ISLET AMYLOID POLYPEPTIDE AGGREGATION IS A LOCAL TRIGGER FOR PANCREATIC ISLET INFLAMMATION

by

Clara Yolande Westwell-Roper

B.Sc. Hons., The University of British Columbia, 2008

A THESIS SUBMITTED IN PARTIAL FULFILLMENT OF
THE REQUIREMENTS FOR THE DEGREE OF

DOCTOR OF MEDICINE AND DOCTOR OF PHILOSOPHY

in

THE FACULTY OF GRADUATE AND POSTDOCTORAL STUDIES
(Pathology and Laboratory Medicine)

THE UNIVERSITY OF BRITISH COLUMBIA
(Vancouver)

May 2014

Abstract

Patients with type 2 diabetes experience an inevitable deterioration of glycemic control leading to long-term complications and dependence on exogenous insulin. Amyloid deposition, macrophage infiltration, and upregulation of pro-inflammatory cytokines are common pathological features of both type 2 diabetic and transplanted islets. Islet amyloid is comprised primarily of aggregates of islet amyloid polypeptide (IAPP), a peptide that is co-secreted with insulin by beta cells. IAPP fibrils share a common cross-β-sheet structure with other amyloids of mammalian and microbial origin that activate innate immune cells via interaction with pattern recognition receptors. We therefore hypothesized that IAPP aggregation acts as a local trigger for islet inflammation.

We found that human IAPP, but not non-amyloidogenic rodent IAPP, induced a potent pro-inflammatory response in islets and macrophages that was amplified by autocrine/paracrine induction of interleukin-1 (IL-1). Pre-fibrillar IAPP activated the membrane-associated pattern recognition receptor Toll-like receptor 2 (TLR2) to induce expression of proIL-1β. Secretion of mature IL-1β required fibrillar IAPP and was attenuated by inhibitors of caspase-1 and the cytosolic NLRP3 inflammasome. Pancreatic islets from transgenic mice with beta cell expression of human IAPP expressed higher levels of pro-inflammatory cytokines than islets from wild-type littermates. Transgenic expression of human IAPP also altered the activation state of resident islet macrophages, the primary cell type responsible for IAPP-induced upregulation of IL-1β. Clodronate liposome-mediated macrophage depletion improved islet function in human IAPP transgenic mice. Moreover, administration of IL-1 receptor antagonist improved human IAPP-induced glucose intolerance in mouse models of islet transplantation and type 2 diabetes. Inhibition of a local IAPP-induced pro-inflammatory response mediated by islet macrophages may therefore help to explain the islet-specific effects of anti-IL-1 therapies in patients with type 2 diabetes.

Collectively, these data suggest a novel – and potentially reversible – mechanism by which IAPP aggregation contributes to beta cell dysfunction and implicate the resident islet macrophage as a critical mediator of chronic islet inflammation in the setting of amyloid formation. Strategies to block TLR2 or NLRP3 activation, inhibit IL-1 signalling, or alter

macrophage polarization may improve IAPP-induced islet dysfunction in type 2 diabetes and islet transplantation.

Preface

Animal studies were reviewed and approved by the University of British Columbia Committee on Animal Care under protocols A11-0202 (Breeding), A12-0260 (Amyloid-induced islet inflammation and beta cell dysfunction), A12-0049 (Processing of proIAPP: role in islet amyloid formation), and A11-0419 (Islet amyloid and transplant failure).

C. Westwell-Roper conceived of the research questions addressed in these studies and designed the experiments with guidance from C.B. Verchere and J.A. Ehses. All experimental work, animal monitoring, and data analysis described herein was conducted by C. Westwell-Roper, with technical assistance as follows: (1) In Chapters 3-5, islet isolation was performed by D. Dai or G. Soukhatcheva. (2) In Chapter 5, immunostaining of pancreas sections from C57BL/6×FVB mice and quantitative image analysis of thioflavin S staining was performed by C.A. Chehroudi, an undergraduate Pathology Summer Fellowship Program trainee, and by V. Kim, a Child & Family Research Institute Mini Med School Studentship recipient. Both students were supervised by C. Westwell-Roper. (3) In Chapter 5, western blotting experiments with MIN6 cells were performed with assistance from C. Chehroudi. (4) In Chapter 5, islet transplant surgery was performed by G. Soukhatcheva or D. Dai. Some material in this thesis has been previously published or is similar to published material, as described below.

1. Concepts presented in Chapter 1 have been described in Montane *et al. Diabetes, Obes, Metabol* (2012) 14(S3):68-77. C. Westwell-Roper wrote the section on islet inflammation, edited the manuscript, and generated the sole data figure in the manuscript, which is included in modified form as Figure 5.11 of this thesis. The discussion of islet transplantation in Chapter 1 also includes ideas published in Potter *et al. Diabetes* (2014) 63:12-9, for which C. Westwell-Roper wrote the draft of the section on islet inflammation and edited the manuscript. Figure 1.7 and Figure 1.8 were initially prepared by C. Westwell-Roper and J.A. Ehses for Westwell-Roper *et al.* (2014) *Immunol Cell Biol* 92(4):314-23. These figures have been significantly modified to fit the context of the chapter.
2. Methods described in Chapter 2 have been published in Westwell-Roper *et al.* (2013) *Methods Mol Biol* 1040:9-18.

3. A portion of the studies presented in Chapter 3 has been published in Westwell-Roper *et al.* (2011) *J Immunol* 187(5):2755-2765. A summary of the TLR2 signalling studies presented in Chapter 2 has been published in abstract form in Westwell-Roper *et al.* (2012) *Can J Diab* 36(5):S18.
4. Data from Chapter 4 have been published in Westwell-Roper *et al.* (2014) *Diabetes* 63(5):1698-711.
5. The transplant experiments described in Chapter 5 have been published in Westwell-Roper *et al.* (2011) *J Immunol* 187(5):2755–2765.

Table of Contents

List of Tables

List of Figures

List of Abbreviations

A1C	glycated hemoglobin
AA	amyloid A
ACCORD	Action to Control Cardiovascular Risk in Diabetes
ADA	American Diabetes Association
ADOPT	A Diabetes Outcome Progression Trial
ADVANCE	Action in Diabetes and Vascular Disease: Preterax and Diamicron MR Controlled Evaluation
AMP	adenosine 5'-monophosphate
AMP	anti-microbial peptide
Aβ	amyloid-β
ANOVA	analysis of variance
AP-1	activator protein 1
ASC	apoptosis speck-like protein containing a caspase-recruitment domain
ATCC	American Type Culture Collection
ATF	activating transcription factor
ATP	adenosine 5'-triphosphate
AUC	area under the curve
BCA	bicinchoninic acid
BMDM	bone marrow-derived macrophage
BSA	bovine serum albumin
CANTOS	Canakinumab Anti-inflammatory Thrombosis Outcomes Study
CAPS	cryopyrin-associated periodic syndrome
CARD	caspase recruitment domain
CCL	CC chemokine ligand
CD	cluster of differentiation
CDA	Canadian Diabetes Association
CFRI	Child and Family Research Institute
CGRP	calcitonin gene-related peptide
CLOD-lip	clodronate liposomes
CMRL	Connaught Medical Research Laboratories
CPE	carboxypeptidase E
CRP	C-reactive peptide
CTLA4	cytotoxic T-lymphocyte-associated antigen 4
CXCL	chemokine (C-X-C motif) ligand
DAMP	danger-associated molecular pattern
DAPI	di aminido phenyl indol
DAVID	Database for Annotation, Visualization and Integrated Discovery
DCCT	Diabetes Control and Complications Trial

Ddit3	DNA damage-inducible transcript 3
DMEM	Dulbecco's Modified Eagle Medium
DMSO	dimethyl sulfoxide
DNA	deoxyribonucleic acid
DPP	Diabetes Prevention Program
DPP-4	dipeptidyl peptidase-4
EDIC	Epidemiology of Diabetes Interventions and Complications
EDTA	ethylenediaminetetraacetic acid
ELISA	enzyme-linked immunosorbent assay
ER	endoplasmic reticulum
FACS	fluorescence-activated cell sorting
FADD	Fas-associated death domain protein
FBS	fetal bovine serum
FinnDiane	Finnish Diabetic Nephropathy Study
FMF	Familial Mediterranean Fever
FPRL1	formyl-peptide-receptor-like-1
GADA	glutamic acid decarboxylase antibody
GEO	Gene Expression Omnibus
GIP	glucose-dependent insulinotropic polypeptide
GLP-1	glucagon-like peptide-1
GO	Gene Ontology
HBSS	Hank's Balanced Salt Solution
HEK	human embryonic kidney
HEPES	4-(2-hydroxyethyl)-1-piperazineethanesulfonic acid
HFD	high fat diet
HFIP	1,1,1,3,3,3-Hexafluoro-2-propanol
hIAPP	human islet amyloid polypeptide
$hIAPP^{Tg/o}$	human islet amyloid polypeptide transgenic (hemizygous)
HLA	human leukocyte antigen
HMGB1	high mobility group box-1
HSP	heat shock protein
i.p.	intraperitoneal
IA2A	insulinoma-associated autoantigen 2 antibody
IAA	insulin autoantibody
IAP	inhibitor of apoptosis protein
IAPP	islet amyloid polypeptide
IBMIR	instant blood-mediated inflammatory response
IFN	interferon
Ig	immunoglobulin
IKK	inhibitor of κB kinase
IL	interleukin
IL-1R	interleukin-1 receptor

IL-1Ra	interleukin-1 receptor antagonist
INOH	Integrating Network Objects with Hierarchies
IPGTT	intraperitoneal glucose tolerance test
IRAK	interleukin-1 receptor-associated kinase
IRF	interferon regulatory factor
IRS	insulin receptor substrate
ITT	insulin tolerance test
JNK	c-Jun N-terminal kinase
KDAC	lysine deacetylase
KEGG	Kyoto Encyclopedia of Genes and Genomes
KRB	Krebs-Ringer bicarbonate buffer
LADA	latent autoimmune diabetes of adulthood
LDH	lactate dehydrogenase
LPS	lipopolysaccharide
LRR	leucine-rich repeat
MafA	v-maf musculoaponeurotic fibrosarcoma oncogene family, protein A
mAb	monoclonal antibody
MALT1	mucosa-associated lymphoid tissue lymphoma translocation protein 1
MAPK	mitogen-activated protein kinase
MHC	major histocompatiblity complex
M-CSF	macrophage colony-stimulating factor
MODY	maturity-onset diabetes of the young
mRNA	messenger RNA
MyD88	myeloid differentiation primary response gene 88
NACHT	NAIP (neuronal apoptosis inhibitor protein), C2TA (MHC class 2 transcription activator), HET-E (incompatibility locus protein from *Podospora anserina*) and TP1 (telomerase-associated protein)
NCD	normal chow diet
NF-κB	nuclear factor-κB
NLR	NOD-like receptor
NLRP3	NACHT, LRR and PYD domains-containing protein 3
NO	nitric oxide
NOD	nucleotide oligomerization domain
NOD/SCID	non-obese diabetic/severe combined immunodeficiency mouse (NOD.CB17-Prkdcscid/J)
ORIGIN	Outcome Reduction with Initial Glargine Intervention
PAM	peptidylglycine alpha-amidating monooxygenase
PAMP	pathogen-associated molecular pattern
PBS	phosphate-buffered saline
PBS-lip	control liposomes
PC1/3	prohormone covertase 1/3
PC2	prohormone convertase 2

PCR	polymerase chain reaction
Pdx1	pancreatic duodenal homeobox 1
pH	hydrogen ion concentration; negative logarithm of hydrogen ion activity
PKC	protein kinase C
PLD	phospholipase D
PPAR	peroxisome proliferator-activated receptor
PrP^{C}	prion protein (cellular isoform)
PrP^{Sc}	prion protein (pathogenic scrapie isoform)
PRR	pattern recognition receptor
PSM	phenol-soluble modulin
PYD	pyrin domain
rIAPP	rodent islet amyloid polypeptide
RIP1	receptor-interacting protein 1
RIPA	radioimmunoprecipitation assay
RNA	ribonucleic acid
ROS	reactive oxygen species
RPMI	Roswell Park Memorial Institute medium
RT-qPCR	reverse transcription quantitative polymerase chain reaction
SAA	serum amyloid A
s.c.	subcutaneous
SD	standard deviation
SDS	sodium dodecyl sulphate
SDS-PAGE	sodium dodecyl sulphate polyacrylamide gel electrophoresis
SEM	standard error of the mean
siRNA	small interfering RNA
TLR	Toll-like receptor
TNF-α	tumor necrosis factor-α
TNFR	tumour necrosis factor receptor
TRAPS	TNF receptor-associated periodic syndrome
TRIF	Toll/IL-1 receptor domain containing adaptor inducing interferon-γ
Tris	tris(hydroxymethyl)aminomethane
TUNEL	terminal deoxynucleotidyl transferase dUTP nick end labelling
TXNIP	thioredoxin interacting protein
UKPDS	UK Prospective Diabetes Study
VADT	Veterans Affairs Diabetes Trial
WT	wild-type
ZnT8A	zinc transporter 8 autoantibody

Acknowledgements

This work was supported by operating grants from the Canadian Institutes for Health Research (CIHR) and the Canadian Diabetes Association (CDA). I am grateful for salary support provided by a CIHR-Vancouver Coastal Health UBC MD/PhD Studentship, a Michael Smith Foundation for Health Research Junior Graduate Studentship, the BC Transplant Training Program, and a CIHR Vanier Canada Graduate Scholarship.

I have been the fortunate recipient of much guidance and encouragement from outstanding mentors during my graduate studies. First, thank you to my supervisor, Dr. Bruce Verchere, for providing a very supportive training environment that has allowed me to explore my interests freely; for encouraging optimism despite seemingly insurmountable technical challenges; for helping me become a better scientist, writer, and communicator; for encouraging me to go where the data leads; for editing my written work at any hour of the day or night; and for much kindness and humour along the way. Second, thank you to Dr. Jan Ehses for invaluable contributions to the direction of this work; many helpful discussions about methods, data, and relevant literature; the chance to work with him on a commentary and a review; and frank conversations about science and academia. Third, thank you to Dr. Paul Orban for advice on both technical and theoretical matters; for keeping me up to date on important publications; and for setting a high standard for a thoughtful, logical, and humble approach to science. Finally, I am grateful to the members of my supervisory committee for their helpful suggestions: Dr. Haydn Pritchard, Dr. James Johnson, Dr. Rusung Tan, Dr. Stuart Turvey, and Dr. Jan Dutz.

I am also grateful to the UBC MD/PhD Program for support: Dr. Lynn Raymond, Dr. Torsten Neilsen, and Jane Lee. I am fortunate to have found a home in the outstanding graduate program of the UBC Department of Pathology and Laboratory Medicine, and I am particularly grateful to Dr. Haydn Pritchard and Aleya Abdulla for monitoring my progress and offering many opportunities for academic and professional development. Thank you also to the staff at CFRI who have assisted with my research or taken care of important administrative tasks: Angel Lam and Meg Hughes (Diabetes Research Program), Lisa Xu (flow cytometry), Kaiji Hu (high throughput imaging), Mitsu Komba (islet core), Baoping Song (histology core), Jingsong Wang (imaging core), and Claire Harrison (Animal Care Facility). I am also grateful to the other labs in the Diabetes Research Program at CFRI for generously lending reagents and equipment.

Many friends and colleagues have helped me reach this point in the balancing act that is an MD/PhD. Thank you to Jaques Courtade, Sigrid Alvarez, Dr. Kathryn Potter, Dr. Mercè Obach, Dr. Joel Montane, Dr. Derek Dai, Dr. Galina Soukhatcheva, Dr. Loraine Bischoff, Dr. Agnieska Klimek-Abercrombie, and Dr. Meredith Hutton. Thank you also to the high school and undergraduate students who have maintained the energy level at my lab bench: Janice Pang, Zoey Li, Jordan Cheng, Sam Aynsley, Cyrus Chehroudi, and Valerie Kim.

Finally, I am grateful for the support and love of my parents, Drs. Yolande and Andrew Westwell-Roper, whose early encouragement of open discussion and respectful debate has shaped my approach to academic questions. To my husband, Dr. Dave Grant, who in the lyric that was his wedding vow promised to double-check my data on IL-1 beta: thank you for sharing the successes of this research project alongside me, and for your support through the disappointments as well. You help sustain my energy and enthusiasm, and I look forward to the many more challenges that we will tackle together.

Chapter 1: Introduction

1.1 Diabetes mellitus

1.1.1 Disease burden

Diabetes mellitus is a heterogeneous group of conditions characterized by hyperglycemia. Approximately 5-10% of affected individuals have type 1 diabetes (1), which remains the most common form of the disease among children and adolescents (2). Most of the remaining 90% have been diagnosed with type 2 diabetes, a condition that has now reached pandemic proportions due to increasingly sedentary lifestyles and rising rates of obesity. Worldwide, diabetes represents one of the most common and devastating non-communicable diseases, affecting over 382 million people (1). An additional 316 million have impaired glucose tolerance and are at high risk for progression to diabetes. This figure is projected to reach 471 million by 2035 (1). Importantly, 80% of individuals with diabetes live in low- and middle-income countries, where limited resource availability contributes to a disproportionate impact on morbidity and mortality (3). Economic development in the Middle East, Western Pacific, sub-Saharan Africa, and South-East Asia has led to significant lifestyle changes in recent years, making these regions emerging hotspots for the disease (1). In May 2013, the 66th World Health Assembly adopted a global action plan for the prevention and control of non-communicable diseases aimed at achieving nine targets by 2025, including a halt in the rising prevalence of diabetes and obesity (4).

In Canada, diabetes rates have doubled over the past decade. Close to 2.4 million adults (6.8% of the population) had been diagnosed with type 1 or type 2 diabetes in 2009, a figure expected to grow to 3.7 million by 2019 (5). It is estimated that by 2020, one in three Canadians will have either pre-diabetes or diabetes (6). Almost 50% of people newly diagnosed with diabetes are between 45 and 64 years old (6). Without optimal glycemic control, diabetes leads to devastating micro- and macrovascular complications that impact an individual's quality of life and – in Canada – shorten lifespan by 5-15 years. These complications include heart disease, stroke, blindness, kidney failure, and limb amputations. Consequently, diabetes causes a considerable financial burden, with an estimated cost to the Canadian healthcare system of $16.9 billion per year by 2020 (6). Vulnerable populations are most severely affected by diabetes;

Aboriginal people are three to five times more likely than the general population to develop the disease (7). Other high-risk populations for type 2 diabetes include those of Hispanic, Asian, South Asian, and African descent (6). Caucasians of northern European descent are more likely to develop type 1 diabetes (1).

1.1.2 Diagnosis

The Canadian Diabetes Association (CDA) Clinical Practice Guidelines were updated in April 2013 (8). These guidelines provide a national standard for evidence-based care of patients with diabetes and are aimed at promoting diabetes prevention efforts, enhancing quality of life for individuals living with diabetes, and reducing the social and economic burden of the disease (9). A major theme emphasized by this recent guideline update is the need for individualized glucose targets and management strategies. Another significant change is the addition of glycated hemoglobin (A1C) levels to the diagnostic parameters, which are determined based on their capacity to predict the development of retinopathy, a significant long-term microvascular complication of chronic hyperglycemia (8).

The diagnosis of diabetes can be made based on (a) a fasting plasma glucose of $\geq$7.0 mmol/L; (b) a two-hour plasma glucose of $\geq$11.1 mmol/L in a 75 g oral glucose tolerance test; (c) an A1C value of $\geq$6.5%; or (d) a random plasma glucose of 11.1 mmol/L. In the absence of symptoms, a repeat confirmatory laboratory test must be performed on another day. The term "prediabetes" refers to impaired fasting glucose (6.1-6.9 mmol/L), impaired glucose tolerance (7.8-11.0 mmol/L at two hours in a 75 g oral glucose tolerance test), or an A1C of 6.0-6.4%, each of which is associated with a high risk of progression to diabetes (8).

In addition to the 6.8% of Canadians diagnosed with diabetes, it is estimated that 1.4% are unaware that they have the disease. Patients with type 1 diabetes are more likely to present with classic symptoms of hyperglycemia: polyuria, polydipsia, polyphagia, weight loss, and ketoacidosis. Patients with type 2 diabetes can be asymptomatic or present with non-specific complaints. Screening of asymptomatic adults at high risk of diabetes as determined by a validated risk calculator (Finnish Diabetes Risk Score or Canadian Diabetes Risk Questionnaire) is recommended every 3-5 years, while those at very high risk should be screened annually (10). Risk calculators take into account age, obesity, history of elevated glucose levels, history of

hypertension, family history of diabetes, limited activity levels, and a diet with limited intake of fruits and vegetables (10).

1.1.3 Etiology and pathogenesis

The American Diabetes Association (ADA) classifies diabetes into one of four categories based on etiology: type 1 diabetes, type 2 diabetes, gestational diabetes, and other specific types (11). However, recent studies suggest that the distinction between type 1 and type 2 diabetes is far less clear – and the disease far more heterogeneous – than this categorization implies (12). Moreover, the clinical distinction based on characteristics such as age, abruptness of onset, ketosis, obesity, and insulin dependence is not always clear (13). Diabetes is perhaps more accurately described as a continuum, with the autoimmunity of type 1 diabetes at one end and the metabolic dysfunction of type 2 diabetes at the other (12,14).

1.1.3.1 Type 1 diabetes

Type 1 diabetes is characterized by autoimmune-mediated destruction of insulin-producing beta cells, leaving patients dependent on exogenous insulin (8). The incidence of type 1 diabetes varies based on geography, age, gender, and family history and has increased over the past 30 years, primarily in younger children (1). This observation has been attributed to changes in environmental factors – including possible increases in enteroviral infection, exposure to dietary toxins, shorter duration of breastfeeding, increasing childhood obesity, and insufficient vitamin D – although attempts are currently underway to remedy the lack of high-quality environmental data (15). Both the hygiene hypothesis and the accelerator hypothesis provide conceptual frameworks to explain the increasing incidence of disease. The hygiene hypothesis suggests that reduced exposure to infectious agents impairs the development of immune-regulatory mechanisms that protect from allergy and autoimmunity (16). The accelerator hypothesis points to insulin resistance associated with increasing average body weight as a cause for earlier diabetes onset in children (17). Further evidence supporting a role for environmental modulation comes from the observation that both disease incidence and autoantibody production vary with changes in season (18,19).

Both geography and ethnicity are important determinants of prevalence: type 1 diabetes is more common among children of northern European descent, and Canada has one of the highest rates of disease in the world (6). The risk of type 1 diabetes is increased in relatives of patients with the disease, with a lifetime risk of 50% for monozygotic twins compared to ~10% for dizygotic twins (20). Discordance is more likely between twins with fewer susceptibility genes (21). Over 40 known loci contribute to type 1 diabetes susceptibility (22). At least 30% of genetic susceptibility can be explained by association with the human leukocyte antigen (HLA) region on chromosome 6, the *IDDM1* locus, and in particular the HLA-DRB1, -DQA1, and -DQB1 loci (23). Non-HLA chromosomal regions such as the insulin gene hypervariable region have also been consistently implicated (24). Genetic studies have provided insight into the innate and adaptive immune dysregulation that leads to disease development, and in particular the mechanisms leading to loss of self-tolerance (25). In individuals with an immune-related genetic predisposition, precipitating events may occur *in utero* or later in life, perhaps in association with normal beta cell turnover or immune system development, ultimately leading to overt immunological abnormalities and beta cell loss (26).

Histological analyses of pancreata soon after disease onset suggest that ~60-90% of insulin-expressing beta cell mass may have been lost (27), although this figure is age-dependent and likely an overestimate for most patients (28). A significant proportion of islets lack immune cell infiltrates and appear normal, with insulitic lesions found throughout the pancreas in a lobular distribution (29). Differences in histological patterns among patients may also suggest the possibility of distinct subsets of type 1 diabetes (30). The amount and progression of insulitis appears to be highly variable, even among islets within a single pancreas (25), and some have suggested that beta cell loss can show a relapsing or remitting pattern throughout the natural history of the disease (26).

Autoantibodies to islet cell antigens, either alone or in combination, can predict diabetes onset among relatives of patients with type 1 diabetes (31). Up to 90% of patients have antibodies to one or more islet antigens, including glutamic acid decarboxylase (GADA), insulin (IAA), insulinoma-associated autoantigen 2 (IA2A), and zinc transporter 8 (ZnT8A) (32). Autoantibodies can be detected months to years before onset of symptoms and are thought to arise secondary to beta cell damage (12). While another traditional hallmark of type 1 diabetes is

a very low C-peptide level at diagnosis, indicative of minimal endogenous insulin secretion, recent data using more sensitive assays suggests considerably more residual beta cell function than previously thought (33). A recent study of 50-year Joslin Medalists – awarded this distinction by the Joslin Diabetes Institute for having lived with diabetes for at least 50 years – included C-peptide measurements in 411 individuals and postmortem examination of nine pancreata. Both analyses provided support for the persistence and function of insulin-producing beta cells (34). These data point to the possible utility of therapies designed to preserve or enhance existing beta cell function rather than a sole focus on replacement of lost beta cell mass.

One less common class of patients included under the ADA's diagnostic umbrella of type 1 diabetes are those with so-called latent autoimmune diabetes of adulthood, or LADA (35). These patients are typically diagnosed as adults, have detectable islet cell antibodies, and present without ketoacidosis (13). Thus, their clinical presentation is similar to that of type 2 diabetes, although they become insulin dependent more rapidly. This condition has also been termed "latent type 1 diabetes," "double diabetes," and "type 1.5 diabetes" (36). Another group of patients with phenotypic type 2 diabetes but negative for islet autoantibodies exhibit T cells that are reactive to islet proteins (T-LADA). The presence of T cell responses in patients with type 2 diabetes may be associated with a more severe beta cell lesion (37).

1.1.3.2 Type 2 diabetes

Type 2 diabetes is a complex polygenic disease characterized by insufficient secretion of insulin to compensate for insulin resistance, which is typically associated with obesity. Patients who do not fulfill the criteria for type 1 diabetes, LADA, secondary diabetes, or monogenic forms of the disease (see below) are considered to have type 2 diabetes, although islet autoantibodies and autoreactive T cells are rarely measured in phenotypic type 2 diabetes.

Concordance rates for type 2 diabetes in monozygotic twins are over 75%, compared to 20-30% in dizygotic twins (38), emphasizing the importance of genetic risk factors. Genome-wide association studies have identified close to 75 susceptibility loci (39), most of which are linked with beta cell function rather than obesity and insulin resistance (40). Nevertheless, known susceptibility loci account for only a small proportion of the estimated heritability (39), and changes in genetics cannot explain the rapidly increasing prevalence of type 2 diabetes.

There is a clear association between obesity and type 2 diabetes: 80 to 90% of individuals with type 2 diabetes are obese (8). Increased caloric intake, decreased energy expenditure, and changes in dietary nutrient composition may all contribute to increased adipose tissue mass and adipose tissue remodelling. A recent study in rodents suggested that hyperinsulinemia may also be a cause of obesity (and not simply a result of beta cell compensation for insulin resistance) (41); in humans, such hyperinsulinemia might be associated with certain patterns of nutrient consumption, although this hypothesis remains to be tested. Obesity is also associated with hypothalamic injury in rodent models (42), and pathology in the hypothalamus, including inflammation leading to insulin and leptin resistance, may contribute to the pathogenesis of obesity (43). The gut microbiome is also a critical environmental mediator of energy homeostasis. Recent metagenome-wide association studies point to microbial dysbiosis predictive of type 2 diabetes (44,45). Notably, fecal transplantation from lean donors into individuals with metabolic syndrome can improve insulin sensitivity (46). In addition, environmental factors *in utero*, affected by overnutrition in the mother, may cause epigenetic changes that determine the offspring's metabolic risk as an adult (47). An increased amount of dysfunctional adipose tissue – and in particular, increased visceral fat (48) – leads to the release of adipokines, including pro-inflammatory cytokines (49), that impair insulin signalling and may also directly affect islet function. Adipose tissue also produces hormones that regulate energy balance, including leptin, adiponectin, and resistin (50). The role of adipose tissue inflammation in type 2 diabetes is discussed in Chapter 1.3.

Despite the association between obesity and type 2 diabetes, most obese individuals do not develop the disease. While the relative contributions of insulin resistance and beta cell dysfunction to the pathogenesis of type 2 diabetes was a subject of early debate, it is now clear that glucose homeostasis requires integrated crosstalk between beta cells and insulin-sensitive tissues (51). Indeed, beta cells themselves can become insulin resistant (52). Even for glucose levels within the normal range, progression toward impaired glucose tolerance appears to be due to a continuous decline in beta cell function (53) that eventually leads to type 2 diabetes (54,55). Other factors contributing to disease progression include the dysregulated release of glucagon by alpha cells (56,57). Indeed, patients with type 2 diabetes have chronically elevated plasma glucagon levels (58) and antagonism of glucagon can lower glycemia in diabetic rodents (59,60).

Data from rodent models also suggest that hypothalamic glucagon signalling may be involved in counter-regulation of hepatic glucose production and is suppressed in obesity (61). Other important contributors to beta cell insulin secretion that may be dysregulated in type 2 diabetes include the incretin hormones, glucose-dependent insulinotropic polypeptide (GIP) and glucagon-like peptide 1 (GLP-1) (62), and neuronal inputs to the pancreas and liver. The vagus nerve is important in regulating islet function (63) as well as many other processes, including chronic inflammation (64). Finally, the hypothalamus contributes to the regulation of insulin secretion by integrating multiple signals, including glucoregulatory hormones and nutrient stimuli such as lipids (65,66).

Beta cells exhibit several functional defects in patients with type 2 diabetes. First-phase glucose-stimulated insulin secretion is already lower than in normal controls in individuals with impaired fasting glucose or impaired glucose tolerance (67). By the time of clinical diabetes onset, insulin secretion in response to glucose is nearly absent and is also reduced in response to other secretagogues such as arginine (67). Other abnormalities include impaired pulsatile insulin release leading to decreased diurnal and ultradian oscillations in serum insulin (68). Furthermore, proinsulin levels and the plasma proinsulin:insulin ratio are significantly elevated in patients with type 2 diabetes, pointing to a defect in proinsulin processing by the beta cell (69). Autopsy studies have also revealed a decrease in beta cell mass associated with increased beta cell apoptosis (70). One such study reported that beta cell volume was decreased by 40% in obese humans with impaired glucose tolerance and by 63% in those with diabetes compared to non-diabetic obese controls (70), and other studies have suggested a range of reduction in beta cell mass from 20-65% (71). However, this decrease in mass cannot fully explain the absence of first-phase insulin release, emphasizing the combined contribution of decreased mass and a functional impairment in the remaining viable beta cells (67).

Multiple mechanisms contribute to progressive beta cell dysfunction. Increased secretory demand on beta cells in the face of insulin resistance promotes beta cell endoplasmic reticulum (ER) and oxidative stress (72-74). The synergistic toxic effect of hyperglycemia and lipids, or glucolipotoxicity (75,76), is also a likely contributor. Increasing evidence suggests that islet amyloid (70,77,78) and islet inflammation (79) both play an important role in the progressive decline in insulin secretion; this thesis examines the potential relationship between these two

factors, which are discussed further below. Figure 1.1 provides a simplified schematic showing major pathways that contribute to the development of obesity, insulin resistance, and impaired beta cell function in type 2 diabetes.

1.1.3.3 Other forms of diabetes mellitus

The third ADA classification is gestational diabetes, which affects 3-20% of pregnant women (9). Risk factors include age over 35, ethnicity (Aboriginal, Hispanic, South Asian, Asian, and African populations are at higher risk), obesity, use of corticosteroids, prediabetes, a family member with type 2 diabetes, and conditions associated with insulin resistance (8). While there is some controversy over the appropriate diagnostic criteria for this condition (80), it is clear that significant hyperglycemia during pregnancy increases the risk of fetal macrosomia and is also a risk factor for subsequent development of type 2 diabetes in the mother (8).

The fourth ADA category includes all other specific etiologies (11). The most common, maturity onset diabetes of the young (MODY), accounts for 1-2% of individuals with diabetes and results from autosomal dominant genetic defects that impair beta cell function. For example, hepatocyte nuclear factor-1α, also known as MODY type 3, is the most common single-gene cause of diabetes (36). Other forms of the disease are associated with genetic defects in insulin action or are secondary to disease of the exocrine pancreas, endocrinopathies, drug or chemical triggers, infections, or other genetic syndromes. Lean individuals with no evidence of insulin resistance, dyslipidemia, or other cardiovascular risk factors typically associated with type 2 diabetes may present a significant diagnostic challenge (36), but an understanding of the specific pathophysiology is important in determining optimal treatment.

1.1.4 Treatment

1.1.4.1 Type 1 diabetes

Preservation of insulin secretion following disease onset is an important therapeutic goal in type 1 diabetes, as endogenous secretion is associated with less retinopathy and reduced severity of iatrogenic hypoglycemia later in the disease (81). Multiple methods for glucose monitoring and insulin delivery exist. Daily injections using a combination of a long-acting insulin analogue to provide basal insulin and rapid-acting insulin administered before meals is a

common approach (8). Pumps that deliver a continuous subcutaneous insulin infusion are also increasingly utilized (82). The combination of insulin pump and continuous glucose monitoring is known as sensor-augmented pump therapy. Devices that integrate both systems are available for clinical use in Europe but are still under evaluation in North America (26).

Other potential therapies for type 1 diabetes include new insulin analogues, incretins, and other hormones such as pramlintide (an analogue of islet amyloid polypeptide, or IAPP) and leptin (26). Previously proposed immunomodulatory therapies include anti-CD20 (rituximab); anti-CD3 (teplizumab, otelixizumab); a CTLA4-immunoglobulin fusion protein (abatacept); and antigen therapies with glutamic acid decarboxylase 65, heat shock protein-60, or an altered peptide ligand of the insulin B chain (26). None of these monotherapies has achieved phase three endpoints, despite some evidence of temporary C-peptide preservation. Approaches that involve limiting innate immune activation, such as blockade of the type 1 IL-1 receptor (IL-1R) with the IL-1R antagonist (IL-1Ra) anakinra, also failed to demonstrate efficacy in recent-onset diabetes (83). Combination immunotherapy targeting multiple aspects of immune activation and regulation may prove more successful.

An alternative approach to therapy in type 1 diabetes is the replacement of beta cells with whole pancreas grafts (typically performed as a combined kidney/pancreas transplant) or with transplanted islets. Significant advances in clinical islet transplantation over the past 15 years are attributable to enhanced surgical methods for islet isolation and transplantation, engraftment of a large number of healthy islets, and an improved glucocorticoid-free immunosuppressive regime (84). However, an international trial of the Edmonton protocol revealed that approximately 75% of patients returned to exogenous insulin therapy within two years (85). The Collaborative Islet Transplant registry recently reported a 52% rate of insulin-independence after two years (86). Even among patients requiring exogenous insulin, islet transplantation can slow the progression of micro- and macrovascular complications (87). Moreover, at the time of graft failure, many patients have serum C-peptide above pre-transplant levels, suggesting residual graft function (85). Many factors contributing to beta cell dysfunction in transplanted islets may be independent of specific allo- and autoimmune responses and are likely shared with islets in type 2 diabetes (88).

1.1.4.2 Type 2 diabetes

Initial management of type 2 diabetes requires lifestyle intervention, including nutrition therapy and physical activity. The biguanide metformin is often started immediately in patients with A1C ≥8.5%, and insulin (potentially in combination with metformin) is initiated in patients with symptomatic hyperglycemia and metabolic decompensation (8). In patients unable to achieve glycemic targets with initial therapy, an additional agent should be added, taking into consideration its blood glucose-lowering efficacy, risk of inducing hypoglycemia, effect on weight, contraindications, side effects, and cost. Agents included in the 2013 CDA treatment guidelines include the alpha-glucosidase inhibitor acarbose; incretin agents, including dipeptidyl peptidase-4 (DPP-4) inhibitors and GLP-1 receptor agonists; insulin; the insulin secretagogues, meglitinides and sulfonylureas; thiazolidinediones; and the weight loss agent orlistat (8). Additional therapeutic classes include sodium/glucose cotransporter-2 inhibitors (e.g. canagliflozin), bile-acid-binding resins (e.g. colesevelam), dopamine receptor agonists (e.g. bromocriptine), and pramlintide (89).

The progressive nature of type 2 diabetes is due to increasing beta cell dysfunction over the course of the disease. The Diabetes Outcome Progression Trial (ADOPT), in which recently diagnosed and previously untreated patients were placed on glibenclamide, metformin, or rosiglitazone for four years, demonstrated the most sustained glucose-lowering effects with rosiglitazone and intermediate maintenance of glycemic control with metformin. Trials focused on prevention of type 2 diabetes onset in individuals with impaired glucose tolerance, including the Diabetes Prevention Program (DPP) study (90), have shown that lifestyle modifications are more effective than any drug except thiazolidinediones, but that many drugs slow progression to diabetes. It is unclear whether short-term improvements in beta cell function can offer sustained benefit after withdrawal of therapy, although such effects have been suggested for troglitazone in DPP and insulin glargine in the Outcome Reduction with Initial Glargine Intervention (ORIGIN) trial (89). Additional studies are currently underway to evaluate changes in beta cell function associated with medical and surgical approaches to treatment in both adults and children with impaired glucose tolerance or recently diagnosed diabetes (90).

Alternate approaches to slow the loss of beta cell function are urgently needed. Anti-inflammatory agents such as anti-IL-1 therapies have shown promising improvements in A1C in

early clinical trials (79). Bariatric surgery has also received recent attention for glucose-lowering effects beyond those attributable to caloric restriction (91). Gastric bypass in combination with medical therapy restores beta cell function as measured by oral disposition index relative to medical therapy alone or medical therapy with sleeve gastrectomy (92). Other experimental approaches are aimed at increasing insulin sensitivity, including the salicylic acid derivative salsalate (93) and interventions that manipulate the gut microbiota (94).

1.1.5 Complications

The long-term consequences of both type 1 and type 2 diabetes include microvascular (retinopathy, nephropathy, neuropathy) and macrovascular (stroke, myocardial infarction) complications (95). These result from the death and dysfunction of cells that accumulate high amounts of intracellular glucose in the presence of hyperglycemia, including endothelial and mesangial cells. Toxicity arises from several mechanisms, including increased flux through the polyol pathway leading to oxidative stress, intracellular production of advanced glycation end products, activation of the protein kinase C pathway, and increased hexosamine pathway activity leading to pathological changes in gene expression (96).

Up to 70-80% of people with diabetes die of a cardiovascular event, often without prior signs or symptoms of cardiovascular disease (97). Indeed, patients with type 1 diabetes have a ten-fold higher risk of cardiovascular events than non-diabetic individuals of the same age (98). Several large studies have evaluated long-term complications in patients with type 1 diabetes. The Epidemiology of Diabetes Interventions and Complications (EDIC) study of the Diabetes Control and Complications Trial (DCCT) found that intensive treatment reduced the risk of cardiovascular events by 42% compared with conventional treatment (99); similarly, the risk for retinopathy and nephropathy decreased with intensive therapy in patients with type 1 diabetes (100). The same study found beneficial effects of intensive therapy on cardiac autonomic neuropathy (101) and progression of diabetic retinopathy (102). The EDIC study also found fewer long-term renal complications in patients with intensive glycemic control, blood pressure control, and favourable lipid panels (103). The Finnish Diabetic Nephropathy Study (FinnDiane) found that variations in A1C predicted the incidence of progression to renal disease and the

incidence of cardiovascular disease (104). FinnDiane also identified an association between the severity of kidney disease and premature mortality in type 1 diabetes (105).

In type 2 diabetes, the UK Prospective Diabetes Study (UKPDS) reported that improved glucose control with sulfonylureas and insulin reduced microvascular complications with no clear benefit for macrovascular disease (106). This led to the design of four interventional trials to examine the effects of more intensive therapy on cardiovascular outcomes. The Action to Control Cardiovascular Risk in Diabetes (ACCORD) trial (107), the Veterans Affairs Diabetes Trial (VADT) (108), and the ORIGIN trial (109) used insulin as a major component of glucose-lowering interventions, while patients in the Action in Diabetes and Vascular Disease (ADVANCE) trial (110) received the sulfonylurea gliclazide. In all four studies, intensive glucose lowering did not reduce cardiovascular events, and in some patients was associated with potential harmful effects. Microvascular benefits were demonstrated in ACCORD and ADVANCE. Thus, intense glucose control can reduce microvascular complications but – unlike in type 1 diabetes – does not appear to reduce cardiovascular events. Additional therapeutic agents to reduce blood pressure and lipids appear to have more of a risk-modifying effect on cardiovascular outcomes in type 2 diabetes (111). Additional studies are underway to examine changes in cognitive function – a poorly characterized long-term complication of diabetes – among participants in the DPP study (89).

1.2 Amyloid

1.2.1 Definition and structure

Amyloids are composed of protein monomers that convert from a soluble native state to an insoluble, non-branching fibril 2-20 nm in diameter and several microns in length (112). Described as “waxy” deposits in the spleen, liver, and kidneys as early as the 1700’s, amyloid (from the Latin *amylum,* for starch) was named by Rudolph Virchow in the early 1900’s based on the erroneous conclusion that it contained starch (113). Traditionally, amyloid fibrils have been identified within plaques in human disease based on their tinctorial properties, including the appearance of apple-green birefringence under polarized light when the deposit is stained with the dye Congo Red (114). Based on this histological definition, more than 20 amyloid-forming proteins have been associated with disease in humans.

The contemporary biophysical definition of amyloid (115) encompasses all ordered arrangements of peptides or proteins with a cross-β-sheet conformation as determined by X-ray diffraction (116). The cross-β-sheet structure is defined by β-strands that lie perpendicular to the axis of the fibril with a central steric zipper formed by the side chains of apposing β-sheets (117). According to this definition, amyloids need not be associated with extracellular pathological deposits (118). Indeed, many proteins are likely capable of forming amyloid-like structures under specific conditions (119). There are no shared amino acid sequences among amyloid-forming proteins, although the propensity of a peptide to form amyloid can be predicted based on hydrophobic residues and intrinsic disorder that drive aggregation into this lower-energy state (120). The presence of short sequences with self-complementary side chains is also thought to be a determinant of amyloid formation, allowing interlocking of adjacent β-sheets (121). Hydrogen bonding between glutamine or asparagine side chains and intersheet ionic bonds between charged side chains also stabilize the fibril structure (122).

Recent advances in biophysical techniques – including hydrogen-deuterium exchange, X-ray crystallography, solid-state nuclear magnetic resonance, and cryoelectron microscopy – have revealed that amyloids display a wider structural diversity than previously thought (123). Fibril morphologies and stacking patterns differ among peptides (124), and there is also substantial polymorphism among fibrils derived from the same monomer (123). Peptide strands may stack in either parallel or antiparallel sheets; the parallel in-register β-sheet structure is most common in pathological amyloid and yeast prions. In other amyloids, the peptide alone may form distinct folded subunits (125). Although many protein aggregates exhibit an amyloid-like conformation, proteins can also assemble into ordered aggregates via other pathways, including domain-swapping, end-to-end stacking, and silk-type β-sheet polymerization (126).

The polymerization of amyloidogenic peptides *in vitro* is typically characterized by three phases: an initial lag phase during formation of fibril nuclei, an elongation phase, and a steady-state phase during which fibrils and monomers are in equilibrium (127). Many amyloid-forming peptides appear to follow similar aggregation pathways (128) with intermediate aggregates (or pre-fibrillar oligomers) that display common exposed epitopes (129,130). For example, yeast prion proteins sample at least two conformational states similar to those of amyloid-β (Aβ), as determined by binding of an antibody ("A11") raised in rabbits against soluble Aβ oligomers.

Another antibody raised against Aβ fibrils ("OC") (131) also binds some species of yeast prion protein aggregates. Although controversial due to the ability of these antibodies to bind multiple antigens and poor validation in many studies (132), A11-immunoreactive aggregates have been described for IAPP, α-synuclein, and prion protein. These are presumably pre-fibrillar oligomers on the path to fibril formation (133), although such species could also represent off-pathway aggregates that lack the capacity to become fibrils. A cylindrical barrel structure containing antiparallel strands has been suggested as a generic oligomeric structure (134), although others have argued that the very different fibril structures of diverse amyloids makes it unlikely that they all transition through similar intermediates (125).

Soluble oligomeric species – rather than amyloid fibrils – are thought to be the primary species that effect tissue damage (132), largely based on evidence that soluble aggregates correlate better with cognitive impairment than amyloid plaque load in Alzheimer's disease (135). However, disruption of the tissue architecture by fibrillar deposits is likely to impair nutrient and oxygen delivery to cells and consequently also contribute to parenchymal dysfunction. Indeed, amyloid deposits in type 2 diabetes are associated with beta cell apoptosis (136). Importantly, rapid nucleation with subsequent consumption of oligomers on the path to fibril formation is a key property of functional amyloids that distinguishes them from the amyloid assembly in disease, in which there is no selection pressure for efficient amyloid formation (131).

Hydrophobic interactions help drive the conversion of native proteins to an amyloid-like state (137), a process proposed to occur according to one of three general models (122). First, the protein may unfold and then refold into a different structure stabilized by backbone hydrogen bonds. Second, natively disordered peptides may give rise to cross-β-sheet structure derived from segments with little structure in the native state. Third, a change in the conformation of a protein may leave a segment free for interaction with other monomers (122). Surface exposure of hydrophobic residues may also explain the toxicity of oligomers (138). At least *in vitro,* oligomeric aggregates appear to damage cells via common mechanisms, including membrane disruption, calcium dysregulation, accumulation of reactive oxygen species, and induction of apoptosis (131). Recent studies (reviewed below) also suggest that amyloids can activate innate

immune pathways, causing indirect damage to nearby cells by inducing a chronic pro-inflammatory state.

An understanding of amyloid structure is critical in the design of therapeutics aimed at inhibiting amyloid formation, deposition, and toxicity. The transient nature of amyloid oligomers makes them difficult to study, and most structural characterization of amyloid has been restricted to fully-formed fibrils. Moreover, the amyloid deposits found in human tissue are often too large and heterogeneous to allow high-resolution structural studies, so most structural analyses have been carried out on fragments of disease-related peptides. A recent analysis of amyloid fibrils seeded from brain lysates of patients with Alzheimer's disease has opened the door to new possibilities for understanding the nature of amyloidogenic peptide aggregates and their contribution to human disease (139).

1.2.2 Functional amyloids

Many organisms have evolved to make use of the amyloid fold. Functional amyloids appear to transition through some of the same oligomeric intermediates as pathogenic amyloids on the pathway to amyloid formation (131). However, they assemble more efficiently, with rapid consumption of monomers and oligomers (140,141). Thus, amyloids that have evolved to make use of the cross-β-sheet fold may spend very little time in a pre-fibrillar state. On the other hand, pathogenic amyloids – many of which are associated with age-related diseases – accumulate as a heterogeneous population of pre-fibrillar species with no selective pressure for efficient aggregation. Functional amyloids were first identified in bacteria, fungi, and insects prior to their discovery in humans (142). They are found in many organisms, from bacteria to mammals and exhibit remarkable diversity of function.

1.2.2.1 Functional amyloids in mammals

Many mammalian proteins can form amyloids under certain physical conditions, a property that has been suggested to allow their controlled release from secretory granules (143). This proposal arose from a study demonstrating that 25% of randomly selected peptide hormones spontaneously formed amyloid fibrils *in vitro,* and the majority of hormones formed fibrils in the presence of heparin (143). The authors suggested that aggregation of prohormones may facilitate

the formation of dense granule cores that exclude non-aggregating, constitutively-secreted proteins. The inherent membrane-binding property of amyloid aggregates may also promote the formation of a granule membrane (143).

The prototypical functional amyloid in mammals is formed by aggregation of the protein Pmel17, which facilitates melanin synthesis (144). Pmel17 provides a template to accelerate the polymerization of melanin, a process that is tightly controlled by membrane sequestration and proteolytic processing (145). Fibrin-related peptides also form amyloid fibrils that act as a scaffold to activate plasmin, a key regulatory element in coagulation (146). Other functional mammalian amyloids include some forms of endostatin, which have antiangiogenic activity (147).

The recent addition of several anti-microbial peptides (AMPs) to the list of mammalian amyloids raises the intriguing possibility that amyloidogenic peptides contribute to host defense. Most AMPs contain both hydrophobic and cationic domains arranged in a variety of structures from α-helices to antiparallel β-sheets, and oligomerization is important in the targeting and permeabilization of bacterial membranes. The well-characterized AMP LL-37 forms amyloid-like aggregates (148) and shares a similar anti-microbial profile with the pathogenic amyloid-β (Aβ) peptide involved in Alzheimer's disease (149). Moreover, corneal amyloidosis, a local amyloid disease in humans, is characterized by subepithelial accumulation of the AMP lactoferrin (150). Finally, AMPs derived from semenogelin may form a major component of seminal vesicle amyloid (151). It has therefore been proposed that amyloid formation by these peptides is a consequence of their increased concentration during innate immune responses to infectious or endogenous pro-inflammatory triggers (149).

1.2.2.2 Functional amyloids in other organisms

Most known amyloids from bacteria and fungi serve important functions in biofilm formation, the fungal life cycle, virulence, and epigenetic inheritance (152). These functions exploit the strength of amyloid fibrils and their capacity for self-propagation. Multiple mechanisms for regulation of amyloid formation exist among different organisms. For example, yeast have evolved chaperone networks that enable the propagation and degradation of prions while preventing toxicity (142). However, further studies are needed to understand other

microbial regulatory mechanisms, which may have implications for the development of drugs that target pathogenic amyloids in humans. Evidence for four major functions of amyloid in bacteria and fungi is summarized below.

1.2.2.2.1 Adhesion and biofilm formation

Amyloid-forming adhesins, cell-surface proteins that facilitate binding to other cells and surfaces, are widespread in biofilms of many phyla (153). Pathogenic fungi such as *Candida*, the most frequent cause of invasive fungal infections, adhere tightly to endothelial and epithelial surfaces due to amyloid formation by the Als family of adhesins (154). These cell-surface glycoproteins enable zipper-like interactions between cells in response to mechanical stimuli (155). Similarly, *Staphylococcus aureus*, the cause of diseases ranging from mild skin conditions to fatal systemic infections, forms biofilms containing phenol-soluble modulins (PSMs), virulence factors conserved across strains. Ordered aggregation of PSMs into amyloid promotes biofilm stability (156). Dissociation of fibrils stored as amyloids may liberate monomers, which contribute to further biofilm disassembly, antimicrobial activity against normal flora, and lysis of neutrophils (156). In *Bacillus subtilus*, the antimicrobial and spore coat protein TasA also assembles into amyloid-like fibrils during biofilm growth.

Curli fibrils produced by enteric bacteria were the first characterized functional amyloids and also participate in biofilm formation. The major subunit of curli, CsgA, contains five repeats that fold into the cross-β-sheet structure. *Escherichia coli* and *Salmonella spp* secrete CsgA in a soluble form, and its fibrillization is then nucleated by CgsB through a highly regulated process affected by temperature, salt, and nutrient concentration. Curli fibers are thought to be involved in host invasion and pathogenesis through the activation of host extracellular matrix remodeling enzymes (157).

1.2.2.2.2 Virulence factor regulation

Amyloidogenic peptides contribute to unique virulence mechanisms in addition to biofilm formation. Harpins are heat-stable type III-secreted proteins produced by Gram-negative bacteria pathogenic to plants. They cause a hypersensitive response in plants leading to programmed cell death. For example, HpaG is a harpin produced by *Xanthomonas* (158). It

forms a functional, toxic amyloid similar in structure to yeast prion proteins, and – like pathogenic amyloids – may cause membrane destabilization and pore formation. Similarly, the Gram-positive bacterium *Klebsiella pneumoniae* produces the amyloidogenic bacteriocin microcin E492, which has antimicrobial activity against related strains, a property that can be turned off through assembly into a stable amyloid. Interestingly, the cytotoxic properties of microcin E492 and its potential for slow release from a stable fibrillar depot has led some to suggest its development as an anti-tumour therapy (159).

1.2.2.2.3 Sporulation

Recent studies suggest that amyloid fibril production is much more widespread among Gram-positive bacteria than previously thought (160). It likely acts as an important structural component of the spore and cell envelope in many *Actinobacteria* and *Firmicutes.* Multicellular organisms, including insects and fish, also take advantage of the mechanical strength of amyloid for the protection of larvae; for example, the chorion protein within the eggshell forms amyloid fibers (161). The process of sporulation is made more efficient by amyloidogenic proteins. For example, *Streptomyces coelicolor* produces several small proteins known as chaplins that aggregate to form an amphipathic film at air-water interfaces (162). This film reduces surface tension, conferring hydrophobicity to submerged hyphae that allow them to grow into the air and form spores (142). Similarly, most fungi employ hydrophobins to enable formation of aerial structures. Like chaplins, these assemble into monolayers of amphipathic fibrils at hydrophobic/hydrophilic interfaces (163).

1.2.2.2.4 Epigenetic inheritance

Prions are proteins that can exist in at least two forms, one of which is capable of recruiting other members. They were first discovered as the causative agent of Creutzfeld-Jacob disease and Kuru (164). The yeast proteins Sup35, Ure2, Rnq1, Swi1, and Mot3 contain prion domains, large segments with high hydrophilic amino acid content and fewer charged and hydrophobic amino acids (142). Most are thought to share a common structure comprised of parallel in-register β-sheets. Yeast prions reversibly form cytoplasmic amyloid, leading to a

phenotype that is passed from mother to daughter cells upon division. The prion aggregation state and resulting phenotype is thus a form of epigenetic inheritance in yeast (164).

1.2.3 Pathogenic amyloids in humans

Amyloid diseases are the most common protein misfolding diseases, and at least 28 amyloidogenic proteins have been linked to hereditary and acquired disorders (165). Increasingly frequent reports of previously uncharacterized amyloid-like structures raises the possibility that there are more. While not all misfolded proteins involved in disease adopt an amyloid state, the cross-β-sheet structure confers several distinguishing features to pathogenic proteins: self-propagation, protease resistance, and – in some cases – transmissibility (165). Amyloid diseases are divided into two general classes based on the location of amyloid deposits. Systemic amyloidoses are characterized by extracellular amyloid deposits at one or more sites that are distinct from the location of precursor protein synthesis. Often, multiple organs and systems are affected (166). In localized amyloidosis, intra- or extracellular amyloid deposits occur only in the tissue in which the precursor protein is synthesized.

1.2.3.1 Systemic amyloidoses

At least 14 systemic amyloid diseases have been described to date (167). They often share common non-specific presenting symptoms including fatigue, weakness, loss of appetite, and weight loss. In recent years, the combination of laser microdissection and mass spectrometry has allowed for identification of the specific protein in biopsy specimens, improving the accuracy of diagnosis (168). Many systemic amyloidoses involve mutations in amyloidogenic proteins that render them unstable prior to aggregation, overproduction of a protein by expansion of a secretory cell population, or loss of effective chaperones for the protein (167).

The most common systemic amyloidosis is light chain amyloidosis, in which immunoglobulin light chain deposits in the heart, kidney, and liver following clonal expansion of plasma cells (169). Other systemic amyloid diseases include heavy chain amyloidosis, associated with myeloma; senile systemic amyloidosis, characterized by gradual accumulation of transthyretin aggregates in the heart; secondary amyloidosis associated with chronic inflammatory disease, in which fragments of serum amyloid A (SAA) accumulate in the kidney,

liver, and spleen; dialysis-related amyloidosis, a complication of long-term hemodialysis due to aggregation of β2 microglobulin; and other amyloidoses caused by hereditary mutations in transthyretin, apolipoprotein AI, apolipoprotein AII, apolipoprotein AIV, fibrinogen, gelsolin, cystatin C, and BriPP (167). Most of these conditions have no cure, and many questions remain regarding the mechanisms of protein aggregation and tissue damage. Existing animal models of systemic amyloidosis generally do not recapitulate the pathology of human disease (170).

1.2.3.2 Local amyloidoses

In the local amyloidoses, amyloid aggregates may be found either intra- or extracellularly within the tissue in which the precursor protein is synthesized (167). Many local amyloid diseases are associated with neurodegeneration and neuroinflammation (171), but sub-acute and rarer forms of local amyloid can be found in many tissues (172). Amyloidogenic proteins involved in neurodegeneration include Aβ in Alzheimer's disease, tau in Alzheimer's disease and frontotemporal dementia, and prion protein in the spongiform encephalopathies. Prion protein exists in a normal, cellular prion protein isoform (PrP^{C}) and in an abnormal, misfolded form (PrP^{Sc}). The misfolded form accumulates in extracellular aggregates and is transmissible by ingestion. Interestingly, a series of recent reports suggests that other amyloidogenic proteins might also transmit misfolded structure by a prion-like mechanism (173). Although not initially identified as amyloids *in vivo,* two other peptides involved in neurodegenerative disease can form amyloid fibrils: α-synuclein, a protein found in Lewy bodies in Parkinson's disease (174), and huntingtin with a polyglutamine expansion, the cause of Huntington's disease (175). Some protein misfolding diseases affecting the nervous system are caused by the formation of amorphous aggregates that are not characterized by the cross-β-sheet amyloid structure. These include inherited forms of amylotrophic lateral sclerosis, for example, in which intracellular inclusions contain misfolded superoxide dismutase (176).

In Alzheimer's disease, Aβ is a product of proteolytic cleavage of amyloid precursor protein and exists as two species, $Aβ_{1-40}$ and $Aβ_{1-42}$, the latter of which has a greater propensity to form amyloid fibrils. Monomeric Aβ has several proposed physiological roles, although the aggregates are neurotoxic (177). The familial form of Alzheimer's disease is associated with mutations that alter the rate of production or the primary structure of Aβ (178), and the sporadic

form is also associated with altered processing of amyloid precursor protein giving rise to increased levels of $A\beta_{1-42}$ (179). Other amyloidogenic peptides that form deposits in the tissues in which they are synthesized include IAPP in the islets of Langerhans (see below), associated with type 2 diabetes and insulinomas; atrial natriuretic factor in the cardiac atria; prolactin in the aging pituitary and prolactinomas; exogenous insulin at injection sites; lactadherin in the aorta; procalcitonin in C-cell thyroid tumours; keratoepithelin and lactoferrin in the cornea; semenogelin I in the seminal vesicles; and leukocyte chemotactic factor 2 in the kidney (115).

Notably, patients with Alzheimer's disease and type 2 diabetes share similar cardiometabolic risk factors (180,181). The risk of developing late-onset Alzheimer's is 1.4- to 4.3-fold higher among patients with type 2 diabetes, and it has been suggested that cognitive function should be included as a standard end-point in the evaluation of potential therapies for type 2 diabetes (182). Metabolic and vascular dysfunction may affect innate immune activity in both disease states, which in turn appears to play a central role in the formation and clearance of amyloid plaques (183). The epidemiological link between Alzheimer's disease and type 2 diabetes and the potential for common pathogenic mechanisms – including inflammation, insulin resistance, and amyloidosis (184) – raises the possibility of common therapeutic approaches (185).

1.2.4 Islet amyloid in type 2 diabetes

Up to 90% of patients with type 2 diabetes have visible islet amyloid at autopsy (186-188), a finding that is uncommon in pancreata of non-diabetic humans (136). The degree of amyloid deposition correlates with disease severity (189), reduced beta cell mass (77,190,191), and development of hyperglycemia in transgenic mice (192-195). Islet amyloid deposits form by aggregation of IAPP (196,197), also called amylin (198), a 37-amino-acid peptide that is synthesized, processed, and secreted with insulin by beta cells (199-203). The monomeric form of IAPP appears to contribute to glucose homeostasis by regulating gastric emptying and satiety, among other proposed functions (204), and is available in non-amyloidogenic form as the drug pramlintide (see above). The amyloidogenic and cytotoxic properties of IAPP are conferred by a region in the mid-portion of the molecule that participates in β-sheet formation (189). In rodents, three proline substitutions between amino acids 20 and 29 disrupt the β-sheet formation required

for aggregation (Figure 1.2A). Consequently, synthetic rodent IAPP (rIAPP) is soluble, non-toxic (205), and does not form fibrils *in vitro* (205,206). Thus, mice and rats do not develop islet amyloid except with transgenic expression of human IAPP (hIAPP) (207).

A missense mutation (serine to glycine) at position 20 of IAPP occurs at a higher frequency in a subpopulation of type 2 diabetic patients compared to nondiabetic controls and is associated with a more severe form of the disease (208). Mutations in the IAPP gene promoter may also predispose to the development of type 2 diabetes in some populations (209). Furthermore, the increased diabetes susceptibility observed in hIAPP transgenic mice suggests that IAPP aggregation is a cause and not merely a consequence of beta cell dysfunction (192,210,211). Indeed, pre-fibrillar aggregates of synthetic IAPP are directly toxic to beta cells *in vitro* (212,213). IAPP aggregation is also associated with beta cell death in cultured human islets (214,215) and with recurrence of hyperglycemia following islet transplantation (216,217). While definitive evidence for a causative role of IAPP in diabetes will require testing of inhibitors of amyloid formation for their capacity to ameliorate disease, a hexapeptide inhibitor of IAPP aggregation can improve beta cell survival in cultured human islets (214), and siRNA-mediated inhibition of IAPP expression has a similar protective effect (215).

Structural studies of IAPP in solution are difficult because it rapidly forms fibrils under physiological conditions. Some reports suggest that IAPP is natively disordered (218), but it may also adopt a transient helical structure (219). Crystallographic studies are hindered by its propensity to aggregate, but structural data have been obtained by generating a fusion protein with maltose binding protein (220). This study identified α-helical structure at residues 8-18 and 22-27, consistent with previous nuclear magnetic resonance measurements (219,221,222). The structure also suggests that IAPP can dimerize by interacting at a helical interface centered around an aromatic stack of two phenylalanine residues. The authors suggest that parallel orientation of the two helices may orient the C-terminal residues of both IAPP molecules to permit stacking in a two-stranded β-sheet, forming a tetrameric fibril nucleus (220).

While the presence of an amyloidogenic sequence is essential for amyloid formation, other factors contributing to IAPP aggregation in type 2 diabetes are poorly understood. Elevated IAPP production and secretion likely contribute (210), but minimal deposition of extracellular islet amyloid resembling that in human islets has been observed in most transgenic lines (207),

suggesting that simple overproduction of an amyloidogenic form of IAPP is insufficient for amyloid formation (223). Most models require additional factors to drive amyloid formation, such as insulin resistance due to leptin deficiency (224), expression of the agouti viable yellow allele (194), glucocorticoid deficiency (225), or high fat feeding (211). Male mice are more susceptible to hIAPP-induced islet amyloid and hyperglycemia, perhaps due to decreased insulin sensitivity relative to female mice (226). In each of these models, increased stress on the beta cell may affect the trafficking and processing of the IAPP precursor, proIAPP.

Impaired proIAPP processing and increased secretion via the constitutive pathway may promote the extracellular secretion of proIAPP, which can interact with heparan sulphate proteoglycans to form a seed for further (pro)IAPP aggregation (227-229). Like proinsulin, proIAPP is processed by sequential cleavage at two dibasic residues, first at its C-terminus by prohormone convertase (PC) 1/3 to produce an N-terminally extended intermediate, followed by PC2 cleavage at its N-terminus (230-232). Residual C-terminal basic residues following PC1/3 cleavage are removed by carboxypeptidase E (233). A schematic of proIAPP processing is shown in Figure 1.2B, and possible pathways to extracellular amyloid formation are outlined in Figure 1.3. Cytokines such as IL-1β, alone or in combination with TNF-α or IL-6, impair proinsulin processing by downregulation of PC1/3 and PC2 (234,235). Islet inflammation may also contribute to the impaired processing of proIAPP, a hypothesis tested in Chapter 5 of this thesis.

1.2.5 Amyloid in islet transplantation

As described in Chapter 1.1, replacement of beta cells by islet transplantation is a potential therapeutic approach to treat type 1 diabetes. Since the initial publication of the Edmonton protocol almost 15 years ago (84), over 400 islet transplants have been performed by other groups (236). The procedure continues to be limited by a shortage of donor pancreata and loss of beta cells during the pre-transplant culture period and following transplantation (236,237). While islet amyloid may takes years to develop in type 2 diabetes (77,238), it forms in human islets within two weeks of transplantation into non-obese diabetic/severe combined immunodeficiency (NOD/SCID) mice (239) and is associated with hyperglycemia in the recipient (217). Moreover, islets from hIAPP transgenic mice rapidly develop amyloid following

transplantation into diabetic syngeneic recipients and fail to maintain normoglycemia (216). A recent case report identified extensive amyloid deposits in islets from a human recipient five years following transplantation (240). Thus, therapeutic approaches that limit IAPP-induced islet dysfunction may protect the beta cell in both type 2 diabetes and islet transplantation.

1.3 Amyloid-induced inflammation

1.3.1 Evidence for amyloid-induced inflammation

Inflammation is a complex physiological response to potentially harmful stimuli and represents one of the first lines of host defense against infection (241). The cardinal signs of inflammation – swelling, redness, heat, and pain – result from local production of cytokines and chemokines, increased vascular permeability, and infiltration of immune cells such as neutrophils and monocytes. Persistence of the stimulus or dysregulation of the innate immune response may lead to chronic inflammation that causes irreversible tissue damage. Classical instigators of the inflammatory response include microbial motifs common to certain classes of pathogens (called pathogen-associated molecular patterns, or PAMPs) and – in sterile inflammation – products released from dysfunctional or dying cells (called danger-associated molecular patterns, or DAMPs) (242,243). These stimuli are sensed by cells of the innate immune system and by a variety of other cell types equipped with pattern recognition receptors (PRRs) that recognize PAMPs and DAMPs. Increasing evidence suggests that amyloid-forming peptides of both microbial and mammalian origin can activate innate immune cells by interacting with PRRs. This section reviews the evidence for chronic inflammation as a mediator of tissue damage in amyloid disease.

Early evidence for amyloid-associated inflammation was based on autopsy specimens from patients with Alzheimer's disease. Activated microglia and increased expression of pro-inflammatory mediators – such as IL-1, IL-6, TNF-α, CC chemokine ligand (CCL) 4, complement, and oxygen radicals – are associated with amyloid deposition (244-246). Indeed, microglia are found in the vicinity of compact plaques in both the brains of patients with Alzheimer's disease and in transgenic mouse models (247). Rapid plaque formation is accompanied by the appearance of activated microglia (248), with increasing numbers over time due to proliferation and/or infiltration (249). While microglia may exhibit an alternatively

activated (anti-inflammatory) phenotype at some stages of disease, classically activated microglia are more prevalent in older animals (250).

Like Alzheimer's disease, prion disease is characterized by activation of microglia and astrocytes. Microglia appear to be early responders to neurodegeneration (251), proliferate in response to prion deposition (252), and release pro-inflammatory cytokines such as IL-1β (253,254). Network analysis of gene expression in rodent models of prion disease identified a core of immune response-related genes - including *Tgfb1*, *Csf1*, *Tlr2*, *Cebpa*, *Lgals3* and *Stat3* - that regulate prion protein replication, accumulation, and neuronal cell death (255). Similarly, neuroinflammation is a common finding in patients with Parkinson's disease (256). Inclusions containing intracytoplasmic aggregates of α-synuclein are found principally within the substantia nigra, with significant loss of dopaminergic neurons. Rare mutations in familial Parkinson's disease include mutations in α-synuclein, which aggregates to form toxic intermediates on the pathway to amyloid formation (257). Neurons release α-synuclein into the extracellular space (258), where it activates microglia (259) and astrocytes (260). Since the initial observation of upregulated major histocompatibility complex (MHC) class II expression in tissue from Parkinson's disease patients (261), additional studies have reported elevated expression of pro-inflammatory cytokines such as IL-1, TNF-α, and IL-6 within the basal ganglia and cerebrospinal fluid (256).

Amyloid A (AA) amyloidosis occurs secondary to chronic inflammatory disease. SAA is an acute phase reactant produced by the liver that complexes with apolipoprotein A, is taken up by macrophages, and is cleaved into AA fragments that form amyloid (262). One recent study suggested that SAA overexpression leading to amyloid accumulation in mice was not associated with an innate immune response (263). Other studies have found elevated expression of cytokines such as IL-6 and macrophage colony-stimulating factor (M-CSF) at sites of amyloid deposition in systemic AA amyloidosis (42), although it is unclear whether the amyloid or the underlying inflammatory condition is the major cause. Mononuclear cell activation in some models of AA amyloidosis may represent an attempt by these cells to clear the deposits (264) but could also contribute to fibril formation by macrophage cleavage of SAA (265). Epithelioid granulomas also contain AA aggregates, which may play a central role in the pathobiology of sarcoidosis (266). In this disease, SAA is initially synthesized in response to mycobacterial

antigens but subsequently aggregates within granulomas to stimulate macrophage PRRs. Ineffective degradation and clearance of SAA may lead to chronic inflammation and fibrosis (266).

Amyloid formation is also associated with inflammation in other tissues, including the prostate (267). The amyloidogenic S100A8 and S100A9 proteins are major components of corpora amylacea inclusions from prostate glands of patients with prostate cancer and are found in deposits associated with activated macrophages (267). Furthermore, the enterobacterial amyloid curli contributes to nitric oxide production *in vivo*: fibrillogenic curli fibrils are important for the fall in blood pressure in response to systemic *E. coli* infection in mice (268). Other microbial amyloids appear to be relatively inert; indeed, hydrophobins may help fungal conidia avoid clearance by neutrophils and macrophages in the early stages of infection (142).

IAPP fibrils are found within macrophage lysosomes in type 2 diabetes and in hIAPP-expressing transgenic mice (269). Uptake of IAPP fibrils occurs by phagocytosis (270,271), leading to accumulation of amyloid in lysosomes due to its resistance to intracellular proteolysis (270). While it has been suggested that islet macrophages do not contribute to clearance of islet amyloid plaques *in vivo* (270), islet macrophages may effectively clear smaller aggregates or oligomers (272). Like Aβ, IAPP induces IL-6 and IL-8 secretion by human astrocytoma cells (273) and release of IL-1β, TNF-α, IL-6, IL-8, CCL3, and CCL4 by lipopolysaccharide- (LPS-) activated THP-1 monocytes (274). Whether transgenic mouse models of IAPP-induced hyperglycemia show evidence of chronic islet inflammation has not been addressed. In this thesis, we evaluate the effect of IAPP aggregation on pro-inflammatory cytokine secretion by macrophages and islets (Chapter 3) and determine the contribution of islet macrophages (Chapter 4) and IL-1 (Chapter 5) to IAPP-induced inflammation and islet dysfunction.

1.3.2 Activation of pattern recognition receptors

Pattern recognition receptors (PRRs) include membrane-bound receptors (Toll-like receptors, or TLRs, and scavenger receptors), intracellular PRRs (RIG-like helicases and the DNA sensors DA1 and AIM2), and the intracellular nucleotide binding oligomerization domain-(NOD-) like receptors (NLRs), which detect both PAMPs and DAMPs (275). Emerging evidence suggests that many amyloidogenic peptides are recognized by complexes of cell surface

receptors, including scavenger receptors. This initial recognition event facilitates subsequent activation of membrane-bound and cytosolic PRRs (266,276-282).

1.3.2.1 Scavenger receptors

Macrophage uptake of amyloid fibrils is thought to occur by phagocytosis, a process dependent on scavenger receptor-mediated particle recognition (270,271). Macropinocytosis is responsible for clearance of soluble (pre-fibrillar/oligomeric) Aβ from the extracellular space in Alzheimer's disease (272), and may involve different cell surface receptors. Whether this is also the case for oligomeric forms of other amyloidogenic peptides is unclear, but an understanding of the mechanisms of peptide uptake at different stages of aggregation may inform the development of anti-amyloid and anti-inflammatory therapies.

Originally identified based on their capacity to bind and internalize oxidized low density lipoprotein, scavenger receptors are now known to interact with diverse ligands, including microbial components such as LPS (283). They are structurally heterogeneous and divided into nine classes based on their domain architecture (283). It is generally thought that ligand binding to scavenger receptors induces endocytosis or phagocytosis followed by lysosomal degradation (284), while engagement of TLRs (see below) transmits transmembrane signals to activate NF-κB and mitogen-activated protein kinase (MAPK) pathways (285). However, many scavenger receptors also activate signalling pathways upon ligand binding, including the class B scavenger receptor CD36 (286).

Several amyloidogenic peptides bind to CD36. The integrin α6β1, the integrin-associated protein CD47, and CD36 form a complex that recognizes fibrillar Aβ (119). A recent study demonstrated that CD36 binding to soluble Aβ and IAPP aggregates is required for their subsequent activation of NACHT, leucine rich repeat, and PYD domain-containing protein 3 (NLRP3; see below) (287). Uptake of SAA (286), α-synuclein (288), and a neurotoxic prion protein fragment (289) also involves CD36. A number of other mechanisms for Aβ uptake have been described, including interaction with formyl-peptide-receptor-like-1 (FPRL1) (290), a mechanism shared by the prion protein fragment $PrP_{106-126}$ (291). Figure 1.4 summarizes the common cell surface receptors implicated in innate immune cell activation by amyloidogenic peptides.

1.3.2.2 Toll-like receptors

Initially identified by their homology with the transmembrane Toll protein involved in *Drosophila* host defense, mammalian TLRs are a family of membrane-bound pattern recognition receptors that recognize common microbial structural motifs, in addition to endogenous ligands (242). For example, TLR2 complexes with TLR1 or TLR6 to recognize bacterial lipoproteins and is also activated by endogenous free fatty acids (292). Other TLR ligands include double-stranded RNA (TLR3), LPS (TLR4), single-stranded RNA (TLR7 or TLR8), and bacterial DNA (TLR9) (293). TLR activation by ligand recognition at extracellular leucine-rich repeats induces receptor homo- or heterodimerization leading to recruitment of adaptor proteins such as myeloid differentiation factor-88 (MyD88) and, for TLR3 and TLR4, Toll/IL-1R domain-containing adapter inducing interferon-β (IFN-β), or TRIF. In the MyD88-dependent pathway of TLR4 signalling, IL-1 receptor-associated kinases (IRAKs) 1 and 4 are recruited to the complex and phosphorylated, leading to activation of TNF receptor-associated factor 6 and downstream MAPK and inhibitor of κB kinase (IKK) signalling (294). Activation of TRIF leads to phosphorylation of IFN response factor 3 (IRF3) and expression of type 1 IFN-inducible genes, as well as a delayed NF-κB response. Activation of the transcription factors NF-κB, activator protein 1 (AP-1), and IRF family members (295) causes expression of pro-inflammatory cytokines, chemokines, and costimulatory molecules in innate immune cells (293,296). Thus, TLRs can provide the priming signal required to induce *Il1b* transcription and proIL-1β synthesis, the first of two steps required for the secretion of IL-1β (297). In addition, TLR activation increases expression of inflammasome components required for formation of mature IL-1β (see below) and may contribute to their post-translational modification, including deubiquitination of NLRP3 (298), phosphorylation of apoptosis speck-like protein containing a caspase-recruitment domain (ASC) (299), and post-translational activation of NLRP3 mediated by IRAK1 (300).

To date, TLR1, TLR2, TLR4, and TLR6 have all been implicated in the inflammatory response to amyloids (Figure 1.4). Activation of TLR1/2 has also been described as a pro-inflammatory mechanism for Aβ (276,301), SAA (302), lysozyme fibrils (303), curli fibrils (304), and α-synuclein (305). While lysozyme may also activate TLR2/6 (303), for other peptides the TLR2/6 heterodimer is either not required for NF-κB activation in macrophages or

suppresses the TLR2-mediated response. TLR4/6 appears to be activated by Aβ (50). One study suggested that nitric oxide production by macrophages in response to SAA may dependent on TLR4 but is independent of the adaptor protein MyD88 (281). Prion disease pathogenesis is accelerated in TLR4-deficent mice, suggesting a role for TLR4-induced microglial activation but not necessarily an interaction between fibrillar prion peptides and this PRR (306). TLR4 activation is also involved in α-synuclein clearance (307). In addition to CD36, other membrane-bound receptors partner with the TLRs to enhance ligand recognition. These include CD14, a co-receptor for multiple cell-surface and endosomal TLRs (308,309). CD14 interacts with Aβ (277) and curli fibrils (310) and may be involved in the progression of prion disease (311). CD14 does not seem to be required for NF-κB activation by lysozyme (303) or SAA (312). The activation of TLRs by both microbial and endogenous amyloids suggests that inflammation in amyloid disease may be a consequence of the evolution of the innate immune system to respond to foreign peptide aggregates with similar structural motifs.

1.3.2.3 NACHT, LRR and PYD domains-containing protein 3

Inflammasomes are a group of multiprotein complexes that process pro-IL-1β and proIL-18 into their mature forms. Most include three major components: an NLR, involved in sensing the activating stimulus; pro-caspase-1, which cleaves proIL-1β; and ASC, which bridges pro-caspase-1 and the NLR (313). While NLRP3 activation has received considerable attention as a critical mechanism required for cleavage of proIL-1β into its active form (313), other mechanisms for proIL-1β processing have been described and are summarized in Figure 1.5.

Multiple protein aggregation diseases are associated with activation of NLRP3 (314). Importantly, several diseases associated with protein aggregation but not necessarily amyloid formation appear to be IL-1-mediated, suggesting that the unique structure of amyloid or its oligomers is not required for this response (314). Given the general capacity of NLRP3 to respond to particulate ligands, this is not surprising. However, not all amorphous aggregates are capable of activating NLRP3; for example, lysozyme fibrils but not non-fibrillar aggregates trigger NLRP3 (303). Activation of NLRP3 also occurs in response to Aβ (315) and contributes to disease pathogenesis in a transgenic mouse model of Alzheimer's disease (316). Similarly, SAA activates NLRP3 to promote allergic sensitization in mice (317,318). Prion protein also

activates NLRP3 in macrophage cell lines and microglia (319), a mechanism that contributes to neurotoxicity (320). In Chapter 3 of this thesis, we assess the capacity of IAPP to induce pro-inflammatory cytokine secretion by macrophages and evaluate the contribution of caspase-1-dependent IL-1β secretion to this response. Recent work by Masters *et al.* provides direct evidence for IAPP-induced NLRP3 inflammasome activation in bone marrow-derived dendritic cells (297). In Chapters 4 and 5, we show that this mechanism may be relevant in the islet in type 2 diabetes.

1.3.3 Nature of the pro-inflammatory species

Hydrophobic interactions help drive protein aggregation to form amyloids (137). As the ability of CD14, TLR2, and TLR4 to bind multiple ligands has been attributed to broad recognition of exposed hydrophobic domains (321), such interactions may also contribute to TLR binding by pre-fibrillar oligomeric aggregates. Importantly, Aβ oligomers (but not fully-formed fibrils) induce TNF-α expression in monocytes (279). Given similar exposed epitopes in other oligomeric peptides (322), it is possible that the TLR-binding capacity of amyloidogenic peptides could be conferred by shared structural characteristics of pre-fibrillar species.

The nature of the species involved in these activities is of critical importance for the development of therapies that target such interactions without stabilizing toxic or pro-inflammatory intermediates. Many studies to date have attributed pro-inflammatory effects to the fibrillar form of the peptide and have provided some evidence for direct binding to TLRs, although these assays are challenging given the tendency of amyloidogenic peptides to bind non-specifically to many proteins and the frequent lack of appropriate controls in published binding assays. A recent study suggests that CD36 binds both fibrillar and soluble Aβ as well as soluble IAPP, promoting uptake of these peptides and their subsequent aggregation within and disruption of the macrophage lysosome (287). However, it is important to note that fibrillar Aβ was just as effective as oligomeric Aβ at inducing IL-1β secretion following LPS stimulation, suggesting that NLRP3 activation occurs in response to fibrils. Indeed, previous studies by the same group demonstrating NLRP3 activation used fibrillar Aβ peptide that had been prepared by allowing it to aggregate in water for one week (315). Similarly, only fibrillar prion protein activates NLRP3 and causes lysosomal destabilization, a process not triggered by amorphous aggregates or soluble

oligomers (320). This is in contrast to the observations of Masters *et al.,* who reported increased NLRP3 activation due to soluble vs. fibrillar IAPP preparations (314). These authors performed critical experiments using size-exclusion columns and fully-solubilized monomers, but these species were applied to cells over a time course that likely allowed subsequent fibril formation, both in culture media and within the macrophage lysosome. While the nature of the SAA aggregate responsible for NLRP3 activation has not been characterized, it does not cause lysosomal destabilization (318), suggesting that amyloid-induced inflammasome activation may occur by distinct mechanisms for different peptides.

Given the dramatic differences in geometry, exposure of hydrophobic residues, and inherent stability of oligomers vs. fibrils, it seems unlikely that common receptors exist for both species, but this requires further study. One recent publication has attempted to shed light on the pro-inflammatory species of lysozyme aggregates, reported to activate both TLR2 and NLRP3 (303). These authors used thioflavin T binding, transmission electron microscopy, and Fourier transform infrared spectroscopy to characterize fibrils generated by incubation followed by repeated centrifugation to eliminate soluble species. These data suggest that the fibrillar peptide is involved in activation of both NLRP3 and TLR2. Importantly, amorphous aggregates were unable to induce these responses, suggesting a property specific to the amyloid is required – although the exact species that interacts with the receptor is unclear. Similarly, curli fibrils (as confirmed by thioflavin T binding and circular dichroism) interact with TLR2 (304), whereas for Aβ both the oligomeric and fibrillar forms have been implicated in the activation of TLR2 (276,312) and TLR4/6 (276,287) and the fibrillar form may interact with CD14 (277).

Thus, existing evidence suggests that both oligomers and fibrils can activate PRRs. Several models of amyloid formation describe fibrils in equilibrium with monomers that are capable of aggregation when concentrated (127), raising the possibility that – in the presence of certain binding partners – monomers in fibrillar preparations might aggregate to form smaller oligomeric species. While our understanding of the mechanisms of NLRP3 activation is very limited, several studies have suggested a role for protease-resistant fibrils in disrupting lysosomal integrity. Other potential mechanisms including mitochondrial dysfunction and oxidative stress could also explain NLRP3-induced inflammasome activation by amyloidogenic peptides. In

addition, TLR and NLRP3 activation may be secondary to the release of endogenous DAMPs due to direct oligomer- or amyloid-induced membrane disruption.

1.3.4 Consequences of amyloid-induced inflammation

In vitro studies suggest that macrophages and microglia take up and degrade both soluble and fibrillar peptide aggregates, leading to secretion of pro-inflammatory cytokines. Studies in mouse models of amyloidoses have similarly pointed to a dual role for amyloid-induced TLR signalling: to induce amyloid clearance by facilitating removal of extracellular protein aggregates (323), and to promote the chronic release of pro-inflammatory cytokines linked to tissue degeneration (324-326). Microglia from transgenic models of Alzheimer's disease display a decrease in scavenger receptor expression and an increase in IL-1β and TNF-α release (327), suggesting an inverse correlation between cytokine production and phagocytosis (328). Indeed, signalling via a single TLR can induce expression of hundreds of genes with distinct functions, including pro-inflammatory cytokines, anti-inflammatory mediators, AMPs, metabolic regulators, antimicrobial proteins, and proteins involved in regulation of adaptive immunity. Each of these genes has different regulatory requirements according to its anti-microbial activity and potential for tissue damage. Both negative feedback and epigenetic regulation contribute to distinct expression profiles and cellular activities downstream of TLR activation (294). Possible consequences of amyloid-induced PRR activation and factors that may modify the response are discussed in Chapter 6.

Evidence from some animal models of amyloid disease suggests that TLRs play a neuroprotective role, at least in the early stages. In fact, TLR activation may be of therapeutic benefit in clearing cerebral amyloid deposits (329-331), and TLR signalling can enhance phagocytosis by upregulation of complement and scavenger receptors (332). Indeed, activation of microglia with TLR2 or TLR9 ligands promotes Aβ uptake *in vitro* by increasing expression of the G protein-coupled formyl peptide receptor 2 in an NF-κB-dependent manner (333). In anti-microbial responses to enterobacteria, curli fibrils produced by *Salmonella* may aid in the maintenance of intestinal barrier function (334). Bacterial entry into the mucosa leads to the generation of IL-17A and IL-22 in a TLR2-dependent manner (335) and may be important in host defense against amyloid-producing enteric pathogens.

In one study of TLR2 deficiency in a transgenic mouse model of Alzheimer's disease, mice lacking TLR2 had increased Aβ accumulation and accelerated memory impairment. Cognitive impairment could be rescued by expression of TLR2 in bone marrow-derived cells (336). In contrast, a recent study in younger mice suggests that hematopoietic TLR2 deficiency is neuroprotective (337). Interestingly, in a transgenic mouse model of Alzheimer's disease with dysfunctional TLR4, attenuated pro-inflammatory cytokine expression (338) and increased insoluble Aβ accumulation (339) were both observed. TLR4-deficient mice also exhibit accelerated scrapie pathogenesis (306) and increased accumulation of transgenic α-synuclein in association with neuronal loss (307). These data support a role for TLR2 and TLR4 signalling in protection against extracellular protein aggregates. However, PRR activation in distinct cell types may have different effects, making it difficult to interpret the results of global knockout models. For example, TLR signalling in neurons may increase their vulnerability to Aβ and oxidative stress (340). Similarly, TLR activation in beta cells within the pancreatic islet may impair their capacity to secrete insulin in response to glucose (341-345).

The consequences of innate immune activation in local amyloid diseases are likely dependent on the extent of amyloid formation and age of the host (171,346). Transient overexpression of IL-1β in a transgenic mouse model of Alzheimer's disease lowers Aβ deposition in the hippocampus in association with increased microglial activation (347). Acute application of LPS can also reduce plaque load, while chronic intracranial delivery increases amyloid deposition (348). Similarly, the concentration of the stimulus may be relevant: lower concentrations of Aβ promote CD14-mediated binding and internalization of fibrils, while higher concentrations induce IL-6 secretion and increased neurotoxicity (277). The principle aggregation state of the peptide is likely a further determinant: the phagocytic capacity of microglia is decreased in the presence of oligomeric Aβ (349), and this is likely due to the inhibition of phagocytosis by induction of pro-inflammatory cytokines and suppression of scavenger receptors (271). Finally, the function of the innate immune system changes with age in the presence of increased endogenous danger signals, impaired responsiveness to infection (350), dysregulation of TLR signalling (351), and increased NLRP3 activation (352). The consequence is an altered balance of pro- to anti-inflammatory cytokines leading to systemic low-grade inflammation, also termed "inflammaging" (353). This process is particularly relevant to

amyloid diseases in which the onset of symptoms occurs later in life, including Alzheimer's disease and type 2 diabetes.

1.4 Inflammation in type 2 diabetes

1.4.1 Type 2 diabetes as an autoinflammatory disease

Autoinflammatory diseases are defined by sterile inflammation mediated primarily by cytokines of the innate immune system, in particular IL-1β. Unlike autoimmune diseases, in which the defect is more pronounced in cells of the adaptive immune system, there is no initiating antigen-specific B cell or T cell response. However, given the critical interaction between innate and adaptive immunity, autoinflammatory and autoimmune diseases are perhaps better represented as two ends of a continuum of immunological disease (354). A hallmark of autoinflammatory diseases is the induction of inflammation by products of the inflammatory response itself: for example, IL-1 signals via the IL-1R to induce more IL-1 (355). Indeed, the dominant cytokines in autoinflammatory diseases appear to be IL-1α and IL-1β, as determined by clinical outcomes using anti-IL-1 agents such as IL-1Ra (anakinra), an IL-1Ra-IL-1β chimera (EPI-005), anti-IL-1β monoclonal antibodies (mAbs; rilonacept, canakinumab, gevokizumab), the anti-IL-1α mAb MABp1, the anti-IL-1R mAb MEDI-78998, the oral caspase-1 inhibitor VX-765, and inhibitors of ATP-induced inflammasome activation (354). IL-1 signalling is tightly regulated; activation of the type 1 IL-1R is antagonized by endogenous IL-1Ra and by the type 2 IL-1R, which acts as a decoy receptor.

The classic autoinflammatory diseases are rare genetic disorders characterized by recurrent systemic and local episodes of inflammation. Symptoms can include recurrent fevers, general fatigue, muscle and joint pain, loss of appetite, poor sleep, gastrointestinal disturbances, and skin rashes (356). Inflammatory episodes are also characterized by neutrophilia and elevation of acute phase proteins in serum. The major cause appears to be increased release of IL-1β from circulating monocytes (354). Perhaps the most common autoinflammatory disease is Familial Mediterranean Fever (FMF), caused by a mutation in the gene encoding pyrin, a protein that controls the activation of caspase-1 (357). Patients with FMF suffer lifelong, recurrent bouts of fever and abdominal pain. In cryopyrin-associated periodic syndrome (CAPS), a mutation in NLRP3 (initially called cryopyrin) causes symptoms resembling those of FMF following

exposure to cold temperatures (358). CAPS represents a continuum of diseases, including Muckle-Wells syndrome and neonatal-onset multisystem inflammatory disease. Other autoinflammatory diseases include TNF receptor-associated periodic syndrome (TRAPS), an autosomal dominant disease caused by mutations in the TNF receptor that cause it to accumulate intracellularly and induce IL-1 synthesis (359). Hyper-IgD syndrome is an autosomal recessive disorder in which episodes of fever, muscle aches, skin rashes, and painful oral ulcers result from mevalonate kinase deficiency, which among other consequences can lead to inappropriate activation of caspase-1 (360). Many other local and systemic inflammatory conditions may be improved with anti-IL-1 therapy. These include acute-onset ischemic diseases such as myocardial infarction and stroke, cardiac remodeling following myocardial infarction, gout, pseudogout, osteoarthritis, rheumatoid arthritis, and diabetes (354).

In type 2 diabetes, preclinical evidence suggests that chronic inflammation affects multiple organs that regulate glucose metabolism. These include the hypothalamus, insulin sensitive tissues (liver, skeletal muscle, adipose tissue), and the pancreatic islet. The first clinical study targeting IL-1 in type 2 diabetes showed improved A1C after 13 weeks of treatment with anakinra (361). Notably, there was a sustained improvement in proinsulin:insulin ratios 39 weeks following cessation of treatment (362). Multiple clinical trials have now demonstrated improved insulin secretion in response to anti-IL-1 therapy with minimal effects on insulin resistance (79), although relative effects on the islet and peripheral tissues may be determined by the dose and duration of treatment. These trials have included the IL-1Ra anakinra and the anti-IL-1β mAbs gevokizumab, canakinumab, and LY2189102 (79). An ongoing, large-scale trial of the anti-IL-1β mAb canakinumab will evaluate cardiovascular risk in 17,200 patients over four years, with diabetes as a secondary endpoint (363). Other lines of evidence supporting a role for IL-1-mediated inflammation in type 2 diabetes are summarized below and have led to the categorization of type 2 diabetes as a metabolic autoinflammatory disease (364).

1.4.2 Systemic markers of inflammation

Patients with type 2 diabetes have elevated circulating levels of IL-6, IL-1β, C-reactive protein (CRP), and other acute phase reactants (365,366). Combinations of these markers can predict the risk of progression to type 2 diabetes, including IL-1 (367) and IL-18 (368) in

combination with IL-6. Similarly, IL-1β gene polymorphisms and circulating levels of IL-1Ra may be associated with progression to type 2 diabetes in individuals with metabolic syndrome (369), whereas those with high levels of the anti-inflammatory adipokine adiponectin have a lower risk of developing the disease (370).

Peripheral blood mononuclear cells from patients with type 2 diabetes display increased IL-1β secretion in response to NLRP3 stimuli (371) and are also hyper-responsive to TLR2 and TLR4 ligands (372). It is unclear whether these changes are secondary to hyperglycemia, which may itself regulate TLR expression (373) and induce NLRP3 activation (374). Nevertheless, other potential systemic stimuli for TLR2 and TLR4 are also elevated in type 2 diabetes, including the heat shock proteins HSP60 and HSP70, high mobility group box-1, endotoxin, and hyaluronan (372). Other changes in innate and adaptive immune status are associated with obesity; for example, monocytes, neutrophils, and T cells in the circulation of obese individuals are polarized toward a pro-inflammatory phenotype, an observation that correlates with the degree of insulin resistance (375). Moreover, B cells from the circulation of patients with type 2 diabetes interact with T cells to induce pro-inflammatory cytokine secretion, whereas those from normal controls do not (376).

Biomarkers to monitor the efficacy of anti-inflammatory therapies in type 2 diabetes have traditionally included plasma IL-1, IL-6, TNF-α, CRP, and adiponectin, but they may not reliably predict the efficacy of treatment (377,378). Other potential biomarkers include serum IL-1Ra (361) and plasma microRNAs, which generate a unique signature in patients with type 2 diabetes (379). Measurement of T cell autoreactivity can identify autoantibody negative patients with phenotypic type 2 diabetes who have more severe beta cell dysfunction (37).

1.4.3 Adipose tissue inflammation

While a role for inflammation in type 2 diabetes was initially inferred based on the capacity of pro-inflammatory markers to predict disease and the efficacy of therapies with anti-inflammatory effects, the first supporting mechanistic studies showed a role for adipose tissue-derived TNF-α in the pathogenesis of insulin resistance (49). The accumulation of fat, particularly within visceral adipose tissue, alters the differentiation state and size of the adipocyte. This leads to changes in blood flow, hypoxia, and mechanical stress that induce the

release of pro-inflammatory cytokines and adipokines (380). Fat deposition within the liver may also potentiate the systemic inflammatory response. Circulating pro-inflammatory cytokines can impair insulin signalling in the liver, skeletal muscle, fat, islet, and hypothalamus (364). The major mechanisms for this effect include induction of suppressors of cytokine signalling that interfere with the insulin receptor's tyrosine kinase activity and cause ubiquitination of the insulin receptor substrates IRS1 and IRS2 (381,382). Both adipocytes and immune cells in the stromal vascular fraction of adipose tissue secrete pro-inflammatory cytokines and chemokines, leading to further recruitment and activation of macrophages (383) and B cells (384). Regulatory cell populations are diminished in visceral adipose tissue from obese humans compared to lean controls (385), and other adipose-tissue-resident cell populations such as invariant natural killer T cells may also maintain insulin sensitivity under physiological conditions (386).

Expression and activation of NLRP3 in adipose tissue may be an early event in the pathogenesis of insulin resistance (364). NLRP3 or caspase-1 deficiency limits diet-induced obesity and insulin resistance (387) in association with changes in effector T cell populations in adipose tissue (388). In humans with type 2 diabetes, weight loss improves insulin sensitivity in association with reduced adipose tissue NLRP3 expression and reduced circulating IL-18 (388). Free fatty acids increase intracellular ceramide in macrophages (388), which may also contribute to NLRP3 activation as an early initiating event in insulin resistance (389).

Despite the therapeutic efficacy of anti-IL-1 and anti-TNF therapies in preclinical models, they have generally failed to improve insulin sensitivity in patients with type 2 diabetes. While in some cases the human studies were poorly designed and underpowered (79), it is possible that circulating adipokines induce local autoinflammatory processes in multiple tissues at the very early stages of obesity, prior to practical therapeutic intervention in humans (364). This is consistent with the observation that systemic markers of inflammation do not correlate with improved beta cell function following IL-1Ra therapy (361,362), implicating local islet inflammation in the pathogenesis of type 2 diabetes.

1.4.4 Islet inflammation

Chronic exposure to elevated IL-1α or IL-1β is toxic to beta cells, with effects that have been well characterized in the context of type 1 diabetes (390,391). IL-1 impairs beta cell

function by decreasing the transcription of proteins required for glucose-sensing and hormone secretion (392). The toxic effects of IL-1 are mediated by the induction of reactive oxygen species (393), which damage macromolecules and alter gene transcription (Figure 1.6). Other stimuli within the islet, including ER stress (394), may enhance the damaging effects of pro-inflammatory cytokines on the beta cell. While much work has focused on the pro-apoptotic effects of IL-1β, studies in rodent models of type 2 diabetes suggest that the effects of IL-1 inhibition on insulin secretion and processing can occur independently of effects on beta cell mass (395,396), emphasizing the importance of potentially reversible functional deficits induced by activation of these signalling pathways.

The first evidence that chronic inflammation affects pancreatic islets in type 2 diabetes emerged in 2002, when Maedler *et al.* demonstrated increased IL-1β mRNA and protein expression in islets isolated from patients with type 2 diabetes (397,398). The elevated ratio of IL-1β to the endogenous antagonist IL-1Ra further enhances beta cell susceptibility to this pro-inflammatory cytokine (398,399). Consistent with these studies, recent unbiased global gene expression analysis has identified a group of IL-1-related genes highly expressed in islets from patients with type 2 diabetes and associated with reduced insulin secretion (400).

Both high glucose and saturated fatty acids, nutrient stimuli that are elevated in the systemic circulation in obesity, stimulate proIL-1β expression and chemokine secretion by human islets (401). Beta cells from patients with type 2 diabetes also have increased expression of IL-6 and the chemokines CCL2, CCL13, CCL11, and chemokine (CXC motif) ligand (CXCL) 1 (402), which may be induced by autocrine/paracrine IL-1 signalling (292,395). Free fatty acids activate pro-inflammatory pathways by interaction with TLRs, in particular TLR2 (403,404), and other stimuli for proIL-1β gene expression – such as metabolic endotoxemia (405) – may also activate TLRs within the islet, which are expressed by both innate immune cells and beta cells (Figure 1.7). The second stimulus for IL-1β secretion may be provided by NLRP3 activation in response to hyperglycemia (374), extracellular ATP (406) (perhaps following release from the insulin granule), DAMPs released from dying beta cells, endocannabinoids (407), and/or lipids (389) (Figure 1.8). NLRP3 acts as a sensor for diverse stimuli that disturb cellular homeostasis, many of which are associated with changes in oxidative state, disruption of plasma and lysosomal membrane integrity, oxidative and ER stress, impaired autophagy, mitochondrial

damage, increased osmotic pressure, potassium efflux, and calcium signalling (408). How NLRP3 senses these disturbances is unclear, although proposed mechanisms include its direct interaction with thioredoxin interacting protein (TXNIP) (374) and oxidized mitochondrial DNA (409). Mice deficient in the inflammasome proteins NLRP3 and ASC show improved beta cell insulin secretion compared to wild-type mice, with reduced islet IL-1β protein expression, macrophage infiltration, and fibrosis (410).

Macrophages are phagocytic innate immune cells that display remarkable plasticity depending on the tissue microenvironment (411-413). Macrophage activation is often conceptualized along a continuum with classically activated M1 macrophages on one end and alternatively activated M2 macrophages at the other (411-413). Healthy mouse islets each contain 8-10 macrophages in close association with the vascular epithelium (414,415). These cells express the plasma membrane glycoproteins F4/80, CD11b, and CD11c that are common to both dendritic cells and macrophages and likely play an important role in tissue repair, angiogenesis, and immune surveillance (415-417). In type 2 diabetes, there is a modest increase in intra-islet $CD68^+$ macrophages (401,418), and evidence from rodent models also supports an important role for intra-islet macrophages in the pathogenesis of the disease. Eguchi *et al.* demonstrated recruitment of M1 macrophages to the islet following ethyl palmitate infusion (419). In this model, macrophage depletion increased islet *Ins1, Ins2,* and *Pdx1* mRNA expression and glucose-stimulated insulin secretion (419). Another recent study suggested that infiltrating macrophages respond to endocannabinoids in the islets of the Zucker diabetic fatty rat via the peripheral endocannabinoid receptor CB1 and NLRP3 (407). A recent study by Cucak *et al.* characterized resident and infiltrating macrophage subsets within the islet in the *db/db* mouse model of type 2 diabetes (420). They found a shift toward an M1-like phenotype that preceded a systemic shift in macrophage polarization. Recent work on islets isolated from cadaveric human donors with type 2 diabetes provides the first characterization of other immune cell subsets, suggesting an elevation in total $CD45^+$ leukocytes, including $CD11b^+$ myeloid cells, $CD3^+$ T cells, and $B220^+$ B cells compared to non-diabetic controls (421). Further studies are needed to fully characterize the phenotype and function of intra-islet leukocytes.

Finally, recent contrast-enhanced magnetic resonance imaging studies have demonstrated changes in vascular permeability in a rodent model of type 2 diabetes, consistent with the actions

of pro-inflammatory mediators on the endothelium (422). Future studies using a non-invasive magnetic resonance imaging nanoparticle approach that identifies insulitis in humans with type 1 diabetes based on increased microvascular leakiness (423) may be informative for the monitoring of islet inflammation in patients with type 2 diabetes.

Thus, as in other organs, multiple systemic stimuli trigger islet cytokine and chemokine synthesis leading to recruitment of macrophages. Many of these stimuli likely activate TLRs (in particular TLR2 and TLR4) and NLRP3, leading to the synthesis and secretion of IL-1β. However, the relative contributions of endocrine cells and macrophages to islet cytokine synthesis is unclear. Human beta cells express increased proIL-1β protein in type 2 diabetes (397), and laser-captured beta cells from individuals with type 2 diabetes have increased *Il1b* mRNA (398). Some beta cell lines secrete mature IL-1 in response to ER stress (424), and purified rat beta cells can also secrete mature IL-1 (425). However, no study to date has provided direct evidence for NLRP3-induced caspase-1 activation in isolated beta cells, emphasizing the need for further studies to understand the cellular sources and mechanisms of islet IL-1 synthesis.

It is also unclear whether there are islet-specific pro-inflammatory stimuli prior to the onset of hyperglycemia. In human studies, anti-IL-1 therapies appear to improve islet function with relatively little impact on insulin sensitivity (79), and rodent models of diet-induced obesity show only small changes in islet pro-inflammatory gene expression (404). This raises the possibility of an islet-localized trigger for IL-1β. In this thesis, we propose that local amyloid formation by IAPP provides such a stimulus by activating both TLR2 and NLRP3.

1.4.5 Anti-inflammatory therapy in type 2 diabetes

Because similar pathways may contribute to both adipose tissue and islet inflammation, they represent attractive therapeutic targets to treat type 2 diabetes and its complications (426). Agents currently in use that likely modulate pro-inflammatory signalling in diabetes include statins, peroxisome-proliferator-activated receptor-γ (PPARγ) agonists (427), and angiotensin receptor blockers. Metformin was recently shown to inhibit NLRP3 inflammasome activity in monocyte-derived macrophages from individuals with type 2 diabetes via activation of the AMP kinase pathway (371). Other studies have shown anti-inflammatory effects of DPP-4 inhibitors

(428) and salsalate (93), although the effects of salsalate on islet function are unclear. Anti-inflammatory therapies that have shown promise in preclinical models include lysine deacetylase (KDAC) inhibitors, which may both inhibit innate immune cell activation and protect the beta cell (429,430). Evidence in rodent models also points to potential therapeutic benefits of resolvin D1, an enzyme that alters the phenotype of tissue macrophages (431); TLR inhibitors; and strategies that target T and B lymphocytes (432), although the side effects of such non-specific approaches require careful consideration. In addition to a number of anti-IL-1 therapies that have not yet been evaluated in type 2 diabetes (see above), further evaluation of anti-TNF-α therapies in properly designed clinical trials may be warranted (79). Recent clinical studies suggest that the efficacy of immunotherapy may be greater in patients with active inflammation or autoreactivity (432), pointing to benefits of stratifying patients based on their inflammatory or autoimmune status and comorbid conditions.

1.4.6 Similarities with islet transplantation

As in type 2 diabetes, IL-1 secretion by infiltrating innate immune cells may impair beta cell function and survival following islet transplantation. IL-1Ra enhances the survival of human islets during culture (433), is reportedly used as a peri-transplant therapy at multiple islet transplant centers (434), and works in combination with the anti-TNF agent etanercept to preserve the mass of marginal human islet grafts in immunodeficient mice (435). Stimuli for pro-inflammatory cytokine secretion during pre-transplant culture include hypoxic and mechanical injury. Activation of MAPK and NF-κB signalling during islet isolation likely promotes the secretion of cytokines and chemokines (436), levels of which are modulated by components of culture media (437).

The quality of the islet preparation may determine the extent of graft loss due to the instant blood-mediated inflammatory response (IBMIR) in humans (438). Triggered by islet expression of tissue factor and CCL2 upon contact with blood in the portal vein, the IBMIR is characterized by rapid consumption and activation of platelets, consumption of neutrophils and monocytes, and activation of the coagulation and complement systems. IBMIR may underlie loss of up to 60% of transplanted graft mass in the first week following transplantation (439). However, even in mice, which do not exhibit an IBMIR, syngeneic islet grafts express high

levels of cytokines and chemokines (440), including IL-1β (441), and blockade of IL-1β, TNF-α, and IFN-γ with neutralizing antibodies can reduce the number of human islets required to achieve normoglycemia (442). Following transplantation, chemokines secreted by macrophages (443), ductal cells (444), endothelial cells (445), and damaged beta cells (446) likely contribute to the observed recruitment of monocytes to syngeneic grafts (447). Infiltrating monocytes/macrophages activated by islet-derived cytokines (448) also play a critical role in the early function of allografts and xenografts in rodents (449-452).

It is unclear whether current immunosuppressive regimens, which are designed to target allograft rejection, impact innate immune responses in islet transplants (maintenance immunosuppression at Vancouver General Hospital includes tacrolimus and mycophenolate mofetil). Treatments aimed at reducing non-specific inflammation can prevent primary dysfunction of islets following transplantation, but addition of a low-dose immunosuppressant is needed to overcome allorejection (51-58). Nevertheless, anti-inflammatory therapy may preserve early beta cell function enough to reduce the number of islets required to achieve insulin-independence. Further studies are needed to understand the nature of the pro-inflammatory response in failing human islet grafts and the potential benefits of long-term anti-inflammatory therapy in islet transplant recipients.

1.5 Thesis hypothesis and objectives

1.5.1 Summary of rationale

Pancreatic islets from patients with type 2 diabetes exhibit progressive beta cell death and dysfunction, likely due in part to increased expression of pro-inflammatory cytokines, macrophage infiltration, and islet amyloid deposition. Islet amyloid deposits form in both type 2 diabetic and transplanted islets by aggregation of IAPP, a peptide that is co-secreted with insulin by beta cells. IAPP aggregates share a common cross-β-sheet structure with those of other amyloidogenic peptides known to induce a potent pro-inflammatory response by activation of both TLRs and the NLRP3 inflammasome, leading to release of the cytokine IL-1β. Blockade of IL-1 signalling can improve beta cell function in individuals with type 2 diabetes with no effect on insulin sensitivity, although it is unclear whether there are islet-specific triggers for IL-1 synthesis. Given that the aggregation intermediates formed by amyloidogenic peptides share

common structural features, we speculate that IAPP acts as a trigger for islet inflammation by activating similar innate immune pathways.

1.5.2 Hypothesis and objectives

We hypothesize that IAPP aggregates activate islet macrophages via interaction with innate immune receptors, resulting in secretion of IL-1β and other pro-inflammatory cytokines that promote beta cell dysfunction and worsen hyperglycemia. A schematic of this hypothesis is shown in Figure 1.9. The overall objective of this work is to understand the major mechanisms by which IAPP interacts with the innate immune system and the consequences for beta cell function and glucose homeostasis. Three objectives were addressed with the specific aims described below.

Objective 1: **To characterize the pro-inflammatory effects of IAPP in macrophages and islets (Chapter 3).**

- ***Aim 1.1.*** To determine whether IAPP aggregates induce pro-inflammatory cytokine/chemokine secretion by macrophages and islets.
- ***Aim 1.2.*** To determine the role of IL-1 receptor signalling in amplification of IAPP-induced cytokine/chemokine secretion.
- ***Aim 1.3.*** To determine whether IAPP acts as an endogenous TLR ligand.

Objective 2: **To understand the functional consequences of the interaction between IAPP and islet macrophages (Chapter 4).**

- ***Aim 2.1.*** To determine the relative contribution of macrophages to IAPP-induced islet cytokine/chemokine expression.
- ***Aim 2.2.*** To evaluate the phenotype of intra-islet macrophages in a mouse model of type 2 diabetes with islet amyloid formation.
- ***Aim 2.3.*** To determine the effect of macrophage depletion on islet amyloid formation, IAPP-induced islet inflammation, and beta cell dysfunction *in vivo*.

Objective 3: **To determine whether IL-1 receptor blockade improves IAPP-induced islet inflammation and dysfunction (Chapter 5).**

Aim 3.1. To determine the effects of IL-1 receptor antagonist on IAPP-induced islet inflammation and beta cell dysfunction *in vivo.*

Aim 3.2. To determine the effects of IL-1 receptor antagonist on islet amyloid formation.

1.5.3 Significance

These studies contribute to our understanding of the mechanisms by which IAPP induces beta cell dysfunction and suggest an islet-localized trigger for innate immune activation in type 2 diabetes. This work may aid in the development of therapeutic strategies to preserve beta cell function in patients with type 2 diabetes and in islet transplant recipients. Moreover, these studies point to several conserved mechanisms by which protein aggregates interact with the innate immune system, a finding of broad relevance to diabetes and other aging-associated amyloid diseases.

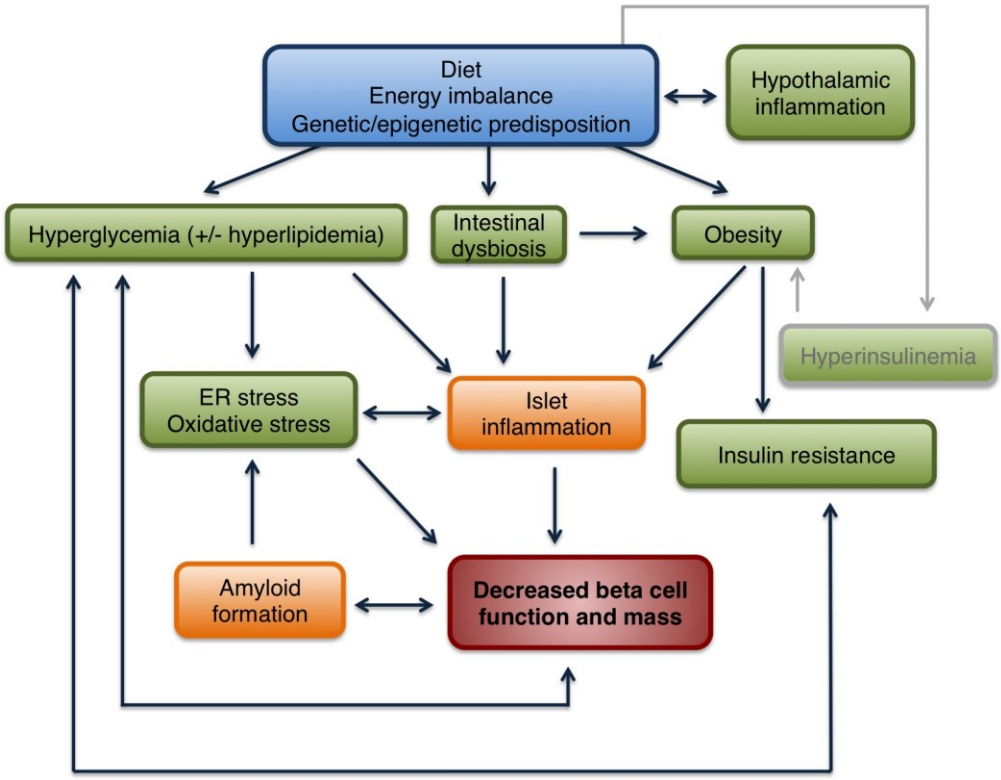

Figure 1.1. Factors contributing to beta cell dysfunction in type 2 diabetes. Excess caloric intake contributes to the development of the obesity that is associated with type 2 diabetes. In rodent models, pathology in the hypothalamus initiated by nutrient stimuli causes dysregulation of many aspects of energy metabolism, including food intake. Diet also affects the diversity of intestinal microbiota, which in turn may regulate body weight and – due to increased intestinal permeability and the presence of microbial components in the blood – drive inflammation in multiple tissues including the islet. Hyperlinsulinemia associated with certain patterns of nutrient intake may also contribute to the pathogenesis of obesity (grey pathway). Insulin resistance in multiple tissues results at least in part from adipose tissue remodeling and secretion of adipokines that interfere with insulin receptor signalling, leading to both an increased requirement for insulin and defective autocrine/paracrine insulin signalling in the beta cell. Most obese individuals do not develop type 2 diabetes, and a defect in beta cell insulin secretion (associated with genetic or epigenetic predisposition) is required for clinical onset. Multiple stimuli including hyperglycemia and hyperlipidemia cause beta cell ER and oxidative stress, which further impair insulin secretion and may also drive islet inflammation. Dysfunctional beta cells have impairments in proinsulin and proIAPP processing, which in turn may contribute to islet amyloid formation due to the aggregation propensity of partially processed proIAPP. Aggregation of IAPP is also a cause of oxidative stress and in some models of intracellular aggregation may contribute to ER stress, which has been linked to islet IL-1 secretion. Pro-inflammatory cytokines such as IL-1 can also induce ER and oxidative stress. This thesis examines the relationship between amyloid formation and islet inflammation. Note that other causative relationships are possible and only those discussed in the text are shown.

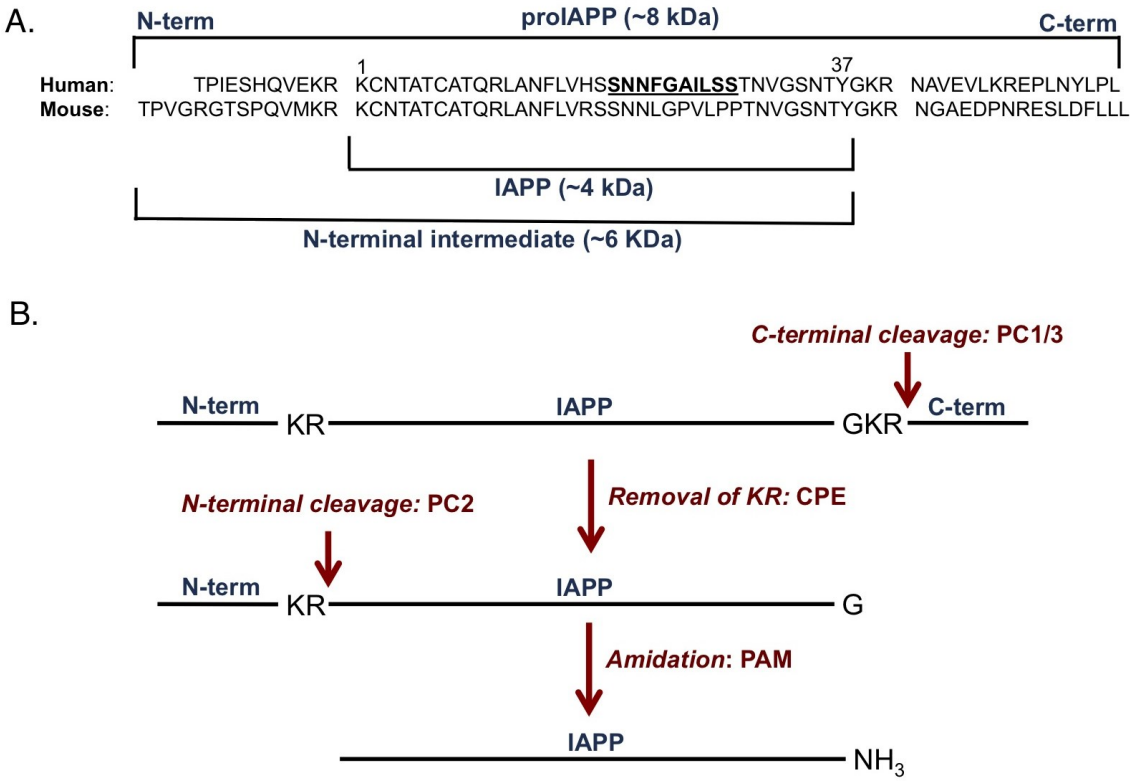

Figure 1.2. ProIAPP processing in beta cells. (A) Sequences of human and mouse proIAPP, the N-terminal intermediate produced during proIAPP processing, and mature IAPP. (B) Schematic of proIAPP processing. Prohormone convertase (PC) 1/3 cleaves proIAPP, followed by carboxypeptidase E- (CPE-) mediated removal of two basic C-terminal residues to produce an N-terminally extended intermediate. Subsequent cleavage by PC2 and amidation by peptidylglycine alpha-amidating monooxygenase (PAM) produces mature IAPP. Adapted from (232).

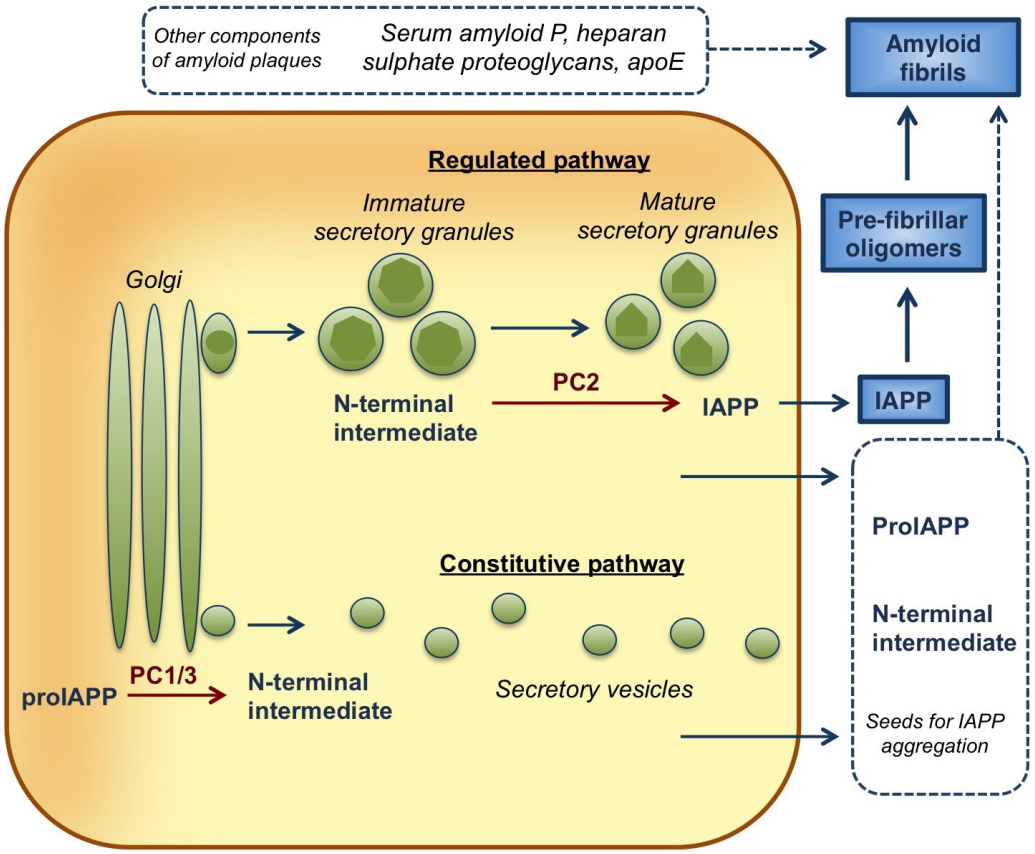

Figure 1.3. IAPP secretion and extracellular amyloid formation. Processing of proIAPP is initiated in the trans-Golgi, where PC1/3 cleaves the C-terminal end to produce an N-terminal intermediate. Constitutive IAPP secretion, which may be a more significant pathway under pathological conditions including high glucose, results in extracellular release of intact proIAPP and the N-terminally extended intermediate. Regulated secretion occurs in response to insulin secretagogues. PC2 cleaves the N-terminal intermediate in the secretory granule, which then releases mature IAPP along with small amounts of proIAPP and the N-terminally extended form, which may form a nucleus that acts as a seed for IAPP aggregation. Other components of amyloid deposits include serum amyloid P, heparan sulphate proteoglycans, and apolipoprotein E (apoE). Adapted from (230).

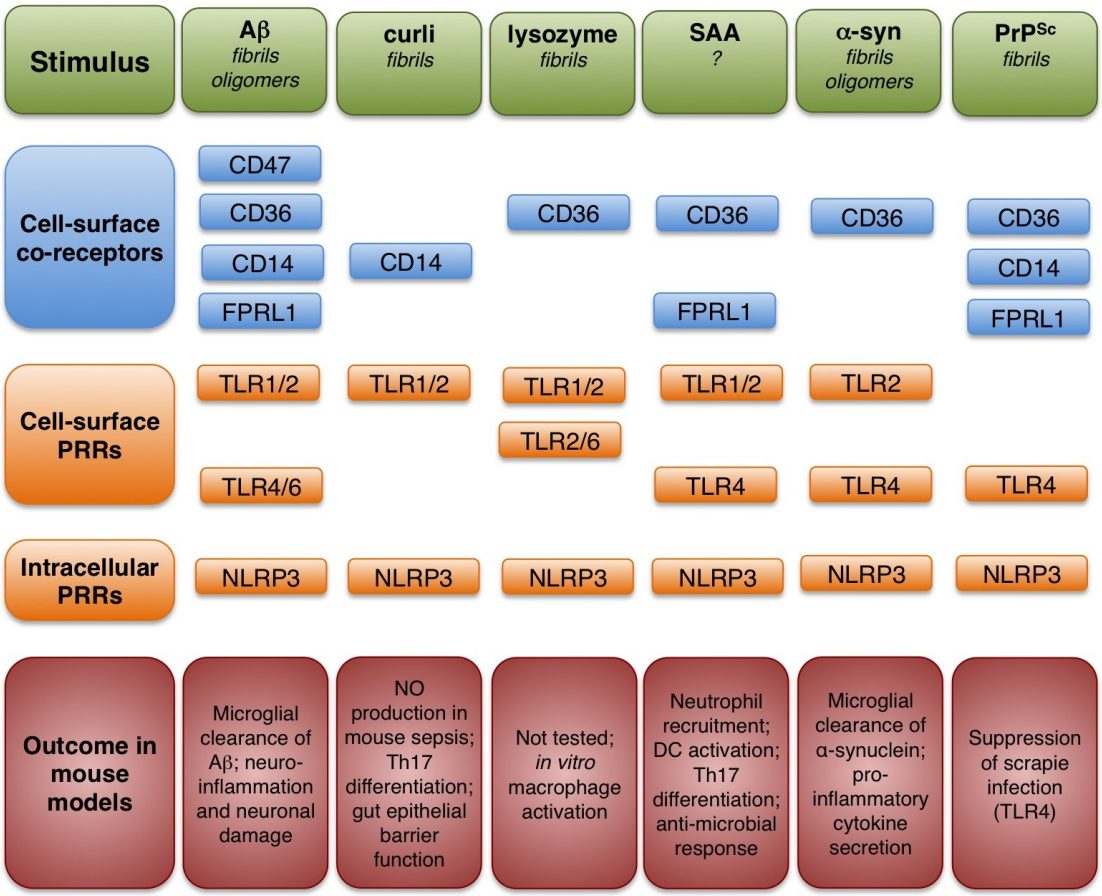

Figure 1.4. Current knowledge of PRRs involved in pro-inflammatory responses to amyloidogenic peptides. Multiple peptides in either fibrillar or pre-fibrillar oligomeric form (green boxes) interact with cell-surface scavenger receptors or TLR co-receptors (blue boxes) leading to enhanced phagocytic uptake and/or pro-inflammatory cytokine secretion. The exact nature of the pro-inflammatory species is not known, but multiple amyloidogenic peptides induce TLR1/2, TLR2/6, TL4, and NLRP3 (orange boxes). The outcome of genetic TLR, MyD88, or NLRP3 deficiency in mouse models of disease (red boxes) appears to depend on the stage of disease and the relative contribution of the signalling pathway to aggregate clearance vs. pro-inflammatory cytokine-induced tissue damage.

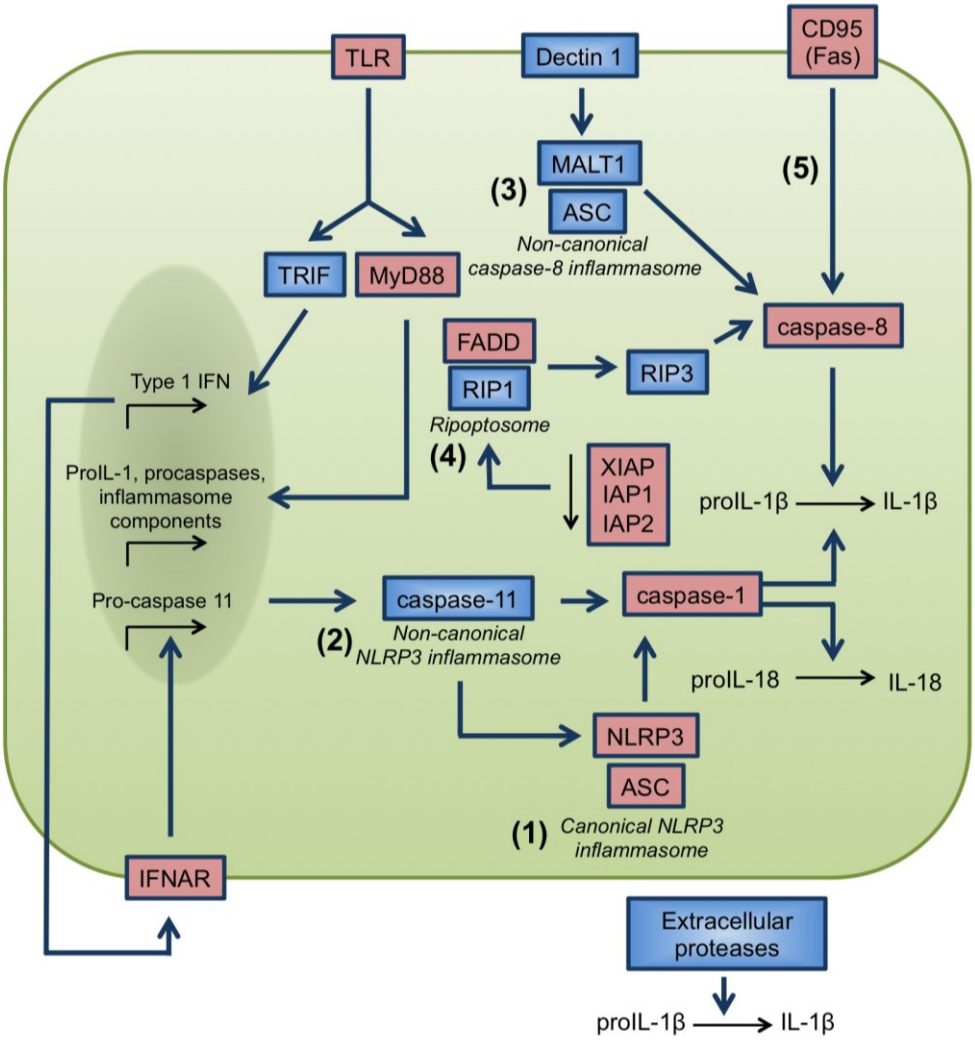

Figure 1.5. Mechanisms of proIL-1β processing. Components implicated in the response to amyloidogenic peptides are shown in red (note that some may be cell-type-specific). Signalling to NF-κB downstream of TLRs or cytokine receptors leads to synthesis of proIL-1 and increased expression (and/or post-translational modification) of inflammasome components. (1) The canonical NLRP3 inflammasome is a cytosolic complex comprised of the sensor NLRP3, the adaptor protein ASC, and caspase-1, which cleaves proIL-1β into its mature form. (2) The IFN-activated caspase-11-induced non-canonical NLRP3 inflammasome is triggered by Gram-negative bacteria and may involve caspase 11-mediated fusion of lysosomes to phagosomes and leakage of bacterial mRNA into the cytoplasm to activate NLRP3. (3) The non-canonical caspase-8 inflammasome consists of mucosa-associated lymphoid tissue lymphoma translocation protein 1 (MALT1), caspase 8, and ASC and is formed in response to stimulation of the lectin receptor dectin-1. Caspase-8 cleaves proIL-1β. (4) The formation of the ripoptosome – consisting of Fas-associated death domain protein (FADD) and receptor-interacting protein 1 (RIP1) – occurs with downregulation of inhibitor of apoptosis proteins (IAPs) and also activates caspase-8. (5) TNF receptor (TNFR) family members such as CD95 (Fas) also activate caspase-8 leading to proIL-1β cleavage. Reviewed in (408).

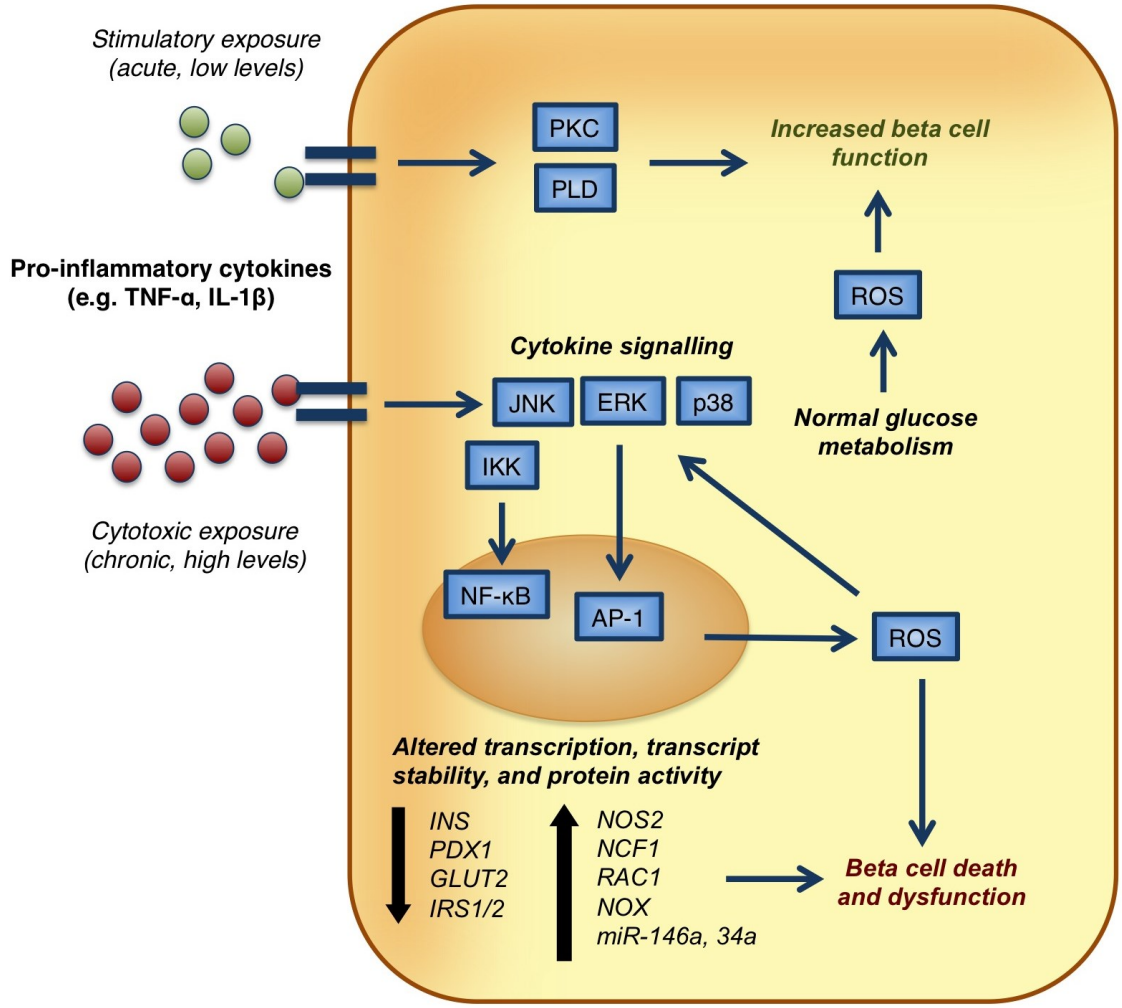

Figure 1.6. Consequences of beta cell exposure to pro-inflammatory cytokines. Short-term exposure to low concentrations of IL-1 can stimulate beta cell insulin secretion via activation of phospholipase D (PLD) and protein kinase C (PKC) signalling pathways. Chronic exposure to high levels of pro-inflammatory cytokines impairs beta cell function by altering transcription, translation, and protein activity. IL-1 and TNF-α signalling initiated by activation of MAPKs and IκB/NF-κB signalling can directly decrease expression of genes required for optimal glucose sensing and insulin secretion. Induction of reactive oxygen species (ROS) leads to subsequent oxidative damage to proteins and nucleic acids. Adapted from (392) and (453).

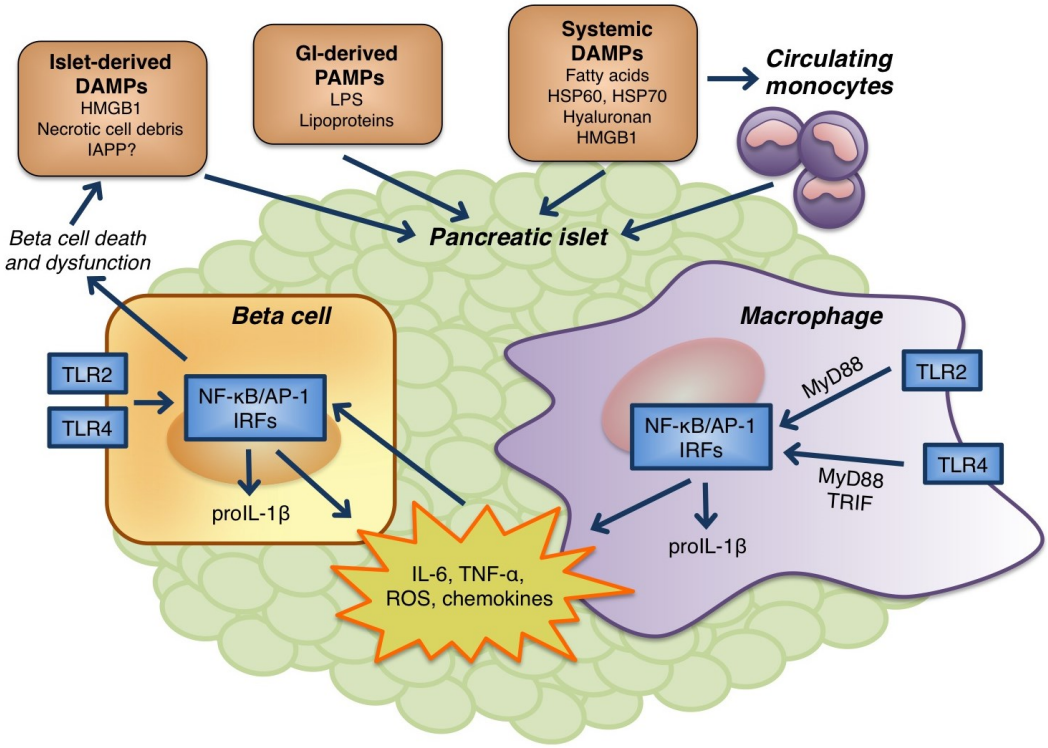

Figure 1.7. Proposed mechanisms of TLR-induced islet inflammation. Systemic stimuli for TLR2 and TLR4 are increased in type 2 diabetes and include microbe-derived PAMPs such as LPS and lipoproteins and endogenous DAMPs such as the heat shock proteins HSP60 and HSP70, high mobility group box-1 (HMGB1), hyaluronan, and saturated fatty acids. Local islet-derived TLR2 and/or TLR4 stimuli may include HMBG1, necrotic cell debris, and IAPP deposits. These endogenous ligands act on islet cells to induce secretion of pro-inflammatory cytokines and chemokines that may recruit monocytes. Recruited monocytes/ macrophages activated by systemic or islet-derived PAMPs and DAMPs may subsequently contribute to impaired beta cell insulin secretion. Chapter 3 of this thesis evaluates the capacity of IAPP to activate TLRs in islets and macrophages.

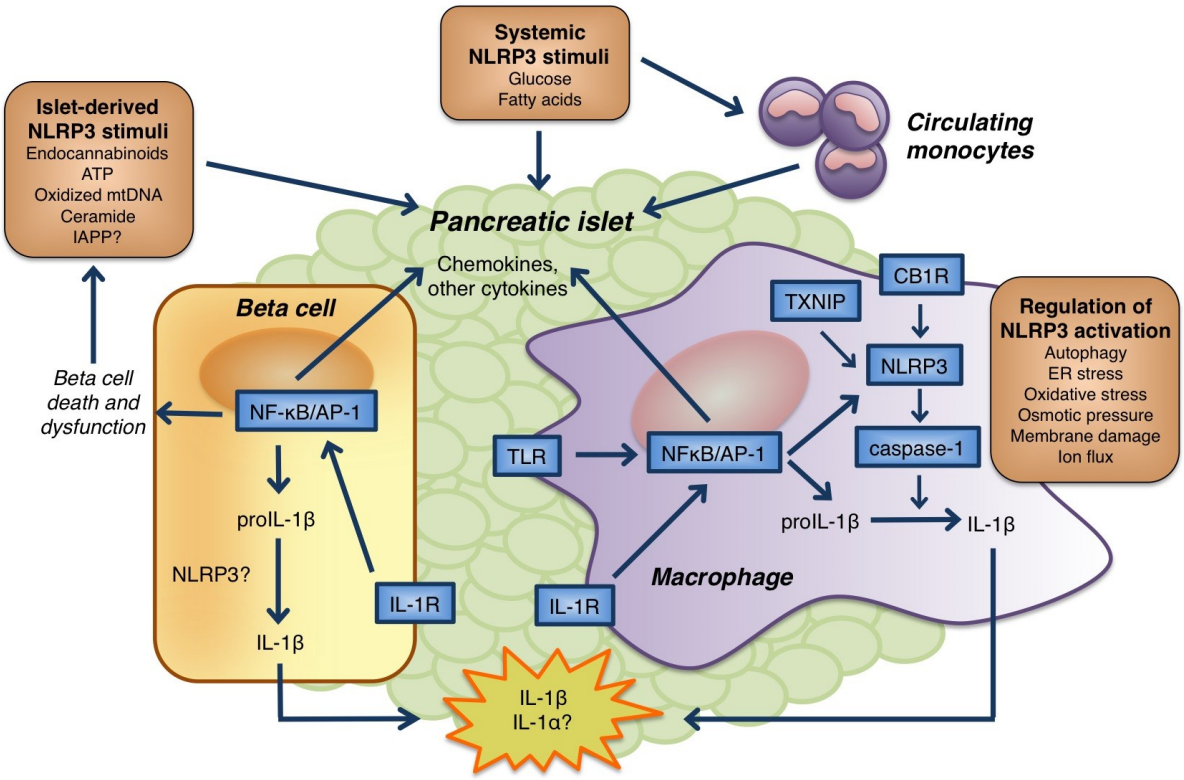

Figure 1.8. Proposed mechanisms of NLRP3-induced islet inflammation. NLRP3 stimuli are increased systemically and locally within islets in type 2 diabetes. These agents act on beta cells (e.g. glucose, fatty acids) and macrophages (e.g. endocannabinoids) to induce secretion of mature IL-1β causing beta cell dysfunction and death. NLRP3 activation may also be modulated by other islet-derived stimuli (e.g. ATP, oxidized mitochondrial DNA, ceramide) or cellular processes (e.g. impaired autophagy, ER stress, oxidative stress, osmotic pressure, membrane damage, and ion flux). IL-1β also acts in a paracrine manner on beta cells and macrophages to induce chemokine production and the secretion of other pro-inflammatory cytokines (e.g. IL-6 and TNF-α). Chapters 3-5 of this thesis examine the ability of IAPP to induce islet IL-1 synthesis and evaluate the consequences for glucose homeostasis in rodent models of amyloid formation.

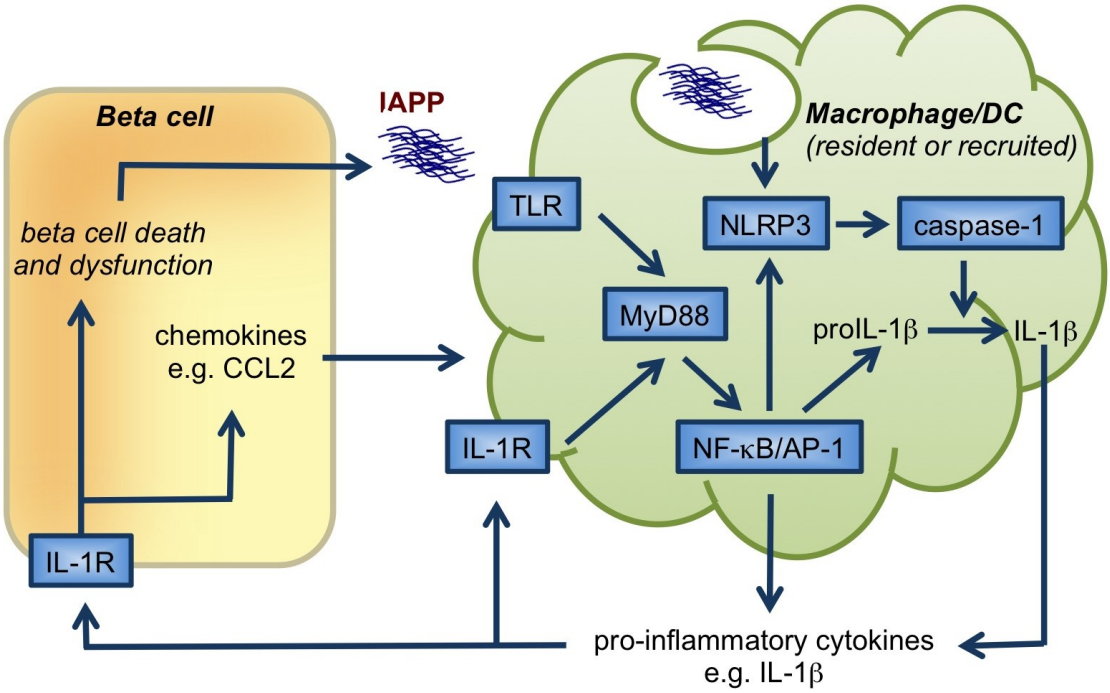

Figure 1.9. Schematic of hypothesis. IAPP secreted by beta cells aggregates to form fibrils in type 2 diabetes. Intermediate aggregates may interact with TLRs expressed by macrophages to induce release of IL-1β, which when present chronically at high concentrations impairs beta cell function. Macrophages may be resident within the islet or recruited by hIAPP-induced chemokines.

Chapter 2: Materials and Methods

2.1 Animals

2.1.1 Rodents

Mouse strains are described in Table 2.1. All strains were initially purchased from The Jackson Laboratory (Bar Harbour, ME). Mice were bred in-house to generate experimental animals and littermate controls, with the exception of the NOD/SCID mice used in transplant experiments, which were used 2-4 weeks after arrival from The Jackson Laboratory. FVB/N-Tg(Ins2-IAPP)RHFSoel/J mice have been described previously (210) and were maintained as hemizygotes (hIAPP$^{Tg/o}$) by breeding of female hIAPP$^{Tg/o}$ mice with male wild-type FVB mice.

Female FVB mice were used in high fat feeding experiments (Chapter 4) as they have no detectable metabolic phenotype up to 24 weeks of age and develop mild hIAPP-induced glucose intolerance after 12-14 weeks on high fat diet (HFD; see below), allowing comparison of normoglycemic mice on a normal chow diet (NCD) with mildly hyperglycemic HFD-fed mice and analysis of early islet dysfunction. No thioflavin-S-positive amyloid deposits can be detected in female FVB hIAPP$^{Tg/o}$ mice, although isolated islets develop amyloid after 4 days of culture at 22 mM glucose (Figure 3.13A), providing an *ex vivo* model of amyloid formation.

To generate hIAPP$^{Tg/o}$ mice and wild-type littermate controls with an agouti viable yellow allele (A^{vy}) at the agouti locus, female hIAPP$^{Tg/o}$ mice were crossed with male B6.C3-A^{vy}/J mice as described previously (194). Male A^{vy}-hIAPP$^{Tg/o}$ mice were employed in experiments to evaluate the role of islet macrophages (Chapter 4) and IL-1 (Chapter 5) in amyloid formation, as they develop extensive islet amyloid by 24 weeks of age (Figure 5.1). Agouti allele status was inferred based on coat colour (i.e. phenotype); only mice with a yellow coat colour (associated with obesity and insulin resistance) were designated A^{vy}-hIAPP$^{Tg/o}$ or A^{vy}-WT. Mice were designated *a*-hIAPP$^{Tg/o}$ or *a*-WT based on brown coat colour; this group includes mice with epigenetic silencing of the A^{vy} allele (454).

Homozygous hIAPP transgenic Sprague-Dawley rats from transgenic Line 9 generated by Butler *et al.* (455) were obtained from Pfizer (New York, NY). Transgenic rats were bred with wild-type Sprague-Dawley rats obtained from the Centre for Disease Modelling (University

of British Columbia, Vancouver, BC) to generate hemizygous hIAPP$^{Tg/o}$ rats and wild-type littermates, which were maintained for islet isolation and culture experiments.

2.1.2 Diets

Mice and rats were maintained on normal chow diet (NCD, 13 kcal% fat, PicoLab Rodent Diet 20-5053, Lab Diet, St. Louis, MO). For high fat feeding, FVB mice were maintained on high fat diet (HFD, 45 kcal% fat; D12451, Research Diets, New Brunswick, NJ). Breeder pairs and pups prior to weaning were maintained on PicoLab Mouse Diet 20-5058 (22 kcal% fat; Lab Diet).

2.1.3 Ethics

Mice and rats were maintained in compliance with Canadian Council on Animal Care guidelines. Studies were approved by the University of British Columbia Committee on Animal Care under current protocols A11-0202 (Breeding), A12-0260 (Amyloid-induced islet inflammation and beta cell dysfunction), A12-0049 (Processing of proIAPP: role in islet amyloid formation), and A11-0419 (Islet amyloid and transplant failure).

2.2 Cell culture

2.2.1 Bone marrow-derived macrophages

To generate bone marrow-derived macrophages (BMDMs), bone marrow was flushed out of mouse femurs and plated in DMEM supplemented with 100 U/ml penicillin, 100 µg/ml streptomycin, 2 mM GlutaMAX™, 1 mM sodium pyruvate, and 10% fetal bovine serum (FBS; all from Invitrogen, Burlington, ON). Freshly-thawed L929-conditioned media (AbLab, Biomedical Research Centre, UBC) was passed through a 0.2 µm filter to remove precipitate and added to media at 15% v/v immediately prior to use. After 24 h, non-adherent cells were transferred to 10 cm tissue culture plates and incubated for 7 days, with addition of fresh media on days 3 and 6. Alternatively, cells were transferred to 6-well plates for experiments requiring subsequent preparation of protein lysates. Adherent BMDMs were detached by incubation with phosphate-buffered saline (PBS) containing 1 mM ethylenediaminetetraacetic acid (EDTA) for 3

min at 37°C followed by gentle pipetting and plated at a density of 100,000 cells per well of a 96-well plate. After 24 h, cells were starved of L929 media for 10-12 h prior to each experiment.

2.2.2 THP-1 cells

THP-1 monocytes (ATCC TIB-202, passages 5-15) were maintained in suspension culture in RPMI 1640 medium supplemented with 100 U/ml penicillin, 100 µg/ml streptomycin, 2 mM GlutaMAX™, 10 mM HEPES, 1 mM sodium pyruvate, and 10% FBS.

2.2.3 RAW 264.7 cells

RAW 264.7 macrophages (ATCC TIB-71, passages 11-16) were maintained in high-glucose DMEM supplemented with 10% FBS, 2 mM GlutaMAX™, and 1 mM sodium pyruvate. For passaging, cells were removed from plates by gentle pipetting in PBS.

2.2.4 MIN6 cells

MIN6 cells (gift from Francis Lynn, UBC, passages 30-40) were maintained in high-glucose DMEM supplemented with 10% FBS, 2 mM GlutaMAX™, and 1 mM sodium pyruvate. For passaging, cells were removed from plates by 5 min incubation with 0.05% trypsin-EDTA at 37°C.

2.2.5 HEK 293 reporter cells

HEK 293 cells co-transfected with mouse TLR2/CD14 or human TLR2/CD14, TLR3, TLR4/CD14, TLR7, or TLR9 and an NFkB/AP-1 SEAP reporter construct were purchased from InvivoGen (San Diego, CA). The parental cell lines, Null1 and Null2, were transfected only with the reporter construct. HEK 293 cells express endogenous TLR1, TLR3, TLR5, TLR6, and NOD1. Cells were maintained in high-glucose DMEM supplemented with 2 mM GlutaMAX™, 10% FBS, 50 U/ml penicillin, 50 µg/ml streptomycin, 100 µg/ml Normocin, and additional antibiotics as per the manufacturer's instructions (TLR2 and TLR4: HEK Blue Selection, a proprietary mixture of Blasticidin, Hygromycin, and Zeocin; TLR3: 30 µg/ml Blasticidin and 100 µg/ml Zeocin; TLR7 and TLR9: 10 µg/ml Blasticidin and 100 µg/ml Zeocin). Secreted alkaline phosphatase activity was measured in cell supernatants using QUANTI-Blue™

detection media (Invivogen) according to the manufacturer's instructions. For passaging, cells were removed from plates by gentle pipetting with PBS.

2.2.6 Assays for viability and cell death

To evaluate mitochondrial activity, supernatants were replaced with fresh media containing 9% Alamar Blue (Invitrogen). BMDMs were incubated for 4-6 h and fluorescence was quantified on a Fluoroskan Ascent Reader (excitation 530 nm; emission 590 nm; Thermo Fisher Scientific, Waltham, MA). To evaluate apoptotic death, BMDMs were fixed in 10% formalin (Anatech, Battle Creek, MI) and stained with terminal deoxynucleotidyl transferase dUTP nick end labelling (TUNEL; Roche Diagnostics, Laval, QC) according to the manufacturer's instructions. TUNEL positivity and the number of cells per 10× objective field were determined using an ArrayScan VTI HCS reader (Thermo Fisher Scientific, Waltham, MA). To assess loss of cell membrane integrity, lactate dehydrogenase (LDH) in cell supernatants was quantified with a colorimetric LDH assay according to the manufacturer's instructions (G-Biosciences, St. Louis, MO).

2.3 Islet isolation and culture

2.3.1 Murine islet isolation

Mouse and rat islets were isolated by ductal collagenase injection and filtration as described previously (456). Mice were anesthetized with isofluorane and euthanized by cervical dislocation. Pancreata were perfused via the pancreatic duct with collagenase (1000 U/ml, type XI, Sigma) dissolved in Hank's Balanced Salt Solution (HBSS; Gibco), then kept on ice until further digestion. Pancreata were incubated at 37°C for 13-15 min, then shaken by hand to disrupt the pancreas until the solution became homogeneous. Digestion was stopped by addition of HBSS with 1 mM $CaCl_2$ on ice. Islets were washed and purified by filtration using a 70 μm nylon cell strainer. Islets were hand-picked and cultured overnight to allow recovery, unless otherwise stated. Islet yield from A^{vy}-hIAPP$^{Tg/o}$ mice with significant amyloid deposition was reduced by ~50% compared to that of wild-type controls; otherwise there was no difference in the islet yield among strains and treatment groups compared in these studies.

2.3.2 Murine islet culture

Islets were maintained at 37°C with 5% CO_2 in RPMI 1640 supplemented with 100 U/ml penicillin, 100 µg/ml streptomycin, 2 mM GlutaMAX™, and 10% FBS. For analysis of cytokine and chemokine release, islets were incubated overnight prior to the start of each experiment. Where required, consistency in islet size and number was verified by comparison of Alamar Blue reduction among treatments at the end of each experiment. Following culture, islets were washed and lysed for RNA or protein isolation, dispersed for flow cytometric analysis, or fixed in 10% formalin and preserved in agar prior to paraffin processing for immunohistochemistry.

2.3.3 Human islet culture

Human islets were obtained at 22°C in CMRL-1066 from the Ike Barber Human Islet Transplant Laboratory (Vancouver General Hospital, Vancouver, BC). Prior to experiments, islets were cultured overnight at 37°C with 5% CO_2 in CMRL-1066 (Gibco) supplemented with 100 U/ml penicillin, 100 µg/ml streptomycin, 50 µg/ml gentamycin, and 2 mM GlutaMAX™.

2.4 Peptides and inhibitors

Synthetic hIAPP and rIAPP (Bachem, Torrance, CA) were dissolved in hexafluoro-2-propanol, lyophilized, and stored at -20°C. Immediately prior to each experiment, IAPP was dissolved in 0.1 M acetic acid and diluted in culture media. Neither rIAPP nor hIAPP induced NF-κB activation in TLR4-expressing HEK 293 cells, evaluated as described in Section 2.2, suggesting minimal endotoxin contamination. Inhibitors described in Table 2.2 or antibodies described in Table 2.4 were added to BMDMs, HEK 293 cells, or islets 1 h prior to treatment with IAPP.

2.5 Thioflavin assays

To assess amyloid fibril formation, IAPP aggregation was monitored by thioflavin T fluorescence as described previously (229). Peptide was dissolved in DMEM containing 10 µM thioflavin T. Fluorescence emission was evaluated on a Fluoroskan Ascent reader (excitation 444 nm; emission 485 nm). For detection of hIAPP aggregates in cultured cells, BMDMs were grown on chamber slides coated with poly-L-lysine (Sigma). Cells were fixed in 10% formalin for 20

min, permeabilized with 0.2% TritonX-100 at room temperature for 5 min, and stained with 0.01% w/v thioflavin S for 10 min at room temperature followed by three washes in 70% ethanol. Cells were wet-mounted using Vectashield mounting medium with DAPI (Vector Laboratories, Burlingame, CA) and visualized on a BX61 microscope (Olympus, Center Valley, PA). Image analyses, including deconvolution of *z*-stacks, was performed using Image-Pro software (MediaCybernetics, Bethesda, MD).

2.6 Analyses of cytokine and chemokine secretion

2.6.1 Multiplexed analysis

Cell culture media was centrifuged following collection to remove debris and supernatants were stored at -80°C prior to analysis. An array of 12 cytokines and chemokines (CCL2, CCL3, CCL4, CCL5, CXCL1, CXCL2, CXCL10, IL-1α, IL-1β, IL-6, TNF-α, IL-12p70) was assessed by multiplex assay (Millipore, Bedford, MA) and analyzed on a Luminex-100 system according to the manufacturer's instructions (Luminex Corporation, Austin, TX).

2.6.2 Enzyme-linked immunosorbent assay

For single cytokine analysis in BMDM and islet supernatants, TNF-α, IL-1β, and CCL2 levels were determined by enzyme-linked immunosorbent assay (ELISA) according to the manufacturer's instructions (eBioscience, San Diego, CA, or BioLegend, San Diego, CA). To evaluate the IAPP species required for IL-1 secretion, BMDMs were treated with a priming stimulus for 3 h to induce proIL-1β synthesis. Cells were then exposed to an NLRP3 activator for 1-16 h. ATP (5 mM; MP Biomedicals, Santa Ana, CA) was used as a positive control for NLRP3 activation. IL-1β in cell supernatants was measured by ELISA according to the manufacturer's instructions (BioLegend).

2.7 Chemotaxis assay

Human islets were plated in CMRL-1066 at a density of 200 islets per well of a 24-well plate and treated with IAPP as indicated (Figure 3.12). Supernatants were centrifuged to remove debris and stored at -80ºC until analysis. Thawed supernatants were diluted 1:1 with RPMI 1640 and 275 µl was added to the bottom chamber of a 96-well Transwell plate (Corning Incorporated,

NY). THP-1 monocytes were suspended at a concentration of 1×10^6 cells/ml in RPMI containing 0.1% bovine serum albumin (BSA) and 70 µl of the suspension was added to the upper chamber of the Transwell plate. After 4 h, the media in the bottom wells were collected and the number of cells was determined by analyzing each sample on a flow cytometer for 15 s and interpolating from a standard curve. The chemotactic index was the ratio of the concentration of migrated cells in the test sample to that in the media control, since in preliminary experiments IAPP alone did not induce monocyte chemotaxis.

2.8 Gene expression analyses

2.8.1 Global gene expression

C57BL/6 BMDMs were treated with hIAPP or rIAPP for 12 h. RNA was isolated using an RNeasy mini kit (Qiagen Inc., Mississauga, ON) and quality was assessed using an Agilent 2100 BioAnalyzer (Agilent Technologies, Santa Clara, CA). All samples had RNA integrity number scores >9.2. Global gene expression was evaluated with an Illumina MouseRef-8 v2 Expression Bead Chip with an Illumina BeadStation 500GX BeadArray Reader (Illumina Inc., San Diego, CA). Data were analyzed with Bead Studio software using rank-invariant normalization. Only transcripts with detection and differential expression *p*-values < 0.05 were included in the analysis. Differentially-expressed genes (absolute fold-difference > 1.5) were uploaded to the Database for Annotation, Visualization and Integrated Discovery (DAVID) functional clustering tool (34). Functional annotation analysis was used to evaluate overrepresentation of biological pathways based on Gene Ontology (GO) terms and Kyoto Encyclopedia of Genes and Genomes (KEGG) pathways. Data were also uploaded to InnateDB (457) for transcription factor binding site overrepresentation analysis (using the CisRED database) and pathway overrepresentation analysis using the KEGG, Integrating Network Objects with Hierarchies (INOH), and Reactome databases. The significance of over-represented terms was determined by a Benjamini *p*-value to correct for multiple comparisons. Array data were deposited in NCBI's Gene Expression Omnibus database as series GSE23534 (http://www.ncbi.nlm.nih.gov/geo/query/acc.cgi?acc=GSE23534).

2.8.2 RNA isolation

RNA was isolated with a Purelink RNA micro kit (Invitrogen) according to the manufacturer's instructions. For analysis of islet gene expression without *in vitro* treatment, islets were allowed to recover for 4 h following isolation prior to lysis, unless otherwise stated.

2.8.3 Reverse transcription quantitative PCR

Synthesis of cDNA was performed using 100-400 ng RNA and a qScript™ cDNA synthesis kit (Quanta Biosciences, Gaithersburg, MD) or a Superscript VILO™ cDNA synthesis kit (Invitrogen), both with a combination of oligo(dT) primers and random hexamers. Reverse transcription quantitative PCR (RT-qPCR) was performed using Power SYBR® Green PCR Master Mix or Fast SYBR® Green Master Mix (ABI, Warrington, UK). Reactions were run on an ABI 7500 Fast or Viia™ 7 Real-Time PCR System. Most primer sequences and cycle protocols were obtained from the public database PrimerBank (458) and are listed in Table 2.3. Differential expression was determined by the $2^{-\Delta\Delta CT}$ method (459) with *Gapdh* (Figure 3.3) or *Rplp0* (all other experiments) as the internal control.

Gene expression in islets isolated from 24-week-old A^{vy}-hIAPP$^{Tg/o}$ and control mice was assessed using a mouse Inflammatory Response and Autoimmunity array (SA Biosciences, Qiagen). Data were analyzed online using SA Biosciences RT^2 Profiler PCR Array Data Analysis version 3.5. Volcano plots were generated based on a *p*-value threshold of 0.05 (determined by Student's t-test) and a fold-change threshold of 2.

2.9 Western blotting

For analysis of IL-1β protein expression (Figure 4.6), BMDMs and islets were treated with IAPP as indicated, rinsed with ice-cold PBS, and lysed on ice with radioimmunoprecipitation assay (RIPA) buffer containing protease and phosphatase inhibitors (Cell Signaling Technology, Danvers, MA). For analysis of IAPP, PC1/3, and PC2 expression, MIN6 cells (Figure 5.13) or islets (Figure 5.14) were treated with recombinant IL-1β (eBioscience, San Diego, CA) for 24 h prior to lysis. Protein concentration in lysates was quantified by bicinchoninic acid (BCA) assay according to the manufacturer's instructions. Lysates were diluted in Laemmli buffer and loaded into 15% tris-tricine gels for detection of

IAPP; 4-20% tris-glycine gradient gels (Bio-Rad Laboratories, Mississauga, ON) for detection of IL-1; or 12% gels for detection of IL-1, PC1/3, and PC2. Proteins were separated by SDS-PAGE and blotted onto nitrocellulose. Blots were blocked with 5% skim milk for 2 h at room temperature and incubated overnight with primary antibody at 4°C in 5% skim milk, as indicated in Table 2.5. HRP-conjugated secondary antibodies (1:10,000; GE Healthcare, Baie d'Urfe, QC) were applied for 1 h at room temperature. Blots were incubated with electrochemiluminescent substrate (BioRad) and exposed to X-ray film. Band densitometry was performed with ImageJ (460).

2.10 Islet transplantation

Islets were isolated from 12- to 16-week-old hIAPP$^{Tg/o}$ mice or wild-type FVB littermate controls and allowed to recover overnight prior to transplantation. Eleven-week-old male NOD/SCID islet transplant recipients were rendered hyperglycemic by a single intraperitoneal (i.p.) injection of 200 mg/kg streptozotocin (Sigma) in citrate buffer. Recipient mice were transplanted with 150 islets into the left renal subcapsular space 4 days after streptozotocin injection, when blood glucose levels were between 20-30 mmol/L. Animals were monitored for non-fasting tail vein blood glucose levels using a glucometer (OneTouch, Burnaby, BC), daily for one week following transplantation and twice weekly for the rest of the experiment. After evaluation of glucose tolerance 8 weeks following transplantation, removal of the islet graft-bearing kidney was performed to rule out effects of residual pancreatic islet function. All mice included in our analyses returned to hyperglycemia within 24 h. Grafts were fixed in 10% formalin and embedded in paraffin for histology.

2.11 IL-1Ra administration

2.11.1 Islet transplant recipients

One day prior to transplantation, NOD/SCID recipient mice were implanted subcutaneously with an ALZET mini-osmotic pump (Durect Corporation, Cupertino, CA) containing PBS or IL-1Ra (anakinra), released at a continuous dose of 100 mg/kg per day. Pumps were replaced every two weeks for a total of eight weeks of IL-1Ra treatment.

2.11.2 Agouti viable yellow mice

Sixteen-week-old male A^{vy}-hIAPP$^{Tg/o}$ mice and control littermates were injected subcutaneously with 50 mg/kg per day IL-1Ra. The drug could not be sufficiently concentrated to allow for continuous release given the body weights of these mice. Metabolic testing was performed between 7-8 following the start of IL-1Ra treatment. After 8 weeks, a small piece of the tail of the pancreas was fixed in 10% formalin and embedded in paraffin for histology. Islets were isolated from the remaining pancreas, allowed to recover overnight, and lysed for RNA isolation and gene expression analysis.

2.12 Clodronate liposome-mediated macrophage depletion

2.12.1 Cultured islets

For *in vitro* macrophage depletion, isolated islets were treated with 1 mg/ml clodronate delivered in liposomes prepared with phosphatidylcholine and cholesterol (461) (ClodLip BV, Amsterdam, The Netherlands). Islets were washed three times after 24-36 h to remove residual liposomes and depletion of macrophages was verified by immunostaining and RT-qPCR (Figure 4.4).

2.12.2 Human IAPP transgenic mice

For *in vivo* macrophage depletion, female HFD-fed hIAPP$^{Tg/o}$ mice and wild-type FVB littermate controls (Figure 4.15, Figure 4.16) or male A^{vy}-hIAPP$^{Tg/o}$ mice and wild-type FVB×C57BL/6 littermate controls (Figure 4.18) were injected i.p. with 100 mg/kg clodronate in liposomes or PBS control liposomes every 4 days for 4 weeks, starting at 20 weeks of age.

2.13 *In vivo* metabolic testing

2.13.1 Glucose tolerance test

To assess glucose tolerance, mice were fasted for 4 h prior to i.p. injection with glucose at a dose of 0.75 g/kg (FVB mice), 1 g/kg (FVB×C57BL/6 mice), or 1.5 g/kg (NOD/SCID mice). Tail vein glucose was monitored at 0, 15, 30, 60, and 120 min by glucometer. Blood was collected from the saphenous vein at 0, 15, and 30 min for plasma insulin measurement by ELISA (ALPCO Diagnostics, Salem, NH).

2.13.2 Insulin tolerance test

To assess insulin sensitivity, mice were fasted for 4 h prior to i.p. injection with 0.5 U/kg (FVB) or 1 U/kg (FVB×C57BL/6) insulin (Novolin®ge Toronto; Novo Nordisk, Mississauga, ON). Glycemia was measured at 0, 15, 30, 60, and 90 min by glucometer.

2.14 *In vitro* analysis of glucose-stimulated insulin secretion

Glucose-stimulated insulin secretion in isolated islets was assessed as described previously (462). Isolated islets were pre-incubated in Krebs-Ringer bicarbonate buffer (KRB) supplemented with 10 mM HEPES, 0.25% BSA, and 1.67 mM glucose for two hours. Islets were transferred to fresh KRB buffer supplemented with either 1.67 or 16.7 mM glucose for 1 h, with a density of 20 islets per well of a 96-well plate. Islets and supernatants were collected from each well and stored at -80°C until further analysis. Islets were lysed with RIPA buffer and insulin content in media and islets was analyzed by ELISA (ALPCO Diagnostics). Insulin content was normalized to total protein content in islet lysates as determined by BCA assay.

2.15 Immunostaining

2.15.1 Immunohistochemistry

Formalin-fixed, paraffin-embedded sections (5 μm) from 2-3 areas of the pancreas or graft were deparaffinized and rehydrated. Antigen retrieval was performed as indicated in Table 2.6 in a vegetable steamer for 20 min. Sections were blocked with 10% normal serum (Vector Laboratories) or 0.25% casein (Protein Block; Dako) for 30 min. Primary antibodies were diluted according to Table 2.6 in 0.1% BSA in PBS and applied to sections overnight at 4°C or at room temperature (MafA and Pdx1). For nuclear staining, sections were permeabilized with 0.25% Triton-X100 (Sigma) for 15 min prior to blocking. Alexa 594 goat anti-guinea pig and Alexa 488 goat anti-rat secondary antibodies (1:100; Invitrogen) were applied for 1 h at room temperature. For thioflavin S staining, sections were incubated with 0.1% thioflavin S for 2 min followed by a brief wash in 70% ethanol. Slides were mounted using Vectashield mounting medium with DAPI (Vector Laboratories) and imaged on a BX61 microscope (Olympus, Center Valley, PA). Quantification was performed using Image-Pro software (MediaCybernetics, Bethesda, MD).

2.15.2 Immunocytochemistry

Cells were seeded in black 96-well clear-bottom plates and cultured as indicated. Cells were fixed with 10% formalin for 15 min at room temperature, permeabilized with 1% Triton X-100 for 15 min, and blocked using a commercial blocking solution optimized for HCS Arrayscan assays (Thermo Fisher Scientific, Waltham, MA). Cells were stained with rabbit anti-mouse NF-κB (1:230, Pierce) for 1 h followed by Dylight 549 goat anti-rabbit IgG (1:400, Pierce) and Hoechst (1 μg/ml) for 1 h. Staining was quantified using an ArrayScan VTI HCS reader and Molecular Translocation BioApplication Software Module (Thermo Fisher Scientific).

2.16 Flow cytometry

2.16.1 Conventional flow cytometry

Islets were dispersed in enzyme-free dissociation buffer (Invitrogen) and passed through a 70 μm nylon strainer. Cells were incubated with Fc block (1:50; eBioscience) for 10 min on ice. For analysis on Aria and Canto instruments (BD Biosciences, San Jose, CA), staining was performed for 30 min on ice with antibodies as described in Table 2.7. Cells were stained with fixable viability dye (1:1000; eFluor450 or 780, eBioscience) for 30 min and fixed with 2% formaldehyde prior to analysis. Gating was performed as in Figure 5.1.

2.16.2 Imaging flow cytometry

For image analysis using the ImageStream^X (Amnis Corporation, Seattle, WA), dispersed islet cells were incubated with 1 μg/ml Hoechst for 5 min at 37°C prior to staining with anti-CD11b antibodies as for conventional flow cytometry. For detection of caspase-1 activity, islets were incubated with FLICA 660-YVAD-FMK (1:30, ImmunoChemistry Technologies, Bloomington, MN) for the final hour of IAPP stimulation. For analysis of IL-1β content, cells were permeabilized with BD Cytofix/Cytoperm and incubated with rabbit anti-mouse total IL-1β (1:100; Santa Cruz Biotechnology, Dallas, TX) for 1 h followed by Alexa 488 goat anti-rabbit secondary antibody (1:100; Invitrogen).

2.16.3 Cell sorting

Dispersed islet cells were prepared as for conventional flow cytometry but without fixation. Sorting of $CD11b^{+}F4/80^{+}$ cells was performed on a FACSAria II cell sorter (BD Biosciences). Cells were collected into lysis buffer for subsequent RNA isolation (Purelink, Invitrogen).

2.17 Statistical analysis

Data were analyzed with Prism Version 5.0a (GraphPad Software Inc., La Jolla, CA) and are expressed as mean±SEM of the indicated number of trials or mean±SD of the indicated number of replicates, as described in figure legends. Differences between two groups were evaluated with a two-tailed t-test. Differences among three or more groups were evaluated with a one-way or two-way ANOVA and Bonferroni post-tests. For figures in which representative experiments are shown, data from other experiments showed the same statistically significant differences but with different absolute values due to variation in IAPP activity among lots of peptide. A p-value <0.05 was considered significant.

Table 2.1. Mouse strains and uses.

Strain name	Abbreviation	Jax strain	Studies
FVB/N-Tg(Ins2-IAPP)RHFSoel/J	hIAPP$^{Tg/o}$ (hemizygote)	008232	Islet culture for *in vitro* modelling of amyloid formation (Chapter 3); analysis of glucose homeostasis after HFD (Chapter 4); islet macrophage phenotyping (Chapter 4); response to clodronate treatment (Chapter 4)
FVB/NJ	FVB	001800	Breeding with hIAPP$^{Tg/o}$ mice to generate hemizygotes and wild-type littermate controls
B6.C3-*A^{vy}*/J	*A^{vy}*	000017	Breeding with hIAPP$^{Tg/o}$ mice to generate A^{vy}-hIAPP$^{Tg/o}$ mice and littermate controls for analysis of glucose homeostasis (Chapter 5), analysis of *in vivo* amyloid formation with clodronate treatment (Chapter 4); analysis of *in vivo* glucose homeostasis and amyloid formation with IL-1Ra treatment (Chapter 5)
C57BL/6J	C57BL/6	000664	Propagation of BMDMs for analysis of response to IAPP *in vitro* (Chapter 3); breeding with B6.C3-*A^{vy}*/J mice to maintain the strain; islet culture for IAPP treatment (Chapter 3); analysis of macrophage content (Chapter 4); analysis of IAPP processing (Chapter 5)
B6.129P2(SJL)-*Myd88$^{tm1.1Defr}$*/J	*Myd88$^{-/-}$*	009088	Propagation of BMDMs for analysis of response to IAPP *in vitro* (Chapter 3)
B6.129-Tlr2^{tm1Kir}/J	*Tlr2$^{-/-}$*	004650	Propagation of BMDMs and isolation of isletsfor analysis of response to IAPP *in vitro* (Chapter 3)
NOD.CB17-*Prkdc^{scid}*/J	NOD/SCID	001303	Islet transplant recipients treated with IL-1Ra or PBS (Chapter 5)

Table 2.2. Compounds tested for ability to inhibit IAPP-induced cytokine secretion *in vitro*.

Inhibitor	Source	Target	Concentration
Polymyxin B	Sigma	LPS lipid A	10 μg/ml
MyD88 inhibitory and control peptides	Imgenex[1]	Homodimerization of MyD88	100 μM
Z-YVAD-FMK	Sigma	Caspase-1	40 μM
Cytochalasin D	Sigma	Actin polymerization	5 μM
CA-074-Me	EMD Chemicals[2]	Cathepsin B	80 μM
Glibenclamide	Sigma	NLRP3 activation	200 μM
Bay 11-7082	Sigma	NF-κB and NLRP3 activation	5 μM
Congo Red	Sigma	IAPP aggregation and interaction with membranes	200 mM
IL-1Ra	Biovitrum AB[3]	type 1 IL-1R	4 μg/ml

[1]Imgenex Corp, San Diego, CA; [2]EMD Chemicals, Gibbstown, NJ; [3]Biovitrum AB, Stockholm, Sweden

Table 2.3. Primers used for RT-qPCR.

Gene	Sequence (5'-3'); forward(F), reverse (R)	Primer Bank Reference
Casp1	F: ACAAGGCACGGGACCTATG R: TCCCAGTCAGTCCTGGAAATG	6753282a1
Ccl2	F: TTAAAAACCTGGATCGGAACCAA R: GCATTAGCTTCAGATTTACGGGT	6755430a1
Ddit3	F: CTGGAAGCCTGGTATGAGGAT R: CAGGGTCAAGAGTAGTGAAGGT	31982415a1
Emr1	F: GCCCTGAACATGCAACCTG R: CTCCTCCACTAGATTCAAGTCCT	2078512a1
Gadph	F: AGGTCGGTGTGAACGGATTTG R: TGTAGACCATGTAGTTGAGGTCA	6679937a1
Hspa5	F: ACTTGGGGACCACCTATTCCT R:ATCGCCAATCAGACGCTCC	31981722a1
Iapp	F: CCACTTGAGAGCTACACCTGT R: GAACCAAAAAGTTTGCCAGGC	6754272a1
Il10	F: CCCATTCCTCGTCACGATCTC R: TCAGACTGGTTTGGGATAGGTTT	6680389a1
Il12b	F: TGGTTTGCCATCGTTTTGCTG R:ACAGGTGAGGTTCACTGTTTCT	6680397a1
Il18	F: GACTCTTGCGTCAACTTCAAGG R: CAGGCTGTCTTTTGTCAACGA	6680413a1
Il18bp	F: CCTACTTCAGCATCCTCTACTGG R: AGGGTTTCTTGAGAAGGGGAC	6754314a1
Il1a	F: CGAAGACTACAGTTCTGCCATT R: GACGTTTCAGAGGTTCTCAGAG	52669a1
Il1b	F: GCAACTGTTCCTGAACTCAACT R: ATCTTTTGGGGTCCGTCAACT	6680415a1
Il1rn	F: GCTCATTGCTGGGTACTTACAA R: CCAGACTTGGCACAAGACAGG	13624317a1
Il6	F: TAGTCCTTCCTACCCCAATTTCC R: TTGGTCCTTAGCCACTCCTTC	13624311a1
Ins1	F: CTCAGGTGGGAATATGGGAGT R: CACCGAGGCAAAAAGTGCTG	12850278a1
Ins2	F: GCTTCTTCTACACACCCATGTC R: AGCACTGATCTACAATGCCAC	6680463a1
Itgam	F: CCATGACCTTCCAAGAGAATGC R: ACCGGCTTGTGCTGTAGTC	132626288b1
Itgax	F: CTGGATAGCCTTTCTTCTGCTG R: GCACACTGTGTCCGAACTCA	10946646a1
Mafa	F: AGGAGGAGGTCATCCGACTG R: CTTCTCGCTCTCCAGAATGTG	23503735a1
Nlrp3	F: ATTACCCGCCCGAGAAAGG R: TCGCAGCAAAGATCCACACAG	22003870a1
Pcsk1	F: CTTTCGCCTTCTTTTGCGTTT R: TCCGCCGCCCATTCATTAAC	26335877a1
Pcsk2	F: AGAGAGACCCCAGGATAAAGATG R: CTTGCCCAGTGTTGAACAGGT	6679229a1
Pdx1	F: GAGGTGCTTACACAGCGGAA R: GGGGCCGGGAGATGTATTT	158518428c3
Pycard	F: CTTGTCAGGGGATGAACTCAAAA R: GCCATACGACTCCAGATAGTAGC	31560222a1
Rplp0	F: AGATTCGGGATATGCTGTTGGC R: TCGGGTCCTAGACCAGTGTTC	6671569a1
Tnf	F: CCCTCACACTCAGATCATCTTCT R: GCTACGACGTGGGCTACAG	7305585a1

Table 2.4. Antibodies used for neutralization experiments.

Target	Manufacturer
TLR2	Invivogen (mab-mtlr2)
TLR1	Invivogen (mabg-htlr1)
TLR6	Invivogen (mabg-htlr6)
CD14	Invivogen (maba-hcd14)
Isotype control (mouse IgG1κ)	BD Biosciences (554721)

Table 2.5. Antibodies used for western blotting.

Target	Manufacturer	Host	Concentration
IL-1β (total)	R&D Systems (AF-401-NA)	goat	1:4000
IL-1β (mature)	Novus (NBP1-42767)	rabbit	1:2000
β-actin	Sigma (A2228)	mouse	1:10,000
IAPP (total)	Bachem (4145)	rabbit	1:1000
PC1/3 ("Thumpa")	Gift from C. Rhodes University of Washington	rabbit	1:1000
PC2	Thermo Fisher Scientific (PIPA512199)	rabbit	1:1000

Table 2.6. Antibodies used for immunostaining.

Target	Manufacturer	Host	Concentration	Antigen retrieval
Insulin	Dako (A0565)	guinea pig	1:200	None
F4/80	Cedarlane (CL89170AP)	rat	1:75	Sodium citrate pH 6.0[1]
Pdx1	Abcam (ab47267)	rabbit	1:200	Tris-EDTA pH 9.0
MafA	Bethyl Laboratories (IHC-00352)	rabbit	1:200	Tris-EDTA pH 9.0
CCL2	Abcam (ab9669)	rabbit	1:100	Sodium citrate pH 6.0[1]
NF-κB (p65)	Thermo Fisher Scientific Pierce (PIPA516545)	rabbit	1:230	N/A (permeabilized with 1% Triton X-100)

[1]Dako Target Retrieval Solution

Table 2.7. Antibodies used for flow cytometry.

Target	Fluorochrome	Manufacturer	Concentration
CD11b	Alexa-700	eBioscience (56-0112-82)	1:150
CD11b	PE	eBioscience (12-1152-82)	1:200
F4/80	APC	eBioscience (17-4801-82)	1:200
CD11c	PerCPCy5.5	eBioscience (45-0114-82)	1:100
IL-1β	Unconjugated	Santa Cruz (sc-7884)	1:100
I-A/E	APC	eBioscience (17-5321-81)	1:200
I-A/E	PerCP-eFluor 710	eBioscience (46-5321-80)	1:200
Ly6C	BV 570	Biolegend (128029)	1:100

Chapter 3: IAPP Aggregates Induce Pro-inflammatory Cytokine Secretion by Islets and Macrophages

3.1 Background

Patients with type 2 diabetes are unable to secrete sufficient insulin to compensate for increased peripheral insulin resistance (463). Their pancreatic islets exhibit progressive beta cell loss (70), likely due in part to increased expression of pro-inflammatory cytokines (398,464), macrophage infiltration (401,418), and islet amyloid deposition (77). Similarly, immune cell infiltration and pro-inflammatory cytokine release impair beta cell function following islet transplantation (237), and isolated islets develop amyloid rapidly during pre-transplant culture (213) and following engraftment (214,216,217,465,466). Anti-inflammatory drugs such as IL-1Ra or anti-IL-1β mAbs can preserve beta cell function in type 2 diabetic patients (361,362,467) and in cultured human islets (397).

Aggregates of hIAPP share a common cross β-sheet structure with those of other amyloidogenic peptides known to induce a potent pro-inflammatory response. The structure of oligomeric and fibrillar peptide aggregates is discussed in Chapter 1.2. Peptides such as enterobacterial CsgA and mammalian Aβ, which forms amyloid plaques in Alzheimer's disease, induce TLR signalling in monocytes (304), providing one potential pathway for amyloid-induced pro-IL-1β synthesis (274,468). Figure 1.4 provides an overview of TLRs activated by other amyloidogenic peptides, as discussed in Chapter 1.3. Several such peptides, including Aβ, also promote proIL-1β cleavage (the second signal required for secretion of mature IL-1β) via activation of the NLRP3 inflammasome (315). We therefore hypothesized that hIAPP may contribute to islet inflammation by activating the same innate immune pathways leading to IL-1β secretion. To address this hypothesis, we first characterized the effects of hIAPP aggregation on cytokine release by BMDMs and chemokine release by islets. We next assessed the contribution of IL-1R and TLR signalling to hIAPP-induced inflammation and determined the form of IAPP aggregate required for the synthesis and secretion of IL-1β.

3.2 Results

3.2.1 IAPP promotes BMDM survival in the absence of M-CSF

To evaluate the effect of hIAPP on macrophage viability, BMDMs were treated with hIAPP or rIAPP (15 μM) in the absence of M-CSF for 12 h. Aggregated peptide was observed as thioflavin S staining of hIAPP- but not rIAPP-treated cells, often in association with cell membranes (Figure 3.1A). Interestingly, both hIAPP and rIAPP inhibited cell death associated with M-CSF deprivation as assessed by LDH release, with a reduction to 83±7% of the vehicle control for rIAPP and 62±3% for hIAPP after 12 h (Figure 3.1B). Similarly, IAPP protected against M-CSF deprivation-induced macrophage loss, with an average cell number per field of 175±26 for hIAPP and 80±14 for rIAPP compared to 57±2 in the control after 12 h (Figure 3.1C). Since both non-amyloidogenic rIAPP and amyloidogenic hIAPP improved macrophage survival during M-CSF deprivation, these data suggest that IAPP can provide a pro-survival signal to macrophages even in the absence of aggregation; however, the more dramatic effect of hIAPP compared to rIAPP suggests that peptide aggregation provides an additional survival stimulus, similar to pro-inflammatory agents such as LPS.

3.2.2 Functional annotation analysis of global gene expression reveals upregulation of pro-inflammatory pathways in macrophages treated with human vs. rodent IAPP

To determine whether hIAPP affects expression of genes associated with an innate immune response, we performed global gene expression analysis to compare expression profiles of hIAPP- and rIAPP-treated BMDMs after 12 h. Approximately 1000 genes were differentially regulated at least 1.5-fold in hIAPP- vs. rIAPP-treated BMDMs (319 were downregulated and 696 were upregulated with $p<0.05$). Functional annotation analysis using DAVID (469,470) revealed significant enrichment of GO terms and KEGG pathways (471) among genes that were differentially expressed in response to hIAPP. Twelve functional annotation clusters enriched more than two-fold were identified, representing pathways involved in angiogenesis, the inflammatory response, apoptosis, lysosomes, nucleotide binding, regulation of cytokine production, leukocyte activation, phagocytosis, and the response to hypoxia. Genes from significantly overrepresented pathways identified in DAVID are shown in Table 3.1.

Differentially expressed genes were also uploaded to InnateDB (457) for transcription factor binding site overrepresentation analysis (using the CisRED database) and pathway overrepresentation analysis using the KEGG, INOH, and Reactome databases. Genes from significantly overrepresented pathways identified in InnateDB are shown in Table 3.2. Only one transcription factor class, activating transcription factor (ATF), was significantly overrepresented following correction for multiple comparisons (p=0.013). Figure 3.2 highlights differentially expressed genes in the KEGG TLR signalling pathway, which was the mostly highly overrepresented KEGG pathway identified by both DAVID and InnateDB.

3.2.3 Human IAPP induces pro-inflammatory cytokine secretion by BMDMs

To explore further the cytokine profile of hIAPP-treated cells, we analyzed supernatants from BMDM cultures treated with hIAPP for 12 h (Figure 3.3A). hIAPP but not rIAPP induced significant levels of IL-1α (11.7±2.3 vs. <2.9 pg/ml), IL-1β (27.2±2.7 vs. 2.6±1.4 pg/ml), TNF-α (134±23 vs. 5.9±0.4 pg/ml), CCL2 (169±8 vs. 18±2 pg/ml), CXCL1 (522 ±110 vs. 91±23 pg/ml), CCL3 (6.96±2.21 vs. 0.10±0.01 ng/ml), CCL4 (4.97±1.41 vs. 0.08±0.01 ng/ml), CCL5 (7.6±5.9 vs. <3.0 pg/ml), and CXCL2 (5.95±0.64 vs. 1.92±0.25 ng/ml). A trend toward increased IL-6 was observed but did not reach statistical significance. Induction of mRNA encoding IL-1α, IL-1β, and TNF-α was confirmed by RT-qPCR (Figure 3.3B). hIAPP also induced nitric oxide production as determined by a six-fold elevation in nitrite levels in cell supernatants (Figure 3.3C).

Since the combination of TNF-α and IL-1β has well-characterized inhibitory effects on insulin secretion and at high concentrations promotes beta cell apoptosis (391), we chose to measure these cytokines in further mechanistic studies. TNF-α induction in BMDMs after 24 h by hIAPP was concentration-dependent (Figure 3.4A) and associated with increased cell viability (as measured by mitochondrial activity) relative to rIAPP-treated cells (181±5 vs.142±5% of the vehicle control, respectively; Figure 3.4B). No apoptotic death of hIAPP-treated BMDMs was observed at concentrations up to 15 μM after 24 h (Figure 3.4C). The LPS inhibitor polymyxin-B had no effect on hIAPP-induced TNF-α release (Figure 3.4D), suggesting that these effects were not due to endotoxin contamination.

3.2.4 Aggregation intermediates are required for induction of TNF-α and IL-1β

To determine which state of hIAPP fibrillogenesis is responsible for TNF-α and IL-1β induction, IAPP was dissolved in media and aggregation was monitored by thioflavin T fluorescence (Figure 3.5A). Thioflavins undergo a red shift in their emission spectra upon binding to β-sheet motifs present in fibrillar hIAPP aggregates (472). BMDMs were treated with freshly-dissolved (soluble) peptide or peptide that had been allowed to aggregate prior to the experiment. Maximal release of TNF-α (Figure 3.5B), IL-1α (Figure 3.5C), and IL-1β (Figure 3.5D) was observed with freshly-dissolved peptide presumably containing primarily pre-fibrillar aggregates (oligomers), whereas hIAPP that had been allowed to aggregate for 6 h prior to addition to BMDMs induced much smaller increases in cytokine levels (TNF-α: 260±43 vs. 968±235 pg/ml; IL-1α: <3.2 vs. 199±68 pg/ml; IL-1β: 160±22 vs. 451±127 pg/ml). Following 7 days of aggregation, induction of both IL-1α and IL-1β by hIAPP fibrils was even further reduced (Figure 3.5C,D). Consistent with these observations, TNF-α secretion induced by freshly-dissolved hIAPP did not follow the kinetics of LPS-induced release (Figure 3.5E), suggesting a mechanism distinct from immediate cell surface TLR activation and a delay in response until the pro-inflammatory species was formed. Furthermore, hIAPP-induced TNF-α release was almost completely inhibited by Congo red (Figure 3.5F), an inhibitor of IAPP fibril formation (473). Taken together, these data suggest that exposure of macrophages to intermediate hIAPP species is required for maximal cytokine secretion.

3.2.5 Pre-fibrillar and fibrillar hIAPP aggregates have distinct effects on the synthesis and secretion of IL-1β

Because secretion of mature IL-1β requires induction of proIL-1β synthesis (signal 1, which can be provided by TLR2 activation) and cleavage of proIL-1β (signal 2, which can be provided by NLRP3-induced caspase-1 activation), we next assessed the relative contributions of pre-fibrillar and fibrillar hIAPP aggregates to each of these processes. Amyloid fibrils were prepared by pre-incubation of hIAPP at 37°C for 16 h and confirmed to contain β-sheet structure by increased thioflavin T fluorescence (Figure 3.6A), which reaches a maximum within ~3 h in culture (Figure 3.5A). First, to determine the kinetics of hIAPP-induced IL-1β secretion following delivery of a distinct stimulus for proIL-1β, BMDMs were treated with LPS for 3 h

(signal 1) followed by rIAPP, freshly-dissolved hIAPP, or pre-aggregated hIAPP for 1 or 16 h (signal 2). BMDMs primed with LPS and then treated with freshly-dissolved or pre-aggregated hIAPP produced similar levels of IL-1β after 16 h (Figure 3.6B), suggesting that fibrillar hIAPP (also formed after ~3 h in cultures treated with freshly-dissolved hIAPP) is the primary stimulus for signal 2, i.e. NLRP3 activation and proIL-1β cleavage. Of note, neither form of hIAPP was able to induce IL-1β secretion after only 1 h of treatment, consistent with a mechanism for NLRP3 activation that requires more time than the response to ATP and may involve phagocytosis with subsequent lysosomal disruption (see below).

Second, we evaluated the capacity of rIAPP, hIAPP, and pre-aggregated hIAPP to induce IL-1β secretion when delivered in sequential combinations as both the priming and activation stimulus. BMDMs were treated with rIAPP, hIAPP, or pre-aggregated hIAPP as a priming stimulus (signal 1) for 3 h followed by 1 h (Figure 3.6C) or 16 h (Figure 3.6D) activation with one of the same three forms of IAPP to provide signal 2. BMDMs treated for 3 h with freshly-dissolved hIAPP but not rIAPP or pre-aggregated hIAPP provided a stimulus for subsequent ATP-induced IL-1β secretion (Figure 3.6C). When the 1 h activation period was increased to 16 h, both soluble and freshly-dissolved hIAPP stimulated IL-1β secretion in cells primed with hIAPP (Figure 3.6D). Cells exposed to additional freshly-dissolved hIAPP for 16 h produced 3.5-fold more IL-1β than those treated with pre-aggregated peptide, suggesting that pro-IL-1β synthesis or NLRP3 priming by soluble hIAPP may be the limiting factor for IL-1β secretion under these conditions, given that rapid aggregation of soluble hIAPP would lead to similar amounts of fibrillar peptide in each case. Delivery of soluble and fibrillar peptide in the opposite order (i.e. pre-aggregated hIAPP prior to freshly-dissolved hIAPP) resulted in two-fold less IL-1β, consistent with soluble aggregates being primarily responsible for priming and suggesting that the aggregation process generates stimuli in the optimal order for a maximal IL-1β response.

3.2.6 IAPP-induced TNF-α secretion by macrophages is dependent on MyD88 and amplified by IL-1R signalling

To determine whether the TLR and IL-1R adaptor protein MyD88 is involved in the macrophage response to hIAPP, we evaluated TNF-α induction in BMDMs from MyD88-deficient mice. hIAPP-induced TNF-α release was markedly attenuated in BMDMs lacking

MyD88 (0.13±0.01 vs. 5.27±0.69 ng/ml, Figure 3.7A). A specific peptide inhibitor of MyD88 homodimerization also reduced hIAPP-elicited TNF-α release in wild-type BMDMs from 3.66±0.28 to 1.68±0.53 ng/ml (Figure 3.7B). Because the IL-1R uses the adaptor protein MyD88, and IL-1 is known to induce TNF-α (474), we evaluated the effect of IL-1 signalling inhibition on hIAPP-induced TNF-α release. Inhibition of proIL-1β cleavage with a caspase-1 inhibitor and blockade of IL-1 signalling with IL-1Ra significantly attenuated hIAPP-induced TNF-α release (Figure 3.7C). To determine whether NLRP3 inflammasome signalling might be involved in caspase-1 activation leading to IL-1β secretion, we evaluated the effects of NLRP3 inflammasome inhibitors on hIAPP-induced IL-1β and TNF-α secretion (Figure 3.7D). Cytokine induction was significantly reduced by Bay 11-7082, an inhibitor of both NF-κB and the NLRP3 inflammasome (475), and by glibenclamide, an inhibitor of ATP-sensitive potassium channels that also blocks NLRP3 activation (476). Cytokine release was dependent on actin polymerization, since it was blocked by cytochalasin D. The potential requirement for phagocytosis is further supported by the significant over-representation of genes related to endosomes/phagosomes in our microarray study (Table 3.2). As described for other inflammasome activators, cytokine release was blocked by CA-074-Me, an inhibitor of the lyososomal enzyme cathepsin B. Thus, hIAPP can provide both signals required for IL-1β secretion, and autocrine or paracrine signalling by IL-1α or IL-1β appears to be at least partially responsible for amplification of TNF-α release.

3.2.7 hIAPP aggregation intermediates activate a TLR2/6 heterodimer

To determine whether the initial signal for induction of proIL-1β synthesis by hIAPP is provided by TLR activation, we next screened a panel of human TLR-expressing HEK 293 cells co-transfected with an NF-κB/AP-1 SEAP reporter construct. hIAPP induced NF-κB/AP-1 activation in HEK 293 cells expressing TLR2 and CD14 but not in the parental cell line or in cells expressing TLR3, TLR4 and CD14, TLR7, or TLR9 (Figure 3.8A). Freshly-dissolved hIAPP but not rIAPP or pre-aggregated fibrillar hIAPP was able to induce this response (Figure 3.8B), which was also observed in HEK 293 cells expressing mouse TLR2 and CD14 (Figure 3.8C). Because TLR2 can form heterodimers with either TLR1 or TLR6, both expressed endogenously by HEK 293 cells, we evaluated the effect of neutralizing antibodies targeting

TLR1, TLR2, and TLR6 on hIAPP-induced reporter activity. NF-κB/AP-1 activation was blocked in cells treated with anti-TLR2 or anti-TLR6 neutralizing antibody, suggesting that IAPP activates a TLR2/6 heterodimer (Figure 3.8D). Blockade of CD14, required for a maximal response to both the TLR1/2 ligand Pam_3CSK_4 and the TLR2/6 ligand FSL-1 (synthetic tri- and diacylated lipoproteins, respectively), did not significantly affect the response to hIAPP (Figure 3.8D), suggesting that this co-receptor is not required for hIAPP-induced TLR2 activation.

3.2.8 TLR2 is required for IAPP-induced NF-κB activation and cytokine secretion by macrophages

To determine whether TLR2 is required for hIAPP-induced pro-inflammatory cytokine secretion by macrophages, we assessed nuclear translocation of the NF-κB p65 subunit in BMDMs from wild-type and TLR2-deficient mice. p65 was observed in the nucleus of wild-type but not *Tlr2*$^{-/-}$ cells 1 h following treatment with hIAPP (Figure 3.9A,B). TLR2 deficiency also prevented IL-1β release in response to 3 h incubation with hIAPP (to induce proIL-1β synthesis) followed by 1 h treatment with ATP (to induce NLRP3 activation and IL-1β secretion; Figure 3.9C). Moreover, hIAPP-induced *Il1b, Tnf,* and *Il6* expression was significantly attenuated in BMDMs from *Tlr2*$^{-/-}$ mice (Figure 3.10A) and in RAW 264.7 cells treated with an anti-TLR2 neutralizing antibody (Figure 3.10B). Because hIAPP also induces the secretion of mature IL-1β after a longer time course of exposure (Figure 3.5E) and others have demonstrated NLRP3 activation by hIAPP (477), we next evaluated the requirement for TLR2 and its downstream adaptor protein MyD88 in hIAPP-induced cytokine and chemokine secretion over a 24 h time course without a second distinct stimulus for NLRP3. Both TLR2 and MyD88 were required for hIAPP-induced secretion of IL-1β, TNF-α, IL-6, CCL2, CCL3, CCL4, CCL5, CXCL1, and IL-10 (Figure 3.11). Thus, both hIAPP-induced TLR2 signalling and autocrine/paracrine amplification via IL-1Ra mediate the pro-inflammatory response to hIAPP in BMDMs.

3.2.9 hIAPP promotes islet chemokine release and monocyte recruitment

To determine whether hIAPP aggregation causes chemokine release from islets, we measured CCL2 and CXCL1 release by whole islets treated with rIAPP or hIAPP for 24 h. We found that both chemokines were markedly upregulated in response to hIAPP but not rIAPP

(Figure 3.12A). To evaluate directly monocyte chemotaxis *in vitro*, we assessed THP-1 cell migration in response to conditioned media from human islets treated with varying concentrations of synthetic IAPP. Media from hIAPP- but not rIAPP-treated human islets induced THP-1 cell chemotaxis, with a chemotactic index of 3.3±0.7 vs. 1.7±0.3 for media from islets treated with hIAPP (Figure 3.12C). These results are consistent with the hypothesis that chemokines produced by resident islet cells attract immune cells to sites of hIAPP aggregation.

To assess the effect of endogenously-produced hIAPP on CCL2 and CXCL1 release, we cultured islets from transgenic mice expressing hIAPP under the control of a beta cell-specific promoter. Male homozygous FVB/N-Tg(Ins2-IAPP)RHFSoel/J mice spontaneously develop diabetes by 8 weeks of age (210), whereas hemizygous animals ($hIAPP^{Tg/o}$) are phenotypically normal and do not develop detectable amyloid deposits (225). However, isolated hemizygous islets form extracellular amyloid deposits after 8 days of culture with high glucose (478). In our experiments, a small amount of thioflavin-S-positive material was also observed in islets cultured with 11 mM glucose for 7 days, but not in freshly isolated islets (Figure 3.13A). After 96 h in culture, we observed higher levels of CCL2 (288±45 vs. 170±34 pg/ml) and CXCL1 (1294±135 vs. 558±116 pg/ml) in supernatants from transgenic islets compared to wild-type littermate controls (Figure 3.13B). Consistent with the macrophage depletion experiments, immunostaining of cultured islets for CCL2 revealed co-localization of this chemokine with insulin (Figure 3.13C). These data suggest that hIAPP could trigger recruitment of macrophages to the site of aggregation by induction of beta cell chemokines. Addition of IL-1Ra to islet cultures reduced both basal and hIAPP-induced release of CCL2 and CXCL1 (Figure 3.13D), suggesting that blockade of IL-1 signalling may not only inhibit hIAPP-induced macrophage cytokine release but may also limit beta cell chemokine secretion and macrophage recruitment to islets, a hypothesis tested in Chapter 5.

3.2.10 TLR2 is required for maximal hIAPP-induced islet cytokine expression

Finally, we assessed the capacity of hIAPP to induce pro-inflammatory cytokine expression in cultured islets, which contain resident macrophages. Synthetic hIAPP caused upregulation of mRNA encoding the pro-inflammatory cytokines IL-1β and TNF-α in isolated islets after 4 h (Figure 3.14A). Expression of both IL-1β and TNF-α was reduced by

approximately 50% in islets from TLR2-deficient mice (Figure 3.14A). Expression of *Il1b* but not *Tnf* was also elevated in hIAPP$^{Tg/o}$ islets expressed after 7 days of culture at 22 mM glucose; both cytokines were significantly inhibited by anti-TLR2 neutralizing antibody (Figure 3.14B). Blockade of TLR2 also preserved insulin content in cultured hIAPP$^{Tg/o}$ islets (Figure 3.14C). Clodronate-liposome-mediated islet macrophage depletion (as confirmed by a decrease in *Itgam* expression) significantly reduced islet *Tnf* and *Il1b* expression (Figure 3.14D), suggesting that macrophages are the major source of these cytokines in both wild-type and hIAPP-expressing islets.

3.3 Discussion

hIAPP fibrils are present within the lysosomes of pancreatic macrophages in type 2 diabetic humans, monkeys, and hIAPP-expressing transgenic mice (479). Autopsy studies have also demonstrated an increased number of islet macrophages together with increased IL-1β expression in type 2 diabetic islets compared to non-diabetic controls (397,398,401,418). The data in this chapter indicate a link between hIAPP aggregation and islet inflammation, with four novel findings: (1) pre-fibrillar hIAPP species induce cytokine/chemokine expression and proIL-1β synthesis in BMDMs; (2) hIAPP-induced TNF-α release is almost entirely dependent on TLR2 and is amplified by the autocrine/paracrine effects of IL-1; (3) freshly-dissolved preparations of hIAPP activate proIL-1β processing and secretion; and (4) hIAPP expression is associated with TLR2- and IL-1Ra-dependent cytokine release by islets *ex vivo*.

We initially analyzed global gene expression in hIAPP- vs. rIAPP-treated BMDMs in an attempt to understand the nature of the macrophage response to hIAPP. This analysis supported the hypothesis that hIAPP aggregates are phagocytosed by macrophages and alter expression of pro-inflammatory cytokines, including IL-1β and TNF-α, a combination that is toxic to beta cells (Figure 1.6) (391). While there are limitations to these microarray data – including the lack of information regarding non-coding RNAs now known to be important in regulating innate immunity (480) – they provide the first evidence that hIAPP can trigger pro-inflammatory signalling pathways in macrophages and suggest important pathways for further analysis. While subsequent experiments in this thesis have helped to define the mechanisms by which hIAPP

activates islet macrophages, additional work will be required to understand the mechanisms involved in hIAPP uptake and the consequences for macrophage phenotype.

Consistent with our pathway overrepresentation analysis, uptake of amyloid fibrils is thought to occur by phagocytosis, a process dependent on scavenger receptor-mediated particle recognition (270,271). For example, the scavenger receptor CD36 and the integrin-associated protein CD47 are necessary for phagocytosis of both Aβ and IAPP aggregates in microglia (271,481). Interestingly, cell surface integrins and the inhibitory FcγRII were upregulated in our global gene expression analysis and are involved in Aβ uptake and neuronal toxicity (482). Macropinocytosis (and not phagocytosis) is responsible for clearance of soluble (pre-fibrillar/oligomeric) Aβ from the extracellular milieu in Alzheimer's disease (272). Whether this is also the case for oligomeric forms of IAPP is unclear, but an understanding of the processes involved in IAPP uptake at different stages of aggregation may inform the development of anti-amyloid and anti-inflammatory therapies.

Our observation that hIAPP aggregation induces release of multiple pro-inflammatory cytokines and chemokines by BMDMs is consistent with previous studies in neurons and glial cells. Like Aβ, hIAPP induced IL-6 and IL-8 secretion by human astrocytoma cells (273) and release of IL-1β, TNF-α, IL-6, IL-8, CCL3, and CCL4 by LPS-activated THP-1 monocytes, a model for human microglia (274). Our data suggest that hIAPP induces pro-inflammatory cytokine release by both macrophages and islets in the absence of priming by a distinct TLR ligand, consistent with previously reported increases in monocyte IL-1β and TNF-α mRNA in response to hIAPP alone (274) and in response to Aβ (315). Unlike monocytes, macrophages do not express constitutively active caspase-1 (354), and we found that hIAPP mediates IL-1β secretion in a caspase-1-dependent manner. hIAPP-induced NLRP3 activation in dendritic cells has since been described by Masters *et al.* (477), although the lack of significant TNF-α and proIL-1β induction reported by these authors may be explained by peptide handling affecting the aggregation state of the peptide or by cell-type-specific effects. That amplification of hIAPP-induced TNF-α release was inhibited not only by MyD88 deficiency but also by blockade of caspase-1 and IL-1R suggests a role for IL-1α or IL-1β release in the autocrine or paracrine amplification of other cytokines. The capacity of IL-1Ra to inhibit hIAPP-induced chemokine secretion by islets and cytokine secretion by BMDMs suggests that anti-IL-1 therapies have the

potential to suppress a central mediator of IAPP-induced islet inflammation. This possibility is further explored in *in vivo* models of amyloid formation in Chapter 5.

Among many potential mechanisms for IAPP-induced pro-inflammatory gene expression and proIL-1β synthesis, we found that activation of a TLR2/6 heterodimer serves as a critical trigger in both BMDMs and cultured islets. Thus, diverse amyloidogenic peptides (summarized in Figure 1.4 and reviewed in Chapter 1.3), including IAPP, appear to act as endogenous ligands for TLR2. While we found that an anti-TLR2 blocking antibody could preserve insulin content in cultured $hIAPP^{Tg/o}$ islets, additional studies are needed to evaluate the physiological relevance of hIAPP-induced TLR2 activation. Small molecule inhibitors of TLR2 that are currently under development may be helpful in this regard (483,484), although many therapeutic strategies might also interfere with pathways leading to hIAPP-induced NF-κB activation (Figure 6.1). Importantly, studies in mouse models of amyloidoses have suggested a dual role for TLR signalling: to facilitate removal of extracellular protein aggregates (323), and to promote the chronic release of pro-inflammatory cytokines linked to tissue degeneration (324-326). TLR2 stimulation early in the disease may help clear hIAPP aggregates and delay the progression to overt diabetes, but chronic TLR activation may promote pro-inflammatory cytokine release and inhibit amyloid clearance.

The cytotoxicity of synthetic hIAPP toward beta cells depends on the peptide's aggregation state and on the association of growing fibrils with the plasma membrane (212). Inhibitors of hIAPP aggregation, which protect cultured human islets from hIAPP-induced cell death (214), may achieve this effect in part by limiting IL-1β secretion. Understanding the nature of the toxic, TLR2-activating, NLRP3-activating, and inert hIAPP species is critical in the development and screening of aggregation inhibitors. Our data support the hypothesis that pre-fibrillar hIAPP aggregates act as the principal stimulus for NF-κB activation and proIL-1β synthesis. Indeed, the ability of hIAPP to induce both TNF-α and IL-1β release declined when the peptide was added to macrophages in a more aggregated form, and pre-aggregated hIAPP was unable to induce TLR2 activation in HEK 293 cells or NLRP3 priming in BMDMs. This finding is consistent with a previous report of maximal TNF-α induction by pre-fibrillar Aβ species (485). We also found that fibrillar hIAPP preparations are sufficient to induce IL-1β secretion in macrophages primed with LPS, and that exposure of cells to pre-fibrillar aggregates

does not lead to a further increase in IL-1β secretion. It is therefore likely that a fibrillar form of hIAPP is the principle species responsible for activating caspase-1. Thus, hIAPP – in two distinct forms – appears to provide sequential signals for priming and activation of the NLRP3 inflammasome. Masters *et al.*(477) reported NLRP3 activation by prefibrillar hIAPP oligomers; however, these authors compared IL-1β release induced by pre-aggregated fibrils and soluble peptide after overnight culture. Since hIAPP rapidly aggregates to form fibrils during the first few hours of culture, it is likely that cells in those studies were primarily exposed to fibrillar species and not only the intended smaller aggregates. Other studies have suggested that fibrillar aggregates of amyloidogenic peptides such as lysozyme are responsible for activation of TLR2 (303); whether fibrils exist in equilibrium with smaller species that interact with the receptor or whether indirect mechanisms for TLR2 activation are involved (e.g. liberation of other TLR2-activating DAMPs) should be addressed by future work.

Recent data suggest that hIAPP-induced NLRP3 activation, like that of Aβ, is associated with lysosomal damage in dendritic cells (477), and hIAPP fibrils condense within macrophage lysosomes to form proteolysis-resistant protofilaments (270). Consistent with these reports, we have shown that hIAPP-induced IL-1β secretion in macrophages is blocked by the cathepsin B inhibitor CA-074-Me. Since CA-074-Me and the inhibitor of actin polymerization cytochalasin D also attenuated TNF-α release, lysosomal damage may be a major mechanism mediating the pro-inflammatory activity of hIAPP. However, further studies are needed to elucidate the mechanisms by which IAPP aggregates – and indeed, numerous other particulate stimuli – induce NLRP3 activation.

Hemizygous expression of the hIAPP transgene in beta cells induces islet amyloid formation under conditions that increase beta cell secretory demand and dysfunction, including high fat feeding (211), *ex vivo* culture (478), and islet transplantation (216). Here, we have shown that both synthetic and endogenously-produced hIAPP potentiate islet chemokine release *ex vivo*. Migration of monocytes toward media conditioned by hIAPP-treated human islets suggests that the chemokine release observed in transgenic islets has functional implications. One previous study reported no difference in macrophage density between amyloid-containing and amyloid-free human and monkey islets (479); however, immune cell recruitment may occur prior to formation of extensive fibrillar deposits, which likely accompany resolution of the

inflammatory response. This hypothesis is consistent with our finding of maximal pro-inflammatory activity of pre-fibrillar hIAPP in BMDM cultures and with chemokine release by transgenic islets in the absence of widespread amyloid deposition. Chapter 5 provides further evidence for recruitment of monocytes/macrophages *in vivo* to hIAPP$^{Tg/o}$ islet grafts, although not all *in vivo* models of hIAPP-induced islet inflammation discussed in this thesis display an increase in intra-islet macrophage content (despite altered resident macrophage phenotype). The stage of amyloid formation and disease progression are likely important variables in this response.

Finally, a number of potential macrophage-independent mechanisms for IAPP-induced inflammation must be considered in future studies, some of which may involve fibrils rather than pre-fibrillar species. For example, fibrillar IAPP induces complement activation and may contribute to beta cell death via anaphylotoxin release or membrane attack complex formation (486). In addition to islet macrophages, endocrine cells, endothelial cells, and dendritic cells may modulate hIAPP-induced effects *in vivo*. Our data demonstrate that hIAPP aggregation causes release of chemokines such as CCL2 by whole islets, including beta cells. Our clodronate-mediated islet macrophage depletion study suggests that islet macrophages are a major source of the pro-inflammatory cytokines TNF-α and IL-1β and may therefore be required for hIAPP-induced inflammation leading to beta cell dysfunction. This hypothesis is tested in Chapter 4.

In conclusion, this study points to a novel role for IAPP in triggering macrophage activation and islet chemokine secretion, suggesting that IAPP aggregates can act as endogenous danger signals to trigger activation of both TLR2/6 and NLRP3. Thus, hIAPP aggregates may promote islet dysfunction not only via direct toxicity to beta cells but also by triggering a localized inflammatory response. Strategies aimed at reducing hIAPP expression and aggregation may ameliorate deficits in insulin secretion associated with pro-inflammatory cytokine release. Since IL-1R signalling contributes to the amplification of hIAPP-induced cytokine and chemokine secretion by islets and macrophages, these data suggest a possible mechanism by which blockade of TLR2, IL-1R, or hIAPP aggregation may significantly alter the inflammatory milieu of the pancreatic islet to improve beta cell function.

Table 3.1. Functional annotation analysis of differentially expressed genes using GO pathways in DAVID.[1]

Pathway	FE	*p*	Genes
Immune response (GO 6955)	2.3	0.0001	*Tollip, Ly86, Tlr4, Il15, Tlr8, Klhl6, Clec4e, Oasl2, Ticam2, Il1b, Fas, Il1a, Gm6097, Cnpy3, Nlrp3, Loc100046097, Lat2, Tnfsf13b, Gadd45g, Lilrb4, Cx3cr1, Oas1a, Clec5a, Oas1g, Lcp1, Tnfaip1, Cd300ld, Tnfaip8l2, Cxcl1, Ccl3, Tnf, Gm8762, Ccl2, Cxcl2, Hfe, Rsad2, Il7r, Ccl4, Ccl7, Mif, Gp49a, Sqstm1, Loc641240, Pou2f2, Gm16379, Msh6, Rmcs2, H2-M2, Loc100047704, Gm10169, Il1rn, Tlr13, H2-Ab1, Malt1, Tnfsf9, Fcgr1, Vav1, Cd180, Loc100048875, Fcgr2b, P2ry14, H2-Dma, Loc100044948, Cd14*
Response to wounding (GO 9611)	2.4	0.0007	*Cxcl1, Gna13, Ccl3, Gm8762, Tnf, Ccl2, Nfkbid, Tollip, Ly86, Pparg, Cxcl2, Tlr4, Sgms1, Ccl4, Tlr8, Ccl7, Mif, Cd44, Mtpn, Bcl2, Map3k1, Cnr2, Ticam2, Il1b, Gm16379, Il1a, Klf6, Gm3655, F10, Plek, Gm6097, Pik3cb, Gm10169, Map2k3, Tlr13, Sphk1, Anxa5, Nlrp3, Fcgr1, Cd180, Plaur, Hbegf, Id3, Loc100044948, Cd14, Igfbp4, Lcp1*
Regulation of cell proliferation (GO 42127)	2.1	0.0005	*Apobec1, Pdgfb, Marcksl1, Pdgfa, Pparg, Edn1, Tlr4, Il15, Pnp, Slfn2, Cdca7, Ptges, Gm15645, Hmox1, Hlx, Chst11, Gm6742, Gnl3, Irs2, Ptger2, Gm3655, Gtpbp4, Ccdc88a, Gm6097, Gm7278, Loc676173, Il11ra1, Cd40, Vegfc, Hhex, Cd80, Tnfsf13b, Jun, Eif2ak2, Smarca2, Ccl2, Tnf, Gm8762, Csf1, Bcl2l1, Timp2, Mif, Cd9, Loc100044675, Bcl2, Gm7993, Tgm2, B4galt7, Gm16379, Tes, Col18a1, Odc1, Gm9115, Loc100045567, Marcksl1-Ps3, Gm10169, Sphk1, Anxa1, Igf1, Pold4, Notch1, Fcgr2b, Dbp, Eef1e1, Cd274, Hbegf, Loc100044948, Klf4, Sash3, Plau*
Vasculature development (GO 1944)	2.5	0.0043	*Gna13, Mef2c, Pdgfa, Tnfrsf12a, Edn1, Anpep, Srf, Cited2, Zfp36l1, Arhgap22, Loc100048867, Hmox1, Itgav, Tgm2, Il1b, Zc3h12a, Rhob, Lox, Angpt2, Rapgef1, Ppap2b, Col18a1, Pdpn, Sphk1, Mmp14, Junb, Anxa2, Vegfc, Notch1, Jmjd6, Mapk14, Hbegf*
Blood vessel development (GO 1568)	2.5	0.0059	*Gna13, Mef2c, Pdgfa, Tnfrsf12a, Edn1, Anpep, Srf, Cited2, Zfp36l1, Arhgap22, Loc100048867, Hmox1, Itgav, Tgm2, Il1b, Zc3h12a, Rhob, Lox, Angpt2, Rapgef1, Ppap2b, Col18a1, Sphk1, Mmp14, Junb, Anxa2, Vegfc, Notch1, Jmjd6, Mapk14, Hbegf*
Cell activation (GO 1775)	2.5	0.0058	*Gna13, Tnf, Tlr4, Il15, Il7r, Bcl2, Wwp1, Pou2f2, Ndrg1, Fas, Gm13416, Egr1, Fyb, Msh6, Gm3655, Gm12141, Plek, Pik3cb, Loc100047704, Il11ra1, Malt1, Cd40, Nfam1, Vav1, Bcl2a1d, Lat2, Cd86, Fcgr2b, Loc100048875, Jmjd6, Cx3cr1, Gadd45g, Hspd1, H2-Dma, Lcp1*
Endosome (GO 5768)	2.5	0.0034	*Vps29, Slc9a9, Cytip, Tnf, Chmp4b, Mmd, Vps37b, Arf6, Rhov, Atp6v0b, Gm5884, Cd68, Sqstm1, Rabgef1, Rhob, Ehd1, Atp6v0d1, Vps18, Rmcs2, H2-Ab1, Ldlrap1, Abcg1, Anxa2, Tmem55a, Atp6v1e1, Sort1, Tom1, Arl8a, Arl8b, H2-Dma, Rin3*
Toll-like receptor signalling pathway (KEGG 4620)	3.3	0.0030	*Ccl3, Tnf, Pik3cb, Tollip, Map2k3, Tlr4, Cd40, Ccl4, Tlr8, Cd86, Cd80, Mapk14, Jun, Map3k8, Ticam2, Il1b, Cd14, Spp1*
Inflammatory response (GO 1525)	2.5	0.0062	*Cxcl1, Ccl3, Gm8762, Ccl2, Tnf, Nfkbid, Tollip, Ly86, Cxcl2, Pparg, Tlr4, Sgms1, Ccl4, Ccl7, Tlr8, Mif, Cd44, Cnr2, Ticam2, Il1b, Gm16379, Il1a, Gm6097, Gm10169, Map2k3, Tlr13, Sphk1, Nlrp3, Fcgr1, Cd180, Loc100044948, Igfbp4, Cd14*
Angiogenesis (GO 1525)	3.0	0.0087	*Col18a1, Gna13, Pdgfa, Tnfrsf12a, Edn1, Anpep, Mmp14, Srf, Anxa2, Arhgap22, Vegfc, Notch1, Loc100048867, Hmox1, Mapk14, Itgav, Il1b, Zc3h12a, Rhob, Hbegf, Angpt2*

[1]Cells were treated with hIAPP or rIAPP for 12 h (n=4 per treatment). Global gene expression was analyzed by Illumina microarray. Pathway overrepresentation analysis was performed on genes differentially expressed by at least 1.5-fold using the Database for Annotation, Visualization, and Integrated Discovery (DAVID) functional annotation tool. Enriched Gene Ontology (GO) terms with a Benjamini corrected p-value <0.01 and fold enrichment (FE) >2.0 are shown.

Table 3.2. Functional annotation analysis of differentially expressed genes using KEGG, INOH, and Reactome pathways in InnateDB.[1]

Pathway Name	Ratio	*p*	Gene Symbols
Phagosome (KEGG)	15	0.0009	*5430435G22Rik, Actb, Atp6v0b, Atp6v0d1, Atp6v0e, Atp6v1c1, Atp6v1d, Atp6v1e1, Atp6v1h, Cd14, Fcgr1, Fcgr2b, Fcgr4, H2-Ab1, H2-DMa, H2-M2, Itga5, Itgav, Itgb5, Tcirg1, Tlr4, Tuba1a, Tuba1b, Tubb4b, Tubb6*
Toll-like receptor signalling pathway (KEGG)	19	0.0011	*Ccl3, Ccl4, Cd14, Cd40, Cd80, Cd86, Ctsk, Il1b, Jun, Map2k3, Map3k8, Mapk14, Pik3cb, Spp1, Ticam2, Tlr4, Tlr8, Tnf, Tollip*
Systemic lupus erythematosus (KEGG)	20	0.0012	*Actn1, Actn4, Cd40, Cd80, Cd86, Fcgr1, Fcgr2b, Fcgr4, H2-Ab1, H2-DMa, Hist1h2af, Hist1h2ak, Hist2h2bb, Hist2h2be, Snrpd1, Tnf*
Insulin receptor recycling (REACTOME)	41	0.0016	*Atp6v0b, Atp6v0d1, Atp6v0e, Atp6v1c1, Atp6v1d, Atp6v1e1, Atp6v1h*
Neurotrophin signalling pathway (KEGG)	16	0.0020	*Atf4, Bcl2, Camk2d, Gab1, Gsk3b, Irak2, Irs2, Jun, Kras, Map3k1, Mapk14, Mapkapk2, Nfkbie, Ngfrap1, Pik3cb, Rapgef1, Rps6ka2, Sort1, Ywhag, Ywhah*
Transferrin endocytosis and recycling (REACTOME)	37	0.0028	*Atp6v0b, Atp6v0d1, Atp6v0e, Atp6v1c1, Atp6v1d, Atp6v1e1, Atp6v1h*
MAPK signalling pathway (KEGG)	12	0.0028	*Atf4, Cd14, Ddit3, Dusp1, Dusp16, Dusp3, Dusp4, Dusp7, Dusp8, Fas, Gadd45b, Gadd45g, Il1a, Il1b, Jun, Kras, Map2k3, Map3k1, Map3k11, Map3k14, Map3k8, Mapk14, Mapk6, Mapkapk2, Mef2c, Pdgfa, Pdgfb, Prkx, Rasa2, Rps6ka2, Srf, Tnf*
Activation of Genes by ATF4 (REACTOME)	50	0.0049	*Asns, Atf3, Atf4, Ddit3, Herpud1*
Phagosomal maturation (REACTOME)	29	0.0055	*Atp6v0b, Atp6v0d1, Atp6v0e, Atp6v1c1, Atp6v1d, Atp6v1e1, Atp6v1h, Tcirg1*
Activation of Matrix Metalloproteinases (REACTOME)	38	0.0056	*Col18a1, Mmp10, Mmp13, Mmp14, Mmp3, Timp2*
Hematopoietic cell lineage (KEGG)	17	0.0061	*Anpep, Cd14, Cd33, Cd44, Cd9, Csf1, Fcgr1, Il11ra1, Il1a, Il1b, Il6ra , Il7r, Itga5, Tnf*
Meiotic Synapsis (REACTOME)	19	0.0083	*H3f3b, Hist1h2af, Hist1h2ah, Hist1h2ai, Hist1h2ak, Hist1h2be, Hist2h2aa2, Hist2h2bb, Hist2h2be, Lmna, Lmnb1*
Osteoclast differentiation (KEGG)	15	0.0084	*Csf1, Ctsk, Fcgr1, Fcgr2b, Fcgr4, Il1a, Il1b, Irf9, Jun, Junb, Map3k14, Mapk14, Nfatc1, Pik3cb, Pparg, Sqstm1, Tnf*
Interleukin-1 signalling (REACTOME)	23	0.0094	*Cul1, Il1a, Il1b, Il1rn, Irak2, Map3k8, Peli2, Sqstm1, Tollip*

[1]Cells were treated with hIAPP or rIAPP for 12 h (n=4 per treatment). Global gene expression was analyzed by Illumina microarray. Pathway over-representation analysis was performed on genes differentially-expressed by at least 1.5-fold using the InnateDB pathway overrepresentation tool. Enriched terms with a Benjamini corrected p-value <0.01 are shown. Ratio: % of curated genes differentially expressed.

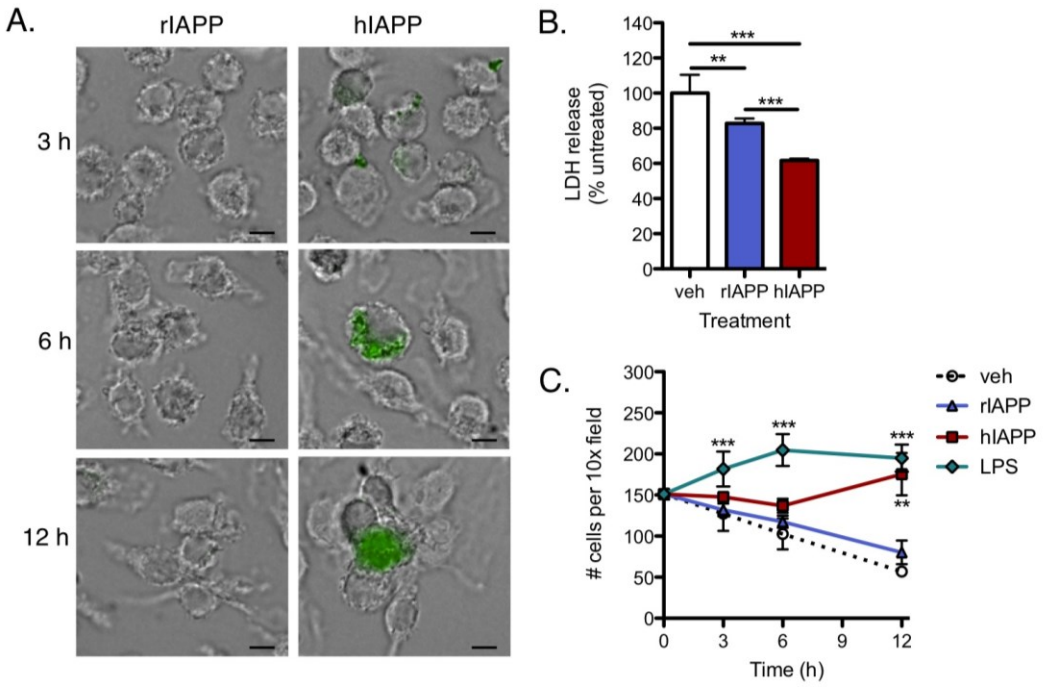

Figure 3.1. IAPP aggregates preserve BMDM viability in the absence of M-CSF. (A) BMDMs were deprived of M-CSF for 12 h, cultured with hIAPP or rIAPP (15 μM) for the indicated time period, fixed in formalin, and stained with thioflavin S to detect amyloid fibrils (green fluorescence, overlaid on brightfield). Scale bar: 5 μM. (B) LDH content in culture supernatants was analyzed by a colorimetric assay as a measure of cell death. (C) The number of cells per field was determined at each time point for cells treated with IAPP or LPS (100 ng/ml) using a Thermo Fisher ArrayScan VTI HCS instrument. Statistical significance is shown relative to the vehicle control. Data represent mean±SD of 3-4 replicates per treatment and are representative of 3 independent experiments. veh: vehicle control. ** $p<0.01$, *** $p<0.001$.

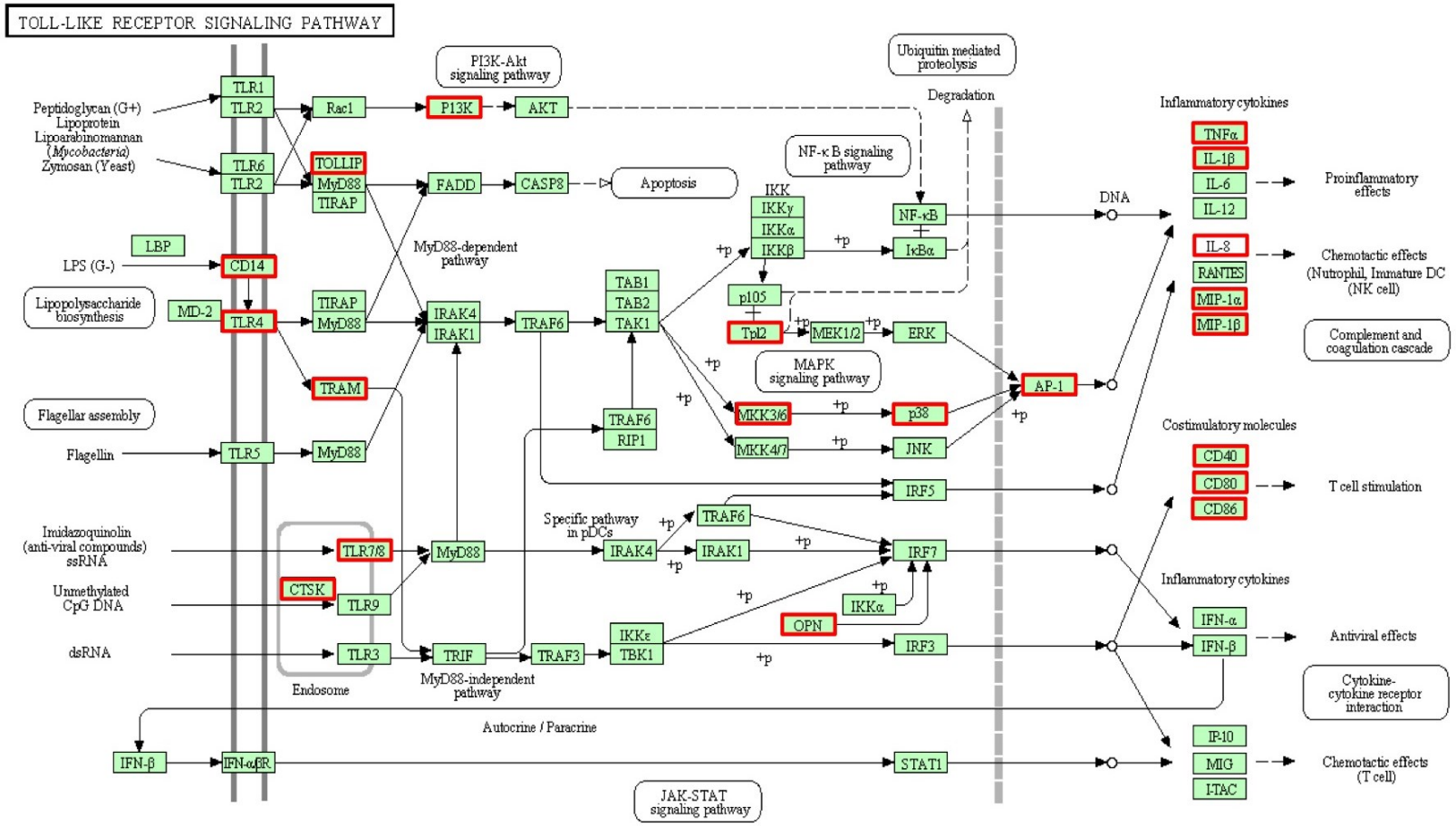

Figure 3.2. KEGG TLR pathway genes upregulated in hIAPP- vs. rIAPP-treated BMDMs. BMDMs were treated with hIAPP or rIAPP for 12 h (*n*=4 per treatment). Global gene expression was analyzed by Illumina microarray. Pathway over-representation analysis was performed on genes differentially expressed by at least 1.5-fold ($p<0.05$) using the InnateDB functional annotation tool. TLR signalling was one of two significantly over-represented KEGG pathways and was also identified by analysis using DAVID. Complexes that include upregulated genes are outlined in red (none was downregulated). The mouse homologue of IL-8 is CXCL1, which was upregulated. Pathway diagram was generated using KEGG (471).

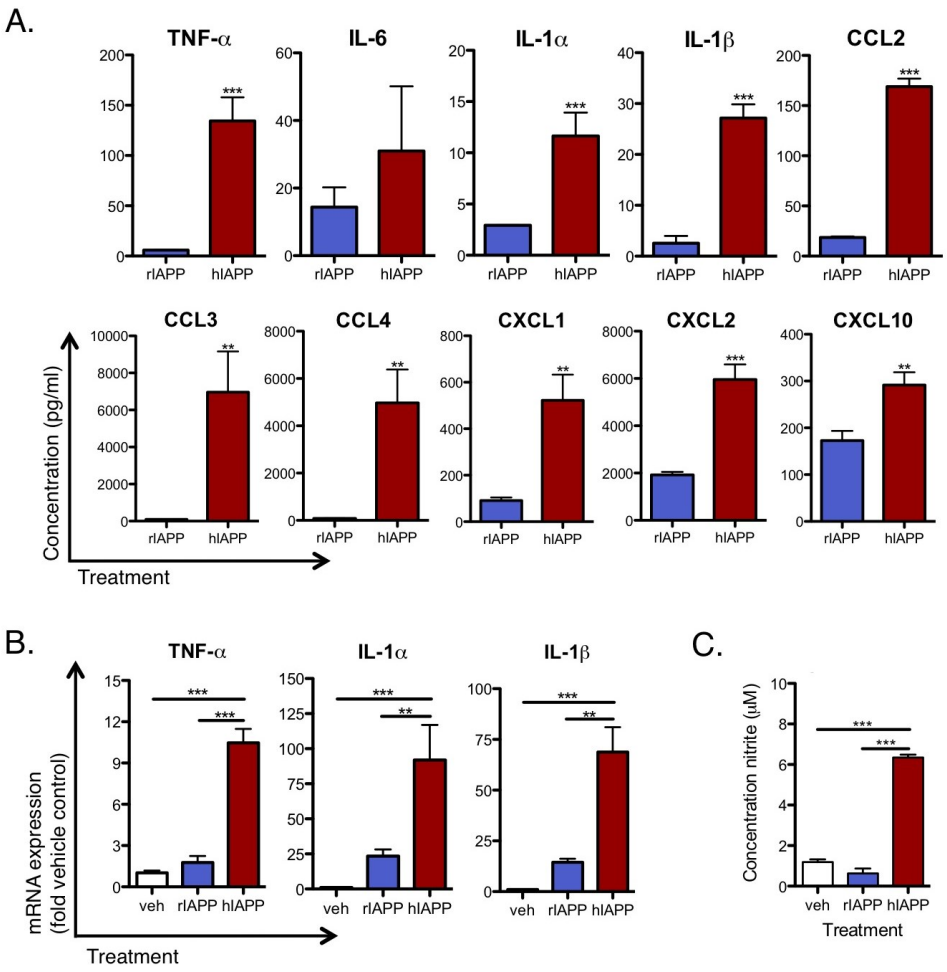

Figure 3.3. hIAPP induces pro-inflammatory cytokine secretion by BMDMs. (A) Cells were incubated with hIAPP or rIAPP (15 μM) for 12 h. Supernatants were assessed for pro-inflammatory cytokines and chemokines with a Luminex assay. (B) Gene expression was evaluated by RT-qPCR and normalized to *Gapdh* as the internal control. (C) Nitrite content in supernatants was measured by Griess assay. Data represent mean±SD of 4 replicates per treatment and are representative of 3 independent experiments. veh: vehicle control. ** $p<0.01$, *** $p<0.001$

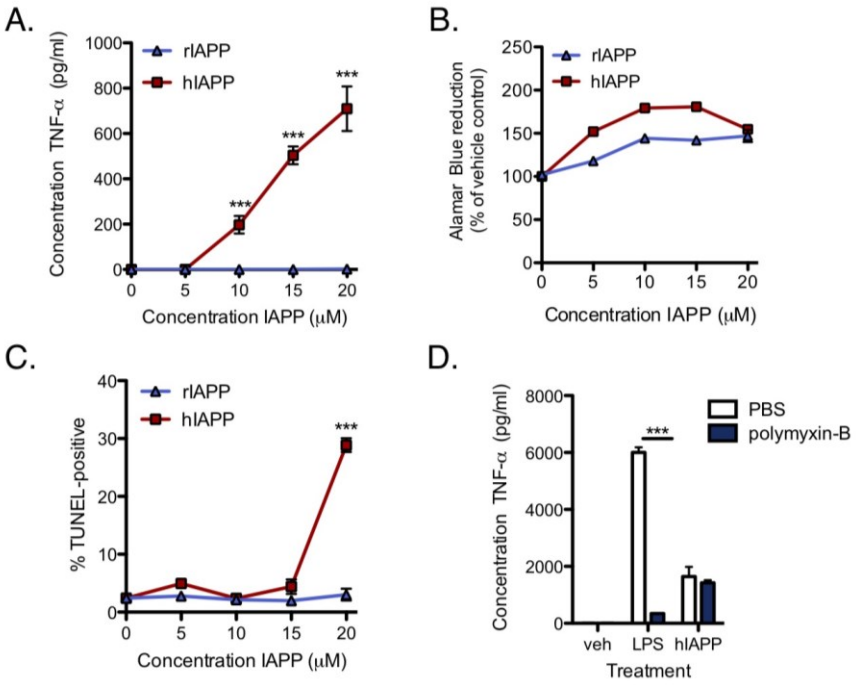

Figure 3.4. hIAPP-induced TNF-α release is independent of cell death and endotoxin contamination. (A) TNF-α production in response to treatment with 5-20 μM IAPP for 24 h was determined by ELISA. (B) Viability was assessed by Alamar Blue fluorescence. (C) Cells were fixed after 24 h and cell death was evaluated by ArrayScan VTI HCS analysis of TUNEL staining. (D) hIAPP-induced TNF-α release was evaluated in the presence of the cationic peptide polymyxin-B (10 μg/ml). Data represent mean±SD of 3 replicates per treatment and are representative of 5 independent experiments. veh: vehicle control. *** $p<0.001$.

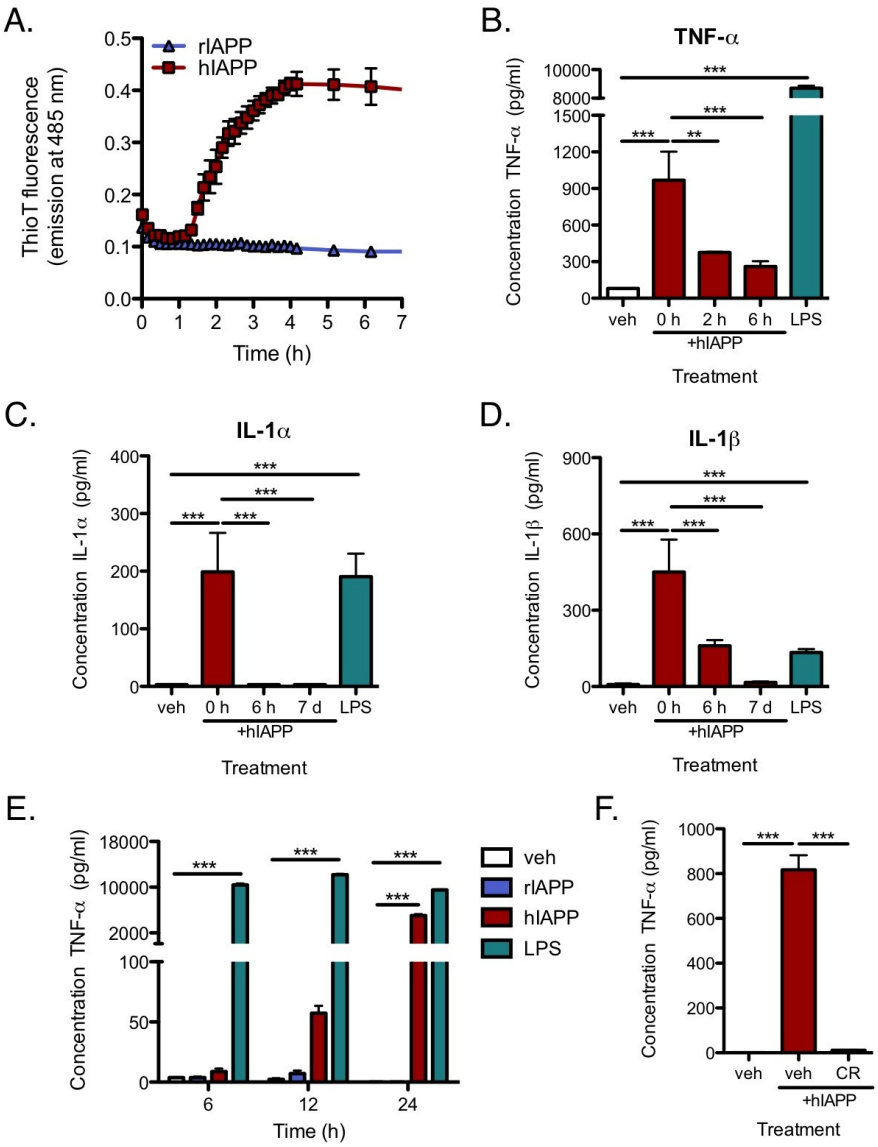

Figure 3.5. hIAPP aggregation intermediates induce maximal TNF-α and IL-1 secretion by BMDMs. (A) hIAPP or rIAPP (15 μM) was dissolved in DMEM and fibril formation was monitored by thioflavin T fluorescence. Peptide was removed at the indicated time points and added to BMDM cultures for 24 h. Levels of (B) TNF-α, (C) IL-1α, and (D) IL-1β in cell supernatants were determined by Luminex assay. (E) Freshly-dissolved hIAPP was evaluated for TNF-α induction after 6, 12, and 24 h and compared with the kinetics of induction by LPS (100 ng/ml). (F) TNF-α levels were assessed following co-incubation with Congo red (200 mM, CR), an inhibitor of hIAPP fibrillogenesis. Data represent mean±SD of 3 replicates per treatment and are representative of 3 independent experiments. veh: vehicle control. ** $p<0.01$, *** $p<0.001$.

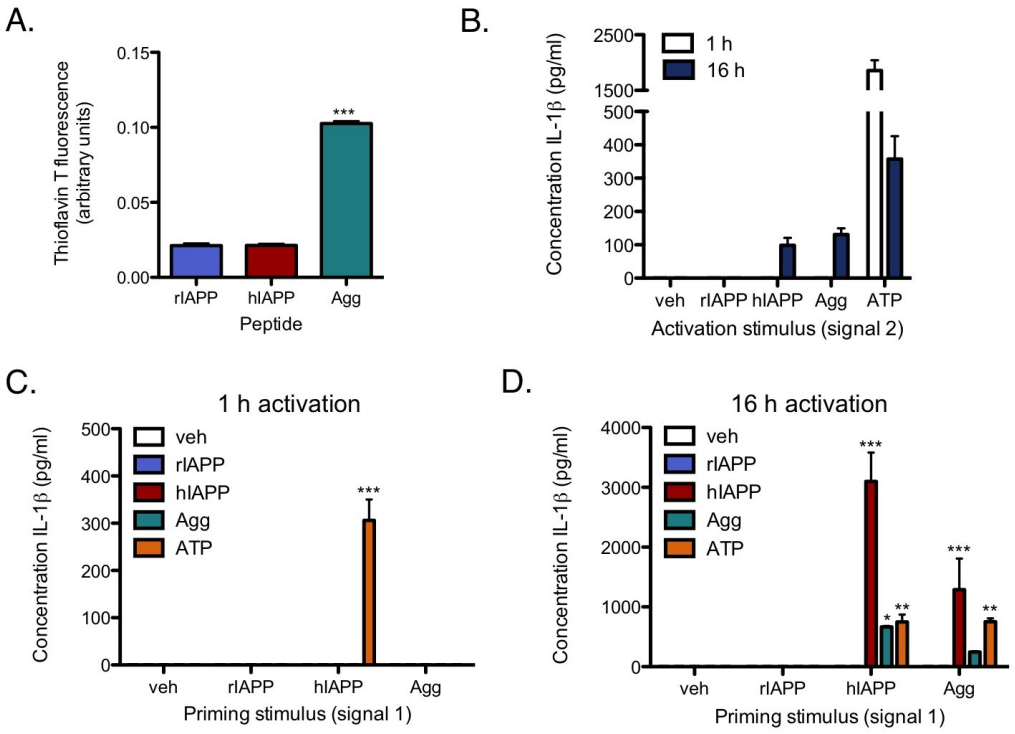

Figure 3.6. Pre-fibrillar and fibrillar hIAPP aggregates have distinct effects on the synthesis and secretion of IL-1β. (A) Amyloid fibril content was determined by measurement of thioflavin T fluorescence in freshly-dissolved preparations of rIAPP or hIAPP (10 μM) or in hIAPP that was allowed to pre-aggregate for 24 h at 37°C (Agg). (B) BMDMs were treated with LPS for 3 h (signal 1, to induce proIL-1β synthesis) followed by treatment with the indicated activation stimulus for 1 or 16 h (signal 2, to induce proIL-1β cleavage and mature IL-1β secretion). IL-1β in supernatants was measured by ELISA as an indicator of NLRP3 activation. (C) BMDMs were treated with the indicated priming stimulus (signal 1) for 3 h followed by 1 h or (D) 16 h activation (signal 2) with the indicated form of IAPP (10 μM) or ATP (5 mM). IL-1β in supernatants was measured by ELISA as an indicator of combined proIL-1β synthesis and NLRP3 activation. veh: vehicle control. Data represent mean±SD of 3 replicates per treatment and are representative of 2 independent experiments. * $p<0.05$, ** $p<0.01$, *** $p<0.001$.

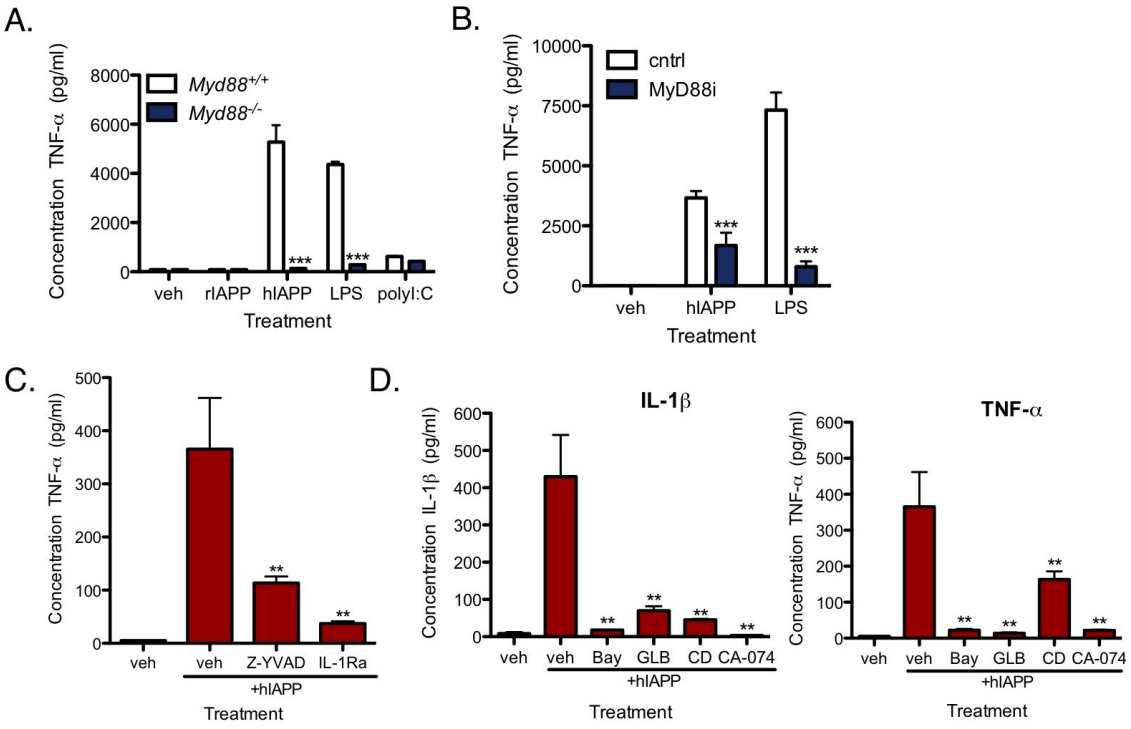

Figure 3.7. hIAPP-induced TNF-α release by BMDMs is dependent on MyD88 and IL-1R. (A) C57BL/6 wild- and *Myd88*$^{-/-}$ BMDMs were evaluated for TNF-α release by ELISA after 24 h incubation with IAPP (15 μM) or the TLR agonists LPS (100 ng/ml) and polyI:C (10 μg/ml). (B) Wild-type BMDMs were pre-treated with MyD88 homodimerization inhibitory peptide (MyD88i) or control peptide (both 100 μM) for 12 h prior to addition of IAPP (15 μM) or LPS (10 ng/ml) for 24 h. TNF-α levels were determined by ELISA. (C) The caspase-1 inhibitor Z-YVAD-FMK (40 μM) and IL-1Ra (4 μg/ml) were added to BMDM cultures 2 h prior to treatment with hIAPP for 24 h. TNF-α levels were determined by ELISA. (D) TNF-α and IL-1β levels were determined by Luminex assay following 24 h culture with hIAPP in the presence of the NLRP3 inhibitors Bay 11-7082 (Bay, 5 μM), glibenclamide (GLB, 200 μM), cytocholasin D (CD, 5 μM), or CA-074 Me (CA-074, 80 μM). Data represent mean±SD of 3 replicates per treatment and are representative of 3 (B-D) or 6 (A) independent experiments. veh: vehicle control. ** p<0.01, *** p<0.001 relative to vehicle control.

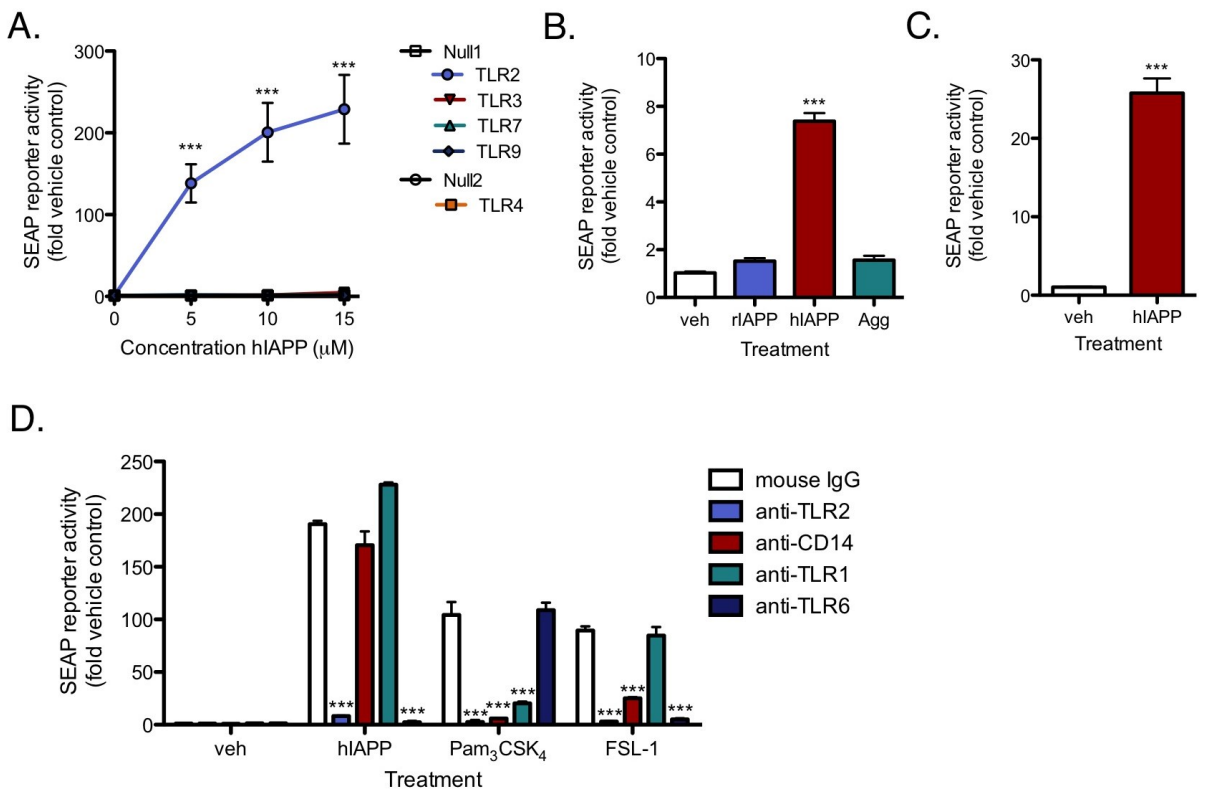

Figure 3.8. hIAPP activates a TLR2/6 heterodimer. (A) Human embryonic kidney (HEK 293) cells co-transfected with the indicated human TLR, CD14 (TLR2- and TLR4-expressing cells), and a secreted alkaline phosphatase (SEAP) NF-κB/AP-1 reporter gene were treated with freshly-dissolved hIAPP for 24 h. SEAP activity was determined by colorimetric assay. Null1 and Null2 represent the parental cell lines. (B) TLR2-overexpressing cells were treated with rIAPP or hIAPP (10 μM) or the mass equivalent of hIAPP that had pre-aggregated for 24 h. (C) HEK 293 cells expressing mouse TLR2 were treated with freshly-dissolved hIAPP (10 μM) for 24 h to confirm similar results with the rodent receptor. (D) Human TLR2-overexpressing HEK cells (with endogenous TLR1 and TLR6 expression) were pre-treated with anti-TLR1, TLR2, TLR6, or CD14 neutralizing antibody (5 μg/ml) or mouse IgG isotype control for 1 h prior to addition of hIAPP (10 μM) or control ligands for TLR1/2 (Pam_3CSK_4) or TLR2/6 (FSL-1) at 10 ng/ml. veh: vehicle control. *** $p<0.001$ relative to vehicle control (A-C) or isotype control (D). Data represent mean±SD of 3 replicates per treatment and are representative of 3 independent experiments.

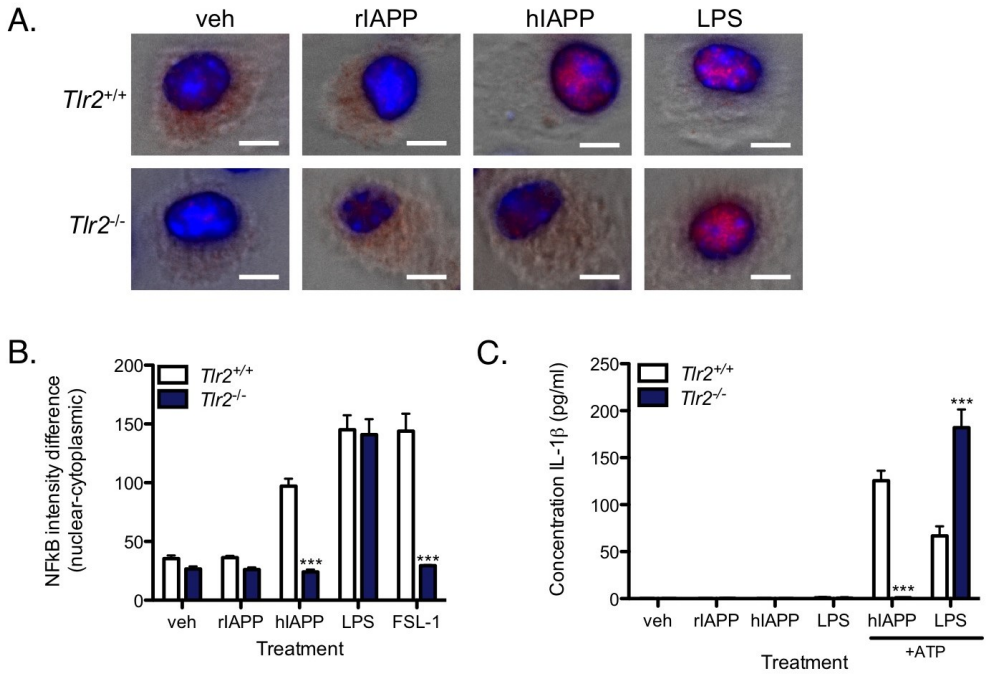

Figure 3.9. hIAPP-induced NF-κB activation and priming for IL-1β secretion require TLR2 in BMDMs. BMDMs from wild-type (WT) or *Tlr2*$^{-/-}$ C57BL/6 mice were treated with IAPP (10 μM) or LPS (10 ng/ml) for 1 h. (A) Representative staining of BMDMs for the NF-κB p65 subunit (red) and DAPI (blue) overlaid on brightfield images. Scale bar: 5 μm. (B) The difference in staining intensity between nucleus and cytoplasm was quantified with a Thermo Fisher ArrayScan VTI HCS instrument. (C) IL-1β was measured by ELISA in supernatants of BMDMs treated with IAPP (10 μM) or LPS (10 ng/ml) for 3 h with or without an additional 1 h of ATP (5 mM) to induce NLRP3 activation. veh: vehicle control. *** p<0.001 relative to WT or isotype control. Data represent mean±SD of 3 replicates per treatment and are representative of 2 independent experiments.

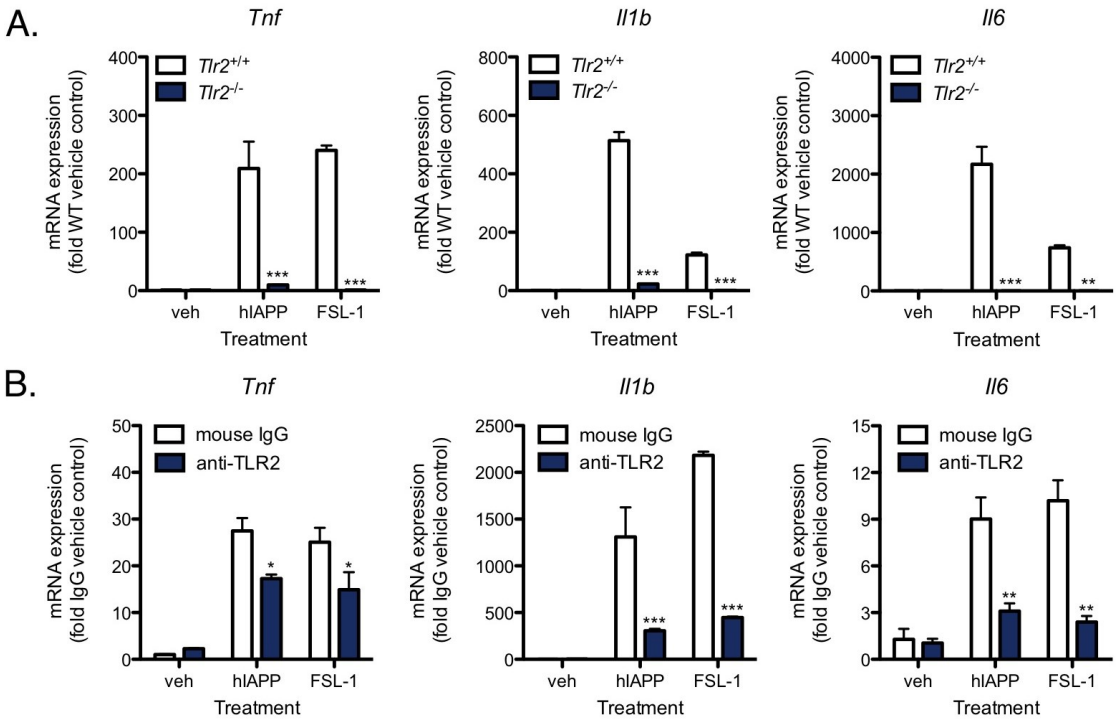

Figure 3.10. Deficiency or neutralization of TLR2 attenuates hIAPP-induced pro-inflammatory gene expression in macrophages. (A) BMDMs from wild-type (WT) or *Tlr2*$^{-/-}$ C57BL/6 mice were treated with IAPP (10 μM) or FSL-1 (10 ng/ml) for 4 h. (B) RAW 264.7 macrophages were pre-incubated with anti-TLR2 neutralizing antibody (5 μg/ml) or mouse IgG isotype control for 30 min prior to addition of hIAPP or FSL-1 for 4 h. mRNA expression of pro-inflammatory cytokines was assessed by RT-qPCR. Expression levels were normalized to the housekeeping gene *Rplp0.* veh: vehicle control. * p<0.05, ** p<0.01, *** p<0.001 relative to WT. Data represent mean±SD of 4 replicates per treatment and are representative of 3 independent experiments.

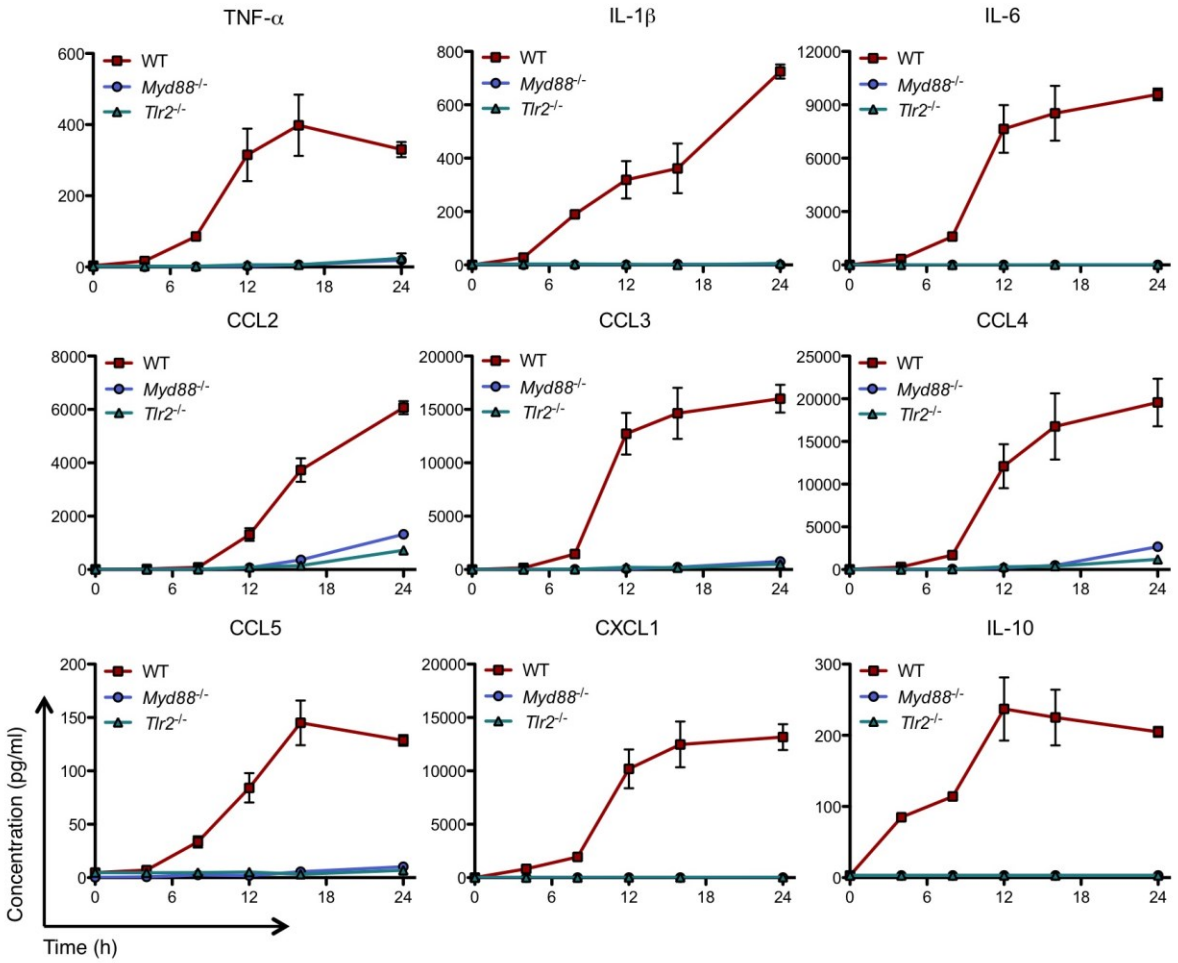

Figure 3.11. Deficiency of TLR2 or MyD88 prevents hIAPP-induced cytokine secretion by BMDMs. BMDMs from wild-type (WT), *Myd88*$^{-/-}$, or *Tlr2*$^{-/-}$ C57BL/6 mice were treated with hIAPP (10 μM) for 0-24 h. Cytokine secretion was measured by Luminex assay. Data represent mean±SD of 3 replicates and are representative of 3 independent experiments. All cytokines/chemokines shown were significantly induced by hIAPP by 8-12 h.

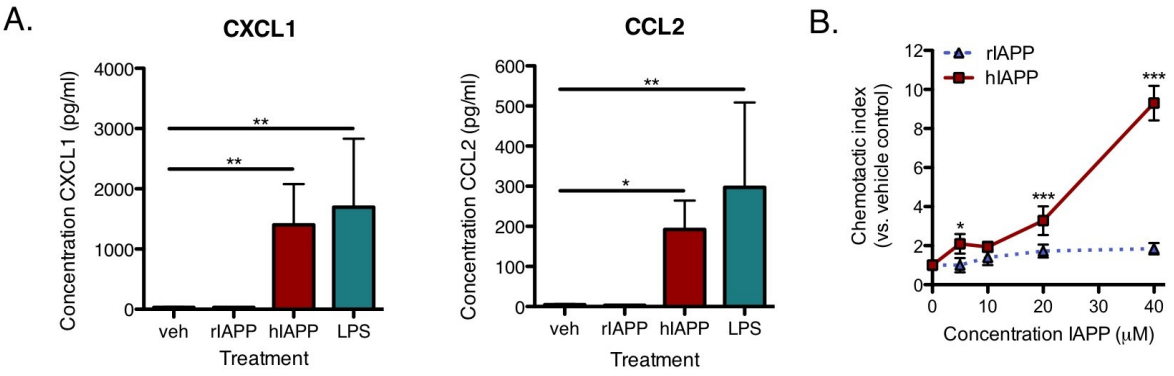

Figure 3.12. Synthetic hIAPP induces islet chemokine secretion and THP-1 monocyte recruitment to cultured human islets. (A) Pancreatic islets were isolated from 12-week-old C57BL/6 mice, allowed to recover overnight, and treated with hIAPP or rIAPP (15 μM) or LPS (100 ng/ml) for 24 h. Supernatants were collected and analyzed for the chemokines CCL2 and CXCL1 by Luminex assay. (B) Human islets from a single cadaveric donor were treated with varying concentrations of synthetic IAPP for 24 h. THP-1 cell chemotaxis in response to islet-conditioned media was evaluated in triplicate in a transwell assay. Data represent mean±SEM of islets from 3 mice per treatment and are representative of 2 independent experiments. veh: vehicle control. * $p<0.05$, ** $p<0.01$, *** $p<0.001$.

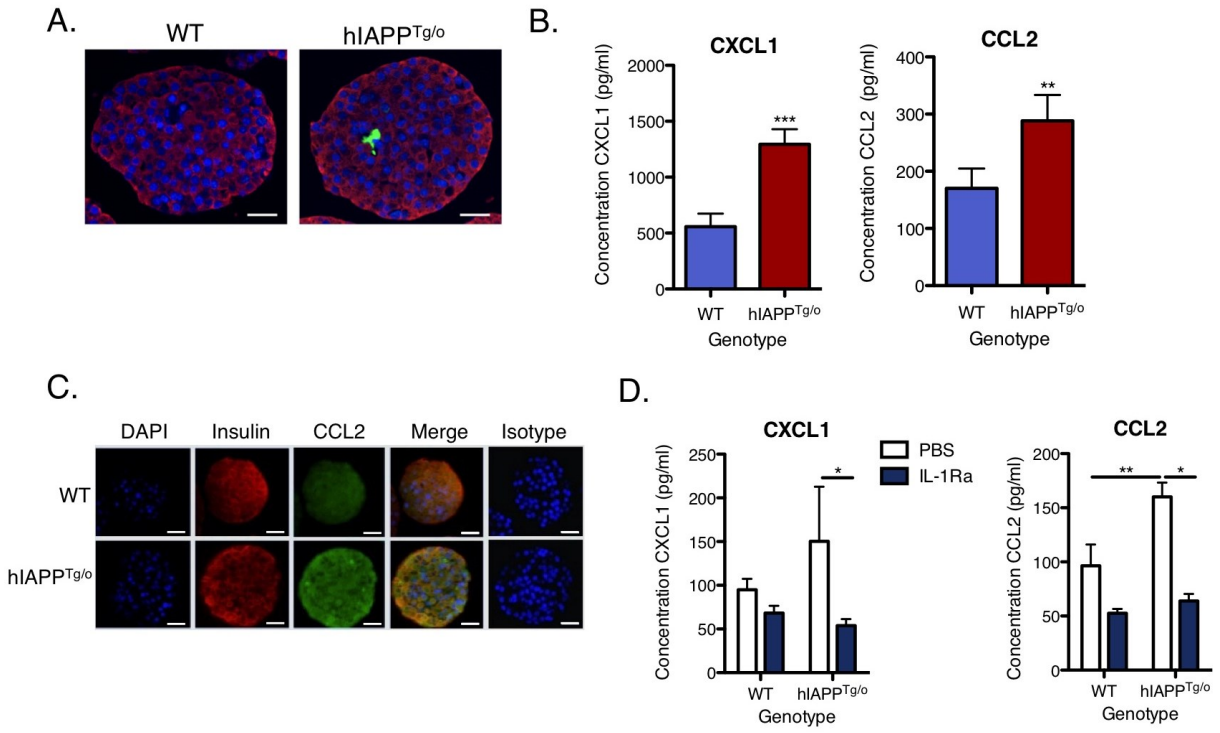

Figure 3.13. Aggregation of endogenous hIAPP promotes islet chemokine secretion. (A) Islets were isolated from 12-week-old hIAPP$^{Tg/o}$ mice and wild-type (WT) littermate controls and cultured for 7 days in RPMI containing 11 mM glucose. Formalin-fixed, paraffin-embedded islet sections were stained for insulin (red), amyloid (thioflavin S), and DAPI (blue). Scale bar: 25 μm. (B) Supernatants were analyzed for CCL2 and CXCL1 by Luminex assay. (C) Islet sections were stained for insulin (red), CCL2 (green), and DAPI (blue). Scale bar: 25 μM. (D) CCL2 and CXCL1 release by WT and hIAPP$^{Tg/o}$ islets were evaluated after 7-day culture in the presence or absence of 4 μg/ml IL-1Ra. Data represent mean±SEM of islets from 3-5 mice per treatment and are representative of 3 independent experiments. veh: vehicle control. * p<0.05, ** p<0.01, *** p<0.001.

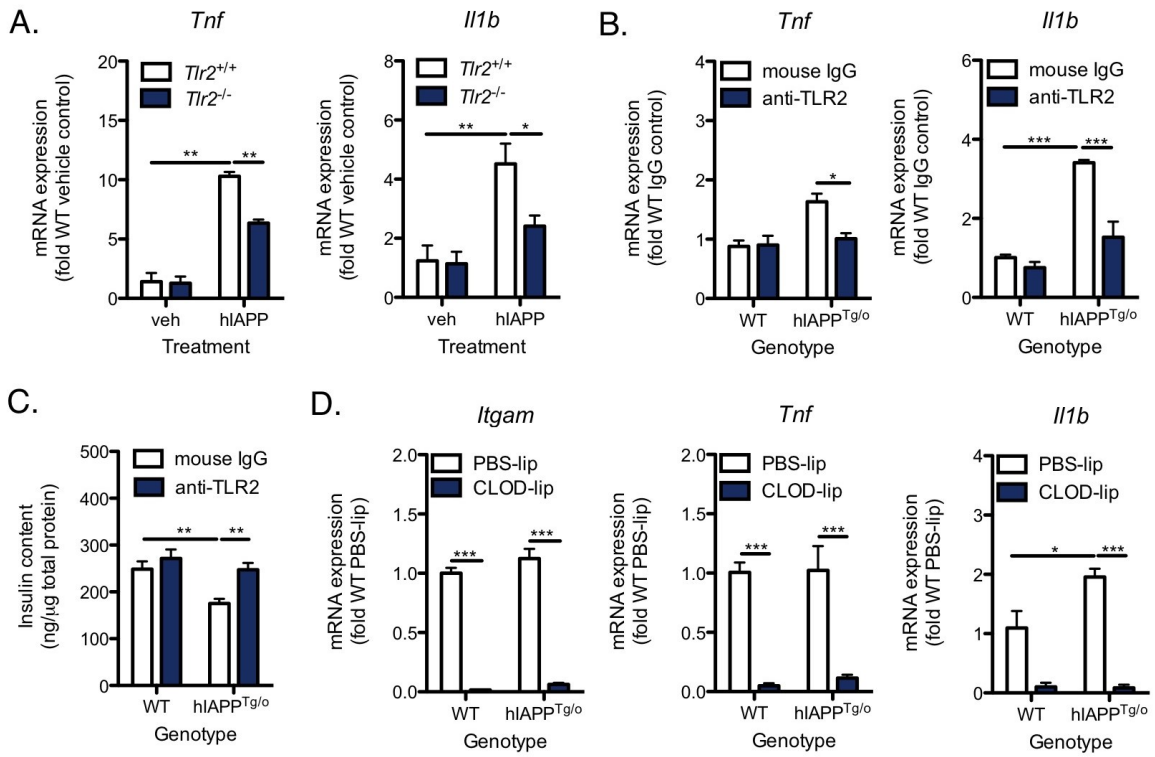

Figure 3.14. Blockade of TLR2 prevents upregulation of islet pro-inflammatory cytokine expression in response to synthetic and endogenous hIAPP. (A) Islets were isolated from 12-week-old wild-type (WT) or *Tlr2*$^{-/-}$ C57BL/6 mice. After overnight recovery, islets were treated with hIAPP (10 µM) for 4 h. *Tnf* and *Il1b* expression were assessed by RT-qPCR. Expression levels were normalized to the housekeeping gene *Rplp0.* (B) Islets from hIAPP$^{Tg/o}$ mice and WT littermate controls were cultured with 10 µg/ml anti-TLR2 neutralizing antibody or isotype control for 7 days at 22 mM glucose to promote amyloid formation. mRNA expression was assessed by RT-qPCR. (C) Insulin content was assessed by ELISA. (D) WT and hIAPP$^{Tg/o}$ islets were treated with clodronate-containing liposomes (CLOD-lip, 1 mg/ml clodronate) or control liposomes (PBS-lip) for 36 h immediately following isolation to determine whether islet phagocytes are a major source of *Tnf* and *Il1b* expression. Islets were subsequently cultured at 22 mM glucose for 4 days to promote amyloid formation. mRNA expression was assessed by RT-qPCR. Data represent mean±SEM of islets from 3 mice per treatment and are representative of 3 independent experiments. veh: vehicle control. * p<0.05, ** p<0.01, *** p<0.001.

Chapter 4: Islet Macrophages Mediate IAPP-induced Islet Inflammation and Dysfunction

4.1 Background

Islet amyloid formation (487), macrophage infiltration (401), and elevated expression of pro-inflammatory cytokines (464) are associated with beta cell dysfunction in patients with type 2 diabetes. Emerging evidence suggests that early aggregates of IAPP, the principal component of islet amyloid, interact directly with innate immune cells to promote the synthesis of pro-inflammatory cytokines, in particular IL-1β (477,488). Other amyloidogenic peptides also trigger an innate immune response by activating cell-surface pattern recognition receptors (276) in addition to the NLRP3 inflammasome (314). In Chapter 3, we found that early aggregates of hIAPP (but not non-amyloidogenic rIAPP) induce *Il1b* mRNA in BMDMs and islets in a TLR2-dependent manner. hIAPP also activates NLRP3 leading to proIL-1β cleavage by caspase-1 (477), an effect likely due to thioflavin-T-positive fibrillar aggregates. Consistent with an important role for IAPP-induced IL-1 signalling in islet inflammation, IL-1Ra limited hIAPP-induced secretion of chemokines by islets and cytokines by BMDMs. Notably, differential expression of IL-1-related genes is a marked characteristic of islets from patients with type 2 diabetes (400), and recent clinical studies suggest improved insulin secretion in response to anti-IL-1 therapy in these patients (79).

Both beta cells (374,397,398,425) and macrophages (419,489) are potential sources of pro-inflammatory cytokines within the islets of patients with type 2 diabetes. Healthy mouse islets each contain 8-10 macrophages in close association with the vascular endothelium. These cells are characterized by cell surface expression of CD11b, CD11c, F4/80, and MHC class II (415). Highly phagocytic and with limited migratory capacity, islet-resident monocyte-derived cells are functionally more similar to macrophages than dendritic cells (490) and play an important role in immune surveillance (415). Amyloid-associated macrophages are a major source of cytokines such as IL-1β in other amyloid diseases (491,492), and IAPP fibrils have been observed within human islet macrophage lysosomes (269). In Chapter 3, we found that clodronate liposome-mediated depletion of islet phagocytes eliminated a major source of *Il1b* mRNA expression in cultured hIAPP$^{Tg/o}$ islets, pointing to macrophages as potential mediators of

hIAPP-induced islet inflammation. The aim of this study was to determine whether hIAPP aggregates alter the phenotype of resident islet macrophages and to assess the consequences for islet function.

4.2 Results

4.2.1 Macrophages survive in islets cultured at 37°C in RPMI

To determine whether macrophages are present in cultured islets and might contribute to islet gene expression, we evaluated the proportion of $F4/80^{+}CD11b^{+}$ cells in isolated islets after 1 and 5 days in suspension culture in RPMI at 37°C (since 22°C culture has been shown to cause macrophage depletion (493)). Islets were dispersed and analyzed by flow cytometry according to the gating strategy in Figure 4.1. $F4/80^{+}CD11b^{+}$ cells comprised 1-2% of viable islet cells, a proportion that remained unchanged with culture (Figure 4.2A,B). Expression of MHC class II but not CD11b or F4/80 was significantly decreased after 5 days (Figure 4.2C), suggesting a phenotypic change but no alteration in cell number. Consistent with these data, expression of the macrophage genes *Emr1* and *Itgam* and the beta cell genes *Pdx1, Ins1,* and *Ins2* did not change during the culture period (Figure 4.2D).

4.2.2 Resident macrophages are required for stimulation of pro-inflammatory gene expression in pancreatic islets by synthetic hIAPP

To determine the effect of hIAPP on islet pro-inflammatory gene expression, we treated isolated islets with synthetic IAPP for 4 h. Both hIAPP and the TLR2/6 ligand FSL-1 induced expression of genes encoding the chemokines CCL2 and CXCL1 and the pro-inflammatory cytokines TNF-α, IL-6, IL-1α, and IL-1β in islets compared to non-amyloidogenic rIAPP (Figure 4.3A). We did not observe effects of hIAPP on IL-12 family members such as IL-12p40 (*Il12b*) or on the IL-1 family member IL-18, which like IL-1β is cleaved by the NLRP3 inflammasome (Figure 4.3A). Like FSL-1, hIAPP also caused increased expression of the anti-inflammatory genes *Il1rn* and *Il10* (encoding IL-10 and IL-1Ra, respectively), with no effect on IL-18bp, an endogenous antagonist at the IL-18 receptor. These data are consistent with previously-reported upregulation of anti-inflammatory cytokines in response to other acute pro-inflammatory stimuli and with their transcriptional regulation by NF-κB (494,495).

To determine the contribution of macrophages to hIAPP-induced islet inflammation, freshly-isolated islets were treated with clodronate-containing liposomes, which are selectively toxic to phagocytes (461). Clodronate reduced the number of F4/80-expressing islet cells as determined by immunostaining (Figure 4.4A) and reduced expression of macrophage but not beta cell markers (Figure 4.4B,C). Notably, phagocyte depletion completely prevented hIAPP-induced expression of both pro- and anti-inflammatory cytokines (Figure 4.3). *Ccl2* expression was reduced by only 80%, suggesting that non-phagocytic cells, likely beta cells as suggested in Chapter 3, also contribute to islet hIAPP-induced CCL2 production.

Phagocyte depletion also prevented hIAPP-induced upregulation of genes encoding the pattern recognition receptor TLR2 and the inflammasome components NLRP3 and caspase-1, with no effect on expression of the adaptor protein ASC (*Pycard*) (Figure 4.5A). These data indicate that macrophages are major contributors to hIAPP-induced expression of both pro- and anti-inflammatory cytokines in cultured islets and – at least in the presence of hIAPP or FSL-1 – the major source of innate immune receptors for hIAPP. Neither hIAPP nor clodronate liposome treatment affected expression of the ER stress markers CHOP (*Ddit3)* or BiP (*Hspa5)* (Figure 4.5B).

4.2.3 Synthetic hIAPP induces synthesis of mature IL-1β in macrophages but not other islet cell types

We next assessed the kinetics of IL-1β production in response to aggregating hIAPP. hIAPP but not rIAPP formed amyloid fibrils, as determined by a red shift in the thioflavin T emission spectrum (Figure 4.6A). ProIL-1β was markedly increased in hIAPP-treated BMDMs compared to rIAPP-treated cells within 2 h of exposure to freshly-dissolved peptide (Figure 4.6B,C), suggesting induction of proIL-1β synthesis by pre-fibrillar aggregates prior to the plateau phase of the hIAPP aggregation curve. IL-1β was detected by ELISA in BMDM supernatants after 24 h (Figure 4.6E) and confirmed by western blot to comprise the mature 17 kDa form (Figure 4.6F). Significant levels of mature IL-1β were not detected until 4-24 h after dissolution of the peptide (Figure 4.6F), suggesting that the NLRP3 inflammasome is activated by a fibrillar hIAPP species following stimulation of proIL-1β synthesis and inflammasome priming by pre-fibrillar hIAPP aggregates. No induction of IL-1β was detected in whole islets,

consistent with synthesis by a rare non-beta-cell population (Figure 4.6D,E). Indeed, total IL-1β protein was induced by hIAPP in $CD11b^+$ but not $CD11b^-$ islet cells, as determined by imaging flow cytometry (Figure 4.7A,B), suggesting that sub-toxic concentrations of hIAPP do not cause proIL-1β synthesis in beta cells. Furthermore, hIAPP caused a modest increase in caspase-1 activation only in $CD11b^+$ cells, as determined by both conventional (Figure 4.7E) and imaging (Figure 4.7C,D) flow cytometry, with caspase-1 puncta delineated by the fluorescent probe YVAD-FMK. Because over 98% of $CD11b^+$ islet cells were triple-positive for CD11b, F4/80, and CD11c (Figure 4.12B), $CD11b^+$ islet cells are primarily comprised of islet macrophages. Taken together, these data provide the first direct evidence that resident macrophages are the major islet cell type in which hIAPP stimulates IL-1β synthesis and secretion.

4.2.4 Transgenic mice with beta cell hIAPP expression have impaired islet function associated with an elevated ratio of pro- to anti-inflammatory cytokines

To determine whether hIAPP aggregation contributes to islet inflammation *in vivo*, female FVB mice expressing hIAPP under the control of the rat insulin promoter ($hIAPP^{Tg/o}$) were placed on HFD for 14 weeks, conditions that promote hIAPP aggregation but no detectable amyloid formation until approximately six months of age (211). HFD but not NCD caused elevated fasting glucose (Figure 4.8A) and impaired glucose tolerance (Figure 4.8B,C) in $hIAPP^{Tg/o}$ but not wild-type mice. Consistent with the previously reported resistance of FVB mice to weight gain on HFD (496), there was no significant difference in body weight among the four groups (Figure 4.8D). While no HFD-induced insulin resistance was detected by insulin tolerance testing (Figure 4.8E,F), HFD was associated with increased plasma insulin following i.p. glucose compared to NCD in wild-type mice (Figure 4.8G). $hIAPP^{Tg/o}$ mice did not exhibit this glucose-induced rise in plasma insulin on HFD vs. NCD, suggesting inadequate beta cell compensation (Figure 4.8G). Similarly, isolated islets from HFD-fed $hIAPP^{Tg/o}$ mice had reduced glucose-stimulated insulin secretion *ex vivo* compared to islets from wild-type mice (Figure 4.8H).

Expression of hIAPP in mice on both NCD and HFD was associated with upregulation of the macrophage markers *Emr1* and *Itgam* in isolated islets (Figure 4.9B), with no change in other immune cell markers including *Cd5*, *Cd19*, *Cd3ε*, and *Cd49b* (Figure 4.9A) or in the beta cell

genes *Pdx1* and *Ins2* (Figure 4.9C). HFD caused a marked decrease in expression of the anti-inflammatory cytokines *Il10* and *Il1rn* in both wild-type and hIAPP$^{Tg/o}$ islets (Figure 4.10B) and also decreased *Ccl2* expression (Figure 4.10A), with no other significant effects on islet gene expression. hIAPP$^{Tg/o}$ mice on HFD had increased islet expression of *Il1b* (Figure 4.10A) and *Nlrp3* (Figure 4.11A) compared to wild-type mice, with no other effects on pro-inflammatory cytokines (Figure 4.10A), TLR2 and inflammasome-related proteins (Figure 4.11A), or ER stress markers (Figure 4.11B). These data suggest that hIAPP aggregation is primarily associated with changes in the regulation of IL-1β synthesis. The ratio of *Il1b* to *Il1rn* was significantly increased in islets from hIAPP$^{Tg/o}$ HFD-fed mice compared to both hIAPP$^{Tg/o}$ and wild-type NCD-fed mice (Figure 4.10C), suggesting that conditions that promote IAPP aggregation alter the balance of islet pro- and anti-inflammatory mediators toward a pro-inflammatory milieu.

4.2.5 Transgenic hIAPP expression affects the phenotype but not the number of resident islet macrophages in HFD-fed FVB mice

Because hIAPP$^{Tg/o}$ islets express elevated mRNA encoding the macrophage markers CD11b and CD11c (Figure 4.9B), we next characterized intra-islet macrophages by flow cytometry. HFD caused a modest increase in the number of CD11b$^+$F4/80$^+$ cells relative to total islet cells, consistent with previous studies (401), while hIAPP expression had no effect on the proportion of CD11b$^+$F4/80$^+$ cells (Figure 4.12A,B), most of which were also CD11c$^+$ (Figure 4.12C). In HFD-fed mice, increased cell-surface expression of CD11b within the CD11b$^+$F4/80$^+$ population (Figure 4.12D,E) was consistent with the increase in *Itgam* expression in hIAPP$^{Tg/o}$ islets (Figure 4.12F). Both CD11c and Ly6C, expressed by inflammatory monocytes in other tissues (383,497), were upregulated in macrophages from hIAPP$^{Tg/o}$ mice along with CD11b (Figure 4.12D,E), with no evidence of a distinct CD11c$^+$ infiltrating population. No differences in CD11b or CD11c expression were observed in cells from the spleen or peripheral blood (Figure 4.14). Fluorescence-activated cell sorting (FACS) of CD11b$^+$F4/80$^+$ islet macrophages from HFD-fed mice (Figure 4.13A) revealed that these cells are the major source of TNF-α, IL-1β, and IL-1Ra, but not the sole source of CCL2, IL-6, or IL-10 (Figure 4.12B). The CD11b$^+$F4/80$^+$ population also expressed higher levels of mRNA encoding TLR2 and NLRP3 (Figure 4.13B) compared to other cell types. The increase in islet expression of *Il1b* and the

decrease in *Il10* and *Il1rn* in hIAPP$^{Tg/o}$ vs. wild-type islets were attributable to differential expression of these genes in islet macrophages (Figure 4.13B).

4.2.6 Systemic macrophage depletion improves IAPP-induced islet inflammation and glucose intolerance while increasing islet amyloid

To determine whether macrophage depletion alters hIAPP-induced islet gene expression *in vivo,* we treated HFD-fed hIAPP$^{Tg/o}$ and wild-type mice with clodronate liposomes or PBS control liposomes. Clodronate liposome administration caused a 3-4-fold reduction in islet *Itgam* and *Emr1* and a modest increase in beta cell *Pdx1* expression, with no effect on *Ins1* or *Ins2* mRNA (Figure 4.15A). Consistent with our *in vitro* macrophage depletion, clodronate liposome administration reduced islet expression of *Il1b* and *Tnf,* and to a lesser extent *Il6* and *Ccl2* (Figure 4.15B). Macrophage depletion also reduced islet expression of the anti-inflammatory cytokines *Il1rn* and *Il10* (Figure 4.15B), although the latter was not affected in hIAPP$^{Tg/o}$ mice in which its expression was already significantly reduced relative to wild-type. Clodronate liposome treatment also significantly decreased islet *Nlrp3* expression but had no effect on *Tlr2*, suggesting significant expression (but not necessarily hIAPP-induced activation) of this pattern recognition receptor by other islet cell types.

Clodronate liposome administration did not significantly affect fasting glycemia (Figure 4.16A) but dramatically improved glucose tolerance in hIAPP$^{Tg/o}$ but not wild-type mice (Figure 4.16B,C). Clodronate liposomes also caused a mild improvement in insulin sensitivity in both hIAPP$^{Tg/o}$ and wild-type mice (Figure 4.16E,F), with no change in body weight (Figure 4.16D). Importantly, islets isolated from clodronate-liposome-treated hIAPP$^{Tg/o}$ mice displayed improved *ex vivo* glucose-stimulated insulin secretion compared to islets from mice treated with control liposomes, with no change in insulin content (Figure 4.16G, H). Moreover, islets pre-treated with clodronate liposomes prior to culture under conditions that promote amyloid formation had increased insulin content (Figure 4.17A) and improved glucose-stimulated insulin secretion (Figure 4.17B), providing further evidence that macrophage depletion affects islet function independent of systemic effects. Taken together, these data suggest that islet macrophages impair islet function in the presence of hIAPP and that they are the major source of both pro- and anti-inflammatory cytokines in islets *in vivo.*

Because islet macrophages could contribute to either the formation of islet amyloid (by inducing beta cell dysfunction) or its clearance (by removing IAPP aggregates), we next asked whether macrophage depletion affects amyloid severity. We generated obese hIAPP$^{Tg/o}$ mice expressing the agouti viable yellow allele (A^{vy}-hIAPP$^{Tg/o}$), since these mice develop extensive islet amyloid associated with beta cell dysfunction (194). Islet macrophages were frequently found associated with thioflavin-S-positive amyloid fibrils in A^{vy}- hIAPP$^{Tg/o}$ mice (Figure 4.18A). Clodronate liposome treatment significantly reduced fasting hyperglycemia in A^{vy}-hIAPP$^{Tg/o}$ mice but not wild-type littermate controls (Figure 4.18B). As in the HFD-fed FVB mice, clodronate liposome administration reduced islet *Il1b* and increased *Pdx1* expression (Figure 4.18C). Interestingly, the improved glycemia in clodronate-liposome-treated mice was associated with increased, rather than decreased, amyloid severity (Figure 4.18D,E) and an increase in the average area of each amyloid deposit (Figure 4.18F) with no change in islet area (Figure 4.18G). These data point to a discordance between amyloid deposition and islet function and suggest that pre-fibrillar hIAPP aggregates (present in the absence of thioflavin-S-positive plaques) rather than mature fibrils are the major species associated with islet dysfunction in this model.

4.3 Discussion

Anti-inflammatory agents represent a promising approach to treat type 2 diabetes, and several recent clinical trials have suggested that targeting IL-1 signalling can improve insulin secretion (79). Indeed, recombinant IL-1Ra improves beta cell function in patients with type 2 diabetes without altering insulin sensitivity (361), suggesting that islets are particularly susceptible to IL-1-mediated damage. In Chapter 3, we provided evidence that hIAPP acts as a potent stimulus for macrophage activation and islet chemokine release, with a critical role for IL-1β in amplification of this response. Because phagocytic cells help clear other amyloidogenic peptides (327), resident islet macrophages might also protect beta cells from IAPP aggregates. The major finding of the current study is that phagocytic cells – despite their possible role in limiting extracellular amyloid – are required for IAPP-induced islet inflammation and dysfunction.

Previous studies have demonstrated depletion of up to 98% of islet macrophages after 4-7 days of low temperature culture at 22-24°C in CMRL (489,493,498). Macrophage depletion in RPMI at 37°C has also been reported based on reduced MHC class II staining (499,500). Our data suggest no change in the size of the islet macrophage population based on CD11b and F4/80 expression after 5 days in RPMI at 37°C, despite decreased MHC class II expression. Thus, macrophages must be considered a major source of both pro- and anti-inflammatory cytokines in cultured islets. Indeed, macrophages were required for islet cytokine induction by both hIAPP and the TLR2 ligand FSL-1, although *Ccl2* expression levels were similar in FACS-sorted macrophages compared to other cell types, consistent with beta cell production of CCL2 (419,488).

These data provide the first direct evidence that resident macrophages are the major source of hIAPP-induced islet IL-1β. Masters *et al.* were unable to detect IL-1β in supernatants from hIAPP-treated islets (477), consistent with our western blot and ELISA data suggesting that the islet macrophage population is too small to significantly affect total islet IL-1β. One previous report used immunocytochemistry to demonstrate IL-1β expression induced by LPS and TNF-α in islet macrophages but not beta cells (498), although beta cells may be an important source of IL-1β in response to other stimuli, including double-stranded RNA and elevated glucose (374,397,398,425,501). Our data point to a model in which pre-fibrillar IAPP aggregates contribute to priming of the NLRP3 inflammasome and induction of *Il1b* mRNA in resident macrophages but not beta cells. NLRP3 activation by larger IAPP species likely occurs later in the course of hIAPP aggregation, when we observed cleavage of proIL-1β. Thus, like other amyloidogenic peptides, hIAPP delivers both signal 1 (for proIL-1β expression) and signal 2 (for proIL-1β processing) required for IL-1β secretion. Interestingly, we also observed limited induction of proIL-1β in BMDMs treated with non-amyloidogenic rIAPP (Figure 4.6). Monomeric IAPP is a weak agonist for the calcitonin gene-related peptide (CGRP) receptor (502), and since CGRP can enhance IL-1β synthesis (503), it is possible that rIAPP may also exert its effects via this pathway. This observation is unlikely to be due to microbial contaminants in the synthetic peptide as rIAPP did not activate TLR2 and neither rIAPP nor hIAPP activated TLR4 (Figure 3.8). Furthermore, proIL-1β induction was not observed in

rIAPP-treated islet macrophages by imaging flow cytometry and may therefore be cell-type-specific.

The most striking differences in gene expression in islets from hIAPP$^{Tg/o}$ vs. wild-type mice were increased expression of *Itgam, Emr1,* and *Il1b* concomitant with decreased *Il1rn* and *Il10* expression. This gene expression profile resembles that in the cerebral cortex of a mouse model of Alzheimer's disease (504). Notably, while IL-1 induces other islet cytokines and our analyses in Chapter 3 point to an important role for regulation of IL-1 family members by hIAPP, amyloid formation cannot explain all changes in islet cytokine content associated with type 2 diabetes, including upregulation of IL-12 (505). Moreover, upregulation of some cytokines in response to acute stimulation with hIAPP *in vitro* did not completely mimic the effects of chronic hIAPP aggregation *in vivo.* For example, although *Il1b* and *Nlrp3* expression were elevated in both situations, hIAPP$^{Tg/o}$ islets did not express increased *Tlr2, Tnf,* or *Ccl2* mRNA, unlike hIAPP-treated BMDMs. Furthermore, both *Il10* and *Il1rn* – decreased in islets from hIAPP$^{Tg/o}$ mice, particularly on HFD – were induced acutely in culture, consistent with shared signalling pathways concomitantly mediating both pro- and anti-inflammatory gene expression in response to other stimuli such as LPS (494). As both the extent of IAPP aggregation and the activation state of the macrophage population likely determine the nature of the local inflammatory response, further work is required to evaluate the mechanisms responsible for alterations in cytokine expression at different stages of amyloid formation and their implications for macrophage function during disease progression.

Interestingly, altered expression of *Il1b, Il1rn*, and *Il10* was observed in NCD-fed hIAPP$^{Tg/o}$ mice with no detectable metabolic abnormality, suggesting that hyperglycemia was not a cause of this phenotype. That these changes did not correlate with islet dysfunction except in mice on HFD suggests that (a) some hIAPP aggregation occurs in hIAPP$^{Tg/o}$ mice on NCD, and precedes the development of glucose intolerance; and (b) HFD may both promote amyloid formation and alter the phenotype of macrophages leading to decreased expression of cytokines such as IL-10 and IL-1Ra that inhibit the synthesis or antagonize the actions of IL-1β (506). While we cannot be certain that altered macrophage cytokine secretion is the cause of beta cell dysfunction in this model, Chapter 5 of this thesis suggests that hIAPP-induced islet dysfunction is improved with IL-1Ra treatment, both in cultured islets and in hIAPP$^{Tg/o}$ mice. Moreover, the

improvement in glucose tolerance in hIAPP$^{Tg/o}$ mice lacking islet macrophages suggests that these cells play a critical role in hIAPP-induced islet dysfunction.

Eguchi *et al.* reported that the majority of resident CD11b^{+} islet cells did not express the granulocyte marker Ly6G, were positive for the macrophage/monocyte marker F4/80, and expressed increased *Il10* and decreased *Il1b* compared to infiltrating monocytes following palmitate infusion (419). We did not observe a distinct infiltrating population in our model, but instead a skewing in the resident population away from a physiological M2-like phenotype (419). Ly6C^{high} monocytes are recent immigrants from the bone marrow and have the capacity to migrate to sites of acute peripheral inflammation (507). The beta-2 integrins CD11b and CD11c have diverse functions including adhesion and phagocytosis (508). We observed increased expression of these three cell-surface glycoproteins in macrophages from hIAPP$^{Tg/o}$ islets, associated with elevated *Il1b* and decreased *Il1rn* and *Il10* expression. Macrophages that migrate into adipose tissue during high fat feeding also express elevated CD11b, CD11c, F4/80, and Ly6C compared to resident tissue macrophages, and this M1-like subpopulation is highly pro-inflammatory (383,509). Our data suggest that hIAPP aggregation may affect the differentiation state of monocytes entering the islet and that hIAPP skews resident cells toward a pro-inflammatory phenotype, consistent with the microenvironment driving macrophage plasticity (510). Although we did not detect changes in granulocyte, lymphocyte, or NK cell markers associated with hIAPP expression, further work will be required to fully characterize other intra-islet leukocyte populations associated with amyloid formation, including infiltrating F4/80^{-} CD11b^{-}CD11c^{-} macrophages (420).

Other studies have demonstrated improved insulin sensitivity in response to clodronate liposomes (511). While we cannot rule out effects on the islet secondary to macrophage depletion in other tissues, wild-type mice displayed no change in glucose tolerance in response to clodronate liposomes, suggesting a unique role for macrophages in the setting of hIAPP aggregation. We observed improved glucose-stimulated insulin secretion in isolated islets from clodronate-liposome-treated hIAPP$^{Tg/o}$ mice and in clodronate-liposome-treated hIAPP$^{Tg/o}$ islets cultured in high glucose, conditions demonstrated by others to promote amyloid formation (512). Thus, we believe that improved beta cell function caused by macrophage depletion *in vivo* is largely independent of peripheral effects. Interestingly, despite improved glucose tolerance,

macrophage depletion was associated with increased islet amyloid in hIAPP$^{Tg/o}$ mice. This observation may be attributed to increased fibril formation - perhaps due to reduced clearance of pre-fibrillar oligomers - or to decreased clearance of mature fibrils, which are phagocytosed by macrophages (270). Importantly, mature IAPP fibrils may be less damaging to the islet than pre-fibrillar oligomers (212), consistent with the discordance between increased fibril deposition and reduced fasting glycemia in our model. The extent of amyloid deposition at the beginning of treatment and macrophage activities other than cytokine secretion are likely critical in determining the islet amyloid burden.

In Chapter 3, we found that both TLR2 and caspase-1 are activated by hIAPP (with direct evidence for NLRP3 activation provided by Masters *et al.* (477)). Here, we found that both *Tlr2* and *Nlrp3* are upregulated in islets treated with synthetic hIAPP, and that in the presence of a stimulus such as hIAPP or FSL-1 the islet macrophage is the major islet source of their gene expression. Similarly, FACS-sorted islet macrophages from both wild-type and hIAPP$^{Tg/o}$ mice expressed higher levels of both receptors than other islet cell types, although only *Nlrp3* was upregulated in islets from hIAPP$^{Tg/o}$ mice. Clodronate liposome administration *in vivo* caused significant depletion of *Nlrp3* but not *Tlr2* expression. Thus, islet macrophages are likely a major source of NLRP3 activity within the islet, and they upregulate NLRP3 expression – a limiting step in inflammasome activation and proIL-1β processing – in the presence of hIAPP. On the other hand, endocrine cells appear to make a significant contribution to islet TLR2 expression, which is unaffected by hIAPP aggregation *in vivo*, perhaps reflecting an inability of these cells to mount a pro-inflammatory response to hIAPP. In some instances, relative gene expression levels determined by different methods gave discordant results; for example TLR2 expression was increased in response to hIAPP in the CD11b^{+}F4/80^{+} population when assessed by FACS, even though TLR2 expression was not affected by clodronate liposome-mediated macrophage depletion. This apparent discrepancy may reflect activation of cells during FACS or a response to necrotic debris generated by clodronate liposome-mediated macrophage cell death.

Islet macrophages contribute to beta cell dysfunction by secreting IL-1β and other cytokines (489,493,498), although low levels of IL-1β are also important for normal beta cell function (425,513). Our findings suggest that resident islet macrophages, by chronic production of IL-1β in response to IAPP aggregates, may be important contributors to the pathogenesis of

type 2 diabetes. Indeed, our data point to islet macrophages as the major source of islet IL-1β in response to IAPP aggregation. The studies presented in Chapter 5 of this thesis provide further evidence that IL-1 contributes to IAPP-induced islet inflammation and dysfunction *in vivo*. Thus, despite their apparent capacity to limit extracellular amyloid fibrils, inhibition of the interaction between macrophages and IAPP and suppression of macrophage IL-1β synthesis are potential therapeutic strategies to improve beta cell function in type 2 diabetes.

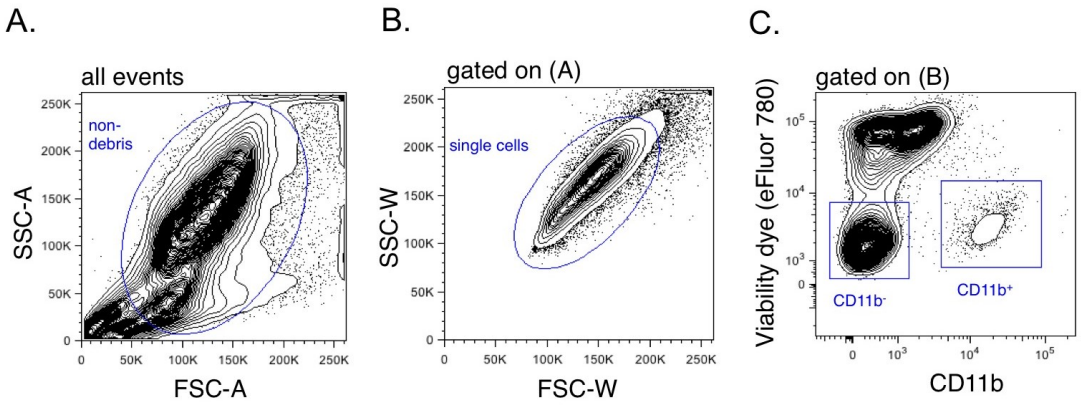

Figure 4.1. Gating strategy for flow cytometric analysis of islet macrophages. Islets were dispersed and analyzed by flow cytometry. (A) Events were gated to exclude debris. (B) Events were gated to exclude doublets. (C) Single cells were gated for analysis of viable $CD11b^+$ and $CD11b^-$ islet cells.

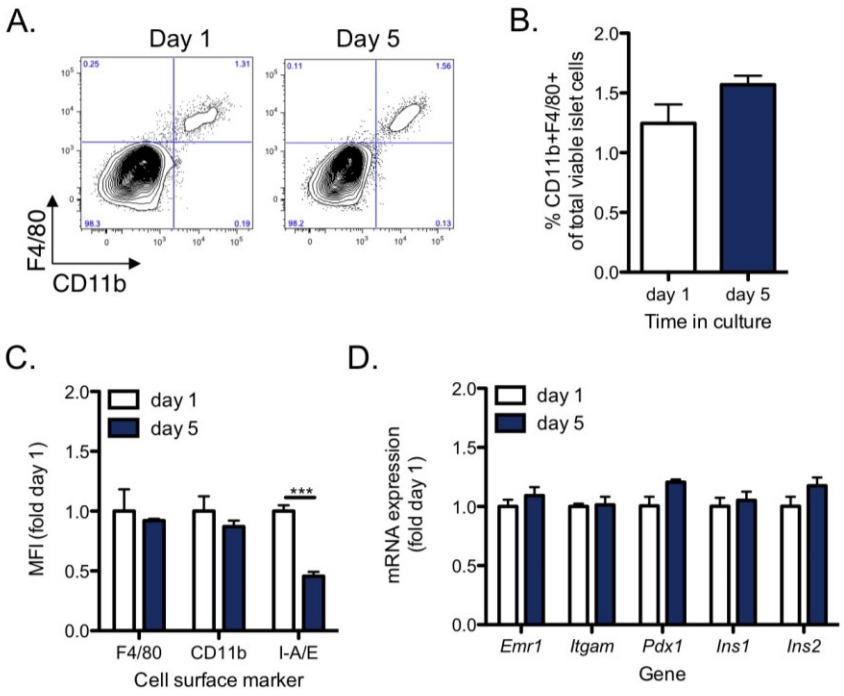

Figure 4.2. Resident macrophages survive in cultured mouse islets. Islets were isolated from 12-week-old C57BL/6 mice and cultured for 1 or 5 days in RPMI at 37°C. (A) Islets were dispersed for analysis of F4/80 and CD11b expression by flow cytometry. (B) The proportion of $CD11b^{+}F4/80^{+}$ cells among all viable islet cells and (C) the mean fluorescence intensity of the indicated cell surface marker were assessed at each time point. (D) mRNA expression of macrophage and beta cell genes was assessed by RT-qPCR. Expression levels were normalized to the housekeeping gene *Rplp0*. *** $p<0.001$. Data represent mean±SEM of islets from 3 mice and are representative of 2 independent experiments.

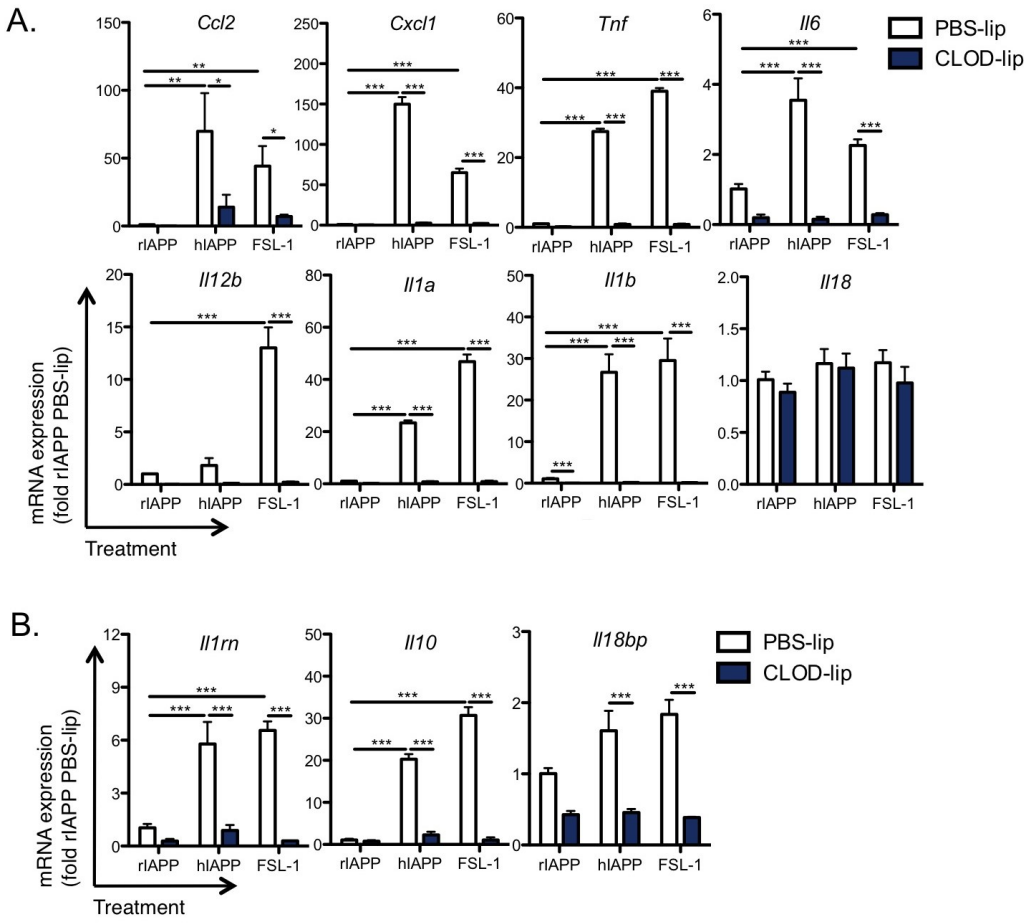

Figure 4.3. Induction of islet pro-inflammatory gene expression by hIAPP is dependent on resident macrophages. Islets were isolated from 12-week-old C57BL/6 mice and immediately treated with clodronate-containing liposomes (CLOD-lip, 1 mg/ml clodronate) or control liposomes (PBS-lip) for 36 h. Islets were washed and allowed to recover for 6 h prior to incubation with hIAPP (10 μM) or the TLR2 ligand FSL-1 (10 ng/ml) for 4 h. mRNA expression of (A) pro-inflammatory and (B) anti-inflammatory cytokines was assessed by RT-qPCR and expression levels were normalized to the housekeeping gene *Rplp0.* Data represent mean±SEM of islets from 4 mice and are representative of 3 independent experiments. * $p<0.05$, ** $p<0.01$, *** $p<0.001$.

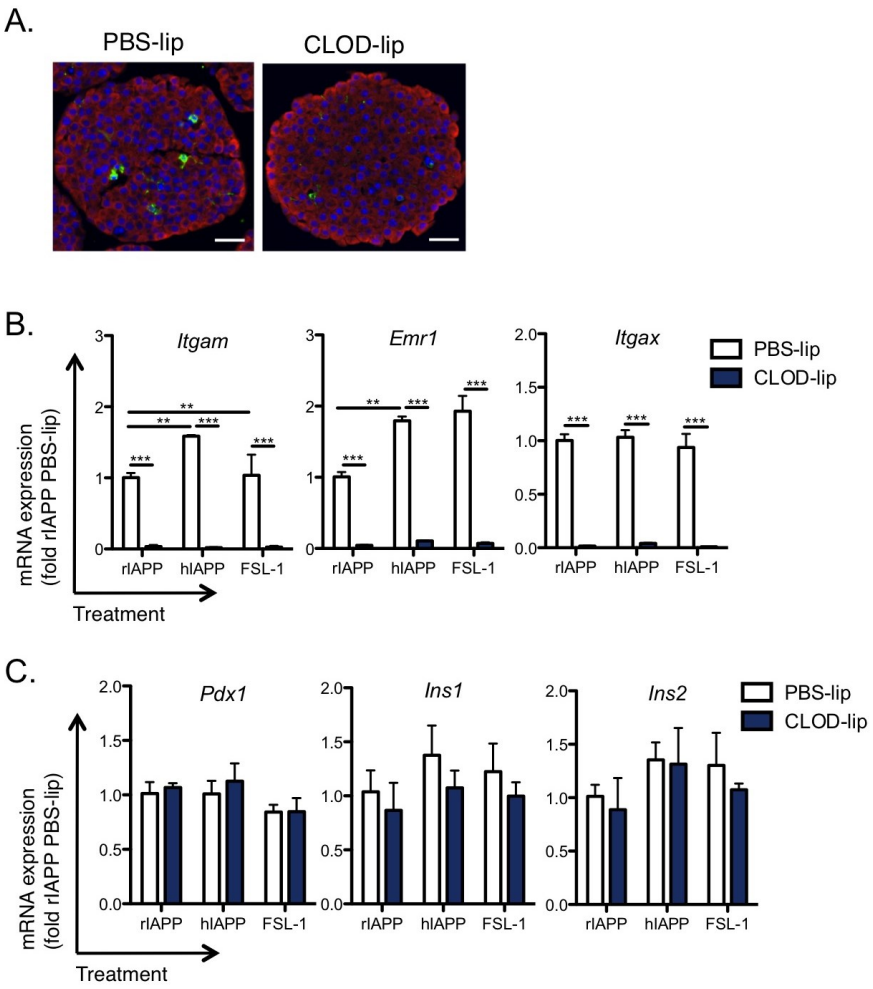

Figure 4.4. Clodronate treatment of islets depletes resident macrophages *in vitro*. Islets were isolated from 12-week-old C57BL/6 mice and immediately treated with clodronate-containing liposomes (CLOD-lip, 1 mg/ml clodronate) or control liposomes (PBS-lip) for 36 h. (A) Islets were fixed with 10% formalin and sections were stained for insulin (red), F4/80 (green), and DAPI (blue). Scale bar: 25 μm. Remaining islets were washed and allowed to recover for 6 h prior to incubation with hIAPP (10 μM) or the TLR2 ligand FSL-1 (10 ng/ml) for 4 h. mRNA expression of (B) macrophage and (C) beta cell markers was assessed by RT-qPCR and expression levels were normalized to the housekeeping gene *Rplp0.* Data represent mean±SEM of islets from 4 mice and are representative of 3 independent experiments. * $p<0.05$, ** $p<0.01$, *** $p< 0.001$.

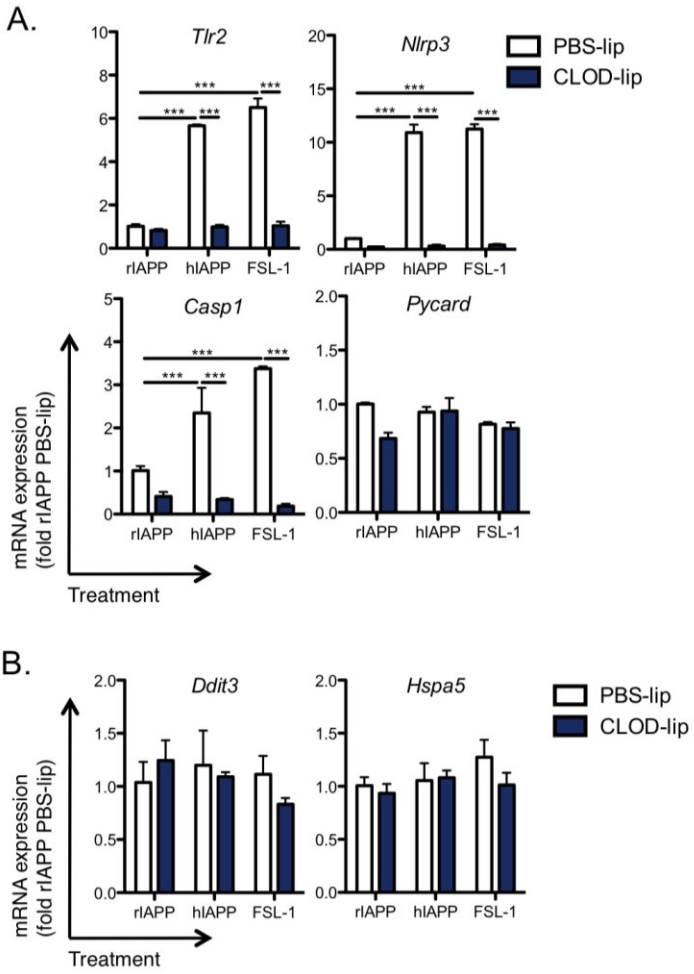

Figure 4.5. hIAPP induces macrophage-dependent expression of PRRs but not ER stress markers in cultured islets. Islets were isolated from 12-week-old C57BL/6 mice and immediately treated with clodronate-containing liposomes (CLOD-lip, 1 mg/ml clodronate) or control liposomes (PBS-lip) for 36 h. Islets were washed and allowed to recover for 6 h prior to incubation with hIAPP (10 μM) or the TLR2 ligand FSL-1 (10 ng/ml) for 4 h. mRNA expression of (A) inflammasome proteins and (B) ER stress markers was assessed by RT-qPCR and expression levels were normalized to the housekeeping gene *Rplp0.* Data represent mean±SEM of islets from 4 mice and are representative of 3 independent experiments. * $p<0.05$, ** $p<0.01$, *** $p<0.001$.

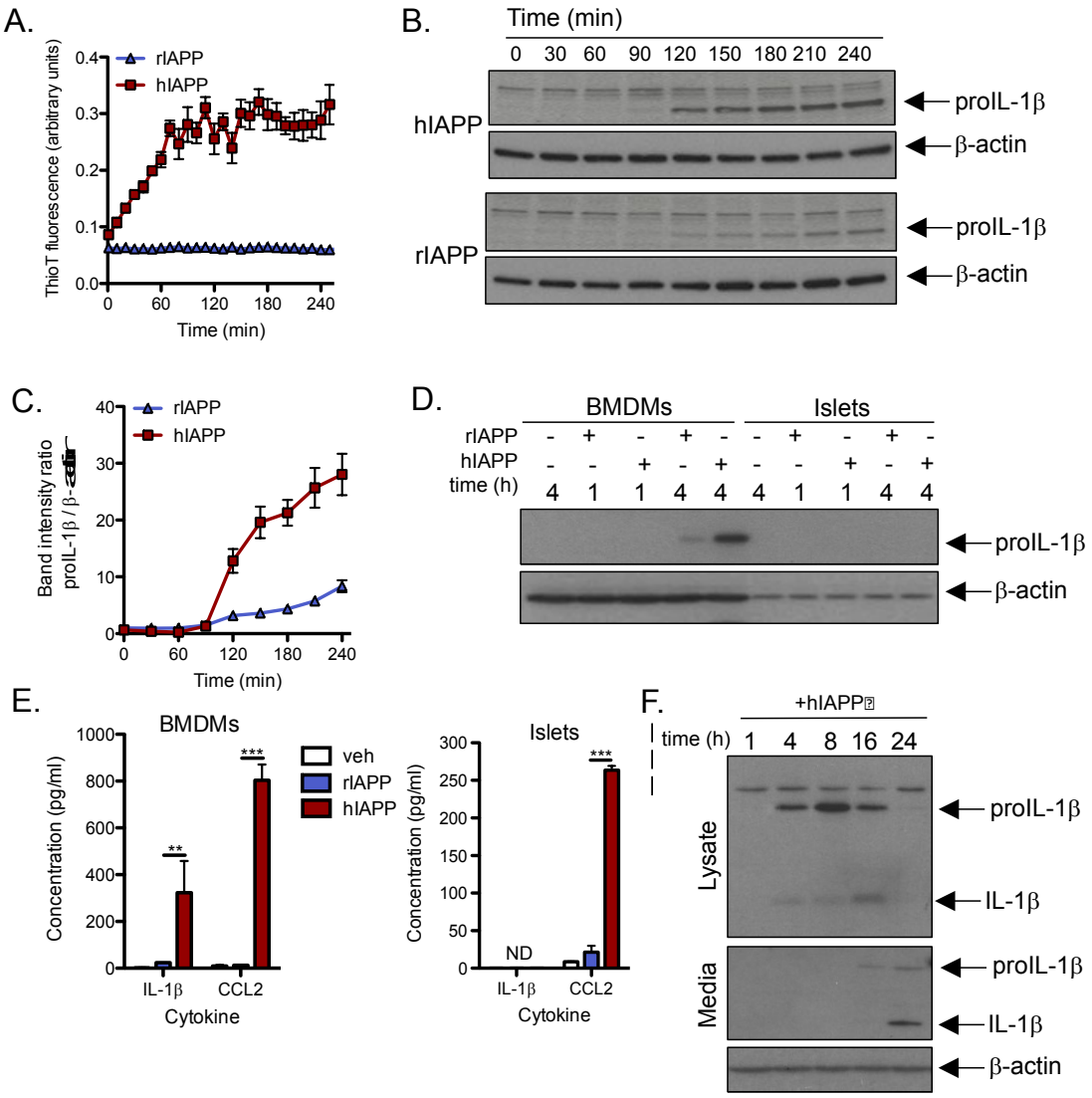

Figure 4.6. hIAPP induces detectable proIL-1β synthesis and mature IL-1β secretion by BMDMs but not whole islets. (A) IAPP (10 μM) was dissolved in DMEM and fibril formation was monitored by thioflavin T fluorescence. (B) hIAPP or rIAPP was added to BMDMs immediately following dissolution and cells were lysed at the indicated time points for analysis of IL-1β expression by western blot using an antibody that detects both proIL-1β (~35 kDa) and mature IL-1β (~17 kDa). (C) Expression of proIL-1β relative to β-actin was quantified by band densitometry and was significantly upregulated by hIAPP after 120 min (p<0.001; no mature IL-1β was detected during this time course). (D) IL-1β protein expression was evaluated in BMDMs and whole islets following 1 or 4 h culture with rIAPP or hIAPP (10 μM). (E) IAPP-induced secretion of IL-1β by BMDMs and islets was evaluated by ELISA after 24 h. (F) Lysates and media were assessed for proIL-1β and mature IL-1β content by western blot. veh: vehicle control. ** p<0.01, *** p<0.001. Data represent mean±SD of 3 replicates (A,C,E) and are representative of 3 independent experiments.

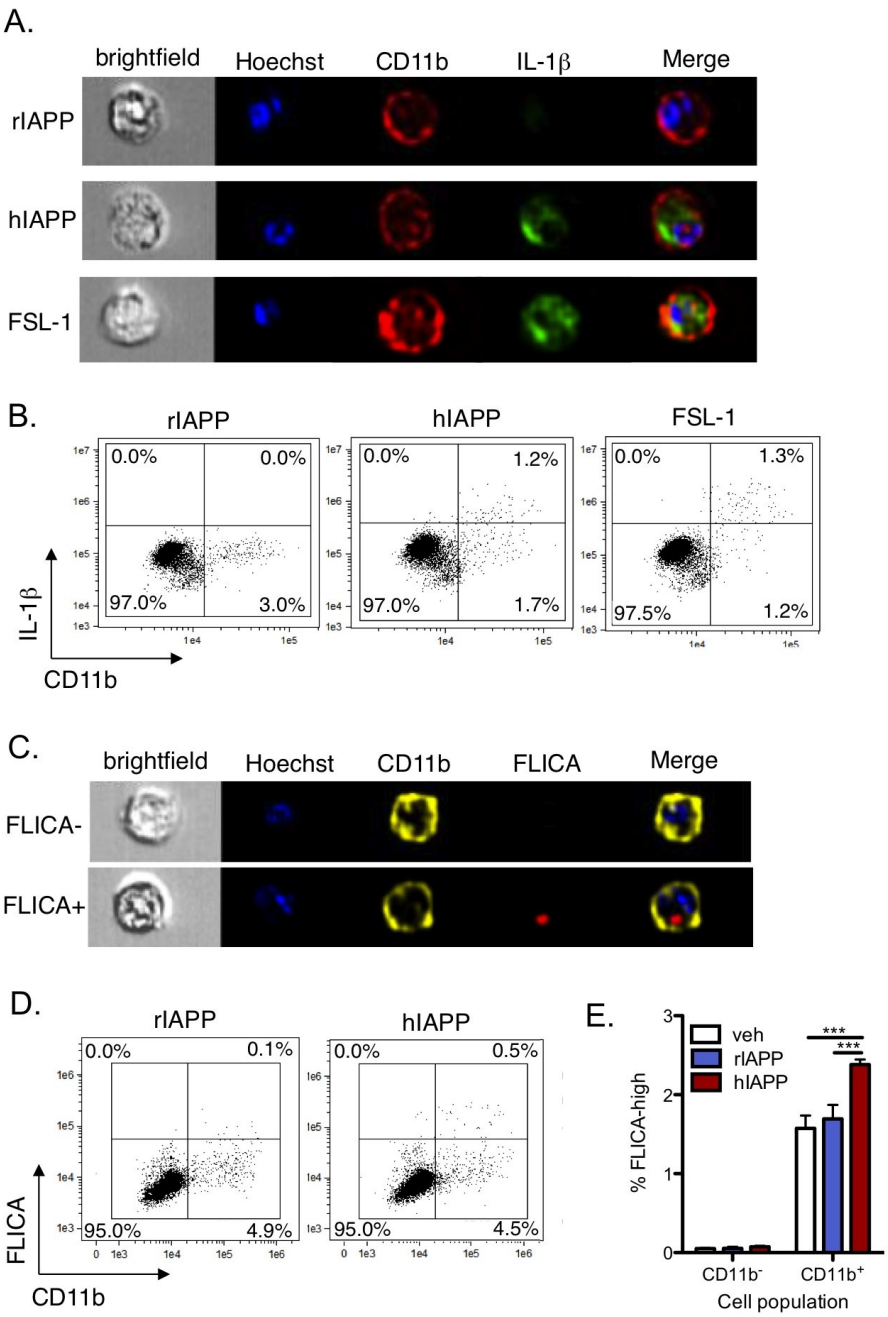

Figure 4.7. Islet macrophages are the major source of hIAPP-induced IL-1β. (A,B) Total IL-1β protein levels in whole islets treated for 4 h with IAPP (10 μM) or FSL-1 (10 ng/ml) were determined by immunofluorescence staining and ImageStream^X analysis with representative images of CD11b$^+$ cells shown in (A). Plots in (B) show all single islet cells. Caspase-1 activation in dispersed islets was analyzed by quantification of FLICA binding by (C,D) ImageStream^X analysis and (E) conventional flow cytometry, with representative examples of caspase-1-positive CD11b$^+$ cells shown in (C). Data represent mean±SEM of 3 independent experiments (E). Images are representative of 3 independent experiments. veh: vehicle control. *** p<0.001.

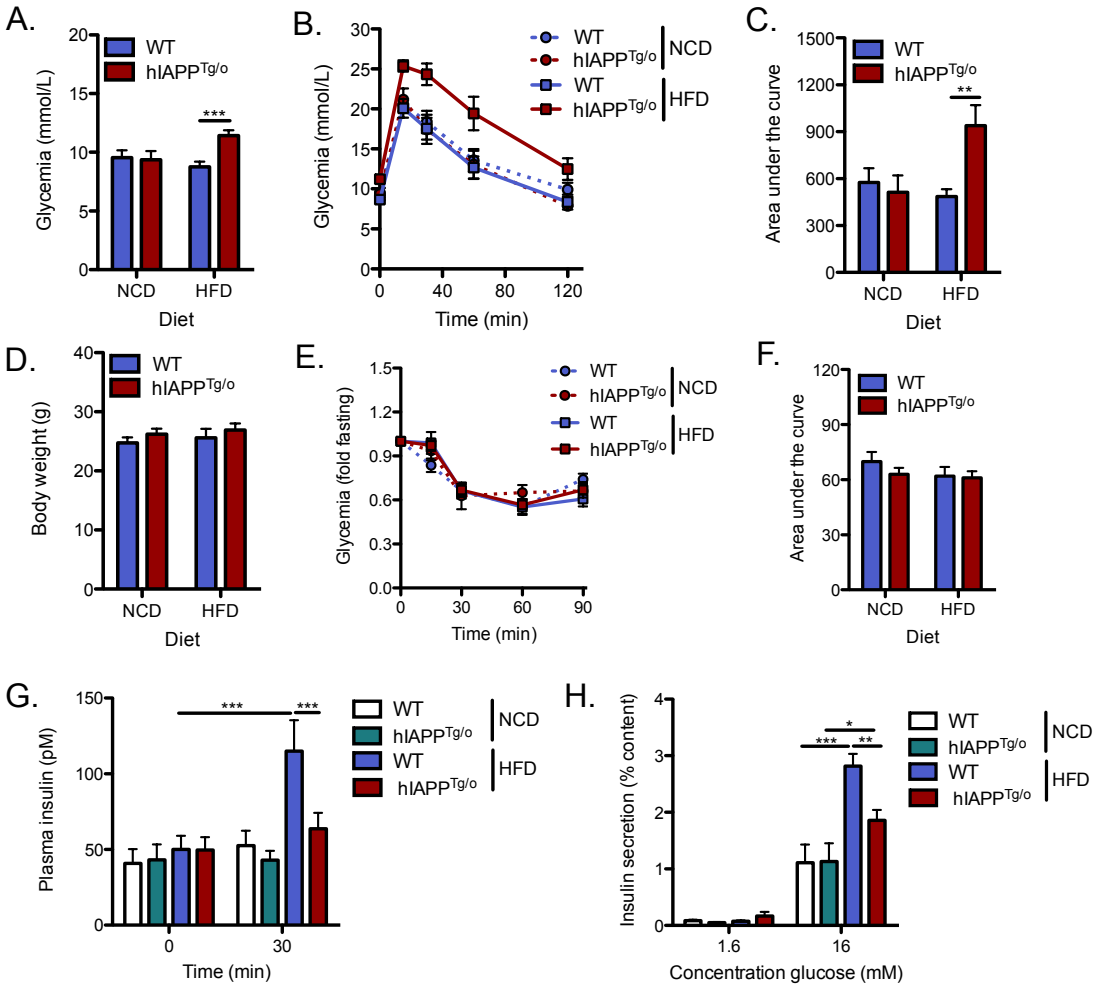

Figure 4.8. Transgenic mice with beta cell hIAPP expression have impaired islet function on HFD. Female FVB hIAPP$^{Tg/o}$ mice and wild-type littermate controls (WT) were placed on NCD (13% kcal from fat) or HFD (45% kcal from fat) for 14 weeks starting at 10 weeks of age. (A) Fasting glycemia and (B) glucose tolerance were assessed at 14 weeks following i.p. injection of 0.75 g/kg glucose and evaluation of (C) area under the glycemia curve up to 120 min (baseline = fasting glycemia). FVB mice were resistant to weight gain on HFD, as determined by (D) body weight assessed at 24 weeks of age. (E) Insulin sensitivity was evaluated by i.p. injection of 1 U/kg insulin and (F) evaluation area under the glycemia curve up to 60 min (baseline = 1.0). (G) Plasma insulin during IPGTT was measured by ELISA. (H) Glucose-stimulated insulin secretion in isolated islets was measured by ELISA and normalized to insulin content, which did not differ among groups. Data represent mean±SEM of 9-14 mice per group and are representative of 3 independent experiments. * p<0.05, ** p<0.01, *** p<0.001.

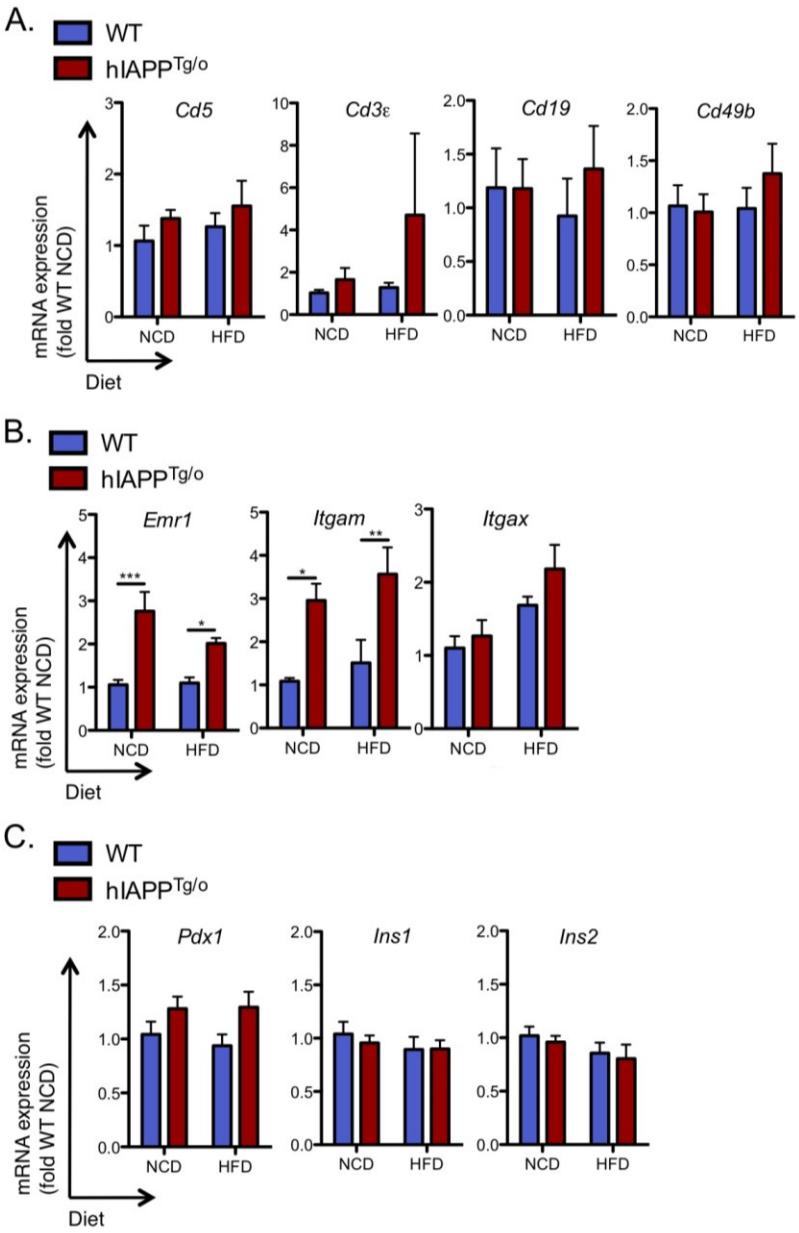

Figure 4.9. Islets from hIAPP$^{Tg/o}$ mice express increased macrophage markers. Female FVB hIAPP$^{Tg/o}$ mice and wild-type littermate controls (WT) were placed on NCD (13% kcal from fat) or HFD (45% kcal from fat) for 14 weeks starting at 10 weeks of age. Islets were isolated and allowed to recover for 4 h prior to gene expression analysis. mRNA expression of (A) leukocyte markers, (B) macrophage markers, and (C) beta cell genes was assessed by RT-qPCR. Expression levels were normalized to the housekeeping gene *Rplp0.* Data represent mean±SEM of 9-14 mice per group and are representative of 3 independent experiments. * $p<0.05$, ** $p<0.01$, *** $p<0.001$.

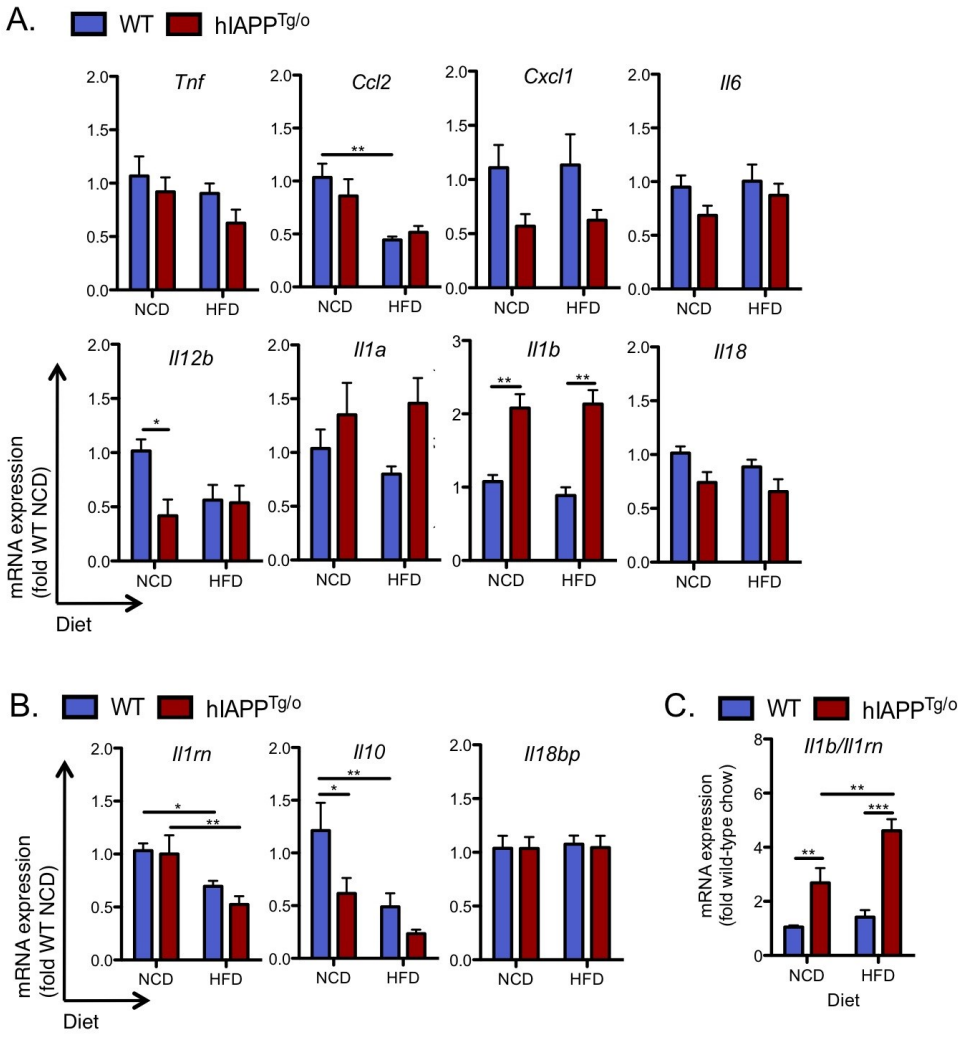

Figure 4.10. Islets from hIAPP$^{Tg/o}$ mice express an elevated ratio of pro- to anti-inflammatory cytokines. Female FVB hIAPP$^{Tg/o}$ mice and wild-type littermate controls (WT) were placed on NCD (13% kcal from fat) or HFD (45% kcal from fat) for 14 weeks starting at 10 weeks of age. Islets were isolated and allowed to recover for 4 h prior to gene expression analysis. mRNA expression of (A) pro-inflammatory cytokines and chemokines, (B) anti-inflammatory cytokines, and (C) the ratio of *Il1b* to the endogenous antagonist encoded by *Il1rn* was assessed by RT-qPCR. Expression levels were normalized to the housekeeping gene *Rplp0*. Data represent mean±SEM of 9-14 mice per group and are representative of 3 independent experiments. * $p<0.05$, ** $p<0.01$, *** $p<0.001$.

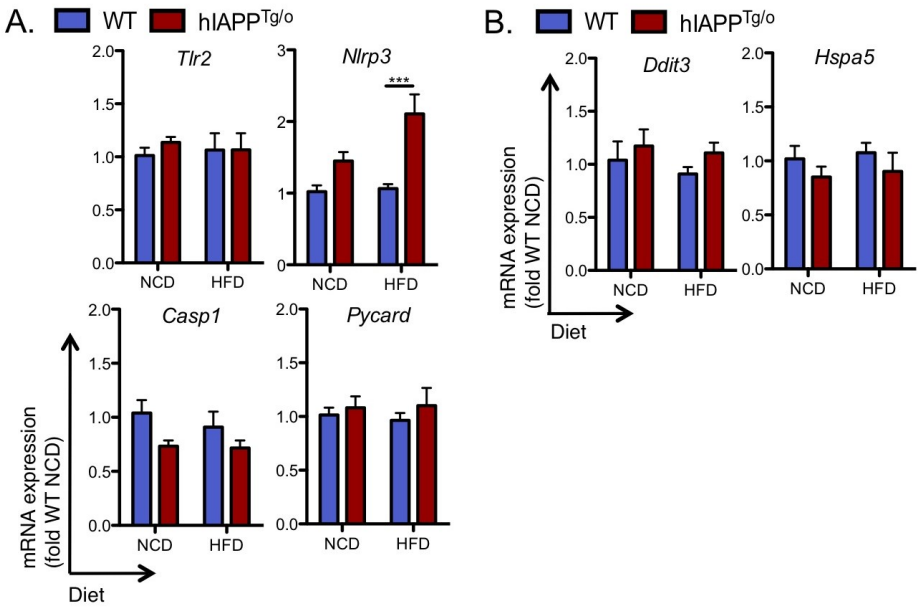

Figure 4.11. Islets from hIAPP$^{Tg/o}$ mice express increased *Nlrp3* with no change in other inflammasome components or ER stress markers. Female FVB hIAPP$^{Tg/o}$ mice and wild-type littermate controls (WT) were placed on NCD (13% kcal from fat) or HFD (45% kcal from fat) for 14 weeks starting at 10 weeks of age. Islets were isolated and allowed to recover for 4 h prior to gene expression analysis. mRNA expression of (A) inflammasome-related proteins and (B) ER stress markers was assessed by RT-qPCR. Expression levels were normalized to the housekeeping gene *Rplp0.* Data represent mean±SEM of 9-14 mice per group and are representative of 2 independent experiments. * $p<0.05$, ** $p<0.01$, *** $p<0.001$.

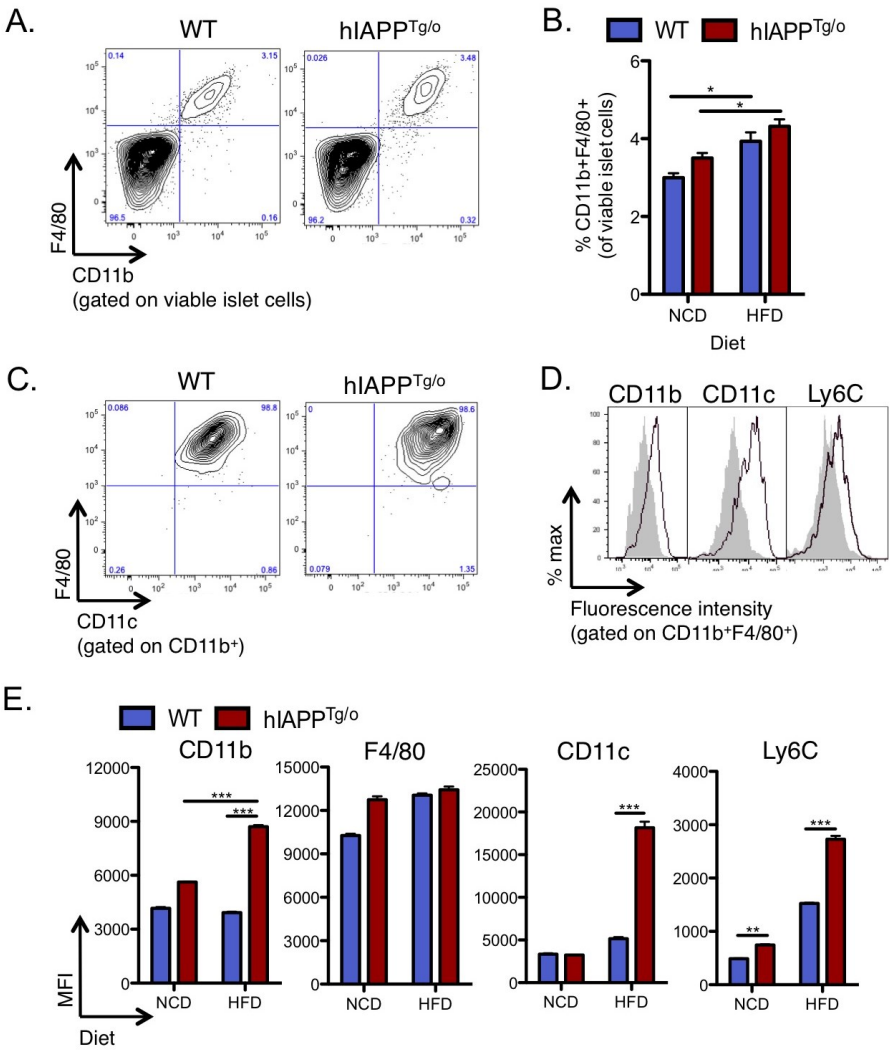

Figure 4.12. Beta cell expression of hIAPP has no effect on size of the CD11b^{+}F4/80^{+} population but alters islet macrophage phenotype. Female FVB hIAPP$^{Tg/o}$ mice and wild-type littermate controls (WT) were placed on NCD (13% kcal from fat) or HFD (45% kcal from fat) for 14 weeks starting at 10 weeks of age. Islets were isolated and dispersed for flow cytometric analysis. (A) Representative plots show staining of macrophages from HFD-fed mice gated on all islet cells, (C) CD11b^{+} cells, and (D) CD11b^{+}F4/80^{+} cells. (B) Proportion of CD11b^{+}F4/80^{+} cells relative to all viable islet cells. (E) Mean fluorescence intensity of the indicated cell surface marker. Data represent mean±SEM of 6-9 mice per group and are representative of 2 independent experiments. * p<0.05, ** p<0.01, *** p<0.001.

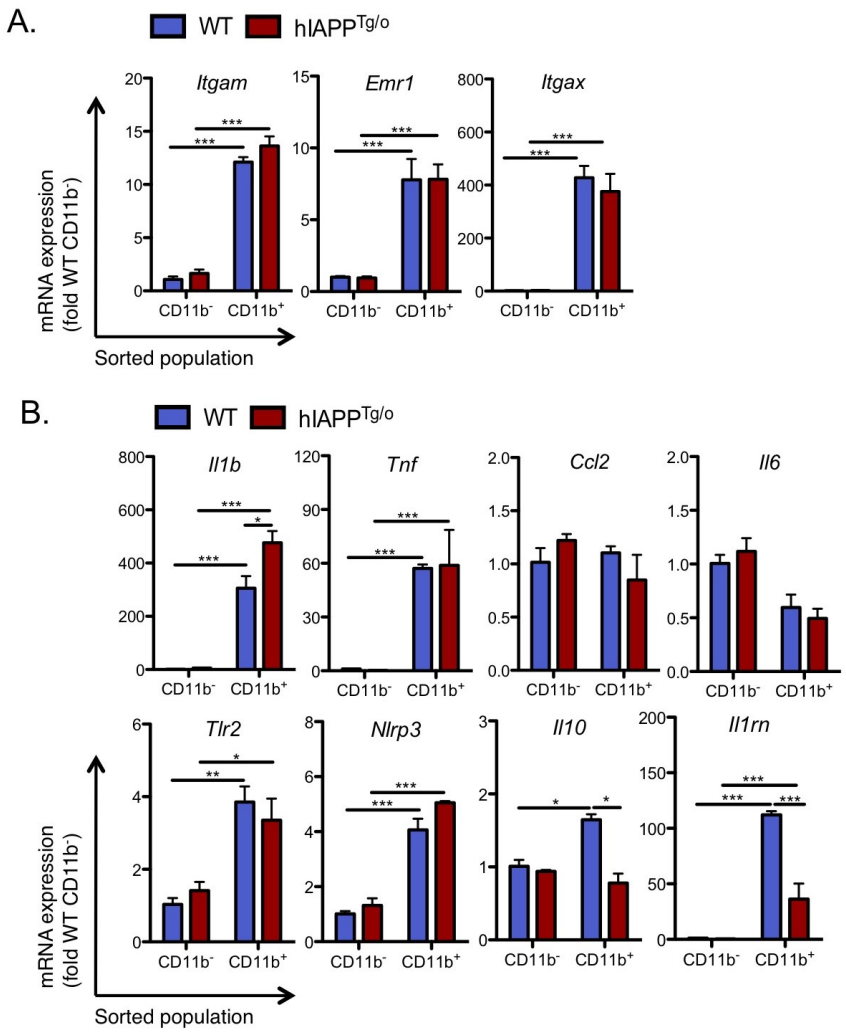

Figure 4.13. Islet macrophages are the major source of altered pro- and anti-inflammatory gene expression in hIAPP$^{Tg/o}$ mice. Female FVB hIAPP$^{Tg/o}$ mice and wild-type littermate controls (WT) were placed on HFD (45% kcal from fat) for 14 weeks starting at 10 weeks of age. Islets were isolated and CD11b^{+}F4/80^{+} cells were sorted from other islet cells. mRNA expression of (A) macrophage markers and (B) cytokines and hIAPP-sensing pattern recognition receptors in the sorted populations was assessed by RT-qPCR. Expression levels were normalized to the housekeeping gene *Rplp0*. Data represent mean±SEM of 6-9 mice per group. * p<0.05, ** p<0.01, *** p<0.001.

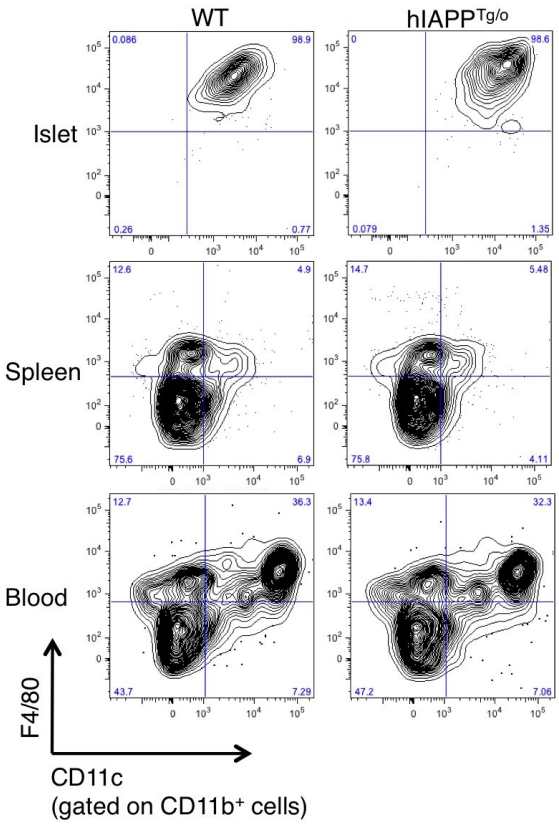

Figure 4.14. Beta cell hIAPP expression increases CD11c expression in CD11b$^+$F4/80$^+$ cells from islets but not peripheral blood or spleen. Female FVB hIAPP$^{Tg/o}$ mice and wild-type littermate controls (WT) were placed on HFD (45% kcal from fat) for 14 weeks starting at 10 weeks of age. Dispersed islets, splenocytes, and peripheral blood leukocytes were analyzed for F4/80 and CD11c expression within the CD11b$^+$ population. Flow cytometry plots are representative of 4-6 mice per group in each of 3 independent experiments.

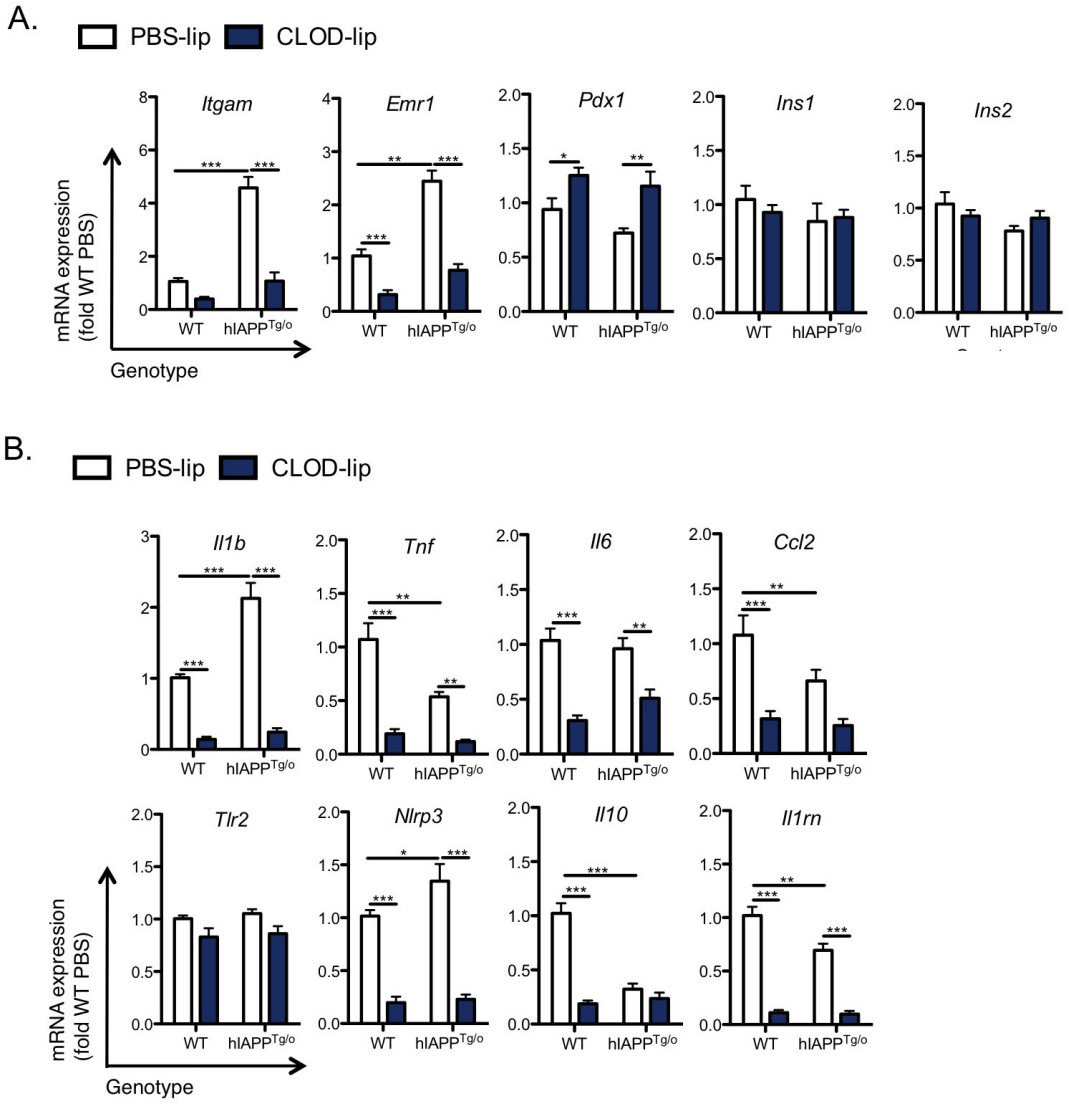

Figure 4.15. Clodronate-liposome-mediated macrophage depletion limits hIAPP-induced islet inflammation. Female FVB hIAPP$^{Tg/o}$ mice and wild-type littermate controls (WT) were placed on HFD (45% kcal from fat) for 14 weeks starting at 10 weeks of age. Mice were treated with 100 mg/kg clodronate- or PBS- containing liposomes (CLOD-lip or PBS-lip, respectively) i.p. every 4 days for the final 4 weeks of HFD. Islets were isolated from 24-week-old mice to evaluate mRNA expression of (A) macrophage and beta cell markers and (B) cytokines and hIAPP-sensing pattern recognition receptors by RT-qPCR. Expression levels were normalized to the housekeeping gene *Rplp0.* Data represent mean±SEM of 6-9 mice per group. * $p<0.05$, ** $p<0.01$, *** $p<0.001$.

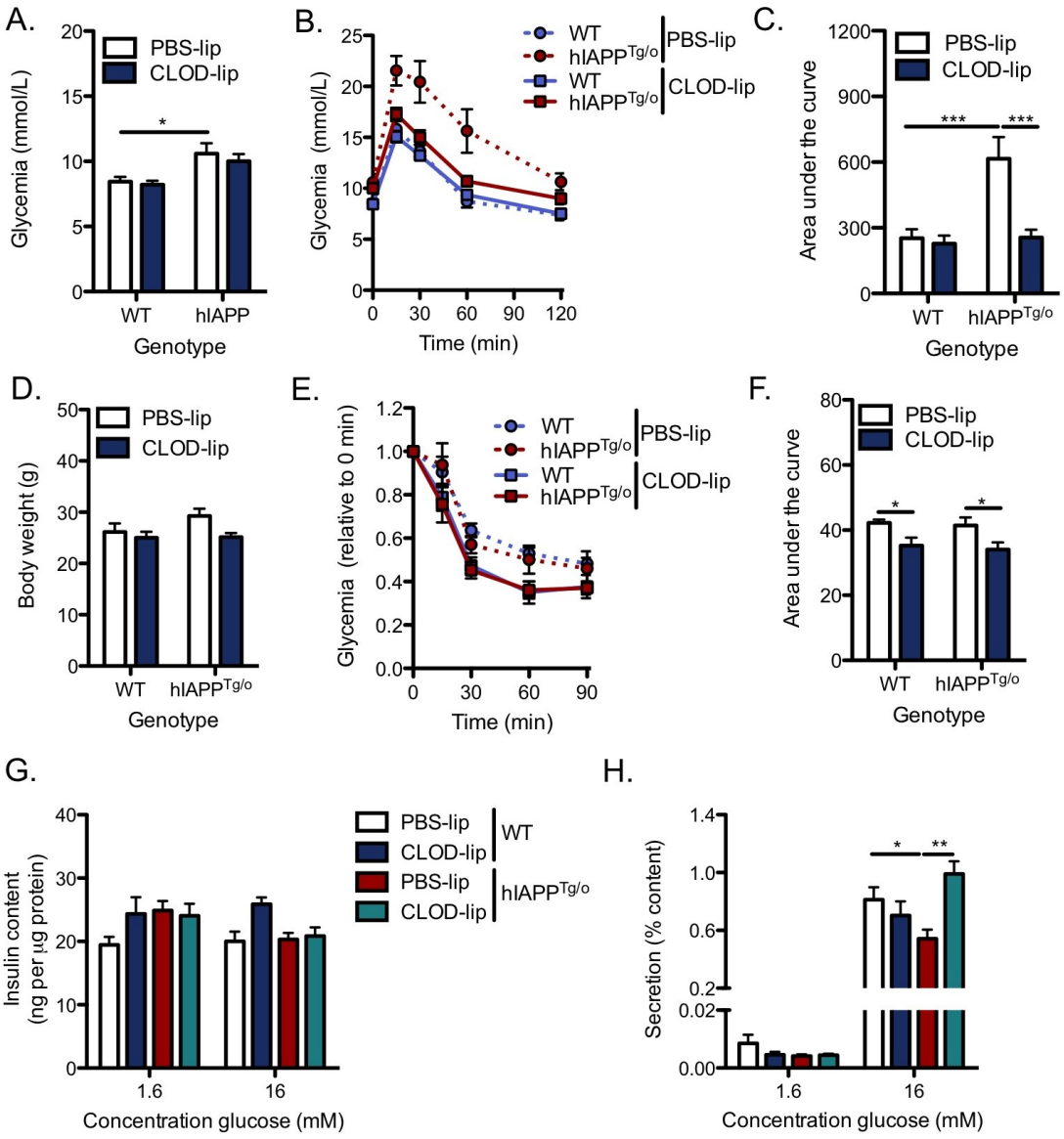

Figure 4.16. Clodronate liposome-mediated macrophage depletion improves hIAPP-induced glucose intolerance. Female FVB hIAPP$^{Tg/o}$ mice and wild-type littermate controls (WT) were placed on HFD (45% kcal from fat) for 14 weeks starting at 10 weeks of age. Mice were treated with 100 mg/kg clodronate- or PBS-containing liposomes (CLOD-lip or PBS-lip, respectively) i.p. every 4 days for the final 4 weeks of HFD. (A) Fasting glycemia was measured at 24 weeks. (B) Glucose tolerance was assessed following i.p. injection of 0.75 g/kg glucose and evaluation of (C) area under the glycemia curve up to 120 min (baseline = fasting glycemia). (D) Body weight and was assessed at 23 weeks of age. (E) Insulin tolerance was assessed following i.p. injection of 0.5 U/kg insulin and (F) evaluation of area under the glycemia curve up to 60 min (baseline = 1.0). (G) Islets were isolated for analysis of insulin content and (H) glucose-stimulated insulin secretion. Data represent mean±SEM of 6-9 mice per group and are representative of 2 independent experiments. * $p<0.05$, ** $p<0.01$, *** $p<0.001$.

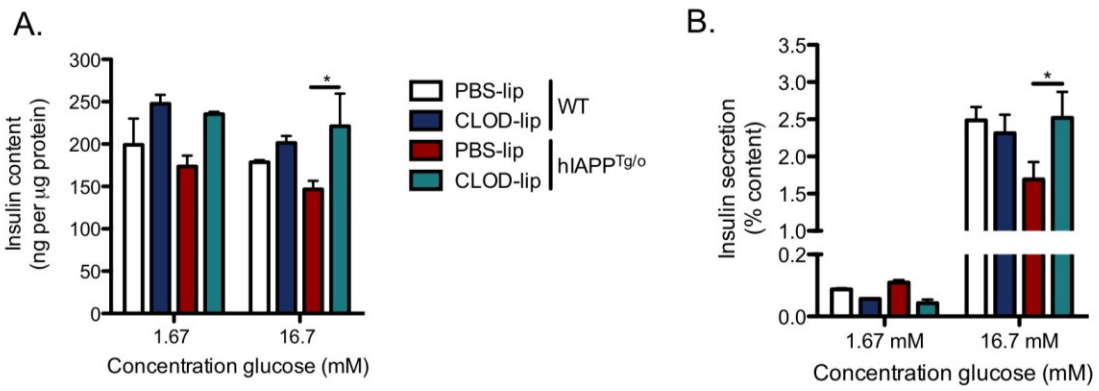

Figure 4.17. Treatment of hIAPP-expressing islets with clodronate liposomes improves insulin secretion *in vitro*. Islets were isolated from 10-week-old wild-type or hIAPP$^{Tg/o}$ FVB mice and immediately treated with CLOD-lip (1 mg/ml clodronate) or PBS-lip for 36 h. Islets were washed and allowed to recover for 6 h prior to culture in RPMI containing 16.7 mM glucose for 5 days to promote amyloid formation. (A) Insulin content and (B) glucose-induced insulin secretion were determined by ELISA. Data represent mean±SEM of 4 mice per group and are representative of 2 independent experiments.

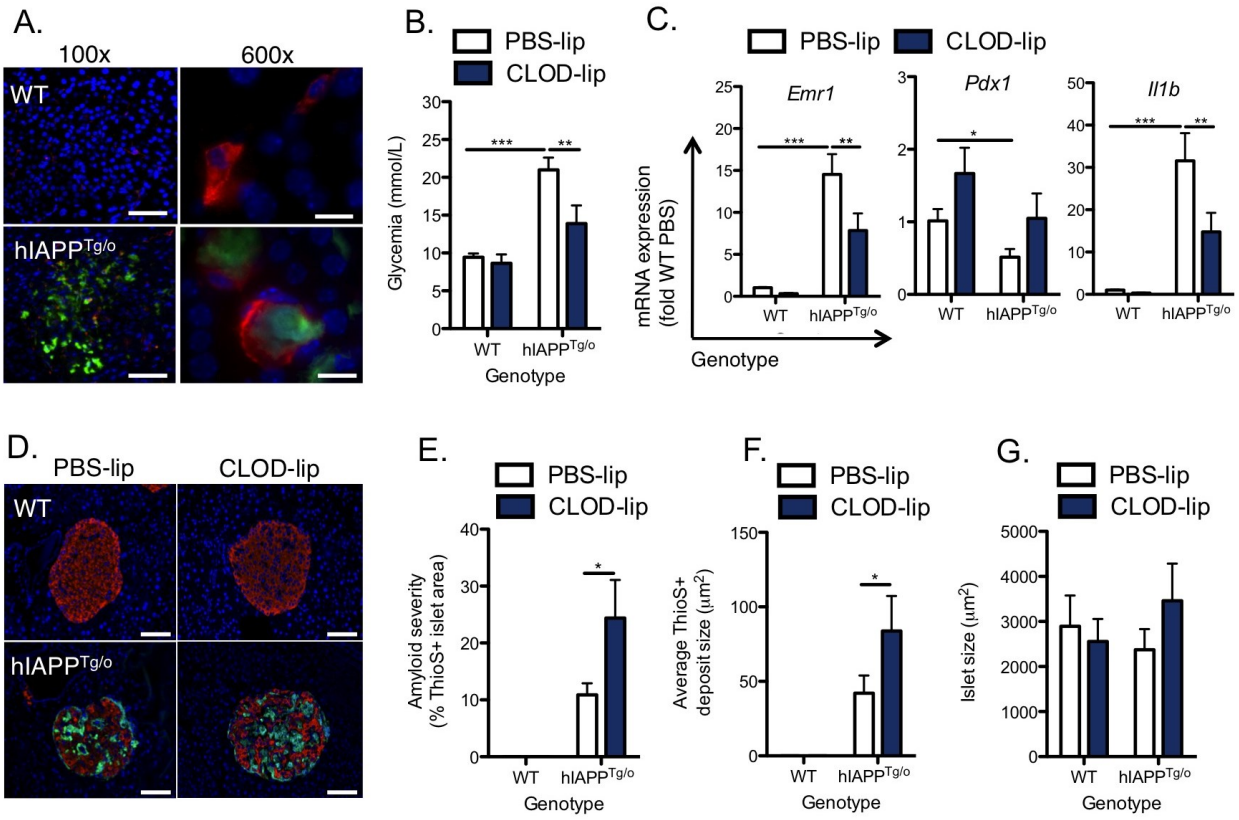

Figure 4.18. Improvement of hIAPP-induced hyperglycemia is accompanied by accumulation of mature amyloid fibrils in clodronate-liposome-treated mice. (A) Islets from 24-week-old FVB×C57BL/6 mice expressing the agouti viable yellow allele were examined to confirm amyloid formation. Representative low power (left) and high power (right) magnification fluorescence micrographs showing staining for F4/80 (red), amyloid (thioflavin S, green), and nuclei (DAPI, blue). Note that due to the broad emission spectrum of thioflavin S there is some detection of this dye by the blue filter. Scale bar: 30 µm (left) or 5 µm (right). (B) 20-week-old FVB×C57BL/6 mice expressing the agouti viable yellow allele were treated with 100 mg/kg clodronate- or PBS-containing liposomes (CLOD-lip or PBS-lip, respectively) i.p. every 4 days for 4 weeks. Fasting blood glucose was assessed at 24 weeks of age. (C) Islets were isolated at 24 weeks of age and mRNA expression of the indicated markers was assessed by RT-qPCR. Expression levels were normalized to the housekeeping gene *Rplp0.* (D) Pancreata were fixed at 24 weeks of age and assessed for amyloid severity. Representative fluorescence micrograph showing staining for insulin (red), amyloid (thioflavin S, green), and nuclei (DAPI, blue). Scale bar: 50 µm. (E) Thioflavin-S-positive area relative to total islet area, (F) average amyloid deposit area, and (G) average islet size were determined by image analysis. Data represent mean±SEM of 4-7 mice per group. * $p<0.05$, ** $p<0.01$, *** $p<0.001$.

Chapter 5: IL-1 Receptor Antagonist Improves IAPP-induced Islet Dysfunction and Limits Amyloid Formation

5.1 Background

Early evidence for islet inflammation in type 2 diabetes came from studies demonstrating elevated IL-1β mRNA and protein expression in islets from patients with type 2 diabetes (397,398). More recently, global gene expression studies have identified a group of IL-1-related genes highly expressed in islets from patients with type 2 diabetes and associated with reduced insulin secretion (400). Both high glucose and saturated fatty acids, nutrient stimuli that are frequently elevated in the systemic circulation, stimulate IL-1 expression and chemokine secretion by human islets (401). Beta cells respond to these stimuli by upregulation of *Il1b* gene expression, which in turn promotes IL-1-induced chemokine secretion and may explain the increase in islet-associated $CD68^+$ macrophages in type 2 diabetes (401,418). While the relative contributions of endocrine cells and innate immune cells to islet IL-1 synthesis is unclear, our work presented in Chapter 4 suggests that islet macrophages are a major source of *Il1b* gene expression in mouse islets, and that transgenic beta cell expression of hIAPP causes upregulation of *Il1b* in macrophages but not other islet cell types.

Clinical studies have also supported a role for IL-1 in islet dysfunction in type 2 diabetes. IL-1Ra reduced glycated A1C without affecting insulin resistance as determined by hyperinsulinemic euglycemic clamp (361), with a sustained reduction in plasma proinsulin:insulin up to 39 weeks after cessation of treatment (362). Remarkably, multiple clinical trials have now demonstrated improved insulin secretion in response to anti-IL-1 therapy with no detectable effects on insulin resistance (79). These include studies using anti-IL-1β mAbs (514-516) and a small clinical study in non-diabetic subjects with the metabolic syndrome (517). That anti-IL-1 agents can improve islet function without obvious systemic effects supports a role for IL-1-induced beta cell dysfunction early in disease development and suggests that the islet may be particularly susceptible to IL-1-induced inflammation. This may be explained both by high IL-1R expression on beta cells (292) and by the presence of an islet-localized stimulus for IL-1 such as hIAPP aggregation.

As in type 2 diabetes, IL-1 secretion by infiltrating innate immune cells may impair beta cell function and survival following islet transplantation. IL-1Ra enhances the survival of human islets during culture (433), is reportedly used routinely as a peri-transplant therapy at some islet transplant centers (435), and works in combination with etanercept to preserve the mass of marginal human islet grafts in immunodeficient mice (435). Amyloid deposits have been reported in human islet graft recipients (240), form within two weeks after transplantation into diabetic immune-deficient mice (239), and are associated with graft failure (217). Islets from hIAPP$^{Tg/o}$ mice also develop amyloid following transplantation into syngeneic mice, corresponding with progressive graft dysfunction (216). Thus, hIAPP aggregation may be a common trigger for islet inflammation in type 2 diabetic and transplanted islets.

In Chapter 3, we found that hIAPP activates the pattern recognition receptors TLR2 and NLRP3 to induce IL-1β secretion by macrophages. Moreover, IL-1Ra limits hIAPP-induced cytokine secretion by BMDMs and chemokine secretion by islets. We propose two potential mechanisms by which IL-1Ra could improve islet function *in vivo*. First, IL-1Ra may suppress IL-1-induced amplification of the inflammatory response to hIAPP as well as the direct inhibitory effect of IL-1 on insulin secretion by beta cells (390,391,397,399,489). Second, improving beta cell function by blocking beta cell IL-1R could reduce the formation of IAPP aggregates. Since impaired proIAPP processing may promote islet amyloid formation (227), it is possible that IL-1-induced beta cell dysfunction alters the processing of proIAPP leading to increased amyloid. Indeed, IL-1β and TNF-α impair proinsulin processing (234), which occurs in parallel with that of proinsulin (230-233). In this chapter, we evaluate the effect of IL-1Ra on glucose homeostasis, islet inflammation, and amyloid deposition in hIAPP$^{Tg/o}$ mice and recipients of hIAPP$^{Tg/o}$ islet grafts.

5.2 Results

5.2.1 Beta cell expression of hIAPP in obese *A^{vy}*-expressing mice promotes amyloid formation and glucose intolerance

We generated obese, insulin-resistant hIAPP$^{Tg/o}$ mice by crossing obese agouti viable yellow C57BL/6 mice (B6.C3-*A^{vy}*/J; *A^{vy}/a* at the agouti locus) with hemizygous FVB hIAPP$^{Tg/o}$ mice (*A/A* at the agouti locus) as described previously (194) and in Chapter 4. We compared the

phenotypes of A^{vy}-expressing mice (yellow, obese; A^{vy}-hIAPP$^{Tg/o}$ or A^{vy}-WT) to their brown, leaner littermates (*a*-hIAPP$^{Tg/o}$ or *a*-WT). hIAPP transgene expression in beta cells of obese male A^{vy}-expressing mice caused islet amyloid formation, with small flecks of amyloid in ~15% of islets at 12 weeks of age and larger pericapillary deposits affecting ~60% of islets and comprising 20% of islet area by 24 weeks of age (Figure 5.1A-C). Expression of the A^{vy} allele in non-transgenic mice was associated with an increase in body weight from 30.0±0.6 to 40.6±1.2 g at 12 weeks of age (Figure 5.1D) and 36.0±1.9 to 49.2±1.9 g at 24 weeks of age (Figure 5.1E; both $p<0.001$). hIAPP transgene expression had no effect on body weight. Amyloid deposition was associated with hyperglycemia in A^{vy}-hIAPP$^{Tg/o}$ but not *a*-hIAPP$^{Tg/o}$ mice, with fasting glycemia of 15.7±1.5 mM vs. 10.6±0.4 mM at 12 weeks of age (A^{vy}-hIAPP$^{Tg/o}$ vs. A^{vy}-WT; Figure 5.1D) and 20.5±2.0 vs. 10.0±0.5 mM at 24 weeks (Figure 5.1E; both $p<0.001$). At 12 weeks of age, A^{vy} expression caused impaired glucose tolerance, with no significant effect of hIAPP$^{Tg/o}$ expression on glucose tolerance (relative to baseline) except that attributable to elevated fasting glycemia (Figure 5.2A,B). The hIAPP-associated hyperglycemia under fasting conditions (preserved throughout the IPGTT) could not be attributed to increased insulin resistance, as A^{vy}-hIAPP$^{Tg/o}$ mice were more sensitive to insulin than their wild-type littermates (Figure 5.2C,D).

5.2.2 Amyloid accumulation in obese A^{vy}-hIAPP$^{Tg/o}$ mice is associated with upregulation of islet pro-inflammatory cytokines

To determine whether amyloid deposition is associated with changes in expression of pro-inflammatory genes, we used an RT-qPCR array (Mouse Inflammatory Response and Autoimmunity; SA Biosciences) to analyze gene expression in isolated islets from 24-week-old *a*-hIAPP$^{Tg/o}$ mice, A^{vy}-hIAPP$^{Tg/o}$ mice, and their wild-type littermates. Of 84 inflammation-related genes evaluated in the array, 66 could be detected in islets (Table 5.1). Differentially expressed genes significantly up- or downregulated by at least two-fold are shown in volcano plots in Figure 5.3. In lean *a*-hIAPP$^{Tg/o}$ mice, only *Itgb2,* which together with *Itgam* encodes the αMβ2 integrin, was significantly upregulated compared to control *a*-WT littermates (Figure 5.3A). Indeed, other pro-inflammatory cytokines, as well as the anti-inflammatory cytokines *Il1rn* and *Il10,* were downregulated, consistent with our observations in HFD-fed FVB mice

described in Chapter 4. The obese, insulin-resistant state caused by A^{vy} expression in wild-type mice also had minimal effects on gene expression, inducing upregulation of *Tlr5, C3, Fos,* and *Il17a,* and downregulation of several chemokines (Figure 5.3B). However, islets from obese A^{vy}-hIAPP$^{Tg/o}$ mice with extensive amyloid deposition showed upregulation of 33 inflammation-related genes (Figure 5.3C), including anti-inflammatory cytokines (such as *Il1rn,* encoding IL-1Ra) that are often induced in parallel, pointing to hIAPP aggregation as an inciting mechanism for islet inflammation.

Because both *Il1b* and *Il1rn* were among the amyloid-associated upregulated genes, we validated these results with a second set of primers and also assessed expression of other IL-1-related genes. Islets from A^{vy}-hIAPP$^{Tg/o}$ mice expressed elevated *Il1a, Il1b, Il1rn, Casp1,* and *Nlrp3* compared to islets from wild-type littermates, while expression of *Il18, Il1r1, Il1rap,* and *Pycard* were unchanged (Figure 5.4A). There was no change in expression of IL-1-related genes in livers from the same mice, suggesting an islet-specific pro-inflammatory response (Figure 5.4C). In wild-type mice, A^{vy} expression was associated with downregulation of the beta cell transcription factors *Pdx1* and *Mafa* as well as the prohormone processing enzymes *Pcsk1* and *Pcsk2*, with no effect on *Ins1* or *Ins2* expression (Figure 5.4B). Expression of hIAPP in lean mice also caused downregulation of *Pdx1*, *Mafa*, and *Pcsk1*, while islets from A^{vy}-hIAPP$^{Tg/o}$ vs. A^{vy}-WT mice displayed significantly reduced expression of all beta cell genes analyzed (Figure 5.4B). Thus, obese, insulin-resistant A^{vy}-hIAPP$^{Tg/o}$ mice show evidence of islet-localized inflammation associated with amyloid deposition, reduced expression of key genes required for beta cell function, and hyperglycemia relative to their A^{vy}-WT littermates.

5.2.3 IL-1Ra improves glucose tolerance in both lean *a*-hIAPP$^{Tg/o}$ and obese A^{vy}-hIAPP$^{Tg/o}$ mice

Because our previous studies identified IL-1 as a central mediator of hIAPP-induced islet cytokine expression (Chapter 3) and both *Il1a* and *Il1b* were upregulated in islets from A^{vy}-hIAPP$^{Tg/o}$ mice (Figure 5.4A), we next evaluated the effects of IL-1R blockade on glucose homeostasis and islet inflammation in hIAPP$^{Tg/o}$ mice. For these studies, we treated 24-week-old lean mice (*a*-hIAPP$^{Tg/o}$ and *a*-WT; Figure 5.5) and obese mice (A^{vy}-hIAPP$^{Tg/o}$ and A^{vy}-WT; Figure 5.6) with IL-1Ra (50mg/kg/day subcutaneously) or PBS for 8 weeks. IL-1Ra had no

effect on body weight or fasting glycemia (Figure 5.5A; Figure 5.6A), although both were lower in A^{vy}-expressing mice (Figure 5.6A-C) compared to the initial cohort (Figure 5.1E). hIAPP expression caused impaired glucose tolerance in both lean *a*-hIAPP$^{Tg/o}$ (Figure 5.5B,C) and obese A^{vy}-hIAPP$^{Tg/o}$ (Figure 5.6B,C) mice relative to wild-type littermates. IL-1Ra improved glucose tolerance in hIAPP$^{Tg/o}$ but not wild-type mice, with no detectable effect on insulin sensitivity in either lean (Figure 5.5D) or obese (Figure 5.6D) mice. Fasting plasma insulin was not significantly decreased in PBS-treated hIAPP$^{Tg/o}$ vs. wild-type mice and was unaffected by IL-1Ra (Figure 5.5E, Figure 5.6E). However, hIAPP expression caused increased plasma proinsulin:insulin ratios in both lean (Figure 5.5F) and obese (Figure 5.6F) mice, which were reduced by IL-1Ra treatment (*a*-hIAPP$^{Tg/o}$: 8±3% vs. 31±10%; A^{vy}-hIAPP$^{Tg/o}$: 6±1% vs. 12±2%; $p<0.01$), consistent with an improvement in hIAPP-induced beta cell dysfunction. We were unable to demonstrate impaired insulin secretion during IPGTT in hIAPP$^{Tg/o}$ mice, unlike in HFD-fed FVB mice (Figure 4.8G), likely due to timing of blood sampling, low levels of detectable insulin, and potential differences in insulin release kinetics among groups. To determine the effects of IL-1Ra on islet function during amyloid formation *in vitro*, we cultured *a*-hIAPP$^{Tg/o}$ islets for 7 days at 16.7 mM glucose. IL-1Ra restored glucose-stimulated insulin secretion in hIAPP$^{Tg/o}$ islets (Figure 5.7A), with no significant effect on insulin content (Figure 5.7B). Thus, IL-1Ra improves hIAPP-induced glucose intolerance and islet dysfunction with no detectable effects on insulin sensitivity.

5.2.4 IL-1Ra limits hIAPP-induced islet inflammation in A^{vy}-hIAPP$^{Tg/o}$ mice

To determine the effect of IL-1Ra on hIAPP-induced islet inflammation, we evaluated expression of pro-inflammatory cytokines and macrophage markers in islets isolated from PBS- and IL-1Ra treated mice following overnight recovery. Of note, islet yield was reduced by an average of ~50% in mice with significant amyloid formation, which may bias the population of isolated islets toward those with less amyloid. Beta cell expression of hIAPP caused modest upregulation of both *Il1a* and *Il1b* but not *Tnf* or *Ccl2* in islets of *a*-hIAPP$^{Tg/o}$ mice and significant upregulation of all four cytokines in association with amyloid deposition in islets of A^{vy}-hIAPP$^{Tg/o}$ mice, an effect that was blocked with IL-1Ra (Figure 5.8A). Expression of the macrophage markers *Itgam* (encoding CD11b) and *Emr1* (encoding F4/80) was upregulated in

both *a*-hIAPP$^{Tg/o}$ and *A^{vy}*-hIAPP$^{Tg/o}$ mice (Figure 5.8A), consistent with our observation of increased macrophage glycoprotein expression by resident macrophages in HFD-fed hIAPP$^{Tg/o}$ FVB mice (Figure 4.12E). IL-1Ra did not prevent this upregulation, suggesting that changes in pro-inflammatory gene expression are not due to significant changes in the size of the islet macrophage population. hIAPP expression was also associated with decreased expression of the beta cell genes *Ins2, Pdx1,* and *Mafa* expression in PBS- but not IL-1Ra-treated mice (Figure 5.8B). One previous study in *db/db* mice showed that IL-1Ra improves beta cell function by preventing translocation of the transcription factor Pdx1 from the nucleus to the cytoplasm (518). However, other groups have observed loss of nuclear MafA in *db/db* mice with no change in Pdx1 (519). We did not detect a significant decrease in nuclear Pdx1 staining intensity with hIAPP transgene expression. However, nuclear MafA intensity was markedly decreased in islet sections from both *a*-hIAPP$^{Tg/o}$ and *A^{vy}*-hIAPP$^{Tg/o}$ mice relative to wild-type littermates (Figure 5.9A,B). IL-1Ra limited the hIAPP-induced loss of nuclear MafA in obese *A^{vy}*-expressing mice, consistent with improved beta cell function.

5.2.5 IL-1Ra limits islet amyloid formation in *a*-hIAPP$^{Tg/o}$ but not *A^{vy}*-hIAPP$^{Tg/o}$ mice

To determine whether improved glucose tolerance and reduced islet inflammation were associated with changes in amyloid deposition, we analyzed thioflavin S staining in islets from IL-1Ra- and PBS-treated hIAPP$^{Tg/o}$ mice (Figure 5.10A). IL-1Ra reduced amyloid severity (proportion of islet area occupied by amyloid; Figure 5.10B) and prevalence (proportion of islets containing amyloid; Figure 5.10C) in *a*-hIAPP$^{Tg/o}$ but not obese *A^{vy}*-hIAPP$^{Tg/o}$ mice. These data suggest that – at least early in disease progression – islet IL-1Ra may act on the beta cell IL-1R to limit IL-1-induced beta cell dysfunction leading to amyloid formation. However, in mice with more extensive amyloid deposits, IL-1Ra improved glucose homeostasis and limited islet inflammation independently of amyloid deposition. To rule out possible peripheral effects of IL-1Ra in the context of amyloid formation, we also evaluated the effects of IL-1Ra on amyloid formation and insulin secretion in cultured hIAPP$^{Tg/o}$ rat islets, which develop islet amyloid after 7 days of culture with 22 mM glucose (Figure 5.11A,B). Islets treated with IL-1Ra showed a two-fold reduction in amyloid severity (Figure 5.12A). As in cultured mouse islets (see above), IL-1Ra also improved glucose-stimulated insulin secretion in hIAPP$^{Tg/o}$ but not wild-type rat

islets (Figure 5.12B). Thus, IL-1Ra can act directly on the islet to limit amyloid formation under conditions of low initial amyloid severity.

5.2.6 IL-1β impairs proIAPP processing in MIN6 cells and islets

To determine whether IL-1 might contribute to islet amyloid formation by impairing proIAPP processing, we evaluated the effect of recombinant IL-1β on MIN6 cell proIAPP expression. We found that 100 pg/ml IL-1β induced significant *Ccl2* expression with no effect on *Ins2* (Figure 5.13A). At this concentration, IL-1β increased expression of both intact proIAPP ($proIAPP_{1-67}$) and the partially processed N-terminally-extended intermediate form ($proIAPP_{1-48}$) while decreasing expression of the mature peptide ($IAPP_{1-37}$; Figure 5.13B,C). The ratios of $proIAPP_{1-67}$ (Figure 5.13D) and $proIAPP_{1-48}$ (Figure 5.13E) to mature IAPP were significantly increased by IL-1β, which also decreased expression of the proIAPP processing enzymes PC1/3 and PC2 (Figure 5.13F,G). Similarly, isolated islets from C57BL/6 mice expressed increased *Ccl2* following 24 h culture with 100 pg/ml IL-1β; however, unlike in MIN6 cells, *Ins2* and *Pdx1* expression were decreased by ~70% at this concentration (Figure 5.14A). IL-1β at 1 pg/ml had no effect on *Pdx1, IAPP,* or *Pcsk1,* despite reduced *Ins2* and *Pcsk2* expression, and IAPP expression was unaffected at up to 10 pg/ml IL-1β (Figure 5.14A). Consistent with our observations in MIN6 cells, IL-1β increased expression of $proIAPP_{1-67}$ and $proIAPP_{1-48}$ while decreasing expression of mature IAPP (Figure 5.14B,C). The ratio of $proIAPP_{1-67}$ (Figure 5.14D) and $proIAPP_{1-48}$ (Figure 5.14E) to IAPP was lower in islets than in MIN6 cells, but as in MIN6 cells was significantly increased by IL-1β. These data suggest one possible mechanism by which IL-1 may contribute to islet amyloid formation– namely, by impairing proIAPP processing.

5.2.7 IL-1Ra attenuates islet graft dysfunction and limits amyloid formation in hIAPP transgenic islet grafts

To test the effect of IL-1Ra on glucose tolerance in a mouse model of islet transplantation, we transplanted islets from FVB $hIAPP^{Tg/o}$ and wild-type littermate control mice into diabetic NOD/SCID recipients treated with 50 mg/kg/day IL-1Ra or PBS. Neither graft expression of hIAPP nor IL-1Ra treatment affected recipient body weight 8 weeks following transplantation (Figure 5.15A). Recipients of transgenic islet grafts displayed elevated non-

fasting glycemia (Figure 5.15B) and impaired glucose tolerance (Figure 5.15C,D) compared to recipients of wild-type grafts. Administration of IL-1Ra reduced hyperglycemia associated with islet hIAPP expression and significantly improved graft function in recipients of transgenic grafts (Figure 5.15B-D). Quantification of intra-graft staining for the macrophage glycoprotein F4/80 demonstrated that hIAPP-expressing grafts contained 50% more macrophages than wild-type grafts, an effect that was significantly inhibited by IL-1Ra (Figure 5.16A,B). Furthermore, a 5-fold reduction in amyloid severity was observed in transgenic grafts from IL-1Ra-treated recipients (Figure 5.16C,D), with no difference in insulin staining among grafts. Interestingly, most thioflavin-S-positive amyloid deposits in transgenic grafts were closely associated with F4/80-expressing macrophages, with thioflavin S staining apparent both within cells and extracellularly, as determined by deconvolution of *z*-stack images (Figure 5.16E,F). These data suggest that, as in obese, insulin resistant mice with hIAPP expression, IL-1Ra improves islet function and limits amyloid formation. Whether IL-1Ra affects the size of the population of resident or infiltrating islet macrophages may depend on variables specific to each model, including the presence of other stimuli such as tissue damage associated with surgery.

5.3 Discussion

Chronic exposure to elevated IL-1 causes beta cell death and dysfunction due to altered gene transcription, changes in protein activity, and induction of oxidative stress (Figure 1.6). Data from clinical studies suggest that anti-IL-1 agents – at least with the dosing regimens and relatively short treatment periods tested to date – can improve beta cell function without affecting insulin sensitivity. The data presented in Chapter 3 show that hIAPP induces IL-1 synthesis and secretion by cultured macrophages. Chapter 4 of this thesis demonstrates that islet macrophages are the major source of hIAPP-induced IL-1β in islets, and that islet macrophage depletion can improve hIAPP-induced islet dysfunction. Here, we present data in support of the hypothesis that IL-1 mediates hIAPP-induced islet inflammation and dysfunction, which – at least at the early stages of disease – may participate in a feed-forward cycle leading to enhanced amyloid formation.

In Chapter 4, we showed that $hIAPP^{Tg/o}$ mice on an FVB background express elevated islet *Il1b* and *Nlrp3* with few other changes in islet pro-inflammatory gene expression. While

these mice serve as a model of early hIAPP-induced islet dysfunction, they do not develop extensive amyloid deposits, even on HFD, consistent with some other transgenic strains (520). Indeed, the background strain appears to be critical to the phenotype and amyloid status of hIAPP transgenic mice (521). Furthermore, homozygous hIAPP$^{Tg/Tg}$ mice spontaneously develop diabetes without extracellular amyloid formation (210), raising the possibility that other mechanisms such as ER stress (522) rather than macrophage activation may be more important mediators of disease in some models. Most strains of hIAPP$^{Tg/o}$ mice develop extracellular islet amyloid resembling that found in type 2 diabetes under conditions that promote beta cell dysfunction, including *ex vivo* culture (488,512,523), treatment with growth hormone and steroids (193), or obesity due to leptin deficiency (520) or expression of the A^{vy} allele (194). Soeller *et al.* showed that A^{vy}-hIAPP$^{Tg/o}$ mice develop slow-onset diabetes associated with extracellular amyloid deposits, decreased plasma insulin and pancreatic insulin content, and decreased beta cell mass by 41-52 weeks of age (194). Here, we show that impaired glucose tolerance is present by 12 weeks of age in the presence of small extracellular flecks of amyloid and becomes more pronounced by 24 weeks of age, in association with increased amyloid severity.

Extensive amyloid deposition and hyperglycemia in A^{vy}-hIAPP$^{Tg/o}$ mice was associated with increased islet expression of a number of pro-inflammatory cytokines and chemokines that were not upregulated in *a*-hIAPP$^{Tg/o}$ mice with low amyloid severity and normoglycemia. In Chapter 3, we showed that both pre-fibrillar and fibrillar hIAPP aggregates are required for increased *Il1b* expression and proIL-1β processing, respectively. Thus, mice with few detectable thioflavin-S-positive amyloid deposits (i.e. lean *a*-hIAPP$^{Tg/o}$ mice) may have insufficient fibrillar hIAPP present to induce maximal NLRP3 activation and IL-1β secretion by islet macrophages, limiting the autocrine/paracrine induction of other pro-inflammatory mediators in the early stages of disease. Alternatively, it is possible that hyperglycemia *per se* and not islet amyloid is the major driver of pro-inflammatory gene expression, either directly or via systemic release of pro-inflammatory cytokines (524). However, several lines of evidence point to a specific role for hIAPP aggregation in islet inflammation. First, hIAPP transgene expression was not associated with the same pro-inflammatory response in liver, a tissue with high content of macrophages that respond to systemic stimuli (525). Second, both synthetic and endogenous hIAPP induced *Il1b*

expression in isolated islets under the same culture conditions as rIAPP-treated or wild-type islets. Third, IL-1Ra improved the function of hIAPP$^{Tg/o}$ but not wild-type rodent islets in high-glucose culture. Finally, A^{vy} expression alone (i.e. in A^{vy}-WT mice) was not associated with elevated expression of IL-1-related genes despite impaired glucose tolerance relative to *a*-WT mice. Careful glycemic control with insulin administration to render hIAPP$^{Tg/o}$ mice normoglycemic would help to rule out the effects of hyperglycemia on islet pro-inflammatory gene expression.

It is also possible that amyloid-associated pro-inflammatory gene expression is due to liberation of stimuli produced by beta cells directly damaged by hIAPP. Whether the *in vivo* action of hIAPP on macrophages is due to direct interaction (e.g. with TLR2) or due to liberation of other pro-inflammatory stimuli requires further study. Indeed, hyperglycemia caused by the beta cell toxin streptozotocin can also be prevented with IL-1Ra (526), and other rodent models of type 2 diabetes that are protected by IL-1Ra, such as the *db/db* mouse (527,528) and Goto-Kakizaki rat (395), demonstrate a similar elevation of islet cytokine expression. It may be difficult to uncouple the toxic and pro-inflammatory effects of hIAPP given that pre-fibrillar oligomers are critical participants in both hIAPP-induced cell death and pro-inflammatory cytokine synthesis. However, we found protective effects of IL-1Ra in two models in which insulin-positive beta cell area is preserved, the *a*-hIAPP$^{Tg/o}$ mouse (194) and the NOD/SCID recipient of hIAPP-expressing islet transplants. Changes in the ratio of proinsulin:insulin provide further evidence for hIAPP-induced islet dysfunction independent of beta cell death. Analysis of beta cell mass and apoptosis at early and advanced stages of amyloid formation may further elucidate the nature of the beta cell defect in the presence of hIAPP aggregates. However, we found no significant differences in the number of TUNEL-positive beta cells among the treatment groups eight weeks following transplantation, suggesting that extensive hIAPP-induced cell death is not a requirement for graft inflammation. Furthermore, we have demonstrated hIAPP-induced chemokine release from transgenic mouse islets *ex vivo* in the absence of significant changes in cell viability as confirmed by Alamar Blue reduction and insulin staining of histological sections. Taken together, these data suggest that hIAPP is likely to act directly on islet macrophages without a requirement for beta cell death.

The transcription factor Pdx1 regulates beta cell function and survival by controlling expression of critical genes such as those encoding insulin, Glut2, and glucokinase (529). Pdx1 deficiency contributes to reduced proliferation and enhanced apoptosis in mouse models of type 2 diabetes such as *Psammomys obesus* and *db/db* mice (530), and overexpression of Pdx1 can restore beta cell mass in *Irs2* knockout mice (531). IL-1β reduces Pdx1 expression (532), and a previous study reported that IL-1Ra can prevent nuclear exclusion of Pdx1 – which can occur in response to stimuli such as oxidative stress and free fatty acids – in islets from *db/db* mice (528). Others have reported a loss of intranuclear MafA with preservation of Pdx1 (519) or a loss of both transcription factors (533) in beta cells of *db/db* mice. Like Pdx1, MafA is a critical regulator of beta cell genes and is required for normal insulin gene expression (534). We found a significant decrease in both *Mafa* and *Pdx1* expression in A^{vy}-hIAPP$^{Tg/o}$ and *a*-hIAPP$^{Tg/o}$ islets relative to wild-type controls, although this effect was more pronounced for *Mafa.* The marked decrease in nuclear MafA expression (not observed for Pdx1), which was partially rescued by IL-1Ra, suggests that this transcription factor is a sensitive indicator of beta cell dysfunction in the setting of amyloid formation. A recent study suggested that beta cell de-differentiation (and loss of detectable insulin) rather than death is the major contributor to the apparent loss of beta cell mass in rodent models of type 2 diabetes (533), and that FoxO1 is required to maintain beta cells in a differentiated state. Examination of this and other transcription factors – in addition to analysis of beta cell mass, apoptosis, and proliferation – may further elucidate the nature of the beta cell defect in the presence of hIAPP aggregates.

The data presented in Chapter 4 suggest that islet macrophages are the major source of hIAPP-induced islet IL-1β. Whether the effects of IL-1Ra are due to blockade of IL-1R signalling in macrophages or in beta cells – or a combination of these effects – remains to be addressed. Future studies should therefore employ models with cell-specific IL-1R deficiency. This can be achieved with either bone marrow transplantation (for reconstitution of islet macrophages) or genetic approaches (e.g. expression of a conditional knockout *Il1r1* allele in macrophages or beta cells in hIAPP$^{Tg/o}$ mice). Moreover, signalling via the IL-1R can be induced not only by IL-1β but also by IL-1α and IL-18 (535). Although we did not observe upregulation of IL-18 expression in A^{vy}-hIAPP$^{Tg/o}$ islets (Figure 5.4A), the relative contributions of IL-1α and IL-1β to IL-1R-mediated islet inflammation requires further study. We attempted several studies

using anti-IL-1β antibody in syngeneic FVB transplant recipients but encountered technical challenges due to poor engraftment rates with this recipient strain. Given current clinical trials underway using anti-IL-1α and anti-IL-1β antibodies (79), which have a longer half-life than IL-1Ra and may be better tolerated due to the absence of injection site reactions, this distinction between IL-1α and IL-1β may be clinically relevant. Other compounds that limit IL-1 secretion, including NLRP3 inflammasome inhibitors and inhibitors of proIL-1β synthesis, are currently under development. Some existing therapies may also limit islet inflammation, including metformin, which inhibits the NLRP3 inflammasome (371); thiazolidinediones, which act via PPARγ to alter macrophage phenotype (427); and DPP-4 inhibitors, which have anti-inflammatory effects (428).

Consistent with hIAPP-induced monocyte recruitment to the islet as reported *in vitro* in Chapter 3, we observed more macrophages within hIAPP$^{Tg/o}$ grafts compared to wild-type grafts, and these cells were present in close association with amyloid plaques. Whereas the number of macrophages in hIAPP$^{Tg/o}$ grafts was reduced when recipients were treated with IL-1Ra, we did not observe a significant change in F4/80 gene expression with IL-1Ra treatment in hIAPP$^{Tg/o}$ mice. This difference between models may be due to the presence of other graft-associated stimuli or to differences in the kinetics of amyloid deposition. Alternatively, our study may be insufficiently powered to detect small changes in gene expression given the technical challenges in isolating amyloid-laden islets and the bias introduced by studying only islets that can be isolated. Further studies are also required to understand the source of intra-graft macrophages (donor vs. recipient) and the kinetics of islet macrophage turnover; for example, it is possible that turnover rates might increase with no net effect on the size of a cell population. Additional characterization of islet macrophage subsets using other markers is also required, including M1-polarized F4/80^{-} populations (420) not detected in these analyses.

Interestingly, IL-1Ra limited amyloid formation in *a*-hIAPP$^{Tg/o}$ mice, FVB hIAPP$^{Tg/o}$ islet grafts, and cultured hIAPP$^{Tg/o}$ rat islets, all models with low amyloid severity. Thus, protection of the beta cell – either by directly inhibiting beta cell IL-1R signalling or by altering the pro-inflammatory milieu – may limit islet amyloid formation. Similarly, the GLP-1R agonist exenatide, which improves beta cell function in cultured islets, may restore proIAPP processing and reduce amyloid formation (536), although this is controversial (537). No effect of IL-1Ra on

amyloid deposition was detected in A^{vy}- hIAPP$^{Tg/o}$ mice, despite improved glucose tolerance, suggesting either a reduction in pre-fibrillar hIAPP aggregates that cannot be detected with thioflavin S or a dominant effect of IL-1Ra on protecting the beta cell from hIAPP-induced IL-1, despite a persistent stimulus. In this more advanced stage of hIAPP deposition, IL-1Ra may be unable to prevent further amyloid formation given the presence of extensive deposits that act as seeds for aggregation. However, in less severe disease, IL-1Ra-mediated improvement in beta cell function may limit amyloid formation, supporting a model in which cytokine production begets amyloid formation (which, in turn, leads to further inflammation) in a feed-forward cycle. This model of our data points to the importance of amyloid and islet inflammation as therapeutic targets in type 2 diabetes and islet transplantation.

We found that IL-1β impairs proIAPP processing in cultured MIN6 cells and islets, pointing to one possible mechanism for reduced amyloid formation in IL-1Ra-treated islets. NH_2-terminally unprocessed proIAPP, which may be secreted at an increased ratio to mature IAPP under conditions of beta cell stress (538), binds to heparan sulphate proteoglycans to create a nidus for extracellular amyloid formation (229). We found that both PC1/3 and PC2, enzymes involved in proIAPP processing (Figure 1.2), are downregulated by IL-1β without a concomitant decrease in IAPP expression. Other enzymes that contribute to proIAPP processing, such as carboxypeptidase E (233), may also be affected and require further study. Our data are consistent with previously reported impairment of proIAPP processing in response to the pro-inflammatory cytokine TNF-α (539) and the chemokine MCP-1 (540), although we did not observe the cytokine-induced upregulation of *Iapp* expression reported in these studies. Further work is required to confirm the effect of IL-1Ra on proIAPP content and secretion in human islets under conditions that promote endogenous IL-1 secretion.

In contrast to IL-1Ra treatment, macrophage depletion by clodronate liposome administration was associated with increased amyloid severity (Chapter 4.2.6), suggesting distinct roles for islet macrophage activity and IL-1β in disease progression. Islet macrophages may play dual roles in the setting of hIAPP aggregation, contributing both to the clearance of hIAPP aggregates and to the secretion of pro-inflammatory cytokines. In each model examined in this thesis, the net effect appears to be detrimental to the beta cell. For example, anti-TLR2 antibody prevented hIAPP-induced upregulation of islet cytokine expression and preserved

insulin content in cultured hIAPP$^{Tg/o}$ mouse islets (Figure 3.14C). Similarly, *in vitro* macrophage depletion preserved insulin content and secretion in FVB hIAPP$^{Tg/o}$ islets (Figure 4.17A), and IL-1Ra also prevented hIAPP-induced reduction in insulin secretion in cultured hIAPP$^{Tg/o}$ mouse and rat islets. *In vivo* clodronate liposome treatment had no effect on islet insulin content or *Ins1* and *Ins2* gene expression (Figure 4.15A), but increased *Pdx1* expression and glucose-stimulated insulin secretion in isolated islets (Figure 4.16G). In hIAPP$^{Tg/o}$ rat islets, which did not exhibit a decrease in insulin content with culture, IL-1Ra nevertheless rescued the impairment in glucose-stimulated insulin secretion. Thus, all three anti-inflammatory approaches can either preserve insulin content or improve glucose responsiveness, an effect that is likely modulated by other factors such as the extent of hIAPP aggregation and the presence of other pro-inflammatory stimuli.

While our *in vitro* studies suggest that interaction of hIAPP with macrophages induces release of cytokines such as IL-1β that at high local concentrations are known to cause beta cell dysfunction, it is likely that IL-1 also plays an important physiological role in regulating islet homeostasis. For example, low concentrations of IL-1β promote beta cell proliferation, and IL-1β knockout mice have impaired glucose tolerance and decreased islet *Pdx1* expression (513). Other classically pro-inflammatory cytokines such as IL-6 may also enhance beta cell insulin secretion under some conditions (541). That IL-1Ra failed to improve glucose tolerance in wild-type mice suggests that blockade of this pathway under physiological conditions provides no benefit, nor causes harm. Moreover, we have found in preliminary experiments that 24 h stimulation of cultured islets with synthetic hIAPP, while inducing upregulation of pro-inflammatory cytokines, enhances rather than impairs insulin secretion. This observation points to the importance of the timing and dose in determining the functional consequents of islet exposure to pro-inflammatory cytokines.

The improved glucose tolerance in IL-1Ra-treated recipients of hIAPP transgenic islet grafts suggests a common mechanism of hIAPP-induced beta cell dysfunction in type 2 diabetic and transplanted islets. Inhibition of hIAPP-mediated IL-1 signalling may partially explain the improvement in beta cell secretory function in type 2 diabetic patients receiving anakinra (15), and our data suggest that blockade of IL-1 signalling may also promote long-term islet graft function. As there was no significant effect of IL-1Ra on glucose tolerance in recipients of wild-

type grafts in our NOD/SCID transplant model, our data suggest a specific effect on hIAPP-associated islet pathology. As in IL-1Ra-treated *a*-hIAPP$^{Tg/o}$ mice, we observed decreased amyloid deposition in hIAPP-expressing grafts in recipients of IL-1Ra, suggesting that IL-1-mediated islet inflammation may not only be a consequence but also a cause of hIAPP aggregation.

Collectively, these findings provide a mechanistic link between two important islet pathologies in type 2 diabetes and islet transplant failure: amyloid and inflammation. They provide the first *in vivo* evidence that IL-1 is an important mediator of hIAPP-induced islet dysfunction and point to hIAPP as an islet-localized trigger for inflammation in type 2 diabetes and islet transplantation. Importantly, our data suggest that hIAPP-induced beta cell dysfunction can be ameliorated even in the presence of widespread amyloid deposition. While no current therapies are available that specifically target islet amyloid formation, anti-TLR2, NLRP3, or IL-1 agents may provide an alternative approach for protecting the beta cell against hIAPP aggregates.

Table 5.1. Differentially-expressed islet pro-inflammatory genes associated with hIAPP expression.[1]

Group	Gene	FC	*p*-value
a-hIAPP$^{Tg/o}$ vs. *a*-WT	*Cxcl10*	-8.3	0.0105
	Ccl4	-6.7	0.0008
	Il10	-5.2	0.0123
	Tnf	-3.9	0.0005
	Ccl12	-3.0	0.0192
	Ccl3	-3.0	0.0005
	Il1rn	-2.7	0.0241
	Tlr9	-2.3	0.0037
	Lta	-2.2	0.0410
	Itgb2	3.8	0.0564
A^{vy}-WT vs. *a*-WT	*Cxcl10*	-4.3	0.0112
	Ccl7	-4.1	0.0449
	Ccl2	-3.6	0.0265
	Ccl22	-3.0	0.0135
	Il10	-2.3	0.0279
	Csf1	-2.2	0.0012
	Lta	-2.2	0.0059
	Tlr5	7.0	0.0111
	C3	4.8	0.0182
	Fos	3.1	0.0011
	Il17a	2.3	0.0313
A^{vy}-hIAPP$^{Tg/o}$ vs. *A^{vy}*-WT	*Fos*	-2.6	0.0005
	Ccl7	63.4	0.0213
	Ccl2	40.2	0.0149
	Ccl17	34.5	0.0111
	Ccl22	25.7	0.0079
	C4b	21.2	0.0008
	Ccr7	19.5	0.0134
	C3ar1	17.0	0.0120
	Sele	14.8	0.0272
	Cxcl1	13.9	0.0216
	Ccl19	13.4	0.0107
	Il1b	12.8	0.0043
	Itgb2	12.6	0.0178
	Ccl11	12.5	0.0077
	Cd14	11.4	0.0006
	Ptgs2	11.2	0.0417
	Ltb	10.1	0.0258
	Cxcl10	10.1	0.0269
	Il6	9.2	0.0112
	Tlr1	7.9	0.0346
	Tlr7	7.8	0.0164
	Ccl5	6.9	0.0349
	Ccl3	6.4	0.0340
	Il1rn	6.0	0.0306
	Tnf	5.3	0.0355
	Cxcl2	4.9	0.0183
	B2m	4.6	0.0008
	Ccl4	4.6	0.0466
	Cd40	4.2	0.0305
	Il10	3.9	0.0495
	Csf1	3.6	0.0187
	Il7	3.5	0.0234
	Tlr4	3.4	0.0180
	Lta	2.1	0.0071

[1]Islets were isolated from 24-week-old male *a*-hIAPP$^{Tg/o}$, *A^{vy}*-hIAPP$^{Tg/o}$, and wild-type (WT) littermates. Islet gene expression was evaluated by RT-qPCR using an SABiosciences Inflammatory Response and Autoimmunity array. Gene expression was normalized to a panel of housekeeping genes (*Actb, Gapdh, Gusb, Hsp90ab1)*. Data represent the average fold-change (FC) of 4 mice per group. *p*-values were determined by Student's t-test.

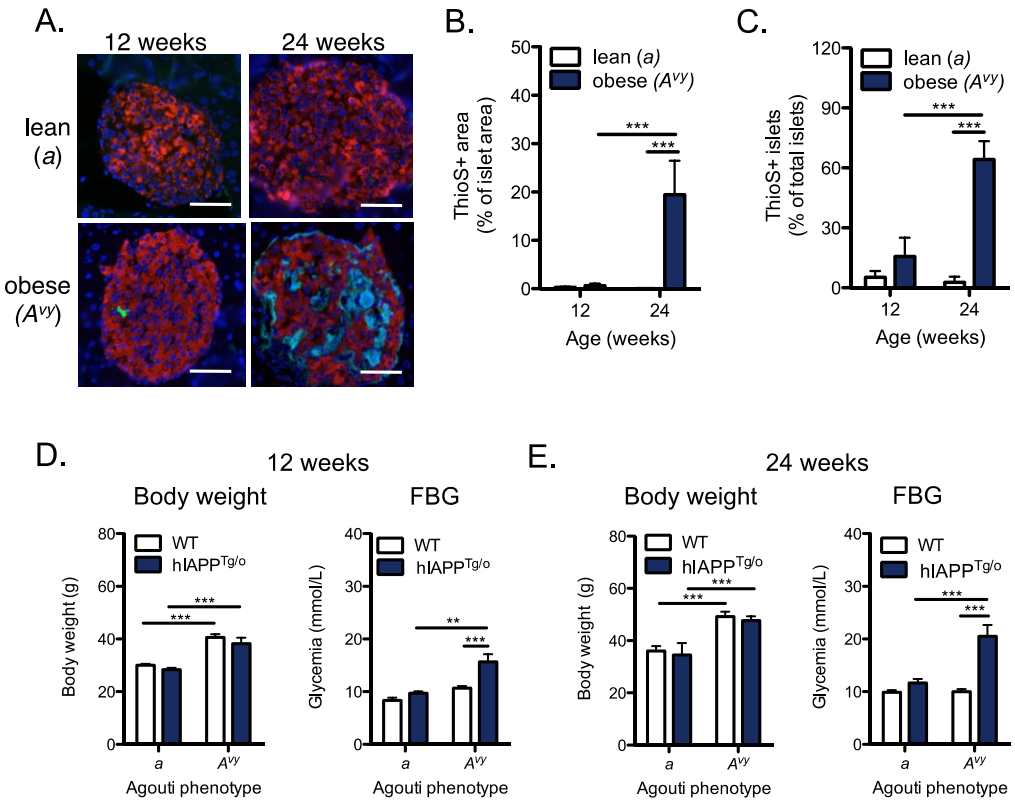

Figure 5.1. Beta cell expression of hIAPP in obese A^{vy}-expressing mice promotes amyloid accumulation and hyperglycemia between 12 and 24 weeks. (A) Pancreata were isolated from 12- and 24-week-old male hIAPP$^{Tg/o}$ or wild-type (WT) mice (C57BL/6×FVB) with or without expression of the agouti viable yellow allele (represented by A^{vy} and *a,* respectively). Sections of formalin-fixed, paraffin-embedded pancreas were stained for insulin (red), amyloid (green, thioflavin S), and DAPI (blue). Note that due to the broad emission spectrum of thioflavin S there is some detection of this dye by the blue filter. Scale bar: 50 μm. (B) Amyloid prevalence (proportion of islets containing amyloid) and (C) amyloid severity (proportion of islet area occupied by amyloid) were assessed at each time point. Body weight and fasting blood glucose (FBG) were assessed at (D) 12 and (E) 24 weeks. Data represent mean±SEM of 7-11 mice per group. ** p<0.01, *** p<0.001.

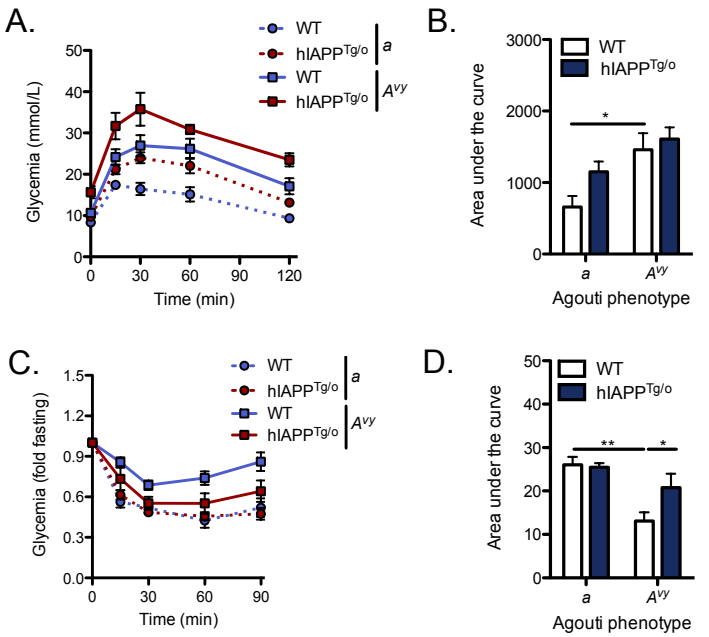

Figure 5.2. Obese A^{vy} mice have impaired glucose tolerance at 12 weeks of age. (A) Glucose tolerance was assessed by i.p. injection of 0.75 g/kg glucose and (B) evaluation of area under the glycemia curve (baseline = fasting glycemia) up to 120 min. (C) Insulin sensitivity was assessed by i.p. injection of 1 U/kg insulin and (D) evaluation of area under the glycemia curve (baseline = 1.0) up to 60 min. Data represent mean±SEM of 7-11 mice per group. * $p<0.05$, ** $p<0.01$.

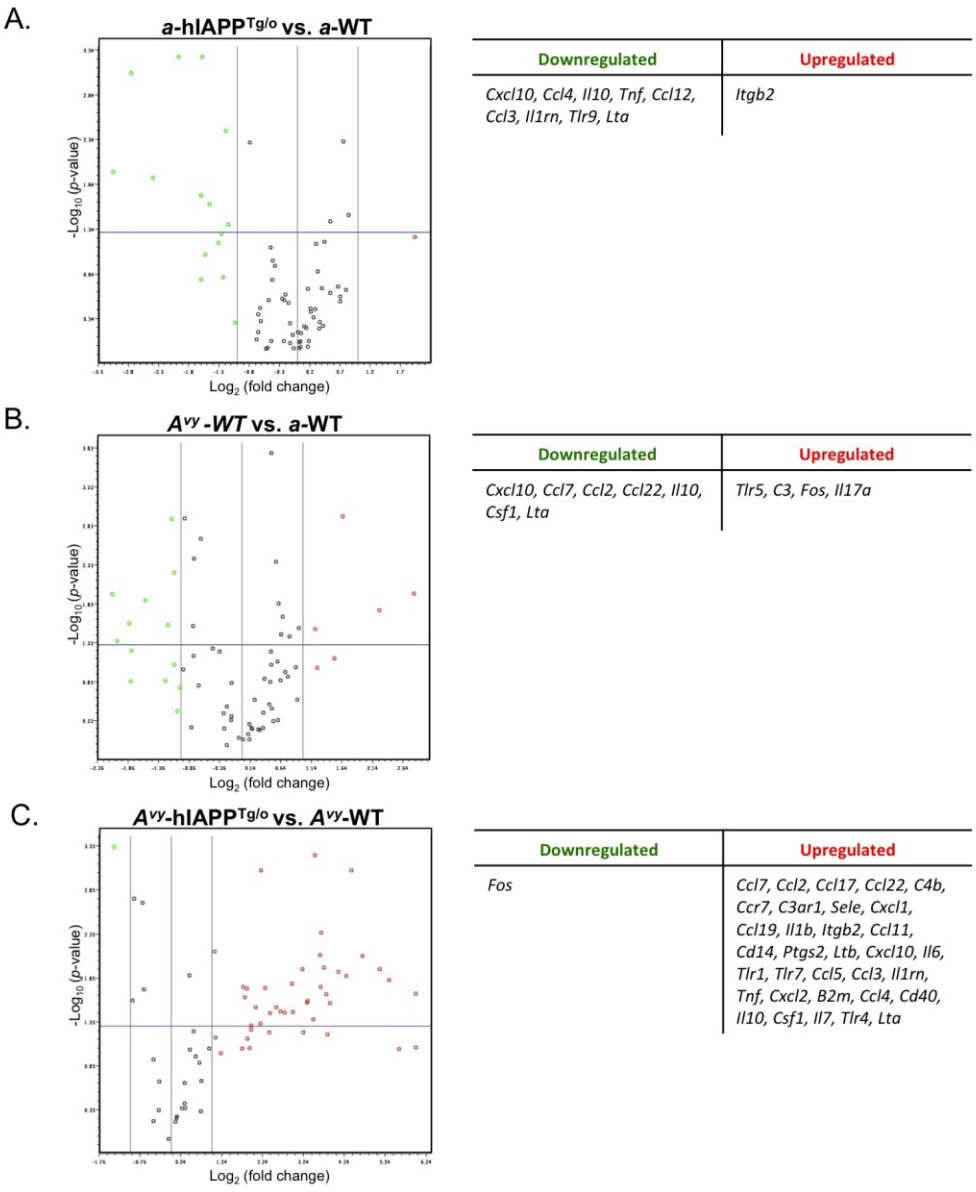

Figure 5.3. hIAPP-induced islet dysfunction in obese A^{vy}-expressing mice is associated with upregulation of islet pro-inflammatory gene expression. Islets were isolated from 24-week-old male hIAPP$^{Tg/o}$ or wild-type (WT) mice (C57BL/6×FVB) with or without expression of the agouti viable yellow allele (represented by A^{vy} and *a,* respectively). Islets were lysed for RNA purification 4 h following isolation and gene expression was evaluated by RT-qPCR using an SABiosciences Inflammatory Response and Autoimmunity array. Volcano plots showing differential gene expression in (A) *a*-hIAPP$^{Tg/o}$ vs. *a*-WT mice, (B) A^{vy}-WT vs. *a*-WT mice, and (C) A^{vy}-hIAPP$^{Tg/o}$ vs. A^{vy}-WT mice show the $\log_2$ fold change in gene expression (*x*-axis, threshold set at 2) relative to the $\log_{10}$ *p*-value as determined by Student's t-test (*y*-axis, threshold set at 0.05). Gene expression was normalized to a panel of housekeeping genes (*Actb, Gapdh, Gusb, Hsp90ab1).* FC: fold change. Data represent the average fold-change of 4 mice per group.

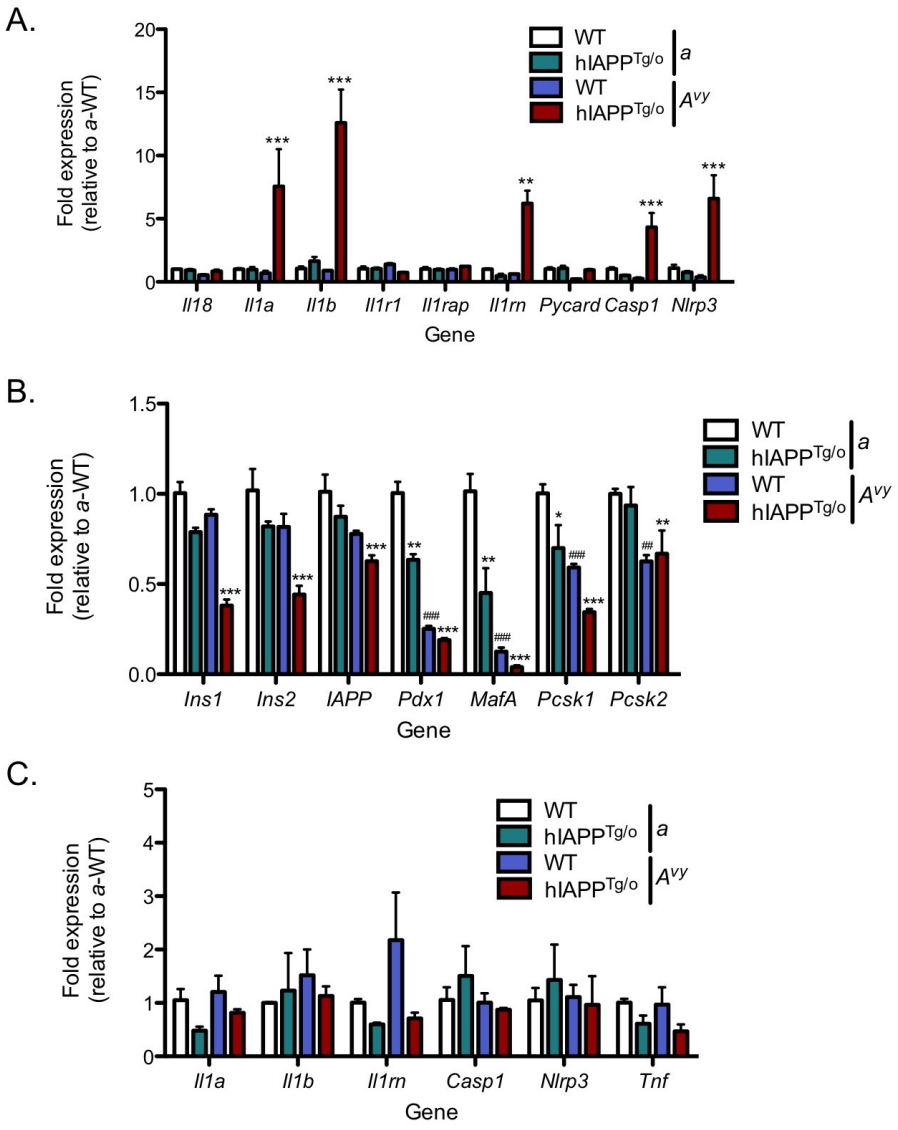

Figure 5.4. hIAPP-induced islet dysfunction is associated with increased expression of IL-1 family members. Islets were isolated from 24-week-old male hIAPP$^{Tg/o}$ or wild-type (WT) mice (C57BL/6×FVB) with or without expression of the agouti viable yellow allele (represented by A^{vy} and *a,* respectively). Islets were lysed for RNA purification 4 h following isolation and expression of (A) IL-1 family genes and (B) beta cell genes was evaluated by RT-qPCR. (C) Expression of IL-1-related genes in liver was evaluated by RT-qPCR. Expression levels were normalized to the housekeeping gene *Rplp0.* * indicates comparison with WT islets with the same agouti phenotype. # indicates comparison between A^{vy}-WT and *a*-WT mice. */# $p<0.05$, **/## $p<0.01$, ***/### $p<0.001$.

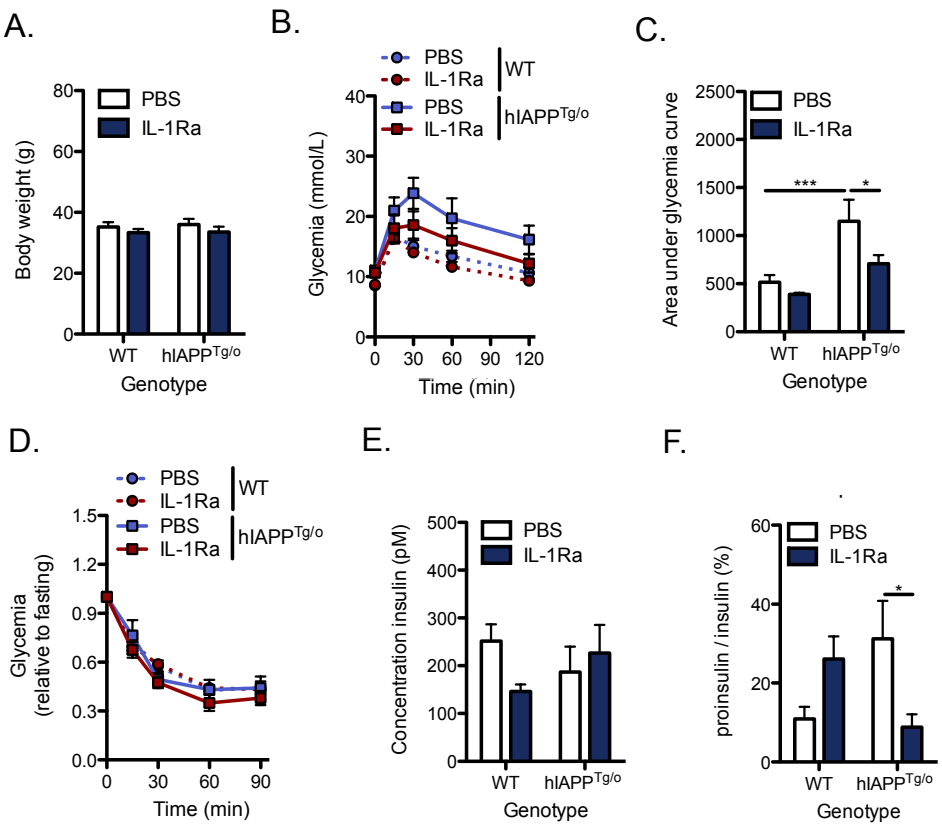

Figure 5.5. IL-1Ra improves islet function in lean *a*-hIAPP$^{Tg/o}$ mice. 16-week-old lean male hIAPP$^{Tg/o}$ or wild-type (WT) mice were treated with 50 mg/kg/day IL-1Ra delivered subcutaneously for 8 weeks. (A) Body weight was assessed at 24 weeks of age. (B) Glucose tolerance was assessed by i.p. injection of 1 g/kg glucose and (C) calculation of area under the glycemia curve (baseline = fasting glycemia). (D) Insulin sensitivity was evaluated following i.p. injection of 1 U/kg insulin. (E) Fasting plasma insulin and (F) the ratio of proinsulin:insulin was determined by ELISA. Data represent mean±SEM of 4-6 mice per group. * $p<0.05$, ** $p<0.01$.

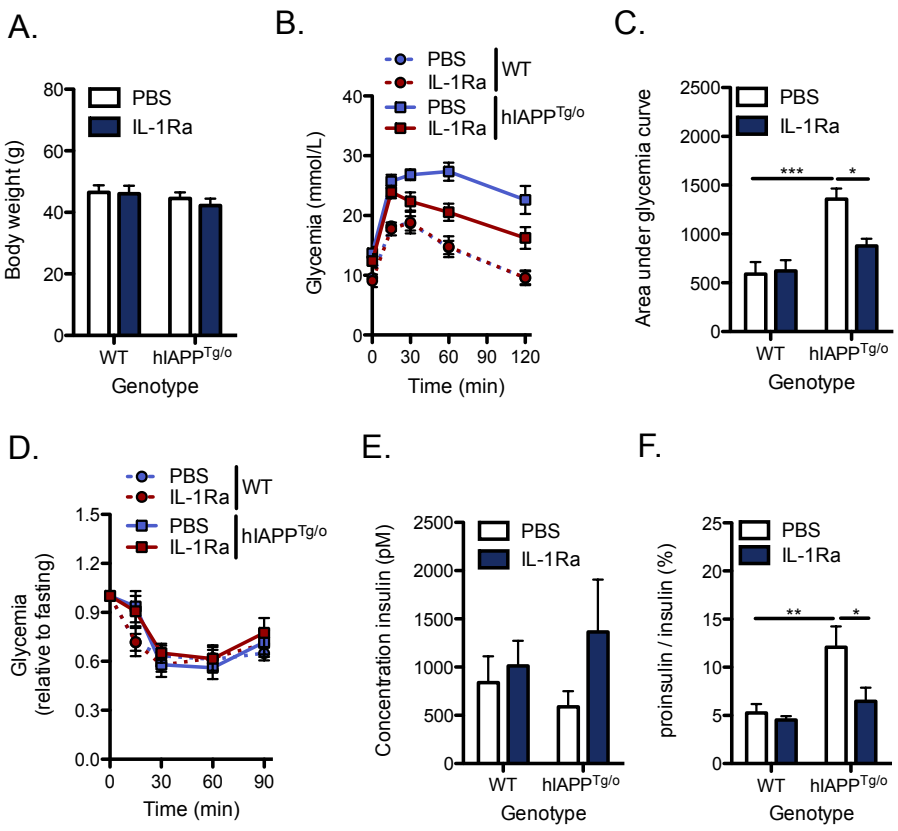

Figure 5.6. IL-1Ra improves glucose tolerance in obese A^{vy}-hIAPP$^{Tg/o}$ mice. 16-week-old obese male hIAPP$^{Tg/o}$ or wild-type (WT) mice (A^{vy} at the agouti locus) were treated with 50 mg/kg/day IL-1Ra delivered subcutaneously for 8 weeks. (A) Body weight was assessed at 24 weeks of age. (B) Glucose tolerance was assessed by i.p. injection of 1 g/kg glucose and (C) calculation of area under the glycemia curve (baseline = fasting glycemia). (D) Insulin sensitivity was evaluated following i.p. injection of 1 U/kg insulin. (E) Fasting plasma insulin and (F) the ratio of proinsulin:insulin was determined by ELISA. Data represent mean±SEM of 4-6 mice per group. * p<0.05, ** p<0.01.

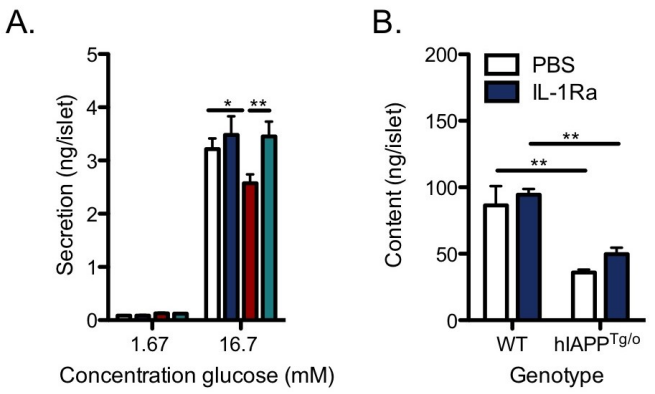

Figure 5.7. IL-1Ra improves glucose-stimulated insulin secretion in cultured hIAPP transgenic islets. Islets were isolated from 12-20-week-old C57BL/6×FVB hIAPP$^{Tg/o}$ mice or wild-type (WT) littermate controls. Islets were cultured for 7 days at 16.7 mM glucose to promote amyloid formation, in the presence or absence of IL-1Ra (2 μg/ml). (A) Glucose-stimulated insulin secretion and (B) insulin content were determined by ELISA. Data represent mean±SEM of islets from 4 mice per group and are representative of 2 independent experiments. * $p<0.05$, ** $p<0.01$, *** $p<0.001$.

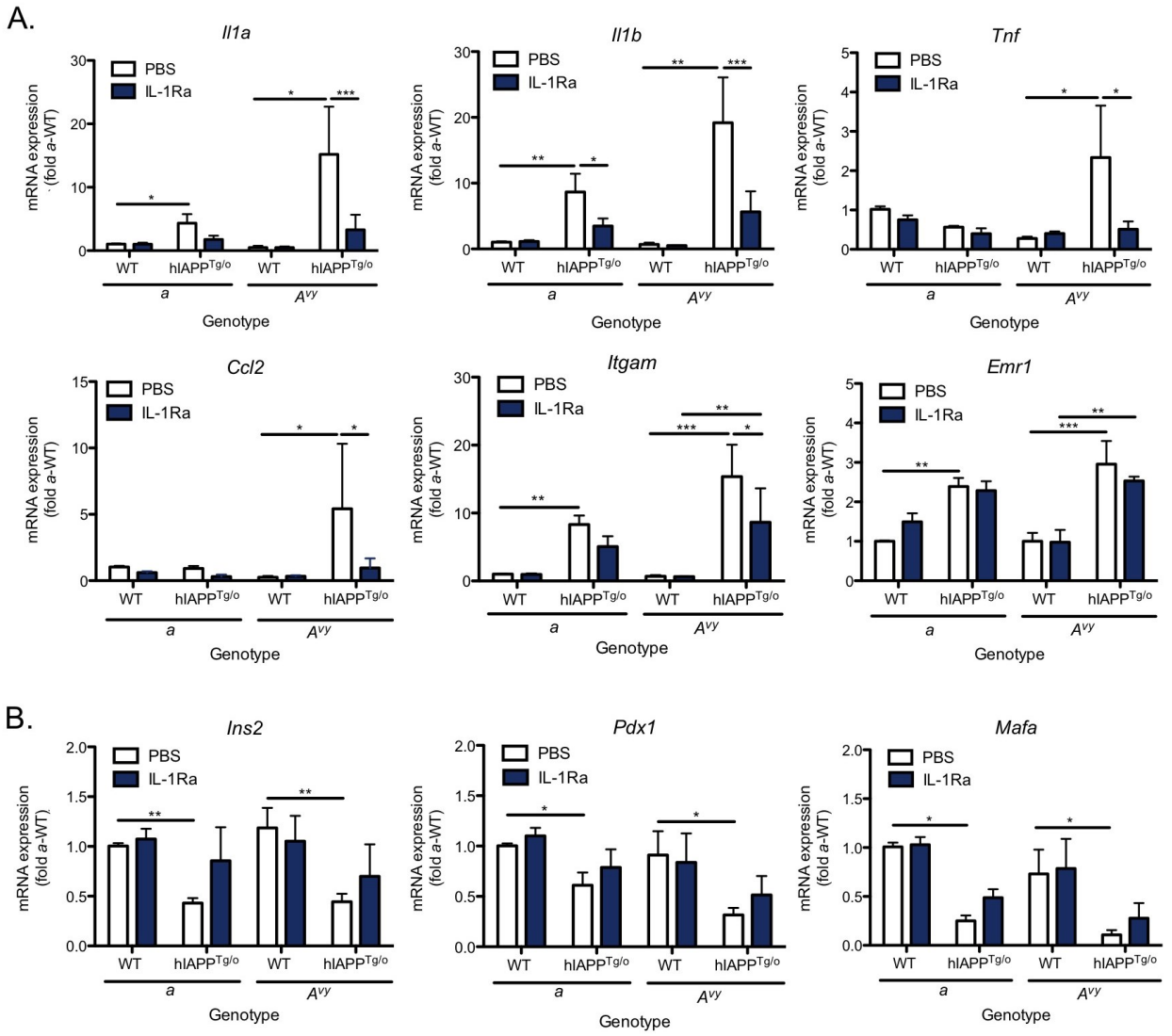

Figure 5.8. IL-1Ra limits islet inflammation in hIAPP$^{Tg/o}$ mice. 16-week-old male hIAPP$^{Tg/o}$ or wild-type (WT) mice with or without expression of the agouti viable yellow allele (represented by A^{vy} and *a,* respectively) were treated with 50 mg/kg/day IL-1Ra delivered subcutaneously. Islets were isolated after 8 weeks and lysed for RNA isolation after overnight recovery. Expression of (A) pro-inflammatory genes and (B) beta cell genes was assessed by RT-qPCR and expression levels were normalized to the housekeeping gene *Rplp0.* Data represent mean±SEM of 4-6 mice per group. * p<0.05, ** p<0.01, *** p<0.001.

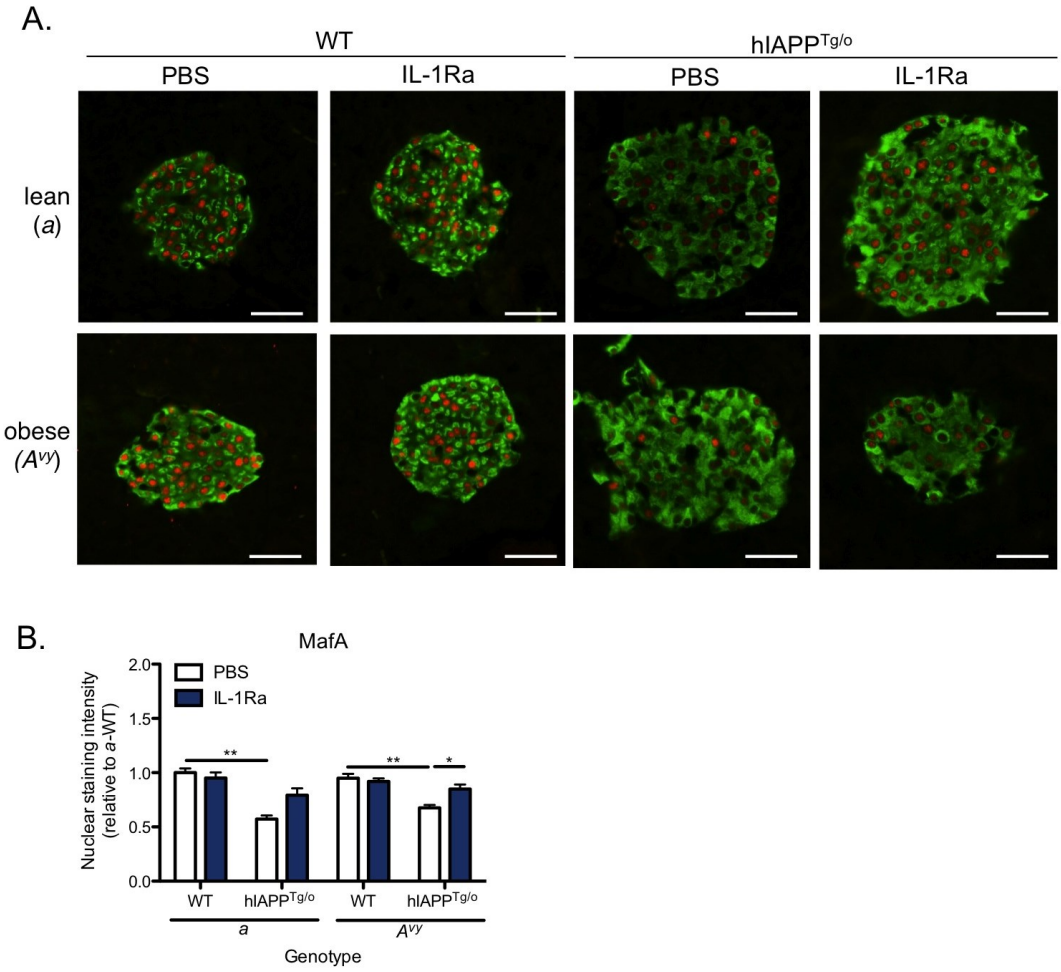

Figure 5.9. IL-1Ra limits loss of nuclear MafA expression in islets of hIAPP$^{Tg/o}$ mice. 16-week-old male hIAPP$^{Tg/o}$ or wild-type (WT) mice with or without expression of the agouti viable yellow allele (represented by A^{vy} and *a,* respectively) were treated with 50 mg/kg/day IL-1Ra delivered subcutaneously for 8 weeks. (A) Nuclear MafA content was assessed by staining of islets from formalin-fixed, paraffin-embedded pancreas sections with insulin (green) and MafA (red). Scale bar: 50 μm. (B) Nuclear staining intensity of MafA was quantified by image analysis of staining represented in (A). Data represent mean±SEM of 4-6 mice per group. * $p<0.05$, ** $p<0.01$.

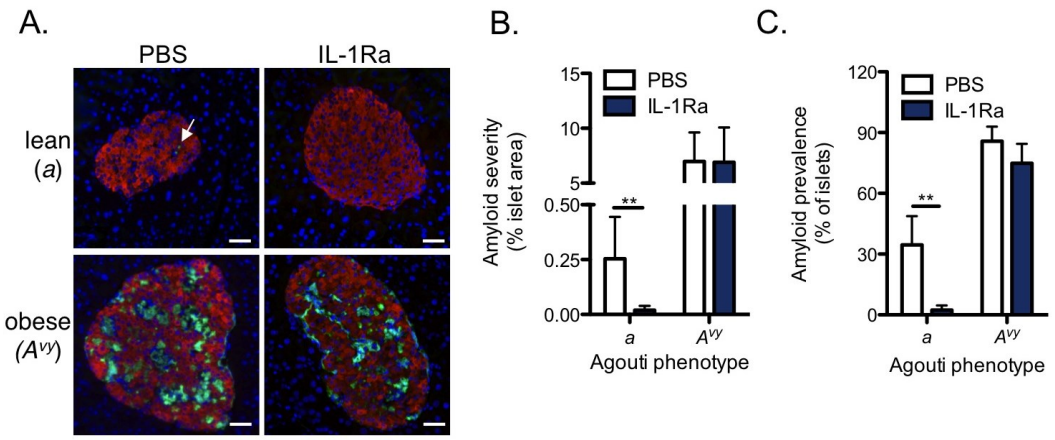

Figure 5.10. IL-1Ra limits islet amyloid severity in lean *a*-hIAPP$^{Tg/o}$ but not obese A^{vy}-hIAPP$^{Tg/o}$ mice. 16-week-old male hIAPP$^{Tg/o}$ or wild-type (WT) mice with or without expression of the agouti viable yellow allele (represented by A^{vy} and *a,* respectively) were treated with 50 mg/kg/day IL-1Ra delivered subcutaneously. Pancreata were isolated after 8 weeks and formalin-fixed, paraffin-embedded sections were stained for insulin (red), amyloid (thioflavin S, green), and DAPI (blue) to assess (B) amyloid severity (proportion of islet area occupied by amyloid) and (C) amyloid prevalence (proportion of islets containing amyloid). Scale bar: 50 μm. Data represent mean±SEM of 4-6 mice per group. ** p<0.01.

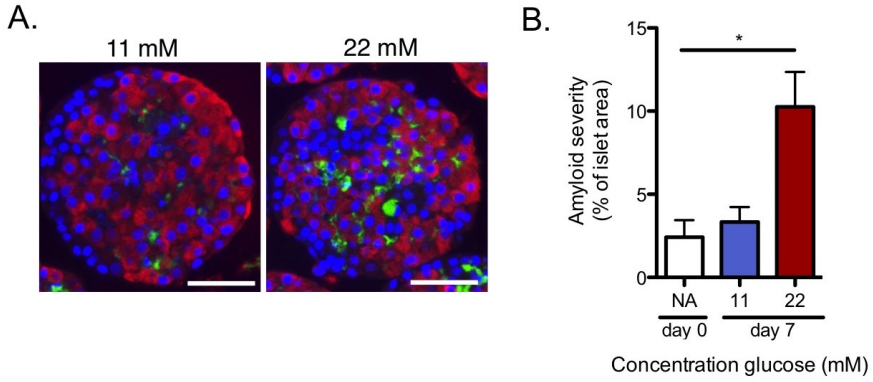

Figure 5.11. hIAPP transgenic rat islets develop amyloid *in vitro* in high-glucose culture. Islets were isolated from 8-week-old hemizygous hIAPP$^{Tg/o}$ mice Sprague-Dawley rats and cultured for 7 days in medium containing either 11 or 22 mM glucose. (A) Sections of formalin-fixed, paraffin-embedded islets were stained for insulin (red), amyloid (thioflavin S, green), and nuclei (DAPI, blue). (B) Thioflavin-S-positive area was quantified as a proportion of total islet area. Data represent mean±SEM of islets from 4 rats. * p<0.05.

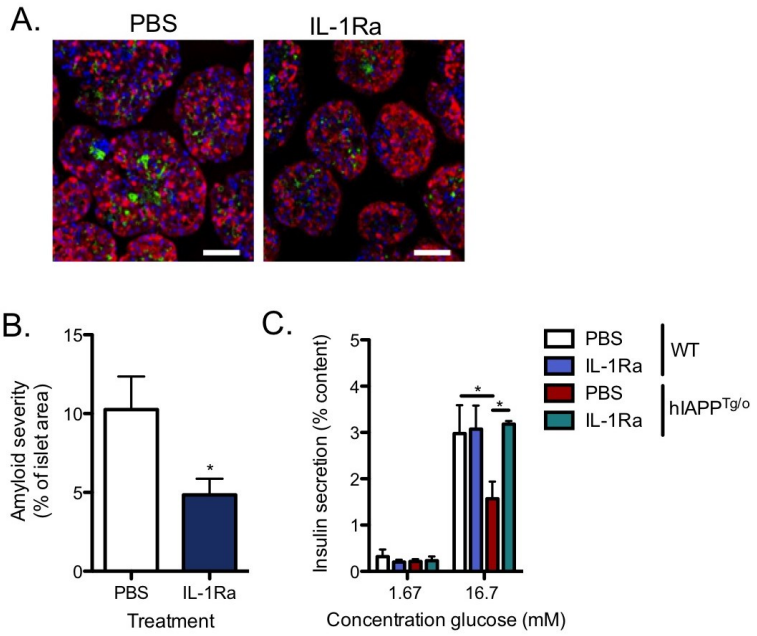

Figure 5.12. IL-1Ra limits islet amyloid formation in cultured hIAPP transgenic rat islets. Islets were isolated from 8-week-old hemizygous hIAPP$^{Tg/o}$ Sprague-Dawley rats and cultured in 22 mM glucose for 7 days in the presence or absence of IL-1Ra (2 μg/ml). (A) Islets were fixed and stained for insulin (red), amyloid (thioflavin S, green), and DAPI (blue) and (B) amyloid area was expressed as a proportion of total islet area. (C) Glucose-stimulated insulin secretion was evaluated by ELISA and expressed relative to insulin content, which did not vary among groups. Scale bar: 50 μm. Data represent mean±SEM of islets from 4 rats. * p<0.05, ** p<0.01.

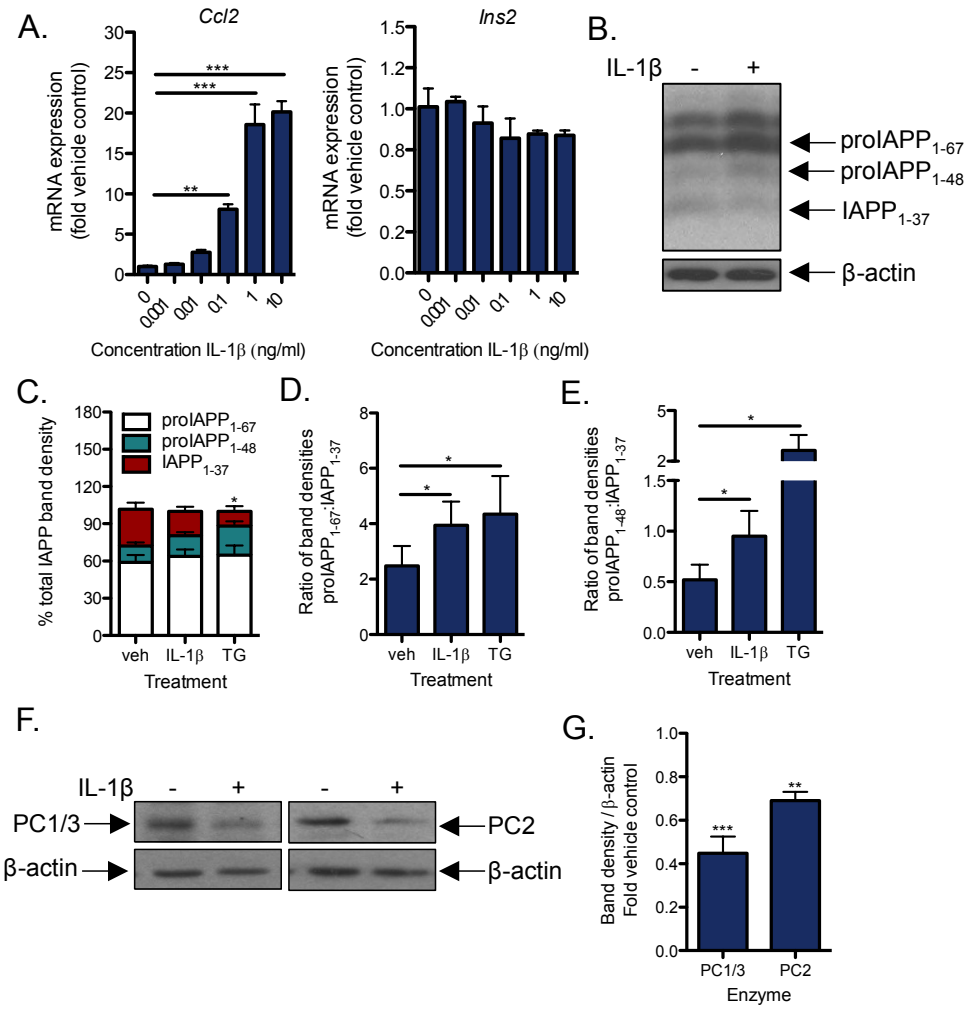

Figure 5.13. IL-1 impairs proIAPP processing in MIN6 cells. MIN6 beta cells were treated with recombinant IL-1β for 24 h. (A) Gene expression was assessed by RT-qPCR with *Rplp0* as the internal control. (B) Expression of proIAPP$_{1-67}$, partially processed proIAPP$_{1-48}$, and mature IAPP$_{1-37}$ in response to 100 pg/ml IL-1β was assessed by western blot. (C) Expression of each species relative to total IAPP (normalized to β-actin), (D) the ratio of proIAPP$_{1-67}$ to mature IAPP, and (E) the ratio of proIAPP$_{1-48}$ to mature IAPP were determined by band densitometry. (F) Levels of active PC1/3 and PC2 in IL-1-treated cells were determined by western blot and (G) expressed relative to vehicle control (normalized to β-actin). Data represent mean±SEM of 4 independent experiments. * p<0.05, ** p<0.01, *** p<0.001.

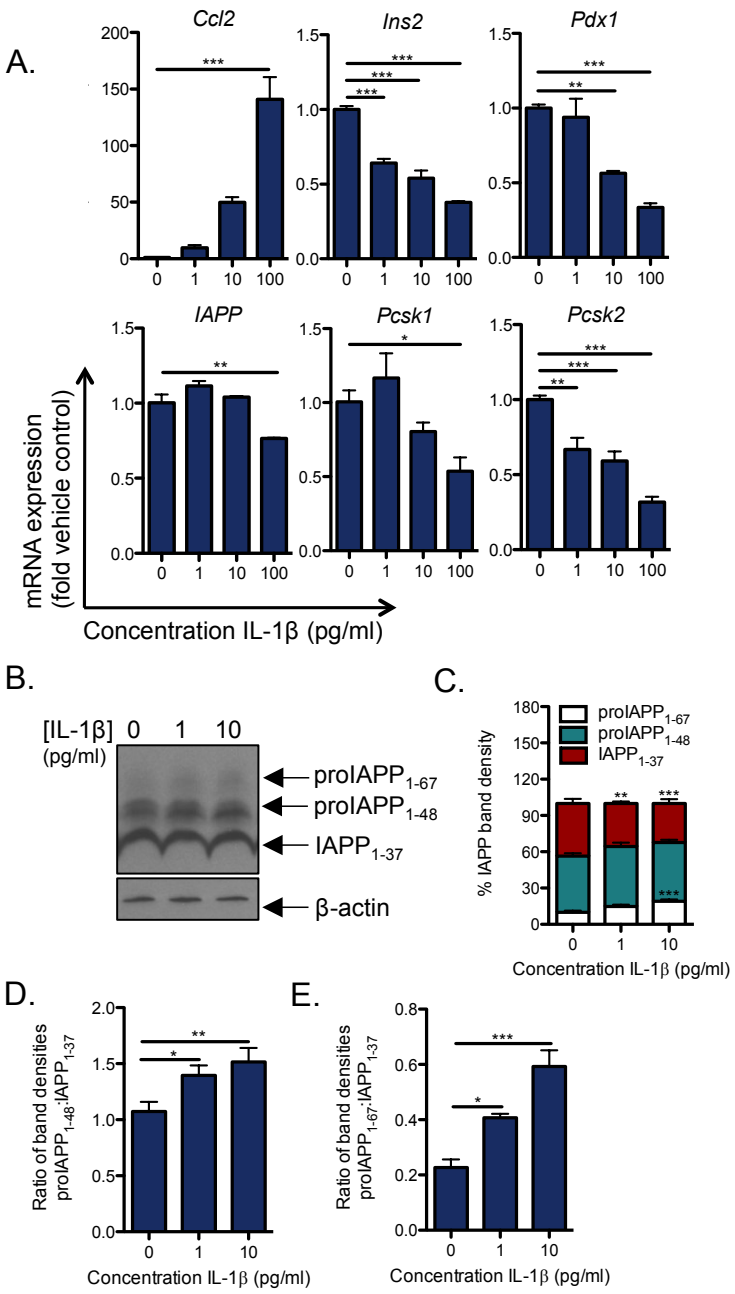

Figure 5.14. IL-1 impairs proIAPP processing in cultured islets. Islets were treated with recombinant IL-1β for 24 h. (A) Gene expression was assessed by RT-qPCR with *Rplp0* as the internal control. (B) Expression of proIAPP$_{1\text{-}67}$, partially processed proIAPP$_{1\text{-}48}$, and mature IAPP$_{1\text{-}37}$ was assessed by western blot. (C) Expression of each species relative to total IAPP (normalized to β-actin), (D) the ratio of proIAPP$_{1\text{-}67}$ to mature IAPP, and (E) the ratio of proIAPP$_{1\text{-}48}$ to mature IAPP were determined by band densitometry. Data represent mean±SEM of islets from 3 mice and are representative of 2 independent experiments. * p<0.05, ** p<0.01, *** p<0.001.

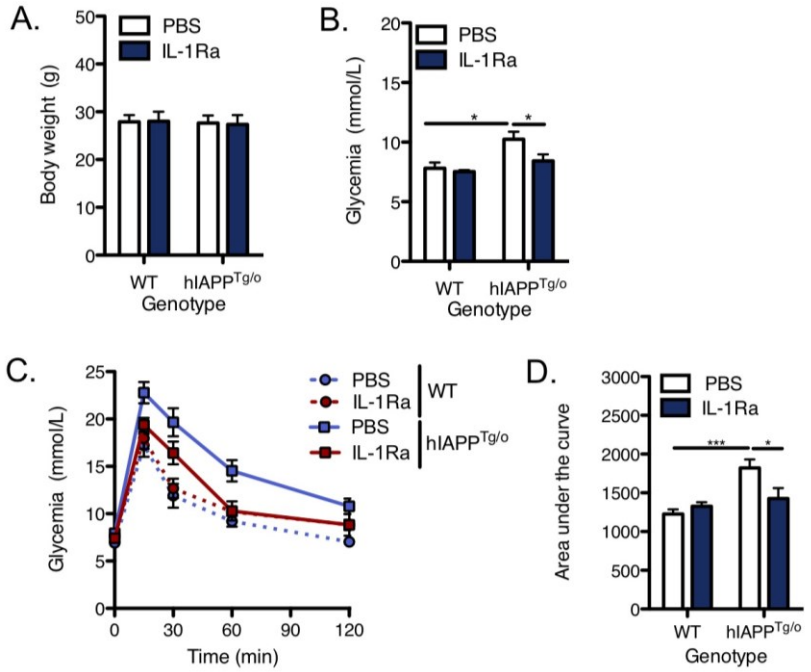

Figure 5.15. IL-1Ra attenuates IAPP-induced islet graft dysfunction. 150 islets from 12- to 16-week-old hIAPP$^{Tg/o}$ mice or wild-type (WT) littermates were transplanted into NOD/SCID recipients implanted with a mini-osmotic pump releasing PBS or IL-1Ra (50 mg/kg/day) for the duration of the experiment. (A) Body weight and (B) fasting glycemia were measured 8 weeks following transplantation. (C) Glucose tolerance was assessed by monitoring tail vein glucose following i.p. injection of 0.75 U/kg glucose, and evaluation of (D) area under the glycemia curve up to 120 min (baseline = 0 mmol/L). Data represent mean±SEM of 7-9 mice per group. * $p<0.05$, *** $p<0.001$.

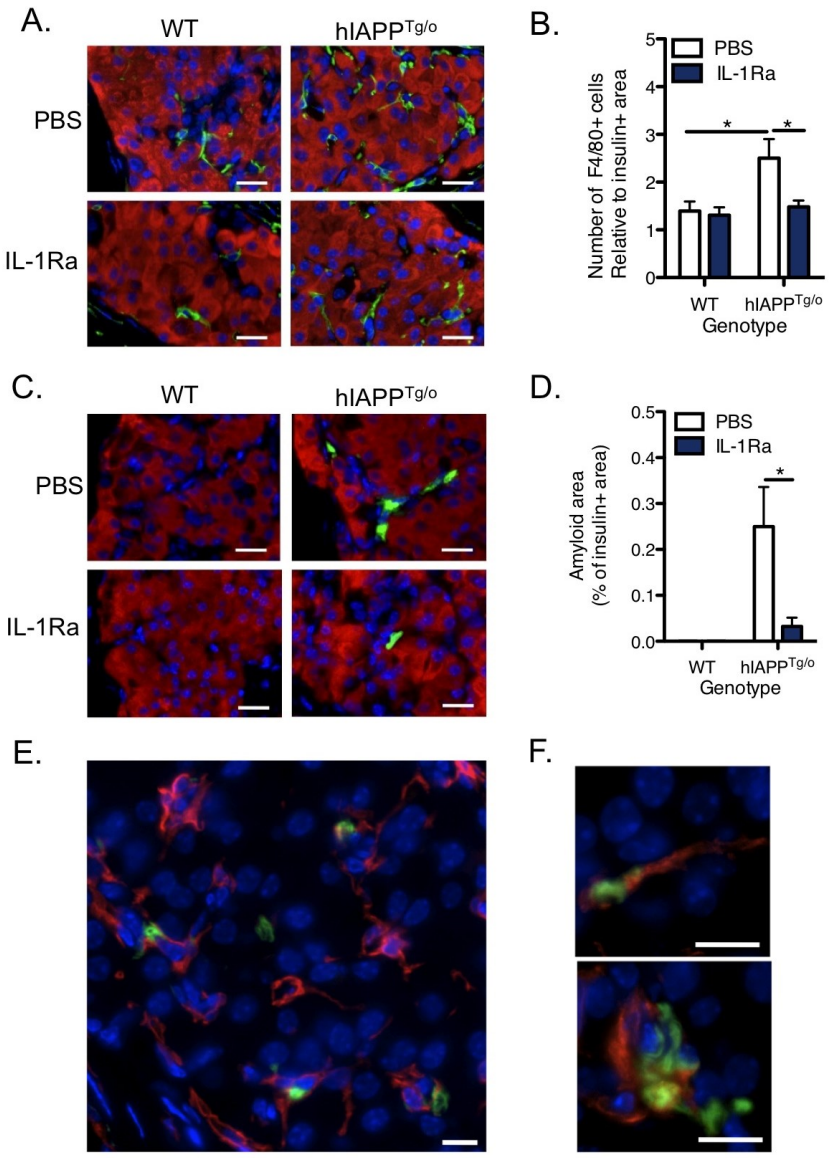

Figure 5.16. IL-1Ra limits amyloid accumulation following islet transplantation. 150 islets from 12- to 16-week-old hIAPP$^{Tg/o}$ mice or wild-type (WT) littermates were transplanted into NOD/SCID recipients implanted with a mini-osmotic pump releasing PBS or IL-1Ra (50 mg/kg/day) for the duration of the experiment. (A) Grafts were stained for insulin (red), F4/80 (green), and DAPI (blue). (B) The number of F4/80-positive cells was expressed relative to the insulin-positive area in each graft, which did not differ among groups. (C) Grafts were stained for insulin (red), amyloid (thioflavin S, green), and DAPI (blue). The amyloid area was expressed relative to the insulin-positive area in each graft. (E) Grafts were stained for F4/80 (red), amyloid (thioflavin S, green), and DAPI (blue). F4/80^{+} cells, at higher magnification in (F), were found associated with most thioflavin-S-positive deposits. Scale bars: 25 μm (A,C,E) or 10 μm (F). Data represent mean±SEM of 7-9 mice per group. * p<0.05.

Chapter 6: Conclusions

Islet amyloid deposition and pro-inflammatory cytokine secretion are associated with beta cell dysfunction in type 2 diabetes. The data presented in this thesis address two critical questions: (a) how does islet amyloid cause beta cell dysfunction; and (b) what are the triggers for islet inflammation? These studies identify IAPP, the principal component of islet amyloid, as an islet-localized trigger for innate immune activation. In Chapter 3, we show that the pro-inflammatory cytokine IL-1 acts as a critical mediator of IAPP-induced macrophage activation and islet cytokine expression. Indeed, IAPP induces at least two major pathways contributing to IL-1β synthesis and secretion: (a) activation of NF-κB via TLR2/6, leading to proIL-1β synthesis; and (b) activation of caspase-1 leading to the maturation and secretion of IL-1β. In Chapter 4, we show that $CD11b^{+}F4/80^{+}$ islet macrophages are the major islet cell type in which this response occurs, and that depletion of islet phagocytes both *in vivo* and *in vitro* improves IAPP-induced islet dysfunction. Finally, Chapter 5 supports an important role for IAPP-induced IL-1 synthesis by demonstrating a therapeutic effect of IL-1Ra in transgenic hIAPP-expressing mouse models of type 2 diabetes and islet transplantation. A schematic overview of the pathways activated by soluble and fibrillar IAPP is shown in Figure 6.1, together with potential targets for therapeutic intervention.

Intriguingly, other amyloidogenic peptides of both bacterial and mammalian origin also activate TLR2 and NLRP3, although in each case it is unclear whether the responsible species is an oligomeric or fibrillar aggregate. An understanding of the nature of the IAPP aggregates that activate TLR2/6 and NLRP3 is important in the development of amyloid inhibitors, which may stabilize on- or off-pathway pre-fibrillar species. Further analysis of IAPP aggregate structure throughout a detailed time course of immune cell activation may provide additional information, making use of methods such as Fourier transform infrared spectroscopy, X-ray diffraction, and atomic force microscopy. While additional studies are also required to determine the nature of the interaction between IAPP and TLR2, screening of candidate aggregation inhibitors for their capacity to stabilize intermediates that activate each pathway may be of some utility. Nevertheless, the physiological significance of IAPP-induced TLR2 activation remains to be determined. It is also unclear whether IAPP interacts directly with TLR2 or whether TLR2/6

activation occurs indirectly via other mechanisms, such as liberation of endogenous DAMPs. In Chapter 3, we provide the first evidence for distinct actions of pre-fibrillar oligomers and amyloid fibrils on TLR2 and NLRP3. An outline of this model is provided in Figure 6.2. Specifically, early IAPP aggregates are the major species responsible for TLR2 activation, whereas fibrils efficiently induce proIL-1β maturation and secretion and are likely the species required for NLRP3 activation. Given increasing evidence for cross-talk between TLR and NLRP3 signalling pathways, IAPP and other amyloidogenic peptides may act as particularly potent pro-inflammatory stimuli because of their capacity to activate both pathways.

Existing methods for isolation and characterization of endogenous amyloid from pancreatic islets are extremely limited; our analysis of IAPP aggregation within the islet was therefore restricted to detection of fibrils with thioflavin S in these studies. While thioflavin staining provides a general indication of the amount and severity of IAPP aggregation, it is unclear how macrophage depletion and IL-1Ra administration affect the formation of pre-fibrillar aggregates *in vivo.* Unfortunately, the A11 antibody that recognizes oligomeric but not fibrillar forms of other amylodogenic peptides (322) has not yielded convincingly specific staining in our hands. Indeed, this antibody recognizes a variety of other proteins, including many molecular chaperones (132). Moreover, while the toxic properties of pre-fibrillar oligomers have been well characterized *in vitro,* the nature of the IAPP species that is toxic to beta cells *in vivo* is unknown. Our data suggest that fibril formation is required for IL-1β secretion. Thus, while smaller aggregates may provide a stimulus for proIL-1β synthesis (as in our models of early IAPP aggregation with limited fibril deposition), a dramatic increase in the expression of other islet pro-inflammatory cytokines was observed only in mice with extensive islet amyloid deposits. This is consistent with an IAPP-induced auto-inflammatory process within the islet mediated by secretion of IL-1.

Our data have several additional therapeutic implications. First, the improved glucose tolerance in clodronate liposome- and IL-1Ra-treated hIAPP$^{Tg/o}$ mice and the improved insulin secretion in cultured islets suggest that IAPP-induced beta cell dysfunction can be prevented without the use of amyloid inhibitors, which – although an area of intensive research – do not yet exist for clinical use. Moreover, in models of early amyloid formation with no defect in beta cell mass – in particular the FVB hIAPP$^{Tg/o}$ mouse, NOD/SCID recipients of FVB hIAPP$^{Tg/o}$ islet

grafts, and the C57BL/6×FVB *a*-hIAPP$^{Tg/o}$ mouse – the protective effects of IL-1Ra and/or macrophage depletion suggest that anti-inflammatory drugs can protect the islet from IAPP aggregates. Our analyses of pancreatic tissue was limited in these studies, as two pieces of pancreas were collected from each mouse (one each for islet isolation and histology), making it difficult to provide accurate measurements of total beta cell mass. Additional evaluation of beta cell mass, death, and markers of cytokine action such as iNOS expression are needed to fully characterize the effects of IL-1Ra and clodronate liposome treatment in our hIAPP$^{Tg/o}$ mice. In addition, while clodronate liposome administration improved glucose tolerance in hIAPP$^{Tg/o}$ mice compared to the pre-treatment phenotype, it is unclear whether the effects of IL-1Ra were due to improvement of already impaired islet function or to prevention of disease progression. Additional cohorts of animals at later stages of disease (i.e. beyond the 12-24 week period during which extensive amyloid deposits form) would be informative in this regard. Further studies making use of control mice overexpressing rIAPP are also needed to rule out an effect of elevated levels of monomeric IAPP; based on our *in vitro* studies, this possibility seems unlikely but nevertheless must be considered.

Second, Chapters 4 and 5 suggest that anti-inflammatory therapies can limit IAPP aggregation at the early stages of disease, providing an alternate (or additional) explanation for improved islet function. However, this was not the case in A^{vy}-hIAPP$^{Tg/o}$ mice, despite markedly improved glycemia with both clodronate liposome and IL-1Ra treatment. Thus, clearance of amyloid fibrils is not a requirement for improved islet function, an observation that is particularly relevant in determining the ideal mechanism of action of IAPP aggregation inhibitors. However, it is possible that IL-1Ra affects the accumulation of pre-fibrillar species that are not detectable with thioflavin S staining, and consequently that the therapeutic response can be partially attributed to a decrease in the pro-inflammatory stimulus. Another likely possibility supported by our *in vitro* data is that an intervention that blocks the cycle of IL-1-induced IL-1 secretion initated by IAPP has protective effects on the beta cell despite the persistence of the initiating stimulus.

Third, anti-inflammatory drugs – including TLR antagonists – are proposed therapeutic agents for increasing insulin sensitivity in type 2 diabetes. However, TLR agonist administration has also been suggested as an approach to amyloid plaque clearance in Alzheimer's disease,

raising the possibility that manipulation of the innate immune response could be detrimental to the function of amyloid-containing tissues. The success of such therapies depends on the maintenance of an appropriate balance between an effective phagocytic response and chronic secretion of toxic pro-inflammatory cytokines. Our data suggest that inhibition of IL-1 or its major intra-islet source, the macrophage, can improve IAPP-induced islet dysfunction. However, since we also show that macrophages may limit the prevalence and severity of islet amyloid, the contribution of each pathway at different stages of disease and in other models of islet amyloid formation requires further evaluation. It is likely that under physiological conditions, macrophages – and indeed, low levels of IL-1β – are critical to maintenance of islet homeostasis. Given the dramatic effects of hIAPP aggregation on the islet inflammatory milieu, existing rodent models of obesity and type 2 diabetes may lack a central trigger for islet inflammation that contributes to beta cell dysfunction. These models may therefore be inadequate for the evaluation of anti-inflammatory therapies, and arguably for any type 2 diabetes therapy.

Fourth, given the central role of IL-1 in mediating IAPP-induced inflammation and the capacity for TLR stimuli to enhance NLRP3 activation, NLRP3 inhibitors or similar therapies may hold promise for limiting IAPP-induced IL-1β secretion and improving islet function. Our data suggest a possible explanation for why anti-IL-1 therapies – at least with the dosing regimens employed in several clinical trials – cause apparent improvement in islet function without affecting insulin sensitivity. The particularly high expression of IL-1R on the beta cell combined with a potent local stimulus for IL-1 may make the islet especially susceptible to this cytokine. Although the short half-life of IL-1Ra and transient injection site reactions make it less likely to be approved for type 2 diabetes, it may be appropriate in some patients with comorbid conditions such as gout, rheumatoid arthritis, or cardiovascular disease. In fact, the Canakinumab Anti-inflammatory Thrombosis Outcomes Study (CANTOS) is currently underway to evaluate the effects of anti-IL-1β antibody on cardiovascular risk in 17,200 patients over four years, with diabetes as a secondary endpoint (363). Other potential targets with therapeutics under development are described in Figure 6.1. While the elevation of islet *Il1b* but not *Il1a* expression appears to precede glucose intolerance in the early model of hIAPP-induced islet dysfunction described in Chapter 4, IL-1α secretion is regulated by other processes and is independent of NLRP3, suggesting that pre-fibrillar hIAPP species may be sufficient for its secretion. As

discussed in Chapter 5, the efficacy of IL-1Ra points to a potential effect of hIAPP on the secretion of IL-1α as well as IL-1β, a distinction that remains to be evaluated.

Finally, preproIAPP has been previously described as a $CD8^+$ T cell epitope in HLA-A*0201 patients with type 1 diabetes (542), suggesting that IAPP may fill dual roles as both a stimulus for activation of antigen-presenting cells and as a beta cell autoantigen. Further work is needed to determine whether hIAPP aggregation accelerates auto- or alloimmunity in mouse models of type 1 diabetes and islet transplantation. To our knowledge, the presence of IAPP aggregates in islets from patients with type 1 diabetes has not been thoroughly investigated and may contribute to beta cell failure by activation of both innate and adaptive immunity.

Among innate immune cells potentially affected by IAPP aggregation, we focused on resident islet macrophages because (a) we found no evidence of increased expression of other leukocyte markers in islets from $hIAPP^{Tg/o}$ mice, (b) the $F4/80^+CD11b^+CD11c^+$ islet population was the major source of islet *Il1b* expression, and (c) islet macrophages/dendritic cells are the only immune cell population characterized in mouse models of type 2 diabetes and found to be present at increased frequency in islets from humans with the disease. However, limited data are available on immune cell populations in islets from human donors. One recent publication provided the first characterization of islet leukocytes, suggesting an increase in the total number of $CD45^+$ cells in islets from patients with type 2 diabetes and an increase in the proportion of B cells relative to other leukocytes (421). Further information regarding immune cell subsets and their activation states will help answer questions regarding the nature and consequences of islet inflammation in type 2 diabetes.

Epidemiological trends toward excess caloric intake and increased life expectancy have emerged only over the last 100 years, in comparison with the evolutionarily ancient mechanisms of innate immunity. That inflammation and infection can drive changes in metabolism is perhaps unsurprising, as increased activity of certain immune cell subsets changes their nutrient and energy requirements. In contrast, innate immune activation in response to diabetes-associated stimuli – including islet amyloid – is a more recent phenomenon, reaches highest prevalence after the peak reproductive years, and seems unlikely to contribute to adaptive fitness. Indeed, the capacity of the immune system to respond to amyloidogenic peptides produced in the setting of metabolic disease may be a consequence of its response to similar motifs produced by

pathogenic bacteria and fungi. Figure 6.3 provides an overview of the possible outcomes of PRR activation by amyloidogenic peptides of either microbial or endogenous origin.

This is an exciting time in the emerging field of immunometabolism, which over the past ten years has provided significant insight into the pathogenesis of diseases involving perturbations in both metabolic and immune homeostasis. Perhaps no other disease at the interface of metabolism and innate immunity poses a threat to global health comparable to that of type 2 diabetes. It is our hope that an increased understanding of the triggers for pancreatic islet inflammation will lead to the development of targeted therapeutic strategies to prevent the onset and limit the progression of beta cell dysfunction. Because increasing evidence suggests an epidemiological and pathological link between type 2 diabetes and neurodegenerative disease, an understanding of the general mechanisms of amyloid-induced innate immune activation may lead to common approaches to the treatment of multiple aging-associated amyloidoses.

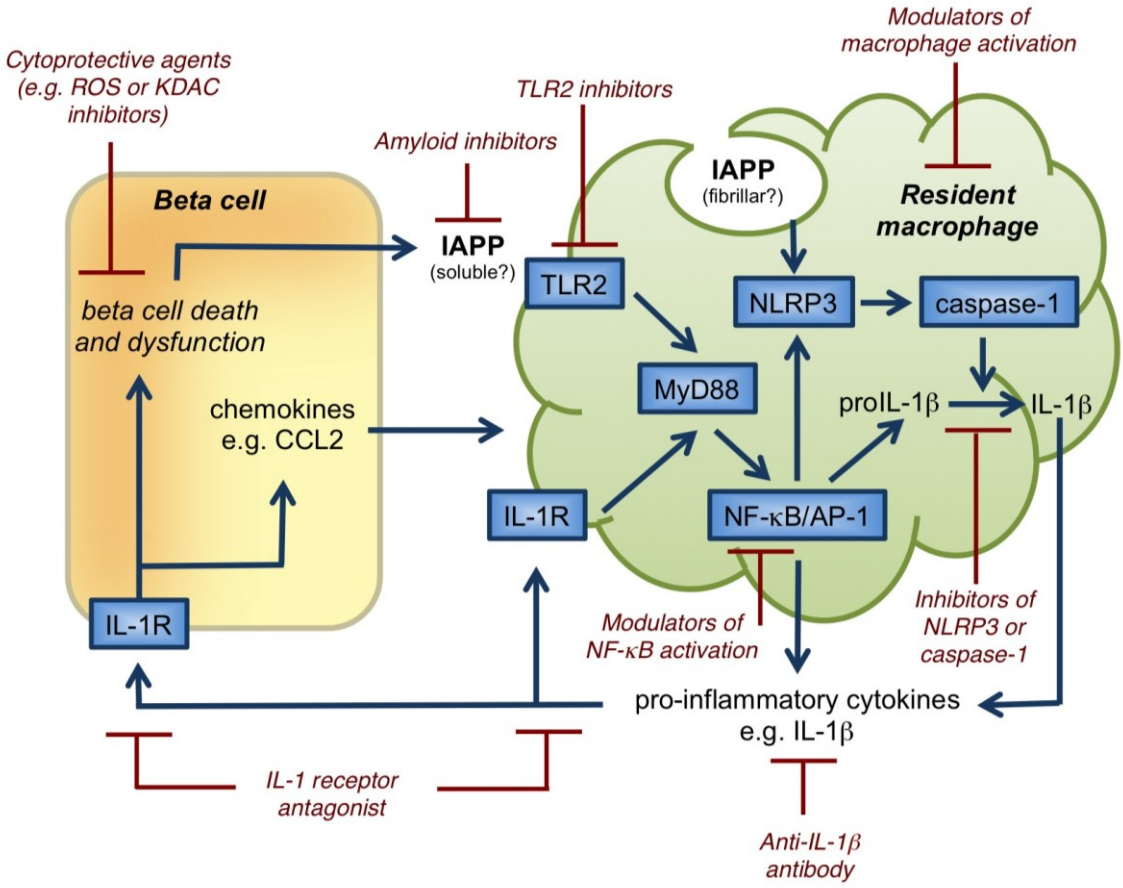

Figure 6.1. Mechanisms of IAPP-induced islet inflammation and potential targets of therapeutic intervention in type 2 diabetes. Aggregates of IAPP formed early during the aggregation process activate TLR2 and its downstream adaptor protein MyD88, leading to nuclear translocation of the transcription factor NF-κB required for synthesis of pro-IL-1β (Chapter 3). Other studies have demonstrated that TLR signalling also promotes NLRP3 activation by increasing expression and post-translational modification of inflammasome components (299,300). Mature IAPP aggregates activate NLRP3 (suggested by us in Chapter 3 and demonstrated directly in (477)), leading to caspase-1-mediated proIL-1β cleavage. Autocrine/paracrine signalling via the IL-1R can directly impair beta cell function and promote chemokine secretion leading to monocyte recruitment (demonstrated *in vitro* in Chapter 3 and in islet transplant recipients in Chapter 5, although we found no change in the number of intra-islet $CD11b^{+}F4/80^{+}CD11c^{+}$ cells within the islets in Chapter 4). Potential therapeutic agents to block amyloid-induced inflammation include inhibitors of IAPP aggregation (e.g. conformation-dependent antibodies or small molecule inhibitors), TLR2 inhibitors (e.g. neutralizing antibodies or small molecules), drugs that modulate macrophage phenotype (e.g. some existing anti-inflammatory and oral anti-diabetic therapies), inhibitors of NLRP3 or caspase-1, anti-IL-1 neutralizing antibodies, modulators of NF-κB activation (e.g. salsalate, KDAC inhibitors), compounds that block cytokine/chemokine receptor activation or signalling (e.g. IL-1Ra), and beta cell cytoprotective agents (e.g. ROS or KDAC inhibitors).

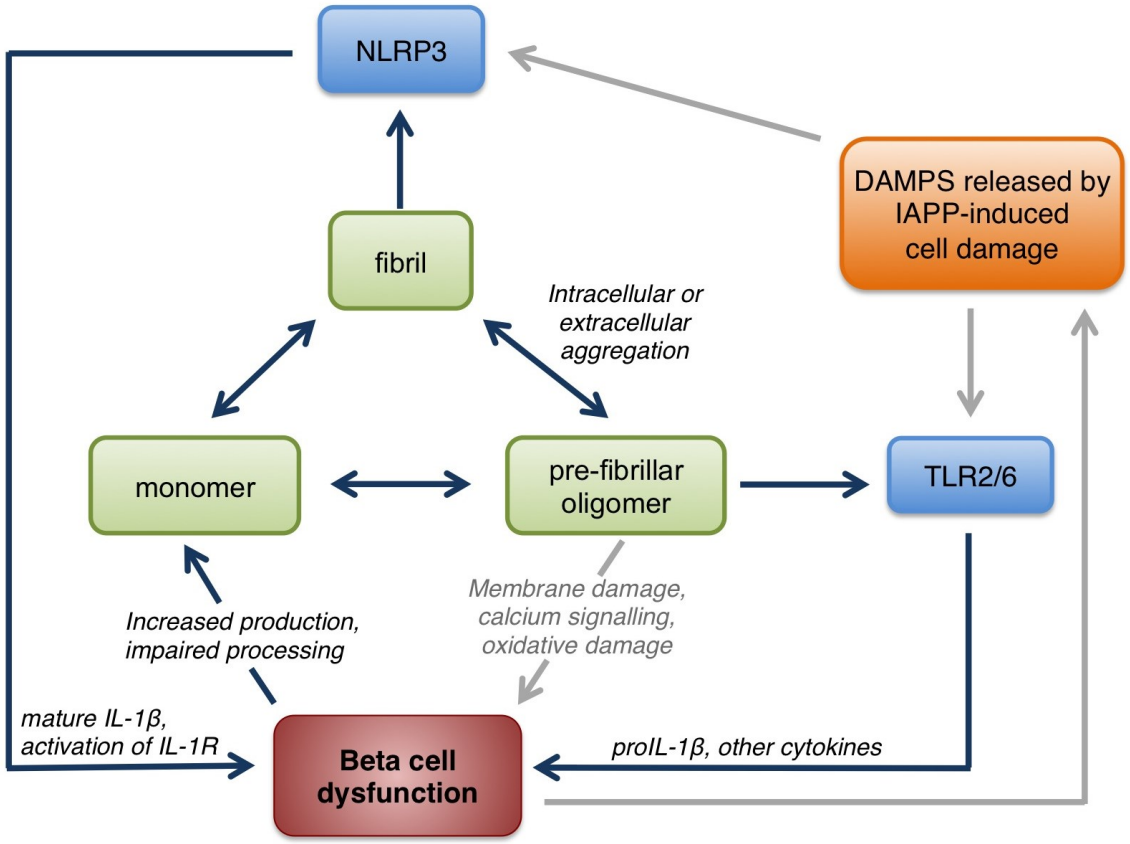

Figure 6.2. Model for PRR activation by oligomeric and fibrillar IAPP. Most models of IAPP aggregation suggest that fibrils exist in equilibrium with monomers, which may aggregate under certain conditions (e.g. in the presence of membrane lipids or certain receptors) to form pre-fibrillar oligomers. TLR2 activation by pre-fibrillar aggregates leads to the synthesis of proIL-1β in macrophages (Chapter 3). Aggregation of monomers can occur extracellularly, leading to phagocytosis of the fibril and NLRP3 activation (477), or aggregation may occur intracellularly within endosomes or lysosomes prior to triggering of NLRP3 (287). Active NLRP3 leads to proIL-1β processing and secretion. IL-1-induced beta cell dysfunction may lead to impaired proIAPP processing and increased secretion of partially processed intermediates that promote amyloid formation. Alternatively, direct damage to beta cells by hIAPP (e.g. via membrane damage, CD95 signalling, oxidative damage, or altered calcium signalling) may lead to release of endogenous DAMPs that activate PRRs (grey pathway).

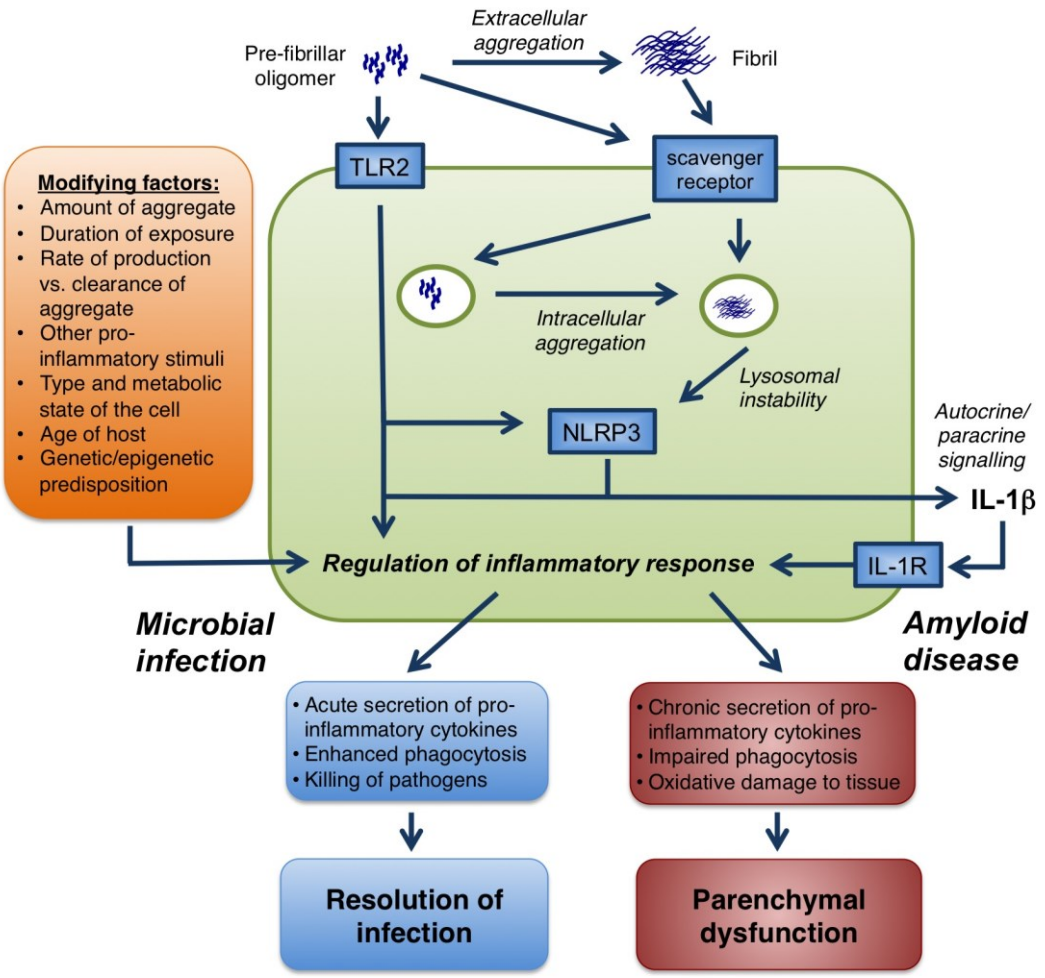

Figure 6.3. Possible outcomes of PRR activation by amyloidogenic peptides. Peptide aggregation may occur intra- or extracellularly, leading to activation of cell-surface scavenger receptors, TLR2 (or TLR4), and the cytosolic NLRP3 inflammasome. Scavenger receptors may facilitate aggregate uptake, promote TLR dimerization, and seed fibril formation within phagosomes (477). IL-R activates the same signalling pathways downstream of the TLRs, and IL-1-induced IL-1 synthesis is a common attribute of many autoinflammatory diseases. The nature of the pro-inflammatory response to amyloidogenic peptides is determined by epigenetic modifications, altered gene transcription, changes in protein activity, and changes in the metabolic state of the cell. The net outcome depends on the nature and duration of the stimulus, the tissue environment, the cell type, and other modifying factors such as the age of the host and the presence of other pro-inflammatory stimuli. In the case of infection with an amyloid-producing microbe, effective phagocytosis and induction of anti-microbial mediators may lead to resolution of infection. However, chronic exposure to endogenous aggregates that are continuously produced in amyloid disease may impair phagocytosis and promote chronic pro-inflammatory cytokine secretion leading to parenchymal dysfunction. Outcomes of the response to TLR stimulation are reviewed in (294) and implications for microglia in Alzheimer's disease are reviewed in (346).

References

1. International Diabetes Federation. IDF Diabetes Atlas, 6th edn. Brussels, Belgium, 2013
2. Maahs DM, West NA, Lawrence JM, Mayer-Davis EJ. Epidemiology of type 1 diabetes. Endocrinol Metab Clin North Am 2010;39:481-497
3. Guariguata L. By the numbers: new estimates from the IDF Diabetes Atlas Update for 2012. Diabetes Res Clin Pract 2012;98:524-525
4. World Health Organization. Global Action Plan for the Prevention and Control of NCDs 2013-2020. Geneva, Switzerland, 2013
5. Public Health Agency of Canada. Diabetes in Canada: Facts and figures from a public health perspective. Ottawa, Ontario, 2012
6. Pelletier C, Dai S, Roberts KC, Bienek A, Onysko J, Pelletier L. Report summary. Diabetes in Canada: facts and figures from a public health perspective. Chronic Dis Inj Can 2012;33:53-54
7. Millar K, Dean HJ. Developmental origins of type 2 diabetes in aboriginal youth in Canada: it is more than diet and exercise. J Nutr Metab 2012;2012:127452
8. Canadian Diabetes Association Clinical Practice Guidelines Expert Committee of the Canadian Diabetes Advisory Board. Canadian Diabetes Association 2013 Clinical Practice Guidelines for the Prevention and Management of Diabetes in Canada. Can J Diabetes 2013;37:S212
9. Cheng AY, Lau DC. The Canadian Diabetes Association 2013 Clinical Practice Guidelines-raising the bar and setting higher standards! Can J Diabetes 2013;37:137-138
10. Pottie K, Jaramillo A, Lewin G, Dickinson J, Bell N, Brauer P, Dunfield L, Joffres M, Singh H, Tonelli M. Recommendations on screening for type 2 diabetes in adults. CMAJ 2012;184:1687-1696
11. American Diabetes Association. Diagnosis and classification of diabetes mellitus. Diabetes Care 2012;35 Suppl 1:S64-71
12. Groop L, Pociot F. Genetics of diabetes - Are we missing the genes or the disease? Mol Cell Endocrinol 2014;382:726-739
13. Naik RG, Brooks-Worrell BM, Palmer JP. Latent autoimmune diabetes in adults. J Clin Endocrinol Metab 2009;94:4635-4644
14. Donath MY, Ehses JA. Type 1, type 1.5, and type 2 diabetes: NOD the diabetes we thought it was. Proc Natl Acad Sci USA 2006;103:12217-12218
15. Hagopian WA, Lernmark A, Rewers MJ, Simell OG, She JX, Ziegler AG, Krischer JP, Akolkar B. TEDDY--The Environmental Determinants of Diabetes in the Young: an observational clinical trial. Ann NY Acad Sci 2006;1079:320-326
16. Bach JF, Chatenoud L. The hygiene hypothesis: an explanation for the increased frequency of insulin-dependent diabetes. Cold Spring Harb Perspect Med 2012;2:a007799
17. Kibirige M, Metcalf B, Renuka R, Wilkin TJ. Testing the accelerator hypothesis: the relationship between body mass and age at diagnosis of type 1 diabetes. Diabetes Care 2003;26:2865-2870
18. Moltchanova EV, Schreier N, Lammi N, Karvonen M. Seasonal variation of diagnosis of Type 1 diabetes mellitus in children worldwide. Diabet Med 2009;26:673-678
19. Kukko M, Kimpimaki T, Korhonen S, Kupila A, Simell S, Veijola R, Simell T, Ilonen J, Simell O, Knip M. Dynamics of diabetes-associated autoantibodies in young children with

human leukocyte antigen-conferred risk of type 1 diabetes recruited from the general population. J Clin Endocrinol Metab 2005;90:2712-2717
20. Kaprio J, Tuomilehto J, Koskenvuo M, Romanov K, Reunanen A, Eriksson J, Stengard J, Kesaniemi YA. Concordance for type 1 (insulin-dependent) and type 2 (non-insulin-dependent) diabetes mellitus in a population-based cohort of twins in Finland. Diabetologia 1992;35:1060-1067
21. Metcalfe KA, Hitman GA, Rowe RE, Hawa M, Huang X, Stewart T, Leslie RD. Concordance for type 1 diabetes in identical twins is affected by insulin genotype. Diabetes Care 2001;24:838-842
22. Concannon P, Rich SS, Nepom GT. Genetics of type 1A diabetes. N Engl J Med 2009;360:1646-1654
23. Davies JL, Kawaguchi Y, Bennett ST, Copeman JB, Cordell HJ, Pritchard LE, Reed PW, Gough SC, Jenkins SC, Palmer SM, et al. A genome-wide search for human type 1 diabetes susceptibility genes. Nature 1994;371:130-136
24. Lucassen AM, Julier C, Beressi JP, Boitard C, Froguel P, Lathrop M, Bell JI. Susceptibility to insulin dependent diabetes mellitus maps to a 4.1 kb segment of DNA spanning the insulin gene and associated VNTR. Nat Genet 1993;4:305-310
25. Maldonado M, Hampe CS, Gaur LK, D'Amico S, Iyer D, Hammerle LP, Bolgiano D, Rodriguez L, Rajan A, Lernmark A, Balasubramanyam A. Ketosis-prone diabetes: dissection of a heterogeneous syndrome using an immunogenetic and beta-cell functional classification, prospective analysis, and clinical outcomes. J Clin Endocrinol Metab 2003;88:5090-5098
26. Atkinson MA, Eisenbarth GS, Michels AW. Type 1 diabetes. Lancet 2014;383:69-82
27. Matveyenko AV, Butler PC. Relationship between beta-cell mass and diabetes onset. Diabetes Obes Metab 2008;10 Suppl 4:23-31
28. Klinke DJ, 2nd. Extent of beta cell destruction is important but insufficient to predict the onset of type 1 diabetes mellitus. PLoS ONE 2008;3:e1374
29. Michels AW, Eisenbarth GS. Immune intervention in type 1 diabetes. Semin Immunol 2011;23:214-219
30. Gianani R, Campbell-Thompson M, Sarkar SA, Wasserfall C, Pugliese A, Solis JM, Kent SC, Hering BJ, West E, Steck A, Bonner-Weir S, Atkinson MA, Coppieters K, von Herrath M, Eisenbarth GS. Dimorphic histopathology of long-standing childhood-onset diabetes. Diabetologia 2010;53:690-698
31. Sosenko JM, Skyler JS, Palmer JP, Krischer JP, Yu L, Mahon J, Beam CA, Boulware DC, Rafkin L, Schatz D, Eisenbarth G. The prediction of type 1 diabetes by multiple autoantibody levels and their incorporation into an autoantibody risk score in relatives of type 1 diabetic patients. Diabetes Care 2013;36:2615-2620
32. Orban T, Sosenko JM, Cuthbertson D, Krischer JP, Skyler JS, Jackson R, Yu L, Palmer JP, Schatz D, Eisenbarth G. Pancreatic islet autoantibodies as predictors of type 1 diabetes in the Diabetes Prevention Trial-Type 1. Diabetes Care 2009;32:2269-2274
33. Wang L, Lovejoy NF, Faustman DL. Persistence of prolonged C-peptide production in type 1 diabetes as measured with an ultrasensitive C-peptide assay. Diabetes Care 2012;35:465-470
34. Keenan HA, Sun JK, Levine J, Doria A, Aiello LP, Eisenbarth G, Bonner-Weir S, King GL. Residual insulin production and pancreatic ss-cell turnover after 50 years of diabetes: Joslin Medalist Study. Diabetes 2010;59:2846-2853

35. Zimmet PZ. The pathogenesis and prevention of diabetes in adults. Genes, autoimmunity, and demography. Diabetes Care 1995;18:1050-1064
36. Steenkamp DW, Alexanian SM, Sternthal E. Approach to the patient with atypical diabetes. CMAJ 2014;10.1503 /cmaj.130185
37. Goel A, Chiu H, Felton J, Palmer JP, Brooks-Worrell B. T-cell responses to islet antigens improves detection of autoimmune diabetes and identifies patients with more severe beta-cell lesions in phenotypic type 2 diabetes. Diabetes 2007;56:2110-2115
38. Medici F, Hawa M, Ianari A, Pyke DA, Leslie RD. Concordance rate for type II diabetes mellitus in monozygotic twins: actuarial analysis. Diabetologia 1999;42:146-150
39. Sanghera DK, Blackett PR. Type 2 Diabetes Genetics: Beyond GWAS. J Diabetes Metab 2012;3:6948
40. McCarthy MI. Genomics, type 2 diabetes, and obesity. N Engl J Med 2010;363:2339-2350
41. Mehran AE, Templeman NM, Brigidi GS, Lim GE, Chu KY, Hu X, Botezelli JD, Asadi A, Hoffman BG, Kieffer TJ, Bamji SX, Clee SM, Johnson JD. Hyperinsulinemia drives diet-induced obesity independently of brain insulin production. Cell Metab 2012;16:723-737
42. Thaler JP, Yi CX, Schur EA, Guyenet SJ, Hwang BH, Dietrich MO, Zhao X, Sarruf DA, Izgur V, Maravilla KR, Nguyen HT, Fischer JD, Matsen ME, Wisse BE, Morton GJ, Horvath TL, Baskin DG, Tschop MH, Schwartz MW. Obesity is associated with hypothalamic injury in rodents and humans. J Clin Invest 2012;122:153-162
43. Thaler JP, Schwartz MW. Minireview: Inflammation and obesity pathogenesis: the hypothalamus heats up. Endocrinology 2010;151:4109-4115
44. Qin J, Li Y, Cai Z, Li S, Zhu J, Zhang F, Liang S, Zhang W, Guan Y, Shen D, Peng Y, Zhang D, Jie Z, Wu W, Qin Y, Xue W, Li J, Han L, Lu D, Wu P, Dai Y, Sun X, Li Z, Tang A, Zhong S, Li X, Chen W, Xu R, Wang M, Feng Q, Gong M, Yu J, Zhang Y, Zhang M, Hansen T, Sanchez G, Raes J, Falony G, Okuda S, Almeida M, LeChatelier E, Renault P, Pons N, Batto JM, Zhang Z, Chen H, Yang R, Zheng W, Li S, Yang H, Wang J, Ehrlich SD, Nielsen R, Pedersen O, Kristiansen K, Wang J. A metagenome-wide association study of gut microbiota in type 2 diabetes. Nature 2012;490:55-60
45. Karlsson FH, Tremaroli V, Nookaew I, Bergstrom G, Behre CJ, Fagerberg B, Nielsen J, Backhed F. Gut metagenome in European women with normal, impaired and diabetic glucose control. Nature 2013;498:99-103
46. Vrieze A, Van Nood E, Holleman F, Salojarvi J, Kootte RS, Bartelsman JF, Dallinga-Thie GM, Ackermans MT, Serlie MJ, Oozeer R, Derrien M, Druesne A, Van Hylckama Vlieg JE, Bloks VW, Groen AK, Heilig HG, Zoetendal EG, Stroes ES, de Vos WM, Hoekstra JB, Nieuwdorp M. Transfer of intestinal microbiota from lean donors increases insulin sensitivity in individuals with metabolic syndrome. Gastroenterology 2012;143:913-916
47. Guenard F, Deshaies Y, Cianflone K, Kral JG, Marceau P, Vohl MC. Differential methylation in glucoregulatory genes of offspring born before vs. after maternal gastrointestinal bypass surgery. Proc Natl Acad Sci USA 2013;110:11439-11444
48. Neeland IJ, Turer AT, Ayers CR, Powell-Wiley TM, Vega GL, Farzaneh-Far R, Grundy SM, Khera A, McGuire DK, de Lemos JA. Dysfunctional adiposity and the risk of prediabetes and type 2 diabetes in obese adults. JAMA 2012;308:1150-1159
49. Hotamisligil GS, Shargill NS, Spiegelman BM. Adipose expression of tumor necrosis factor-alpha: direct role in obesity-linked insulin resistance. Science 1993;259:87-91

50. Havel PJ. Update on adipocyte hormones: regulation of energy balance and carbohydrate/lipid metabolism. Diabetes 2004;53 Suppl 1:S143-151
51. Kahn SE, Prigeon RL, McCulloch DK, Boyko EJ, Bergman RN, Schwartz MW, Neifing JL, Ward WK, Beard JC, Palmer JP, et al. Quantification of the relationship between insulin sensitivity and beta-cell function in human subjects. Evidence for a hyperbolic function. Diabetes 1993;42:1663-1672
52. Kasuga M. Insulin resistance and pancreatic beta cell failure. J Clin Invest 2006;116:1756-1760
53. Stancakova A, Javorsky M, Kuulasmaa T, Haffner SM, Kuusisto J, Laakso M. Changes in insulin sensitivity and insulin release in relation to glycemia and glucose tolerance in 6,414 Finnish men. Diabetes 2009;58:1212-1221
54. Weyer C, Bogardus C, Mott DM, Pratley RE. The natural history of insulin secretory dysfunction and insulin resistance in the pathogenesis of type 2 diabetes mellitus. J Clin Invest 1999;104:787-794
55. Kahn SE, Lachin JM, Zinman B, Haffner SM, Aftring RP, Paul G, Kravitz BG, Herman WH, Viberti G, Holman RR. Effects of rosiglitazone, glyburide, and metformin on beta-cell function and insulin sensitivity in ADOPT. Diabetes 2011;60:1552-1560
56. D'Alessio D. The role of dysregulated glucagon secretion in type 2 diabetes. Diabetes Obes Metab 2011;13 Suppl 1:126-132
57. Unger RH, Cherrington AD. Glucagonocentric restructuring of diabetes: a pathophysiologic and therapeutic makeover. J Clin Invest 2012;122:4-12
58. Reaven GM, Chen YD, Golay A, Swislocki AL, Jaspan JB. Documentation of hyperglucagonemia throughout the day in nonobese and obese patients with noninsulin-dependent diabetes mellitus. J Clin Endocrinol Metab 1987;64:106-110
59. Brand CL, Rolin B, Jorgensen PN, Svendsen I, Kristensen JS, Holst JJ. Immunoneutralization of endogenous glucagon with monoclonal glucagon antibody normalizes hyperglycaemia in moderately streptozotocin-diabetic rats. Diabetologia 1994;37:985-993
60. Johnson DG, Goebel CU, Hruby VJ, Bregman MD, Trivedi D. Hyperglycemia of diabetic rats decreased by a glucagon receptor antagonist. Science 1982;215:1115-1116
61. Mighiu PI, Yue JT, Filippi BM, Abraham MA, Chari M, Lam CK, Yang CS, Christian NR, Charron MJ, Lam TK. Hypothalamic glucagon signaling inhibits hepatic glucose production. Nat Med 2013;19:766-772
62. Quddusi S, Vahl TP, Hanson K, Prigeon RL, D'Alessio DA. Differential effects of acute and extended infusions of glucagon-like peptide-1 on first- and second-phase insulin secretion in diabetic and nondiabetic humans. Diabetes Care 2003;26:791-798
63. Miller RE. Pancreatic neuroendocrinology: peripheral neural mechanisms in the regulation of the Islets of Langerhans. Endocr Rev 1981;2:471-494
64. Pavlov VA, Tracey KJ. The vagus nerve and the inflammatory reflex--linking immunity and metabolism. Nat Rev Endocrinol 2012;8:743-754
65. Le Stunff H, Coant N, Migrenne S, Magnan C. Targeting lipid sensing in the central nervous system: new therapy against the development of obesity and type 2 diabetes. Expert Opin Ther Targets 2013;17:545-555

66. Berthoud HR, Jeanrenaud B. Acute hyperinsulinemia and its reversal by vagotomy after lesions of the ventromedial hypothalamus in anesthetized rats. Endocrinology 1979;105:146-151
67. Kahn SE, Zraika S, Utzschneider KM, Hull RL. The beta cell lesion in type 2 diabetes: there has to be a primary functional abnormality. Diabetologia 2009;52:1003-1012
68. Porksen N, Grofte T, Greisen J, Mengel A, Juhl C, Veldhuis JD, Schmitz O, Rossle M, Vilstrup H. Human insulin release processes measured by intraportal sampling. Am J Physiol Endocrinol Metab 2002;282:E695-702
69. Kahn SE, Halban PA. Release of incompletely processed proinsulin is the cause of the disproportionate proinsulinemia of NIDDM. Diabetes 1997;46:1725-1732
70. Butler AE, Janson J, Bonner-Weir S, Ritzel R, Rizza RA, Butler PC. Beta-cell deficit and increased beta-cell apoptosis in humans with type 2 diabetes. Diabetes 2003;52:102-110
71. Meier JJ, Bonadonna RC. Role of reduced beta-cell mass versus impaired beta-cell function in the pathogenesis of type 2 diabetes. Diabetes Care 2013;36 Suppl 2:S113-119
72. Laybutt DR, Preston AM, Akerfeldt MC, Kench JG, Busch AK, Biankin AV, Biden TJ. Endoplasmic reticulum stress contributes to beta cell apoptosis in type 2 diabetes. Diabetologia 2007;50:752-763
73. Robertson RP. Beta-cell deterioration during diabetes: what's in the gun? Trends Endocrinol Metab 2009;20:388-393
74. Andrikopoulos S. Obesity and type 2 diabetes: slow down!--Can metabolic deceleration protect the islet beta cell from excess nutrient-induced damage? Mol Cell Endocrinol 2010;316:140-146
75. El-Assaad W, Buteau J, Peyot ML, Nolan C, Roduit R, Hardy S, Joly E, Dbaibo G, Rosenberg L, Prentki M. Saturated fatty acids synergize with elevated glucose to cause pancreatic beta-cell death. Endocrinology 2003;144:4154-4163
76. Poitout V, Robertson RP. Minireview: Secondary beta-cell failure in type 2 diabetes--a convergence of glucotoxicity and lipotoxicity. Endocrinology 2002;143:339-342
77. Kahn SE, Andrikopoulos S, Verchere CB. Islet amyloid: a long-recognized but underappreciated pathological feature of type 2 diabetes. Diabetes 1999;48:241-253
78. Höppener JWM, Ahren B, Lips CJM. Islet amyloid and type 2 diabetes mellitus. N Engl J Med 2000;343:411-419
79. Donath MY, Dalmas E, Sauter NS, Böni-Schnetzler M. Inflammation in obesity and diabetes: islet dysfunction and therapeutic opportunity. Cell Metab 2013;17:860-872
80. Ryan EA. Diagnostic criteria for gestational diabetes: who decides? CMAJ 2012;184:1341-1342
81. Steffes MW, Sibley S, Jackson M, Thomas W. Beta-cell function and the development of diabetes-related complications in the diabetes control and complications trial. Diabetes Care 2003;26:832-836
82. Pickup JC. Insulin-pump therapy for type 1 diabetes mellitus. N Engl J Med 2012;366:1616-1624
83. Moran A, Bundy B, Becker DJ, DiMeglio LA, Gitelman SE, Goland R, Greenbaum CJ, Herold KC, Marks JB, Raskin P, Sanda S, Schatz D, Wherrett DK, Wilson DM, Krischer JP, Skyler JS, Pickersgill L, de Koning E, Ziegler AG, Boehm B, Badenhoop K, Schloot N, Bak JF, Pozzilli P, Mauricio D, Donath MY, Castano L, Wagner A, Lervang HH, Perrild H, Mandrup-Poulsen T, Pociot F, Dinarello CA. Interleukin-1 antagonism in type 1 diabetes of

recent onset: two multicentre, randomised, double-blind, placebo-controlled trials. Lancet 2013;381:1905-1915
84. Shapiro AM, Lakey JR, Ryan EA, Korbutt GS, Toth E, Warnock GL, Kneteman NM, Rajotte RV. Islet transplantation in seven patients with type 1 diabetes mellitus using a glucocorticoid-free immunosuppressive regimen. N Engl J Med 2000;343:230-238
85. Shapiro AM, Ricordi C, Hering BJ, Auchincloss H, Lindblad R, Robertson RP, Secchi A, Brendel MD, Berney T, Brennan DC, Cagliero E, Alejandro R, Ryan EA, DiMercurio B, Morel P, Polonsky KS, Reems JA, Bretzel RG, Bertuzzi F, Froud T, Kandaswamy R, Sutherland DE, Eisenbarth G, Segal M, Preiksaitis J, Korbutt GS, Barton FB, Viviano L, Seyfert-Margolis V, Bluestone J, Lakey JR. International trial of the Edmonton protocol for islet transplantation. N Engl J Med 2006;355:1318-1330
86. Alejandro R, Barton FB, Hering BJ, Wease S. 2008 Update from the Collaborative Islet Transplant Registry. Transplantation 2008;86:1783-1788
87. Warnock GL, Thompson DM, Meloche RM, Shapiro RJ, Ao Z, Keown P, Johnson JD, Verchere CB, Partovi N, Begg IS, Fung M, Kozak SE, Tong SO, Alghofaili KM, Harris C. A multi-year analysis of islet transplantation compared with intensive medical therapy on progression of complications in type 1 diabetes. Transplantation 2008;86:1762-1766
88. Potter KJ, Westwell-Roper CY, Klimek-Abercrombie AM, Warnock GL, Verchere CB. Death and Dysfunction of Transplanted beta-Cells: Lessons Learned From Type 2 Diabetes? Diabetes 2014;63:12-19
89. Kahn SE, Cooper ME, Del Prato S. Pathophysiology and treatment of type 2 diabetes: perspectives on the past, present, and future. Lancet 2013;10.1016/S0140-6736(13)62154-6
90. Perreault L, Pan Q, Mather KJ, Watson KE, Hamman RF, Kahn SE. Effect of regression from prediabetes to normal glucose regulation on long-term reduction in diabetes risk: results from the Diabetes Prevention Program Outcomes Study. Lancet 2012;379:2243-2251
91. Schauer PR, Kashyap SR, Wolski K, Brethauer SA, Kirwan JP, Pothier CE, Thomas S, Abood B, Nissen SE, Bhatt DL. Bariatric surgery versus intensive medical therapy in obese patients with diabetes. N Engl J Med 2012;366:1567-1576
92. Kashyap SR, Bhatt DL, Wolski K, Watanabe RM, Abdul-Ghani M, Abood B, Pothier CE, Brethauer S, Nissen S, Gupta M, Kirwan JP, Schauer PR. Metabolic effects of bariatric surgery in patients with moderate obesity and type 2 diabetes: analysis of a randomized control trial comparing surgery with intensive medical treatment. Diabetes Care 2013;36:2175-2182
93. Goldfine AB, Fonseca V, Jablonski KA, Pyle L, Staten MA, Shoelson SE. The effects of salsalate on glycemic control in patients with type 2 diabetes: a randomized trial. Ann Intern Med 2010;152:346-357
94. Gravitz L. Microbiome: The critters within. Nature 2012;485:S12-13
95. Sarwar N, Gao P, Seshasai SR, Gobin R, Kaptoge S, Di Angelantonio E, Ingelsson E, Lawlor DA, Selvin E, Stampfer M, Stehouwer CD, Lewington S, Pennells L, Thompson A, Sattar N, White IR, Ray KK, Danesh J. Diabetes mellitus, fasting blood glucose concentration, and risk of vascular disease: a collaborative meta-analysis of 102 prospective studies. Lancet 2010;375:2215-2222
96. Brownlee M. The pathobiology of diabetic complications: a unifying mechanism. Diabetes 2005;54:1615-1625

97. Booth GL, Kapral MK, Fung K, Tu JV. Relation between age and cardiovascular disease in men and women with diabetes compared with non-diabetic people: a population-based retrospective cohort study. Lancet 2006;368:29-36
98. Orchard TJ, Costacou T, Kretowski A, Nesto RW. Type 1 diabetes and coronary artery disease. Diabetes Care 2006;29:2528-2538
99. Nathan DM, Cleary PA, Backlund JY, Genuth SM, Lachin JM, Orchard TJ, Raskin P, Zinman B. Intensive diabetes treatment and cardiovascular disease in patients with type 1 diabetes. N Engl J Med 2005;353:2643-2653
100. Nathan DM, Zinman B, Cleary PA, Backlund JY, Genuth S, Miller R, Orchard TJ. Modern-day clinical course of type 1 diabetes mellitus after 30 years' duration: the diabetes control and complications trial/epidemiology of diabetes interventions and complications and Pittsburgh epidemiology of diabetes complications experience (1983-2005). Arch Intern Med 2009;169:1307-1316
101. Pop-Busui R, Low PA, Waberski BH, Martin CL, Albers JW, Feldman EL, Sommer C, Cleary PA, Lachin JM, Herman WH. Effects of prior intensive insulin therapy on cardiac autonomic nervous system function in type 1 diabetes mellitus: the Diabetes Control and Complications Trial/Epidemiology of Diabetes Interventions and Complications study (DCCT/EDIC). Circulation 2009;119:2886-2893
102. White NH, Sun W, Cleary PA, Danis RP, Davis MD, Hainsworth DP, Hubbard LD, Lachin JM, Nathan DM. Prolonged effect of intensive therapy on the risk of retinopathy complications in patients with type 1 diabetes mellitus: 10 years after the Diabetes Control and Complications Trial. Arch Ophthalmol 2008;126:1707-1715
103. de Boer IH, Rue TC, Cleary PA, Lachin JM, Molitch ME, Steffes MW, Sun W, Zinman B, Brunzell JD, White NH, Danis RP, Davis MD, Hainsworth D, Hubbard LD, Nathan DM. Long-term renal outcomes of patients with type 1 diabetes mellitus and microalbuminuria: an analysis of the Diabetes Control and Complications Trial/Epidemiology of Diabetes Interventions and Complications cohort. Arch Intern Med 2011;171:412-420
104. Waden J, Forsblom C, Thorn LM, Gordin D, Saraheimo M, Groop PH. A1C variability predicts incident cardiovascular events, microalbuminuria, and overt diabetic nephropathy in patients with type 1 diabetes. Diabetes 2009;58:2649-2655
105. Groop PH, Thomas MC, Moran JL, Waden J, Thorn LM, Makinen VP, Rosengard-Barlund M, Saraheimo M, Hietala K, Heikkila O, Forsblom C. The presence and severity of chronic kidney disease predicts all-cause mortality in type 1 diabetes. Diabetes 2009;58:1651-1658
106. Intensive blood-glucose control with sulphonylureas or insulin compared with conventional treatment and risk of complications in patients with type 2 diabetes (UKPDS 33). UK Prospective Diabetes Study (UKPDS) Group. Lancet 1998;352:837-853
107. Gerstein HC, Miller ME, Byington RP, Goff DC, Jr., Bigger JT, Buse JB, Cushman WC, Genuth S, Ismail-Beigi F, Grimm RH, Jr., Probstfield JL, Simons-Morton DG, Friedewald WT. Effects of intensive glucose lowering in type 2 diabetes. N Engl J Med 2008;358:2545-2559
108. Duckworth W, Abraira C, Moritz T, Reda D, Emanuele N, Reaven PD, Zieve FJ, Marks J, Davis SN, Hayward R, Warren SR, Goldman S, McCarren M, Vitek ME, Henderson WG, Huang GD. Glucose control and vascular complications in veterans with type 2 diabetes. N Engl J Med 2009;360:129-139

109. Gerstein HC, Bosch J, Dagenais GR, Diaz R, Jung H, Maggioni AP, Pogue J, Probstfield J, Ramachandran A, Riddle MC, Ryden LE, Yusuf S. Basal insulin and cardiovascular and other outcomes in dysglycemia. N Engl J Med 2012;367:319-328
110. Patel A, MacMahon S, Chalmers J, Neal B, Billot L, Woodward M, Marre M, Cooper M, Glasziou P, Grobbee D, Hamet P, Harrap S, Heller S, Liu L, Mancia G, Mogensen CE, Pan C, Poulter N, Rodgers A, Williams B, Bompoint S, de Galan BE, Joshi R, Travert F. Intensive blood glucose control and vascular outcomes in patients with type 2 diabetes. N Engl J Med 2008;358:2560-2572
111. Gaede P, Lund-Andersen H, Parving HH, Pedersen O. Effect of a multifactorial intervention on mortality in type 2 diabetes. N Engl J Med 2008;358:580-591
112. Goldsbury C, Baxa U, Simon MN, Steven AC, Engel A, Wall JS, Aebi U, Müller SA. Amyloid structure and assembly: insights from scanning transmission electron microscopy. J Struct Biol 2011;173:1-13
113. Kyle RA. Amyloidosis: a convoluted story. Br J Haematol 2001;114:529-538
114. Maezawa I, Hong H-S, Liu R, Wu C-Y, Cheng RH, Kung M-P, Kung HF, Lam KS, Oddo S, Laferla FM, Jin L-W. Congo red and thioflavin-T analogs detect Abeta oligomers. J Neurochem 2008;104:457-468
115. Buxbaum JN, Linke RP. A molecular history of the amyloidoses. J Mol Biol 2012;421:142-159
116. Eanes ED, Glenner GG. X-ray diffraction studies on amyloid filaments. J Histochem Cytochem 1968;16:673-677
117. Zheng J, Ma B, Nussinov R. Consensus features in amyloid fibrils: sheet-sheet recognition via a (polar or nonpolar) zipper structure. Phys Biol 2006;3:P1-4
118. Eisenberg D, Jucker M. The amyloid state of proteins in human diseases. Cell 2012;148:1188-1203
119. Dobson CM. The structural basis of protein folding and its links with human disease. Philos Trans R Soc Lond B Biol Sci 2001;356:133-145
120. Schmit JD, Ghosh K, Dill K. What drives amyloid molecules to assemble into oligomers and fibrils? Biophys J 2011;100:450-458
121. Nelson R, Sawaya MR, Balbirnie M, Madsen AO, Riekel C, Grothe R, Eisenberg D. Structure of the cross-beta spine of amyloid-like fibrils. Nature 2005;435:773-778
122. Nelson R, Eisenberg D. Recent atomic models of amyloid fibril structure. Curr Opin Struct Biol 2006;16:260-265
123. Toyama BH, Weissman JS. Amyloid structure: conformational diversity and consequences. Annu Rev Biochem 2011;80:557-585
124. Pedersen JS, Andersen CB, Otzen DE. Amyloid structure--one but not the same: the many levels of fibrillar polymorphism. FEBS J 2010;277:4591-4601
125. Shewmaker F, McGlinchey RP, Wickner RB. Structural insights into functional and pathological amyloid. J Biol Chem 2011;286:16533-16540
126. Greenwald J, Riek R. Biology of amyloid: structure, function, and regulation. Structure 2010;18:1244-1260
127. O'Nuallain B, Shivaprasad S, Kheterpal I, Wetzel R. Thermodynamics of A beta(1-40) amyloid fibril elongation. Biochemistry 2005;44:12709-12718
128. Abedini A, Raleigh DP. A role for helical intermediates in amyloid formation by natively unfolded polypeptides? Phys Biol 2009;6:1-6

129. Kayed R. Common structure of soluble amyloid oligomers implies common mechanism of pathogenesis. Science 2003;300:486-489
130. Kayed R, Head E, Sarsoza F, Saing T, Cotman CW, Necula M, Margol L, Wu J, Breydo L, Thompson JL, Rasool S, Gurlo T, Butler P, Glabe CG. Fibril specific, conformation dependent antibodies recognize a generic epitope common to amyloid fibrils and fibrillar oligomers that is absent in prefibrillar oligomers. Mol Neurodegener 2007;2:18
131. Krishnan R, Goodman JL, Mukhopadhyay S, Pacheco CD, Lemke EA, Deniz AA, Lindquist S. Conserved features of intermediates in amyloid assembly determine their benign or toxic states. Proc Natl Acad Sci USA 2012;109:11172-11177
132. Zraika S, Hull RL, Verchere CB, Clark A, Potter KJ, Fraser PE, Raleigh DP, Kahn SE. Toxic oligomers and islet beta cell death: guilty by association or convicted by circumstantial evidence? Diabetologia 2010;53:1046-1056
133. McIntire T, Milton S, Cotman C, Glabe C. Common structure of soluble amyloid oligomers implies common mechanism of pathogenesis. Science 2003;300:486-489
134. Laganowsky A, Liu C, Sawaya MR, Whitelegge JP, Park J, Zhao M, Pensalfini A, Soriaga AB, Landau M, Teng PK, Cascio D, Glabe C, Eisenberg D. Atomic view of a toxic amyloid small oligomer. Science 2012;335:1228-1231
135. Lesne SE, Sherman MA, Grant M, Kuskowski M, Schneider JA, Bennett DA, Ashe KH. Brain amyloid-beta oligomers in ageing and Alzheimer's disease. Brain 2013;136:1383-1398
136. Jurgens CA, Toukatly MN, Fligner CL, Udayasankar J, Subramanian SL, Zraika S, Aston-Mourney K, Carr DB, Westermark P, Westermark GT, Kahn SE, Hull RL. β-cell loss and β-cell apoptosis in human type 2 diabetes are related to islet amyloid deposition. Am J Pathol 2011;178:2632-2640
137. Marshall KE, Morris KL, Charlton D, O'Reilly N, Lewis L, Walden H, Serpell LC. Hydrophobic, aromatic, and electrostatic interactions play a central role in amyloid fibril formation and stability. Biochemistry 2011;50:2061-2071
138. Campioni S, Mannini B, Zampagni M, Pensalfini A, Parrini C, Evangelisti E, Relini A, Stefani M, Dobson CM, Cecchi C, Chiti F. A causative link between the structure of aberrant protein oligomers and their toxicity. Nat Chem Biol 2010;6:140-147
139. Lu JX, Qiang W, Yau WM, Schwieters CD, Meredith SC, Tycko R. Molecular structure of beta-amyloid fibrils in Alzheimer's disease brain tissue. Cell 2013;154:1257-1268
140. Serio TR, Cashikar AG, Kowal AS, Sawicki GJ, Moslehi JJ, Serpell L, Arnsdorf MF, Lindquist SL. Nucleated conformational conversion and the replication of conformational information by a prion determinant. Science 2000;289:1317-1321
141. Shorter J, Lindquist S. Hsp104 catalyzes formation and elimination of self-replicating Sup35 prion conformers. Science 2004;304:1793-1797
142. Fowler DM, Koulov AV, Balch WE, Kelly JW. Functional amyloid--from bacteria to humans. Trends Biochem Sci 2007;32:217-224
143. Maji SK, Perrin MH, Sawaya MR, Jessberger S, Vadodaria K, Rissman RA, Singru PS, Nilsson KP, Simon R, Schubert D, Eisenberg D, Rivier J, Sawchenko P, Vale W, Riek R. Functional amyloids as natural storage of peptide hormones in pituitary secretory granules. Science 2009;325:328-332

144. Berson JF, Theos AC, Harper DC, Tenza D, Raposo G, Marks MS. Proprotein convertase cleavage liberates a fibrillogenic fragment of a resident glycoprotein to initiate melanosome biogenesis. J Cell Biol 2003;161:521-533
145. Harper DC, Theos AC, Herman KE, Tenza D, Raposo G, Marks MS. Premelanosome amyloid-like fibrils are composed of only golgi-processed forms of Pmel17 that have been proteolytically processed in endosomes. J Biol Chem 2008;283:2307-2322
146. Kranenburg O, Bouma B, Kroon-Batenburg LM, Reijerkerk A, Wu YP, Voest EE, Gebbink MF. Tissue-type plasminogen activator is a multiligand cross-beta structure receptor. Curr Biol 2002;12:1833-1839
147. Gebbink MF, Voest EE, Reijerkerk A. Do antiangiogenic protein fragments have amyloid properties? Blood 2004;104:1601-1605
148. Sood R, Domanov Y, Pietiainen M, Kontinen VP, Kinnunen PK. Binding of LL-37 to model biomembranes: insight into target vs host cell recognition. Biochim Biophys Acta 2008;1778:983-996
149. Soscia SJ, Kirby JE, Washicosky KJ, Tucker SM, Ingelsson M, Hyman B, Burton MA, Goldstein LE, Duong S, Tanzi RE, Moir RD. The Alzheimer's Disease-Associated Amyloid beta-Protein Is an Antimicrobial Peptide. PLoS ONE 2010;5:e9505
150. Ando Y, Nakamura M, Kai H, Katsuragi S, Terazaki H, Nozawa T, Okuda T, Misumi S, Matsunaga N, Hata K, Tajiri T, Shoji S, Yamashita T, Haraoka K, Obayashi K, Matsumoto K, Ando M, Uchino M. A novel localized amyloidosis associated with lactoferrin in the cornea. Lab Invest 2002;82:757-766
151. Linke RP, Joswig R, Murphy CL, Wang S, Zhou H, Gross U, Rocken C, Westermark P, Weiss DT, Solomon A. Senile seminal vesicle amyloid is derived from semenogelin I. J Lab Clin Med 2005;145:187-193
152. Blanco LP, Evans ML, Smith DR, Badtke MP, Chapman MR. Diversity, biogenesis and function of microbial amyloids. Trends Microbiol 2012;20:66-73
153. Larsen P, Nielsen JL, Dueholm MS, Wetzel R, Otzen D, Nielsen PH. Amyloid adhesins are abundant in natural biofilms. Environ Microbiol 2007;9:3077-3090
154. Gilchrist KB, Garcia MC, Sobonya R, Lipke PN, Klotz SA. New features of invasive candidiasis in humans: amyloid formation by fungi and deposition of serum amyloid P component by the host. J Infect Dis 2012;206:1473-1478
155. de Groot PW, Bader O, de Boer AD, Weig M, Chauhan N. Adhesins in human fungal pathogens: glue with plenty of stick. Eukaryot Cell 2013;12:470-481
156. Schwartz K, Syed AK, Stephenson RE, Rickard AH, Boles BR. Functional amyloids composed of phenol soluble modulins stabilize Staphylococcus aureus biofilms. PLoS Pathog 2012;8:e1002744
157. Barnhart MM, Chapman MR. Curli biogenesis and function. Annu Rev Microbiol 2006;60:131-147
158. Oh J, Kim JG, Jeon E, Yoo CH, Moon JS, Rhee S, Hwang I. Amyloidogenesis of type III-dependent harpins from plant pathogenic bacteria. J Biol Chem 2007;282:13601-13609
159. Lagos R, Tello M, Mercado G, Garcia V, Monasterio O. Antibacterial and antitumorigenic properties of microcin E492, a pore-forming bacteriocin. Curr Pharm Biotechnol 2009;10:74-85

160. Jordal PB, Dueholm MS, Larsen P, Petersen SV, Enghild JJ, Christiansen G, Hojrup P, Nielsen PH, Otzen DE. Widespread abundance of functional bacterial amyloid in mycolata and other gram-positive bacteria. Appl Environ Microbiol 2009;75:4101-4110
161. Podrabsky JE, Carpenter JF, Hand SC. Survival of water stress in annual fish embryos: dehydration avoidance and egg envelope amyloid fibers. Am J Physiol Regul Integr Comp Physiol 2001;280:R123-131
162. Claessen D, Rink R, de Jong W, Siebring J, de Vreugd P, Boersma FG, Dijkhuizen L, Wosten HA. A novel class of secreted hydrophobic proteins is involved in aerial hyphae formation in Streptomyces coelicolor by forming amyloid-like fibrils. Genes Dev 2003;17:1714-1726
163. Morris VK, Sunde M. Formation of amphipathic amyloid monolayers from fungal hydrophobin proteins. Methods Mol Biol 2013;996:119-129
164. Prusiner SB. Prions. Proc Natl Acad Sci USA 1998;95:13363-13383
165. Maury CPJ. The emerging concept of functional amyloid. J Intern Med 2009;265:329-334
166. Falk RH, Comenzo RL, Skinner M. The systemic amyloidoses. N Engl J Med 1997;337:898-909
167. Blancas-Mejia LM, Ramirez-Alvarado M. Systemic amyloidoses. Annu Rev Biochem 2013;82:745-774
168. Vrana JA, Gamez JD, Madden BJ, Theis JD, Bergen HR, 3rd, Dogan A. Classification of amyloidosis by laser microdissection and mass spectrometry-based proteomic analysis in clinical biopsy specimens. Blood 2009;114:4957-4959
169. Merlini G, Palladini G. Amyloidosis: is a cure possible? Ann Oncol 2008;19 Suppl 4:63-66
170. Buxbaum J. Animal models of human amyloidoses: Are transgenic mice worth the time and trouble? FEBS Lett 2009;583:2663-2673
171. Lyman M, Lloyd DG, Ji X, Vizcaychipi MP, Ma D. Neuroinflammation: The role and consequences. Neurosci Res 2013;10.1016/j.neures.2013.10.004
172. Rongioletti F. Amyloidoses. In *Clinical and Pathological Aspects of Skin Diseases in Endocrine, Metabolic, Nutritional and Deposition Disease* Rongioletti FS, BR, Ed. New York, NY, Springer Science+Business Media LLC, 2010, p. 127-137
173. Moreno-Gonzalez I, Soto C. Misfolded protein aggregates: mechanisms, structures and potential for disease transmission. Semin Cell Dev Biol 2011;22:482-487
174. Conway KA, Harper JD, Lansbury PT. Accelerated in vitro fibril formation by a mutant alpha-synuclein linked to early-onset Parkinson disease. Nat Med 1998;4:1318-1320
175. Scherzinger E, Lurz R, Turmaine M, Mangiarini L, Hollenbach B, Hasenbank R, Bates GP, Davies SW, Lehrach H, Wanker EE. Huntingtin-encoded polyglutamine expansions form amyloid-like protein aggregates in vitro and in vivo. Cell 1997;90:549-558
176. Kerman A, Liu HN, Croul S, Bilbao J, Rogaeva E, Zinman L, Robertson J, Chakrabartty A. Amyotrophic lateral sclerosis is a non-amyloid disease in which extensive misfolding of SOD1 is unique to the familial form. Acta Neuropathol 2010;119:335-344
177. Pearson HA, Peers C. Physiological roles for amyloid beta peptides. J Physiol 2006;575:5-10
178. Gessel MM, Bernstein S, Kemper M, Teplow DB, Bowers MT. Familial Alzheimer's disease mutations differentially alter amyloid beta-protein oligomerization. ACS Chem Neurosci 2012;3:909-918

179. Zhang YW, Thompson R, Zhang H, Xu H. APP processing in Alzheimer's disease. Mol Brain 2011;4:3
180. Leiter LA, Fitchett DH, Gilbert RE, Gupta M, Mancini GB, McFarlane PA, Ross R, Teoh H, Verma S, Anand S, Camelon K, Chow CM, Cox JL, Despres JP, Genest J, Harris SB, Lau DC, Lewanczuk R, Liu PP, Lonn EM, McPherson R, Poirier P, Qaadri S, Rabasa-Lhoret R, Rabkin SW, Sharma AM, Steele AW, Stone JA, Tardif JC, Tobe S, Ur E. Cardiometabolic risk in Canada: a detailed analysis and position paper by the cardiometabolic risk working group. Can J Cardiol 2011;27:e1-e33
181. Webster MW. Clinical practice and implications of recent diabetes trials. Curr Opin Cardiol 2011;26:288-293
182. Strachan MW, Reynolds RM, Marioni RE, Price JF. Cognitive function, dementia and type 2 diabetes mellitus in the elderly. Nat Rev Endocrinol 2011;7:108-114
183. Wyss-Coray T. Inflammation in Alzheimer disease: driving force, bystander or beneficial response? Nat Med 2006;12:1005-1015
184. Lourenco MV, Clarke JR, Frozza RL, Bomfim TR, Forny-Germano L, Batista AF, Sathler LB, Brito-Moreira J, Amaral OB, Silva CA, Freitas-Correa L, Espirito-Santo S, Campello-Costa P, Houzel JC, Klein WL, Holscher C, Carvalheira JB, Silva AM, Velloso LA, Munoz DP, Ferreira ST, De Felice FG. TNF-alpha Mediates PKR-Dependent Memory Impairment and Brain IRS-1 Inhibition Induced by Alzheimer's beta-Amyloid Oligomers in Mice and Monkeys. Cell Metab 2013;18:831-843
185. Gotz J, Ittner LM, Lim YA. Common features between diabetes mellitus and Alzheimer's disease. Cell Mol Life Sci 2009;66:1321-1325
186. Bell ET. Hyalinization of the islets of Langerhans in nondiabetic individuals. Am J Pathol 1959;35:801-805
187. Clark A, Saad MF, Nezzer T, Uren C, Knowler WC, Bennett PH, Turner RC. Islet amyloid polypeptide in diabetic and non-diabetic Pima Indians. Diabetologia 1990;33:285-289
188. Westermark P. Quantitative studies on amyloid in the islets of Langerhans. Ups J Med Sci 1972;77:91-94
189. Westermark P. Amyloid and polypeptide hormones: what is their interrelationship? Amyloid 1994;1:47-58
190. Clark A, Wells CA, Buley ID, Cruickshank JK, Vanhegan RI, Matthews DR, Cooper GJS, Holman RR, Turner RC. Islet amyloid, increased A-cells, reduced B-cells and exocrine fibrosis: quantitative changes in the pancreas in type 2 diabetes. Diabetes Res 1988;9:151-159
191. de Koning EJP, Bodkin NL, Hansen BC, Clark A. Diabetes mellitus in Macaca mulatta monkeys is characterised by islet amyloidosis and reduction in beta-cell population. Diabetologia 1993;36:378-384
192. Verchere CB, D'Alessio DA, Palmiter RD, Weir GC, Bonner-Weir S, Baskin DG, Kahn SE. Islet amyloid formation associated with hyperglycemia in transgenic mice with pancreatic beta cell expression of human islet amyloid polypeptide. Proc Natl Acad Sci USA 1996;93:3492-3496
193. Couce M, Kane LA, O'Brien TD, Charlesworth J, Soeller W, McNeish J, Kreutter D, Roche P, Butler PC. Treatment with growth hormone and dexamethasone in mice transgenic for human islet amyloid polypeptide causes islet amyloidosis and beta cell dysfunction. Diabetes 1996;45:1094-1101

194. Soeller WC, Janson J, Hart SE, Parker JC, Carty MD, Stevenson RW, Kreutter DK, Butler PC. Islet amyloid-associated diabetes in obese A(vy)/a mice expressing human islet amyloid polypeptide. Diabetes 1998;47:743-750
195. Hoppener JW, Oosterwijk C, Nieuwenhuis MG, Posthuma G, Thijssen JH, Vroom TM, Ahren B, Lips CJ. Extensive islet amyloid formation is induced by development of Type II diabetes mellitus and contributes to its progression: pathogenesis of diabetes in a mouse model. Diabetologia 1999;42:427-434
196. Westermark P, Wernstedt C, Wilander E, Sletten K. A novel peptide in the calcitonin gene related peptide family as an amyloid fibril protein in the endocrine pancreas. Biochem Biophys Res Commun 1986;140:827-831
197. Westermark P, Wernstedt C, Wilander E, Hayden DW, O'Brien TD, Johnson KH. Amyloid fibrils in human insulinoma and islets of Langerhans of the diabetic cat are derived from a neuropeptide-like protein also present in normal islets. Proc Natl Acad Sci USA 1987;84:3881-3885
198. Cooper GJS, Willis AC, Clark A, Turner RC, Sim RB, Reid KBM. Purification and characterization of a peptide from amyloid-rich pancreases of type 2 diabetic patients. Proc Natl Acad Sci USA 1987;84:8628-8632
199. Verchere CB, D'Alessio DA, Palmiter RD, Kahn SE. Transgenic mice overproducing islet amyloid polypeptide have increased insulin storage and secretion in vitro. Diabetologia 1994;37:725-728
200. Verchere CB, D'Alessio DA, Prigeon RL, Hull RL, Kahn SE. The constitutive secretory pathway is a major route for islet amyloid polypeptide secretion from neonatal rat beta cells. Diabetes 2000;49:1477-1484
201. Ogawa A, Harris V, McCorkie SK, Unger RH, Luskey KL. Amylin secretion from the rat pancreas and its selective loss after streptozocin treatment. J Clin Invest 1990;85:973-976
202. Kanatsuka A, Makino H, Ohsawa H, Tokuyama Y, Yamaguchi T, Yoshida S, Adachi M. Secretion of islet amyloid polypeptide in response to glucose. FEBS Lett 1989;259:199-201
203. Kahn SE, D'Alessio DA, Schwartz MW, Fujimoto WY, Ensinck JW, Taborsky GJ, Jr., Porte D, Jr. Evidence of cosecretion of islet amyloid polypeptide and insulin by ß-cells. Diabetes 1990;39:634-638
204. Lutz TA. The role of amylin in the control of energy homeostasis. Am J Physiol Regul Integr Comp Physiol 2010;298:R1475-1484
205. Lorenzo A, Razzaboni B, Weir GC, Yankner BA. Pancreatic islet cell toxicity of amylin associated with type 2 diabetes mellitus. Nature 1994;368:756-760
206. Betsholtz C, Christmansson L, Engstrom U, Rorsman F, Svensson V, Johnson KH, Westermark P. Sequence divergence in a specific region of islet amyloid polypeptide (IAPP) explains differences in islet amyloid formation between species. FEBS Lett 1989;251:261-264
207. Matveyenko AV, Butler PC. Islet amyloid polypeptide (IAPP) transgenic rodents as models for type 2 diabetes. ILAR J 2006;47:225-233
208. Sakagashira S, Sanke T, Hanabusa T, Shimomura H, Ohagi S, Kumagaye KY, Nakajima K, Nanjo K. Missense mutation of amylin gene (S20G) in Japanese NIDDM patients. Diabetes 1996;45:1279-1281
209. Poa NR, Cooper GJ, Edgar PF. Amylin gene promoter mutations predispose to Type 2 diabetes in New Zealand Maori. Diabetologia 2003;46:574-578

210. Janson J, Soeller WC, Roche PC, Nelson RT, Torchia AJ, Kreutter DK, Butler PC. Spontaneous diabetes mellitus in transgenic mice expressing human islet amyloid polypeptide. Proc Natl Acad Sci USA 1996;93:7283-7288
211. Hull RL, Andrikopoulos S, Verchere CB, Vidal J, Wang F, Cnop M, Prigeon RL, Kahn SE. Increased dietary fat promotes islet amyloid formation and beta-cell secretory dysfunction in a transgenic mouse model of islet amyloid. Diabetes 2003;52:372-379
212. Janson J, Ashley RH, Harrison D, McIntyre S, Butler PC. The mechanism of islet amyloid polypeptide toxicity is membrane disruption by intermediate-sized toxic amyloid particles. Diabetes 1999;48:491-498
213. Engel MFM, Khemtémourian L, Kleijer CC, Meeldijk HJD, Jacobs J, Verkleij AJ, de Kruijff B, Killian JA, Höppener JWM. Membrane damage by human islet amyloid polypeptide through fibril growth at the membrane. Proc Natl Acad Sci USA 2008;105:6033-6038
214. Potter KJ, Scrocchi LA, Warnock GL, Ao Z, Younker MA, Rosenberg L, Lipsett M, Verchere CB, Fraser PE. Amyloid inhibitors enhance survival of cultured human islets. Biochim Biophys Acta 2009;1790:566-574
215. Marzban L, Tomas A, Becker TC, Rosenberg L, Oberholzer J, Fraser PE, Halban PA, Verchere CB. Small interfering RNA-mediated suppression of proislet amyloid polypeptide expression inhibits islet amyloid formation and enhances survival of human islets in culture. Diabetes 2008;57:3045-3055
216. Udayasankar J, Kodama K, Hull RL, Zraika S, Aston-Mourney K, Subramanian SL, Tong J, Faulenbach MV, Vidal J, Kahn SE. Amyloid formation results in recurrence of hyperglycaemia following transplantation of human IAPP transgenic mouse islets. Diabetologia 2009;52:145-153
217. Potter KJ, Abedini A, Marek P, Klimek AM, Butterworth S, Driscoll M, Baker R, Nilsson MR, Warnock GL, Oberholzer J, Bertera S, Trucco M, Korbutt GS, Fraser PE, Raleigh DP, Verchere CB. Islet amyloid deposition limits the viability of human islet grafts but not porcine islet grafts. Proc Natl Acad Sci USA 2010;107:4305-4310
218. Kayed R, Bernhagen J, Greenfield N, Sweimeh K, Brunner H, Voelter W, Kapurniotu A. Conformational transitions of islet amyloid polypeptide (IAPP) in amyloid formation in vitro. J Mol Biol 1999;287:781-796
219. Williamson JA, Miranker AD. Direct detection of transient alpha-helical states in islet amyloid polypeptide. Protein Sci 2007;16:110-117
220. Wiltzius JJ, Sievers SA, Sawaya MR, Eisenberg D. Atomic structures of IAPP (amylin) fusions suggest a mechanism for fibrillation and the role of insulin in the process. Protein Sci 2009;18:1521-1530
221. Nanga RP, Brender JR, Xu J, Veglia G, Ramamoorthy A. Structures of rat and human islet amyloid polypeptide IAPP(1-19) in micelles by NMR spectroscopy. Biochemistry 2008;47:12689-12697
222. Patil SM, Xu S, Sheftic SR, Alexandrescu AT. Dynamic alpha-helix structure of micelle-bound human amylin. J Biol Chem 2009;284:11982-11991
223. Verchere CB, D'Alessio DA, Wang S, Andrikopoulos S, Kahn SE. Transgenic overproduction of islet amyloid polypeptide (amylin) is not sufficient for islet amyloid formation. Horm Metab Res 1997;29:311-316

224. Höppener JW, Oosterwijk C, Nieuwenhuis MG, Posthuma G, Thijssen JH, Vroom TM, Ahrén B, Lips CJ. Extensive islet amyloid formation is induced by development of Type II diabetes mellitus and contributes to its progression: pathogenesis of diabetes in a mouse model. Diabetologia 1999;42:427-434
225. Couce M, Kane LA, O'Brien TD, Charlesworth J, Soeller W, McNeish J, Kreutter D, Roche P, Butler PC. Treatment with growth hormone and dexamethasone in mice transgenic for human islet amyloid polypeptide causes islet amyloidosis and beta-cell dysfunction. Diabetes 1996;45:1094-1101
226. Hull RL, Verchere CB, Andrikopoulos S, Wang F, Vidal J, Kahn SE. Oophorectomy promotes islet amyloid formation in human islet amyloid polypeptide transgenic mice. Diabetes 2001;50 Suppl 1:S184-185
227. Marzban L, Rhodes CJ, Steiner DF, Haataja L, Halban PA, Verchere CB. Impaired NH2-terminal processing of human proislet amyloid polypeptide by the prohormone convertase PC2 leads to amyloid formation and cell death. Diabetes 2006;55:2192-2201
228. Paulsson JF, Westermark GT. Aberrant processing of human proislet amyloid polypeptide results in increased amyloid formation. Diabetes 2005;54:2117-2125
229. Park K, Verchere CB. Identification of a heparin binding domain in the N-terminal cleavage site of pro-islet amyloid polypeptide. Implications for islet amyloid formation. J Biol Chem 2001;276:16611-16616
230. Marzban L, Trigo-Gonzalez G, Verchere CB. Processing of pro-islet amyloid polypeptide in the constitutive and regulated secretory pathways of beta cells. Mol Endocrinol 2005;19:2154-2163
231. Wang J, Xu J, Finnerty J, Furuta M, Steiner DF, Verchere CB. The prohormone convertase enzyme 2 (PC2) is essential for processing pro-islet amyloid polypeptide at the NH2-terminal cleavage site. Diabetes 2001;50:534-539
232. Marzban L, Trigo-Gonzalez G, Zhu X, Rhodes CJ, Halban PA, Steiner DF, Verchere CB. Role of beta-cell prohormone convertase (PC)1/3 in processing of pro-islet amyloid polypeptide. Diabetes 2004;53:141-148
233. Marzban L, Soukhatcheva G, Verchere CB. Role of carboxypeptidase E in processing of pro-islet amyloid polypeptide in beta-cells. Endocrinology 2005;146:1808-1817
234. Hostens K, Pavlovic D, Zambre Y, Ling Z, Van Schravendijk C, Eizirik D, L., Pipeleers DG. Exposure of human islets to cytokines can result in disproportionately elevated proinsulin release. J Clin Invest 1999;104:67-72
235. Andersson AK, Börjesson A, Sandgren J, Sandler S. Cytokines affect PDX-1 expression, insulin and proinsulin secretion from iNOS deficient murine islets. Mol Cell Endocrinol 2005;240:50-57
236. Harlan DM, Kenyon NS, Korsgren O, Roep BO, Society IoD. Current advances and travails in islet transplantation. Diabetes 2009;58:2175-2184
237. Huang X, Moore DJ, Ketchum RJ, Nunemaker CS, Kovatchev B, McCall AL, Brayman KL. Resolving the conundrum of islet transplantation by linking metabolic dysregulation, inflammation, and immune regulation. Endocr Rev 2008;29:603-630
238. Marzban L, Park K, Verchere CB. Islet amyloid polypeptide and type 2 diabetes. Exp Gerontol 2003;38:347-351

239. Westermark GT, Westermark P, Nordin A, Tornelius E, Andersson A. Formation of amyloid in human pancreatic islets transplanted to the liver and spleen of nude mice. Ups J Med Sci 2003;108:193-203
240. Westermark GT, Westermark P, Berne C, Korsgren O. Widespread amyloid deposition in transplanted human pancreatic islets. N Engl J Med 2008;359:977-979
241. Medzhitov R. Origin and physiological roles of inflammation. Nature 2008;454:428-435
242. Matzinger P. The danger model: a renewed sense of self. Science 2002;296:301-305
243. Sauter B, Albert ML, Francisco L, Larsson M, Somersan S, Bhardwaj N. Consequences of cell death: exposure to necrotic tumor cells, but not primary tissue cells or apoptotic cells, induces the maturation of immunostimulatory dendritic cells. J Exp Med 2000;191:423-434
244. McGeer EG, McGeer PL. Inflammatory processes in Alzheimer's disease. Prog Neuropsychopharmacol Biol Psychiatry 2003;27:741-749
245. Heneka MT, O'Banion MK. Inflammatory processes in Alzheimer's disease. J Neuroimmunol 2007;184:69-91
246. Rojo LE, Fernandez JA, Maccioni AA, Jimenez JM, Maccioni RB. Neuroinflammation: implications for the pathogenesis and molecular diagnosis of Alzheimer's disease. Arch Med Res 2008;39:1-16
247. Eikelenboom P, Veerhuis R, Familian A, Hoozemans JJ, van Gool WA, Rozemuller AJ. Neuroinflammation in plaque and vascular beta-amyloid disorders: clinical and therapeutic implications. Neurodegener Dis 2008;5:190-193
248. Meyer-Luehmann M, Spires-Jones TL, Prada C, Garcia-Alloza M, de Calignon A, Rozkalne A, Koenigsknecht-Talboo J, Holtzman DM, Bacskai BJ, Hyman BT. Rapid appearance and local toxicity of amyloid-beta plaques in a mouse model of Alzheimer's disease. Nature 2008;451:720-724
249. Bolmont T, Haiss F, Eicke D, Radde R, Mathis CA, Klunk WE, Kohsaka S, Jucker M, Calhoun ME. Dynamics of the microglial/amyloid interaction indicate a role in plaque maintenance. J Neurosci 2008;28:4283-4292
250. Jimenez S, Baglietto-Vargas D, Caballero C, Moreno-Gonzalez I, Torres M, Sanchez-Varo R, Ruano D, Vizuete M, Gutierrez A, Vitorica J. Inflammatory response in the hippocampus of PS1M146L/APP751SL mouse model of Alzheimer's disease: age-dependent switch in the microglial phenotype from alternative to classic. J Neurosci 2008;28:11650-11661
251. Rezaie P, Lantos PL. Microglia and the pathogenesis of spongiform encephalopathies. Brain Res Brain Res Rev 2001;35:55-72
252. Williams A, Lucassen PJ, Ritchie D, Bruce M. PrP deposition, microglial activation, and neuronal apoptosis in murine scrapie. Exp Neurol 1997;144:433-438
253. Peyrin JM, Lasmezas CI, Haik S, Tagliavini F, Salmona M, Williams A, Richie D, Deslys JP, Dormont D. Microglial cells respond to amyloidogenic PrP peptide by the production of inflammatory cytokines. Neuroreport 1999;10:723-729
254. Tribouillard-Tanvier D, Striebel JF, Peterson KE, Chesebro B. Analysis of protein levels of 24 cytokines in scrapie agent-infected brain and glial cell cultures from mice differing in prion protein expression levels. J Virol 2009;83:11244-11253
255. Crespo I, Roomp K, Jurkowski W, Kitano H, del Sol A. Gene regulatory network analysis supports inflammation as a key neurodegeneration process in prion disease. BMC Syst Biol 2012;6:132

256. Whitton PS. Inflammation as a causative factor in the aetiology of Parkinson's disease. Br J Pharmacol 2007;150:963-976
257. Danzer KM, Haasen D, Karow AR, Moussaud S, Habeck M, Giese A, Kretzschmar H, Hengerer B, Kostka M. Different species of alpha-synuclein oligomers induce calcium influx and seeding. J Neurosci 2007;27:9220-9232
258. Roodveldt C, Christodoulou J, Dobson CM. Immunological features of alpha-synuclein in Parkinson's disease. J Cell Mol Med 2008;12:1820-1829
259. Zhang W, Wang T, Pei Z, Miller DS, Wu X, Block ML, Wilson B, Zhang W, Zhou Y, Hong JS, Zhang J. Aggregated alpha-synuclein activates microglia: a process leading to disease progression in Parkinson's disease. FASEB J 2005;19:533-542
260. Klegeris A, Giasson BI, Zhang H, Maguire J, Pelech S, McGeer PL. Alpha-synuclein and its disease-causing mutants induce ICAM-1 and IL-6 in human astrocytes and astrocytoma cells. FASEB J 2006;20:2000-2008
261. McGeer PL, Itagaki S, Boyes BE, McGeer EG. Reactive microglia are positive for HLA-DR in the substantia nigra of Parkinson's and Alzheimer's disease brains. Neurology 1988;38:1285-1291
262. Perfetto F, Moggi-Pignone A, Livi R, Tempestini A, Bergesio F, Matucci-Cerinic M. Systemic amyloidosis: a challenge for the rheumatologist. Nat Rev Rheumatol 2010;6:417-429
263. Simons JP, Al-Shawi R, Ellmerich S, Speck I, Aslam S, Hutchinson WL, Mangione PP, Disterer P, Gilbertson JA, Hunt T, Millar DJ, Minogue S, Bodin K, Pepys MB, Hawkins PN. Pathogenetic mechanisms of amyloid A amyloidosis. Proc Natl Acad Sci USA 2013;110:16115-16120
264. Richter GW. The resorption of amyloid under experimental conditions. Am J Pathol 1954;30:239-261
265. Kluve-Beckerman B, Manaloor JJ, Liepnieks JJ. A pulse-chase study tracking the conversion of macrophage-endocytosed serum amyloid A into extracellular amyloid. Arthritis Rheum 2002;46:1905-1913
266. Chen ES, Song Z, Willett MH, Heine S, Yung RC, Liu MC, Groshong SD, Zhang Y, Tuder RM, Moller DR. Serum amyloid A regulates granulomatous inflammation in sarcoidosis through Toll-like receptor-2. Am J Respir Crit Care Med 2010;181:360-373
267. Yanamandra K, Alexeyev O, Zamotin V, Srivastava V, Shchukarev A, Brorsson AC, Tartaglia GG, Vogl T, Kayed R, Wingsle G, Olsson J, Dobson CM, Bergh A, Elgh F, Morozova-Roche LA. Amyloid formation by the pro-inflammatory S100A8/A9 proteins in the ageing prostate. PLoS ONE 2009;4:e5562
268. Bian Z, Yan ZQ, Hansson GK, Thoren P, Normark S. Activation of inducible nitric oxide synthase/nitric oxide by curli fibers leads to a fall in blood pressure during systemic Escherichia coli infection in mice. J Infect Dis 2001;183:612-619
269. de Koning EJ, van den Brand JJ, Mott VL, Charge SB, Hansen BC, Bodkin NL, Morris JF, Clark A. Macrophages and pancreatic islet amyloidosis. Amyloid 1998;5:247-254
270. Badman MK, Pryce RA, Chargé SB, Morris JF, Clark A. Fibrillar islet amyloid polypeptide (amylin) is internalised by macrophages but resists proteolytic degradation. Cell Tissue Res 1998;291:285-294
271. Koenigsknecht J, Landreth G. Microglial phagocytosis of fibrillar beta-amyloid through a beta1 integrin-dependent mechanism. J Neurosci 2004;24:9838-9846

272. Mandrekar S, Jiang Q, Lee CYD, Koenigsknecht-Talboo J, Holtzman DM, Landreth GE. Microglia mediate the clearance of soluble Abeta through fluid phase macropinocytosis. J Neurosci 2009;29:4252-4262
273. Gitter BD, Cox LM, Carlson CD, May PC. Human amylin stimulates inflammatory cytokine secretion from human glioma cells. Neuroimmunomodulation 2000;7:147-152
274. Yates SL, Burgess LH, Kocsis-Angle J, Antal JM, Dority MD, Embury PB, Piotrkowski AM, Brunden KR. Amyloid beta and amylin fibrils induce increases in proinflammatory cytokine and chemokine production by THP-1 cells and murine microglia. J Neurochem 2000;74:1017-1025
275. Takeuchi O, Akira S. Pattern recognition receptors and inflammation. Cell 2010;140:805-820
276. Stewart CR, Stuart LM, Wilkinson K, van Gils JM, Deng J, Halle A, Rayner KJ, Boyer L, Zhong R, Frazier WA, Lacy-Hulbert A, Khoury JE, Golenbock DT, Moore KJ. CD36 ligands promote sterile inflammation through assembly of a Toll-like receptor 4 and 6 heterodimer. Nat Immunol 2010;11:155-161
277. Fassbender K, Walter S, Kühl S, Landmann R, Ishii K, Bertsch T, Stalder AK, Muehlhauser F, Liu Y, Ulmer AJ, Rivest S, Lentschat A, Gulbins E, Jucker M, Staufenbiel M, Brechtel K, Walter J, Multhaup G, Penke B, Adachi Y, Hartmann T, Beyreuther K. The LPS receptor (CD14) links innate immunity with Alzheimer's disease. FASEB J 2004;18:203-205
278. Jana M, Palencia CA, Pahan K. Fibrillar amyloid-beta peptides activate microglia via TLR2: implications for Alzheimer's disease. J Immunol 2008;181:7254-7262
279. Udan MLD, Ajit D, Crouse NR, Nichols MR. Toll-like receptors 2 and 4 mediate Abeta(1-42) activation of the innate immune response in a human monocytic cell line. J Neurochem 2008;104:524-533
280. Cheng N, He R, Tian J, Ye PP, Ye RD. Cutting edge: TLR2 is a functional receptor for acute-phase serum amyloid A. J Immunol 2008;181:22-26
281. Sandri S, Rodriguez D, Gomes E, Monteiro HP, Russo M, Campa A. Is serum amyloid A an endogenous TLR4 agonist? J Leukoc Biol 2008;83:1174-1180
282. Tükel C, Nishimori JH, Wilson RP, Winter MG, Keestra AM, van Putten JPM, Bäumler AJ. Toll-like receptors 1 and 2 cooperatively mediate immune responses to curli, a common amyloid from enterobacterial biofilms. Cell Microbiol 2010;12:1495-1505
283. Canton J, Neculai D, Grinstein S. Scavenger receptors in homeostasis and immunity. Nat Rev Immunol 2013;13:621-634
284. Krieger M, Acton S, Ashkenas J, Pearson A, Penman M, Resnick D. Molecular flypaper, host defense, and atherosclerosis. Structure, binding properties, and functions of macrophage scavenger receptors. J Biol Chem 1993;268:4569-4572
285. Uematsu S, Akira S. Toll-Like receptors (TLRs) and their ligands. Handb Exp Pharmacol 2008;183:1-20
286. Baranova IN, Bocharov AV, Vishnyakova TG, Kurlander R, Chen Z, Fu D, Arias IM, Csako G, Patterson AP, Eggerman TL. CD36 is a novel serum amyloid A (SAA) receptor mediating SAA binding and SAA-induced signaling in human and rodent cells. J Biol Chem 2010;285:8492-8506
287. Sheedy FJ, Grebe A, Rayner KJ, Kalantari P, Ramkhelawon B, Carpenter SB, Becker CE, Ediriweera HN, Mullick AE, Golenbock DT, Stuart LM, Latz E, Fitzgerald KA, Moore KJ. CD36 coordinates NLRP3 inflammasome activation by facilitating intracellular nucleation

of soluble ligands into particulate ligands in sterile inflammation. Nat Immunol 2013;14:812-820
288. Su X, Maguire-Zeiss KA, Giuliano R, Prifti L, Venkatesh K, Federoff HJ. Synuclein activates microglia in a model of Parkinson's disease. Neurobiol Aging 2008;29:1690-1701
289. Kouadir M, Yang L, Tan R, Shi F, Lu Y, Zhang S, Yin X, Zhou X, Zhao D. CD36 participates in PrP(106-126)-induced activation of microglia. PLoS ONE 2012;7:e30756
290. Iribarren P, Zhou Y, Hu J, Le Y, Wang JM. Role of formyl peptide receptor-like 1 (FPRL1/FPR2) in mononuclear phagocyte responses in Alzheimer disease. Immunol Res 2005;31:165-176
291. Brandenburg LO, Koch T, Sievers J, Lucius R. Internalization of PrP106-126 by the formyl-peptide-receptor-like-1 in glial cells. J Neurochem 2007;101:718-728
292. Böni-Schnetzler M, Boller S, Debray S, Bouzakri K, Meier DT, Prazak R, Kerr-Conte J, Pattou F, Ehses JA, Schuit FC, Donath MY. Free fatty acids induce a proinflammatory response in islets via the abundantly expressed interleukin-1 receptor I. Endocrinology 2009;150:5218-5229
293. Kawai T, Akira S. Toll-like receptor and RIG-I-like receptor signaling. Ann NY Acad Sci 2008;1143:1-20
294. Foster SL, Medzhitov R. Gene-specific control of the TLR-induced inflammatory response. Clin Immunol 2009;130:7-15
295. O'Neill LAJ, Bowie AG. The family of five: TIR-domain-containing adaptors in Toll-like receptor signalling. Nat Rev Immunol 2007;7:353-364
296. Trinchieri G, Sher A. Cooperation of Toll-like receptor signals in innate immune defence. Nat Rev Immunol 2007;7:179-190
297. Masters SL, Latz E, O'Neill LA. The inflammasome in atherosclerosis and type 2 diabetes. Sci Transl Med 2011;3:81ps17
298. Juliana C, Fernandes-Alnemri T, Kang S, Farias A, Qin F, Alnemri ES. Non-transcriptional priming and deubiquitination regulate NLRP3 inflammasome activation. J Biol Chem 2012;287:36617-36622
299. Hara H, Tsuchiya K, Kawamura I, Fang R, Hernandez-Cuellar E, Shen Y, Mizuguchi J, Schweighoffer E, Tybulewicz V, Mitsuyama M. Phosphorylation of the adaptor ASC acts as a molecular switch that controls the formation of speck-like aggregates and inflammasome activity. Nat Immunol 2013;10.1038/ni.2749
300. Fernandes-Alnemri T, Kang S, Anderson C, Sagara J, Fitzgerald KA, Alnemri ES. Cutting edge: TLR signaling licenses IRAK1 for rapid activation of the NLRP3 inflammasome. J Immunol 2013;191:3995-3999
301. Reed-Geaghan EG, Savage JC, Hise AG, Landreth GE. CD14 and toll-like receptors 2 and 4 are required for fibrillar A{beta}-stimulated microglial activation. J Neurosci 2009;29:11982-11992
302. He RL, Zhou J, Hanson CZ, Chen J, Cheng N, Ye RD. Serum amyloid A induces G-CSF expression and neutrophilia via Toll-like receptor 2. Blood 2009;113:429-437
303. Gustot A, Raussens V, Dehousse M, Dumoulin M, Bryant CE, Ruysschaert JM, Lonez C. Activation of innate immunity by lysozyme fibrils is critically dependent on cross-beta sheet structure. Cell Mol Life Sci 2013;70:2999-3012

304. Tükel C, Wilson RP, Nishimori JH, Pezeshki M, Chromy BA, Bäumler AJ. Responses to amyloids of microbial and host origin are mediated through toll-like receptor 2. Cell Host Microbe 2009;6:45-53
305. Kim C, Ho DH, Suk JE, You S, Michael S, Kang J, Joong Lee S, Masliah E, Hwang D, Lee HJ, Lee SJ. Neuron-released oligomeric alpha-synuclein is an endogenous agonist of TLR2 for paracrine activation of microglia. Nat Commun 2013;4:1562
306. Spinner DS, Cho IS, Park SY, Kim JI, Meeker HC, Ye X, Lafauci G, Kerr DJ, Flory MJ, Kim BS, Kascsak RB, Wisniewski T, Levis WR, Schuller-Levis GB, Carp RI, Park E, Kascsak RJ. Accelerated prion disease pathogenesis in Toll-like receptor 4 signaling-mutant mice. J Virol 2008;82:10701-10708
307. Stefanova N, Fellner L, Reindl M, Masliah E, Poewe W, Wenning GK. Toll-like receptor 4 promotes α-synuclein clearance and survival of nigral dopaminergic neurons. Am J Pathol 2011;179:954-963
308. Akashi-Takamura S, Miyake K. TLR accessory molecules. Curr Opin Immunol 2008;20:420-425
309. Baumann CL, Aspalter IM, Sharif O, Pichlmair A, Bluml S, Grebien F, Bruckner M, Pasierbek P, Aumayr K, Planyavsky M, Bennett KL, Colinge J, Knapp S, Superti-Furga G. CD14 is a coreceptor of Toll-like receptors 7 and 9. J Exp Med 2010;207:2689-2701
310. Rapsinski GJ, Newman TN, Oppong GO, van Putten JP, Tukel C. CD14 protein acts as an adaptor molecule for the immune recognition of Salmonella curli fibers. J Biol Chem 2013;288:14178-14188
311. Sakai K, Hasebe R, Takahashi Y, Song CH, Suzuki A, Yamasaki T, Horiuchi M. Absence of CD14 delays progression of prion diseases accompanied by increased microglial activation. J Virol 2013;87:13433-13445
312. Liu S, Liu Y, Hao W, Wolf L, Kiliaan AJ, Penke B, Rube CE, Walter J, Heneka MT, Hartmann T, Menger MD, Fassbender K. TLR2 is a primary receptor for Alzheimer's amyloid beta peptide to trigger neuroinflammatory activation. J Immunol 2012;188:1098-1107
313. Martinon F, Mayor A, Tschopp J. The inflammasomes: guardians of the body. Annu Rev Immunol 2009;27:229-265
314. Masters SL, O'Neill LAJ. Disease-associated amyloid and misfolded protein aggregates activate the inflammasome. Trends Mol Med 2011;17:276-282
315. Halle A, Hornung V, Petzold GC, Stewart CR, Monks BG, Reinheckel T, Fitzgerald KA, Latz E, Moore KJ, Golenbock DT. The NALP3 inflammasome is involved in the innate immune response to amyloid-beta. Nat Immunol 2008;9:857-865
316. Heneka MT, Kummer MP, Stutz A, Delekate A, Schwartz S, Vieira-Saecker A, Griep A, Axt D, Remus A, Tzeng TC, Gelpi E, Halle A, Korte M, Latz E, Golenbock DT. NLRP3 is activated in Alzheimer's disease and contributes to pathology in APP/PS1 mice. Nature 2013;493:674-678
317. Ather JL, Ckless K, Martin R, Foley KL, Suratt BT, Boyson JE, Fitzgerald KA, Flavell RA, Eisenbarth SC, Poynter ME. Serum amyloid A activates the NLRP3 inflammasome and promotes Th17 allergic asthma in mice. J Immunol 2011;187:64-73
318. Niemi K, Teirila L, Lappalainen J, Rajamaki K, Baumann MH, Oorni K, Wolff H, Kovanen PT, Matikainen S, Eklund KK. Serum amyloid A activates the NLRP3 inflammasome via P2X7 receptor and a cathepsin B-sensitive pathway. J Immunol 2011;186:6119-6128

319. Shi F, Yang L, Kouadir M, Yang Y, Wang J, Zhou X, Yin X, Zhao D. The NALP3 inflammasome is involved in neurotoxic prion peptide-induced microglial activation. J Neuroinflammation 2012;9:73
320. Hafner-Bratkovic I, Bencina M, Fitzgerald KA, Golenbock D, Jerala R. NLRP3 inflammasome activation in macrophage cell lines by prion protein fibrils as the source of IL-1beta and neuronal toxicity. Cell Mol Life Sci 2012;69:4215-4228
321. Seong S-Y, Matzinger P. Hydrophobicity: an ancient damage-associated molecular pattern that initiates innate immune responses. Nature reviews Immunology 2004;4:469-478
322. Kayed R, Glabe CG. Conformation-dependent anti-amyloid oligomer antibodies. Meth Enzymol 2006;413:326-344
323. Neumann H, Kotter MR, Franklin RJM. Debris clearance by microglia: an essential link between degeneration and regeneration. Brain 2009;132:288-295
324. Trudler D, Farfara D, Frenkel D. Toll-like receptors expression and signaling in glia cells in neuro-amyloidogenic diseases: towards future therapeutic application. Mediators Inflamm 2010;2010
325. Wirths O, Breyhan H, Marcello A, Cotel M-C, Brück W, Bayer TA. Inflammatory changes are tightly associated with neurodegeneration in the brain and spinal cord of the APP/PS1KI mouse model of Alzheimer's disease. Neurobiol Aging 2010;31:747-757
326. Landreth GE, Reed-Geaghan EG. Toll-like receptors in Alzheimer's disease. Curr Top Microbiol Immunol 2009;336:137-153
327. Hickman SE, Allison EK, El Khoury J. Microglial dysfunction and defective beta-amyloid clearance pathways in aging Alzheimer's disease mice. J Neurosci 2008;28:8354-8360
328. Salminen A, Ojala J, Kauppinen A, Kaarniranta K, Suuronen T. Inflammation in Alzheimer's disease: amyloid-beta oligomers trigger innate immunity defence via pattern recognition receptors. Prog Neurobiol 2009;87:181-194
329. Sethi S, Lipford G, Wagner H, Kretzschmar H. Postexposure prophylaxis against prion disease with a stimulator of innate immunity. Lancet 2002;360:229-230
330. DiCarlo G, Wilcock D, Henderson D, Gordon M, Morgan D. Intrahippocampal LPS injections reduce Abeta load in APP+PS1 transgenic mice. Neurobiol Aging 2001;22:1007-1012
331. Herber DL, Mercer M, Roth LM, Symmonds K, Maloney J, Wilson N, Freeman MJ, Morgan D, Gordon MN. Microglial activation is required for Abeta clearance after intracranial injection of lipopolysaccharide in APP transgenic mice. J Neuroimmune Pharmacol 2007;2:222-231
332. Tricker E, Cheng G. With a little help from my friends: modulation of phagocytosis through TLR activation. Cell Res 2008;18:711-712
333. Chen K, Iribarren P, Hu J, Chen J, Gong W, Cho EH, Lockett S, Dunlop NM, Wang JM. Activation of Toll-like receptor 2 on microglia promotes cell uptake of Alzheimer disease-associated amyloid beta peptide. J Biol Chem 2006;281:3651-3659
334. Oppong GO, Rapsinski GJ, Newman TN, Nishimori JH, Biesecker SG, Tukel C. Epithelial cells augment barrier function via activation of the Toll-like receptor 2/phosphatidylinositol 3-kinase pathway upon recognition of Salmonella enterica serovar Typhimurium curli fibrils in the gut. Infect Immun 2013;81:478-486
335. Nishimori JH, Newman TN, Oppong GO, Rapsinski GJ, Yen JH, Biesecker SG, Wilson RP, Butler BP, Winter MG, Tsolis RM, Ganea D, Tukel C. Microbial amyloids induce

interleukin 17A (IL-17A) and IL-22 responses via Toll-like receptor 2 activation in the intestinal mucosa. Infect Immun 2012;80:4398-4408
336. Richard KL, Filali M, Préfontaine P, Rivest S. Toll-like receptor 2 acts as a natural innate immune receptor to clear amyloid beta 1-42 and delay the cognitive decline in a mouse model of Alzheimer's disease. J Neurosci 2008;28:5784-5793
337. Liu S, Liu Y, Hao W, Wolf L, Kiliaan AJ, Penke B, Rübe CE, Walter J, Heneka MT, Hartmann T, Menger MD, Fassbender K. TLR2 is a primary receptor for Alzheimer's amyloid β peptide to trigger neuroinflammatory activation. J Immunol 2012;188:1098-1107
338. Jin JJ, Kim HD, Maxwell JA, Li L, Fukuchi K. Toll-like receptor 4-dependent upregulation of cytokines in a transgenic mouse model of Alzheimer's disease. J Neuroinflammation 2008;5
339. Tahara K, Kim H-D, Jin J-J, Maxwell JA, Li L, Fukuchi K-I. Role of toll-like receptor signalling in Abeta uptake and clearance. Brain 2006;129:3006-3019
340. Tang S, Lathia J, Selvaraj P, Jo D, Mughal M, Cheng A, Siler D, Markesbery W, Arumugam T, Mattson M. Toll-like receptor-4 mediates neuronal apoptosis induced by amyloid beta-peptide and the membrane lipid peroxidation product 4-hydroxynonenal. Exp Neurol 2008;213:114-121
341. Osterbye T, Funda DP, Fundova P, Mansson JE, Tlaskalova-Hogenova H, Buschard K. A subset of human pancreatic beta cells express functional CD14 receptors: a signaling pathway for beta cell-related glycolipids, sulfatide and beta-galactosylceramide. Diabetes Metab Res Rev 2010;26:656-667
342. Kiely A, Robinson A, McClenaghan NH, Flatt PR, Newsholme P. Toll-like receptor agonist induced changes in clonal rat BRIN-BD11 beta-cell insulin secretion and signal transduction. J Endocrinol 2009;202:365-373
343. Garay-Malpartida HM, Mourão RF, Mantovani M, Santos IA, Sogayar MC, Goldberg AC. Toll-like receptor 4 (TLR4) expression in human and murine pancreatic beta-cells affects cell viability and insulin homeostasis. BMC Immunol 2011;12:18
344. Vives-Pi M, Somoza N, Fernandez-Alvarez J, Vargas F, Caro P, Alba A, Gomis R, Labeta MO, Pujol-Borrell R. Evidence of expression of endotoxin receptors CD14, toll-like receptors TLR4 and TLR2 and associated molecule MD-2 and of sensitivity to endotoxin (LPS) in islet beta cells. Clin Exp Immunol 2003;133:208-218
345. Amyot J, Semache M, Ferdaoussi M, Fontes G, Poitout V. Lipopolysaccharides impair insulin gene expression in isolated islets of Langerhans via Toll-Like Receptor-4 and NF-kappaB signalling. PLoS ONE 2012;7:e36200
346. Schlachetzki JC, Hull M. Microglial activation in Alzheimer's disease. Curr Alzheimer Res 2009;6:554-563
347. Shaftel SS, Kyrkanides S, Olschowka JA, Miller JN, Johnson RE, O'Banion MK. Sustained hippocampal IL-1 beta overexpression mediates chronic neuroinflammation and ameliorates Alzheimer plaque pathology. J Clin Invest 2007;117:1595-1604
348. Morgan D, Gordon MN, Tan J, Wilcock D, Rojiani AM. Dynamic complexity of the microglial activation response in transgenic models of amyloid deposition: implications for Alzheimer therapeutics. J Neuropathol Exp Neurol 2005;64:743-753
349. Michelucci A, Heurtaux T, Grandbarbe L, Morga E, Heuschling P. Characterization of the microglial phenotype under specific pro-inflammatory and anti-inflammatory conditions: Effects of oligomeric and fibrillar amyloid-beta. J Neuroimmunol 2009;210:3-12

350. Shaw AC, Goldstein DR, Montgomery RR. Age-dependent dysregulation of innate immunity. Nat Rev Immunol 2013;13:875-877
351. Shaw AC, Panda A, Joshi SR, Qian F, Allore HG, Montgomery RR. Dysregulation of human Toll-like receptor function in aging. Ageing Res Rev 2011;10:346-353
352. Youm YH, Grant RW, McCabe LR, Albarado DC, Nguyen KY, Ravussin A, Pistell P, Newman S, Carter R, Laque A, Munzberg H, Rosen CJ, Ingram DK, Salbaum JM, Dixit VD. Canonical nlrp3 inflammasome links systemic low-grade inflammation to functional decline in aging. Cell Metab 2013;18:519-532
353. Franceschi C, Capri M, Monti D, Giunta S, Olivieri F, Sevini F, Panourgia MP, Invidia L, Celani L, Scurti M, Cevenini E, Castellani GC, Salvioli S. Inflammaging and anti-inflammaging: a systemic perspective on aging and longevity emerged from studies in humans. Mech Ageing Dev 2007;128:92-105
354. Dinarello CA, Simon A, van der Meer JW. Treating inflammation by blocking interleukin-1 in a broad spectrum of diseases. Nat Rev Drug Discov 2012;11:633-652
355. Dinarello CA, Ikejima T, Warner SJ, Orencole SF, Lonnemann G, Cannon JG, Libby P. Interleukin 1 induces interleukin 1. I. Induction of circulating interleukin 1 in rabbits in vivo and in human mononuclear cells in vitro. J Immunol 1987;139:1902-1910
356. Dinarello CA. Interleukin-1 in the pathogenesis and treatment of inflammatory diseases. Blood 2011;117:3720-3732
357. Chae JJ, Aksentijevich I, Kastner DL. Advances in the understanding of familial Mediterranean fever and possibilities for targeted therapy. Br J Haematol 2009;146:467-478
358. Hoffman HM, Mueller JL, Broide DH, Wanderer AA, Kolodner RD. Mutation of a new gene encoding a putative pyrin-like protein causes familial cold autoinflammatory syndrome and Muckle-Wells syndrome. Nat Genet 2001;29:301-305
359. Simon A, Park H, Maddipati R, Lobito AA, Bulua AC, Jackson AJ, Chae JJ, Ettinger R, de Koning HD, Cruz AC, Kastner DL, Komarow H, Siegel RM. Concerted action of wild-type and mutant TNF receptors enhances inflammation in TNF receptor 1-associated periodic fever syndrome. Proc Natl Acad Sci USA 2010;107:9801-9806
360. Stoffels M, Simon A. Hyper-IgD syndrome or mevalonate kinase deficiency. Curr Opin Rheumatol 2011;23:419-423
361. Larsen CM, Faulenbach M, Vaag A, Vølund A, Ehses JA, Seifert B, Mandrup-Poulsen T, Donath MY. Interleukin-1-receptor antagonist in type 2 diabetes mellitus. N Engl J Med 2007;356:1517-1526
362. Larsen CM, Faulenbach M, Vaag A, Ehses JA, Donath MY, Mandrup-Poulsen T. Sustained effects of interleukin-1 receptor antagonist treatment in type 2 diabetes. Diabetes Care 2009;32:1663-1668
363. Ridker PM, Thuren T, Zalewski A, Libby P. Interleukin-1beta inhibition and the prevention of recurrent cardiovascular events: rationale and design of the Canakinumab Anti-inflammatory Thrombosis Outcomes Study (CANTOS). Am Heart J 2011;162:597-605
364. Mandrup-Poulsen T. Type 2 diabetes mellitus: a metabolic autoinflammatory disease. Dermatol Clin 2013;31:495-506
365. Wang X, Bao W, Liu J, Ouyang YY, Wang D, Rong S, Xiao X, Shan ZL, Zhang Y, Yao P, Liu LG. Inflammatory markers and risk of type 2 diabetes: a systematic review and meta-analysis. Diabetes Care 2013;36:166-175

366. Pickup JC, Mattock MB, Chusney GD, Burt D. NIDDM as a disease of the innate immune system: association of acute-phase reactants and interleukin-6 with metabolic syndrome X. Diabetologia 1997;40:1286-1292
367. Spranger J, Kroke A, Mohlig M, Hoffmann K, Bergmann MM, Ristow M, Boeing H, Pfeiffer AF. Inflammatory cytokines and the risk to develop type 2 diabetes: results of the prospective population-based European Prospective Investigation into Cancer and Nutrition (EPIC)-Potsdam Study. Diabetes 2003;52:812-817
368. Thorand B, Kolb H, Baumert J, Koenig W, Chambless L, Meisinger C, Illig T, Martin S, Herder C. Elevated levels of interleukin-18 predict the development of type 2 diabetes: results from the MONICA/KORA Augsburg Study, 1984-2002. Diabetes 2005;54:2932-2938
369. Luotola K, Pietilä A, Zeller T, Moilanen L, Kähönen M, Nieminen MS, Kesäniemi YA, Blankenberg S, Jula A, Perola M, Salomaa V, Studies HaF. Associations between interleukin-1 (IL-1) gene variations or IL-1 receptor antagonist levels and the development of type 2 diabetes. J Intern Med 2011;269:322-332
370. Yamauchi T, Kamon J, Waki H, Terauchi Y, Kubota N, Hara K, Mori Y, Ide T, Murakami K, Tsuboyama-Kasaoka N, Ezaki O, Akanuma Y, Gavrilova O, Vinson C, Reitman ML, Kagechika H, Shudo K, Yoda M, Nakano Y, Tobe K, Nagai R, Kimura S, Tomita M, Froguel P, Kadowaki T. The fat-derived hormone adiponectin reverses insulin resistance associated with both lipoatrophy and obesity. Nat Med 2001;7:941-946
371. Lee HM, Kim JJ, Kim HJ, Shong M, Ku BJ, Jo EK. Upregulated NLRP3 inflammasome activation in patients with type 2 diabetes. Diabetes 2013;62:194-204
372. Dasu MR, Devaraj S, Park S, Jialal I. Increased toll-like receptor (TLR) activation and TLR ligands in recently diagnosed type 2 diabetic subjects. Diabetes Care 2010;33:861-868
373. Dasu M, Devaraj S, Ling Z, Hwang D, Jialal I. High glucose induces Toll-like receptor expression in human monocytes: Mechanism of activation. Diabetes 2008;57:3090-3098
374. Zhou R, Tardivel A, Thorens B, Choi I, Tschopp J. Thioredoxin-interacting protein links oxidative stress to inflammasome activation. Nat Immunol 2009;11:136-140
375. Viardot A, Heilbronn LK, Samocha-Bonet D, Mackay F, Campbell LV, Samaras K. Obesity is associated with activated and insulin resistant immune cells. Diabetes Metab Res Rev 2012;28:447-454
376. DeFuria J, Belkina AC, Jagannathan-Bogdan M, Snyder-Cappione J, Carr JD, Nersesova YR, Markham D, Strissel KJ, Watkins AA, Zhu M, Allen J, Bouchard J, Toraldo G, Jasuja R, Obin MS, McDonnell ME, Apovian C, Denis GV, Nikolajczyk BS. B cells promote inflammation in obesity and type 2 diabetes through regulation of T-cell function and an inflammatory cytokine profile. Proc Natl Acad Sci USA 2013;110:5133-5138
377. Tak PP, Kalden JR. Advances in rheumatology: new targeted therapeutics. Arthritis Res Ther 2011;13 Suppl 1:S5
378. Samaropoulos XF, Light L, Ambrosius WT, Marcovina SM, Probstfield J, Jr DC. The effect of intensive risk factor management in type 2 diabetes on inflammatory biomarkers. Diabetes Res Clin Pract 2012;95:389-398
379. Zampetaki A, Kiechl S, Drozdov I, Willeit P, Mayr U, Prokopi M, Mayr A, Weger S, Oberhollenzer F, Bonora E, Shah A, Willeit J, Mayr M. Plasma microRNA profiling reveals loss of endothelial miR-126 and other microRNAs in type 2 diabetes. Circ Res 2010;107:810-817

380. Rutkowski JM, Davis KE, Scherer PE. Mechanisms of obesity and related pathologies: the macro- and microcirculation of adipose tissue. FEBS J 2009;276:5738-5746
381. Ueki K, Kondo T, Kahn CR. Suppressor of cytokine signaling 1 (SOCS-1) and SOCS-3 cause insulin resistance through inhibition of tyrosine phosphorylation of insulin receptor substrate proteins by discrete mechanisms. Mol Cell Biol 2004;24:5434-5446
382. Rui L, Yuan M, Frantz D, Shoelson S, White MF. SOCS-1 and SOCS-3 block insulin signaling by ubiquitin-mediated degradation of IRS1 and IRS2. J Biol Chem 2002;277:42394-42398
383. Lumeng CN, Bodzin JL, Saltiel AR. Obesity induces a phenotypic switch in adipose tissue macrophage polarization. J Clin Invest 2007;117:175-184
384. Winer DA, Winer S, Shen L, Wadia PP, Yantha J, Paltser G, Tsui H, Wu P, Davidson MG, Alonso MN, Leong HX, Glassford A, Caimol M, Kenkel JA, Tedder TF, McLaughlin T, Miklos DB, Dosch HM, Engleman EG. B cells promote insulin resistance through modulation of T cells and production of pathogenic IgG antibodies. Nat Med 2011;17:610-617
385. Eller K, Kirsch A, Wolf AM, Sopper S, Tagwerker A, Stanzl U, Wolf D, Patsch W, Rosenkranz AR, Eller P. Potential role of regulatory T cells in reversing obesity-linked insulin resistance and diabetic nephropathy. Diabetes 2011;60:2954-2962
386. Schipper HS, Rakhshandehroo M, van de Graaf SF, Venken K, Koppen A, Stienstra R, Prop S, Meerding J, Hamers N, Besra G, Boon L, Nieuwenhuis EE, Elewaut D, Prakken B, Kersten S, Boes M, Kalkhoven E. Natural killer T cells in adipose tissue prevent insulin resistance. J Clin Invest 2012;122:3343-3354
387. Stienstra R, van Diepen JA, Tack CJ, Zaki MH, van de Veerdonk FL, Perera D, Neale GA, Hooiveld GJ, Hijmans A, Vroegrijk I, van den Berg S, Romijn J, Rensen PC, Joosten LA, Netea MG, Kanneganti TD. Inflammasome is a central player in the induction of obesity and insulin resistance. Proc Natl Acad Sci USA 2011;108:15324-15329
388. Vandanmagsar B, Youm YH, Ravussin A, Galgani JE, Stadler K, Mynatt RL, Ravussin E, Stephens JM, Dixit VD. The NLRP3 inflammasome instigates obesity-induced inflammation and insulin resistance. Nat Med 2011;17:179-188
389. Wen H, Gris D, Lei Y, Jha S, Zhang L, Huang MT, Brickey WJ, Ting JP. Fatty acid-induced NLRP3-ASC inflammasome activation interferes with insulin signaling. Nat Immunol 2011;12:408-415
390. Bendtzen K, Mandrup-Poulsen T, Nerup J, Nielsen JH, Dinarello CA, Svenson M. Cytotoxicity of human pI 7 interleukin-1 for pancreatic islets of Langerhans. Science 1986;232:1545-1547
391. Mandrup-Poulsen T, Bendtzen K, Dinarello CA, Nerup J. Human tumor necrosis factor potentiates human interleukin 1-mediated rat pancreatic beta-cell cytotoxicity. J Immunol 1987;139:4077-4082
392. Novotny GW, Lundh M, Backe MB, Christensen DP, Hansen JB, Dahllof MS, Pallesen EM, Mandrup-Poulsen T. Transcriptional and translational regulation of cytokine signaling in inflammatory beta-cell dysfunction and apoptosis. Arch Biochem Biophys 2012;528:171-184
393. Corbett JA, Wang JL, Sweetland MA, Lancaster JR, McDaniel ML. Interleukin 1 beta induces the formation of nitric oxide by beta-cells purified from rodent islets of Langerhans.

Evidence for the beta-cell as a source and site of action of nitric oxide. J Clin Invest 1992;90:2384-2391
394. Miani M, Barthson J, Colli ML, Brozzi F, Cnop M, Eizirik DL. Endoplasmic reticulum stress sensitizes pancreatic beta cells to interleukin-1beta-induced apoptosis via Bim/A1 imbalance. Cell Death Dis 2013;4:e701
395. Ehses JA, Lacraz G, Giroix M-H, Schmidlin F, Coulaud J, Kassis N, Irminger J-C, Kergoat M, Portha B, Homo-Delarche F, Donath MY. IL-1 antagonism reduces hyperglycemia and tissue inflammation in the type 2 diabetic GK rat. Proc Natl Acad Sci USA 2009;106:13998-14003
396. Sauter NS, Schulthess FT, Galasso R, Castellani LW, Maedler K. The antiinflammatory cytokine interleukin-1 receptor antagonist protects from high-fat diet-induced hyperglycemia. Endocrinology 2008;149:2208-2218
397. Maedler K, Sergeev P, Ris F, Oberholzer J, Joller-Jemelka HI, Spinas GA, Kaiser N, Halban PA, Donath MY. Glucose-induced beta cell production of IL-1beta contributes to glucotoxicity in human pancreatic islets. J Clin Invest 2002;110:851-860
398. Böni-Schnetzler M, Thorne J, Parnaud G, Marselli L, Ehses JA, Kerr-Conte J, Pattou F, Halban PA, Weir GC, Donath MY. Increased interleukin (IL)-1beta messenger ribonucleic acid expression in beta -cells of individuals with type 2 diabetes and regulation of IL-1beta in human islets by glucose and autostimulation. J Clin Endocrinol Metab 2008;93:4065-4074
399. Maedler K, Størling J, Sturis J, Zuellig RA, Spinas GA, Arkhammar POG, Mandrup-Poulsen T, Donath MY. Glucose- and interleukin-1beta-induced beta-cell apoptosis requires Ca2+ influx and extracellular signal-regulated kinase (ERK) 1/2 activation and is prevented by a sulfonylurea receptor 1/inwardly rectifying K+ channel 6.2 (SUR/Kir6.2) selective potassium channel opener in human islets. Diabetes 2004;53:1706-1713
400. Mahdi T, Hanzelmann S, Salehi A, Muhammed SJ, Reinbothe TM, Tang Y, Axelsson AS, Zhou Y, Jing X, Almgren P, Krus U, Taneera J, Blom AM, Lyssenko V, Esguerra JL, Hansson O, Eliasson L, Derry J, Zhang E, Wollheim CB, Groop L, Renstrom E, Rosengren AH. Secreted frizzled-related protein 4 reduces insulin secretion and is overexpressed in type 2 diabetes. Cell Metab 2012;16:625-633
401. Ehses JA, Perren A, Eppler E, Ribaux P, Pospisilik JA, Maor-Cahn R, Gueripel X, Ellingsgaard H, Schneider MKJ, Biollaz G, Fontana A, Reinecke M, Homo-Delarche F, Donath MY. Increased number of islet-associated macrophages in type 2 diabetes. Diabetes 2007;56:2356-2370
402. Igoillo-Esteve M, Marselli L, Cunha DA, Ladrière L, Ortis F, Grieco FA, Dotta F, Weir GC, Marchetti P, Eizirik DL, Cnop M. Palmitate induces a pro-inflammatory response in human pancreatic islets that mimics CCL2 expression by beta cells in type 2 diabetes. Diabetologia 2010;53:1395-1405
403. Lee JY, Zhao L, Youn HS, Weatherill AR, Tapping R, Feng L, Lee WH, Fitzgerald KA, Hwang DH. Saturated fatty acid activates but polyunsaturated fatty acid inhibits Toll-like receptor 2 dimerized with Toll-like receptor 6 or 1. J Biol Chem 2004;279:16971-16979
404. Ehses JA, Meier DT, Wueest S, Rytka J, Boller S, Wielinga PY, Schraenen A, Lemaire K, Debray S, Van Lommel L, Pospisilik JA, Tschopp O, Schultze SM, Malipiero U, Esterbauer H, Ellingsgaard H, Rütti S, Schuit FC, Lutz TA, Böni-Schnetzler M, Konrad D, Donath

MY. Toll-like receptor 2-deficient mice are protected from insulin resistance and beta cell dysfunction induced by a high-fat diet. Diabetologia 2010;53:1795-1806
405. Creely SJ, McTernan PG, Kusminski CM, Fisher fM, Da Silva NF, Khanolkar M, Evans M, Harte AL, Kumar S. Lipopolysaccharide activates an innate immune system response in human adipose tissue in obesity and type 2 diabetes. Am J Physiol Endocrinol Metab 2007;292:E740-747
406. Gombault A, Baron L, Couillin I. ATP release and purinergic signaling in NLRP3 inflammasome activation. Front Immunol 2012;3:414
407. Jourdan T, Godlewski G, Cinar R, Bertola A, Szanda G, Liu J, Tam J, Han T, Mukhopadhyay B, Skarulis MC, Ju C, Aouadi M, Czech MP, Kunos G. Activation of the Nlrp3 inflammasome in infiltrating macrophages by endocannabinoids mediates beta cell loss in type 2 diabetes. Nat Med 2013;19:1132-1140
408. Latz E, Xiao TS, Stutz A. Activation and regulation of the inflammasomes. Nat Rev Immunol 2013;13:397-411
409. Shimada K, Crother TR, Karlin J, Dagvadorj J, Chiba N, Chen S, Ramanujan VK, Wolf AJ, Vergnes L, Ojcius DM, Rentsendorj A, Vargas M, Guerrero C, Wang Y, Fitzgerald KA, Underhill DM, Town T, Arditi M. Oxidized mitochondrial DNA activates the NLRP3 inflammasome during apoptosis. Immunity 2012;36:401-414
410. Youm YH, Adijiang A, Vandanmagsar B, Burk D, Ravussin A, Dixit VD. Elimination of the NLRP3-ASC inflammasome protects against chronic obesity-induced pancreatic damage. Endocrinology 2011;152:4039-4045
411. Martinez FO, Helming L, Gordon S. Alternative activation of macrophages: an immunologic functional perspective. Annu Rev Immunol 2009;27:451-483
412. Mosser DM, Edwards JP. Exploring the full spectrum of macrophage activation. Nat Rev Immunol 2008;8:958-969
413. Biswas SK, Mantovani A. Macrophage plasticity and interaction with lymphocyte subsets: cancer as a paradigm. Nat Immunol 2010;11:889-896
414. Hume DA, Halpin D, Charlton H, Gordon S. The mononuclear phagocyte system of the mouse defined by immunohistochemical localization of antigen F4/80: macrophages of endocrine organs. Proc Natl Acad Sci USA 1984;81:4174-4177
415. Calderon B, Suri A, Miller MJ, Unanue ER. Dendritic cells in islets of Langerhans constitutively present beta cell-derived peptides bound to their class II MHC molecules. Proc Natl Acad Sci USA 2008;105:6121-6126
416. Hess D, Li L, Martin M, Sakano S, Hill D, Strutt B, Thyssen S, Gray DA, Bhatia M. Bone marrow-derived stem cells initiate pancreatic regeneration. Nat Biotechnol 2003;21:763-770
417. Tessem JS, Jensen JN, Pelli H, Dai X-M, Zong X-H, Stanley ER, Jensen J, DeGregori J. Critical roles for macrophages in islet angiogenesis and maintenance during pancreatic degeneration. Diabetes 2008;57:1605-1617
418. Richardson SJ, Willcox A, Bone AJ, Foulis AK, Morgan NG. Islet-associated macrophages in type 2 diabetes. Diabetologia 2009;52:1686-1688
419. Eguchi K, Manabe I, Oishi-Tanaka Y, Ohsugi M, Kono N, Ogata F, Yagi N, Ohto U, Kimoto M, Miyake K, Tobe K, Arai H, Kadowaki T, Nagai R. Saturated Fatty Acid and TLR Signaling Link β Cell Dysfunction and Islet Inflammation. Cell Metab 2012;15:518-533

420. Cucak H, Grunnet LG, Rosendahl A. Accumulation of M1-like macrophages in type 2 diabetic islets is followed by a systemic shift in macrophage polarization. J Leukoc Biol 2013;10.1189/jlb.0213075
421. Butcher MJ, Hallinger D, Garcia E, Machida Y, Chakrabarti S, Nadler J, Galkina EV, Imai Y. Association of proinflammatory cytokines and islet resident leucocytes with islet dysfunction in type 2 diabetes. Diabetologia 2014;10.1007/s00125-013-3116-5
422. Medarova Z, Greiner DL, Ifediba M, Dai G, Bolotin E, Castillo G, Bogdanov A, Kumar M, Moore A. Imaging the pancreatic vasculature in diabetes models. Diabetes Metab Res Rev 2011;27:767-772
423. Gaglia JL, Guimaraes AR, Harisinghani M, Turvey SE, Jackson R, Benoist C, Mathis D, Weissleder R. Noninvasive imaging of pancreatic islet inflammation in type 1A diabetes patients. J Clin Invest 2011;121:442-445
424. Oslowski CM, Hara T, O'Sullivan-Murphy B, Kanekura K, Lu S, Hara M, Ishigaki S, Zhu LJ, Hayashi E, Hui ST, Greiner D, Kaufman RJ, Bortell R, Urano F. Thioredoxin-interacting protein mediates ER stress-induced beta cell death through initiation of the inflammasome. Cell Metab 2012;16:265-273
425. Ribaux P, Ehses JA, Lin-Marq N, Carrozzino F, Böni-Schnetzler M, Hammar E, Irminger J-C, Donath MY, Halban PA. Induction of CXCL1 by extracellular matrix and autocrine enhancement by interleukin-1 in rat pancreatic beta-cells. Endocrinology 2007;148:5582-5590
426. Donath MY, Shoelson SE. Type 2 diabetes as an inflammatory disease. Nat Rev Immunol 2011;11:98-107
427. Hevener AL, Olefsky JM, Reichart D, Nguyen MT, Bandyopadyhay G, Leung HY, Watt MJ, Benner C, Febbraio MA, Nguyen AK, Folian B, Subramaniam S, Gonzalez FJ, Glass CK, Ricote M. Macrophage PPAR gamma is required for normal skeletal muscle and hepatic insulin sensitivity and full antidiabetic effects of thiazolidinediones. J Clin Invest 2007;117:1658-1669
428. Dobrian AD, Ma Q, Lindsay JW, Leone KA, Ma K, Coben J, Galkina EV, Nadler JL. Dipeptidyl peptidase IV inhibitor sitagliptin reduces local inflammation in adipose tissue and in pancreatic islets of obese mice. Am J Physiol Endocrinol Metab 2011;300:E410-421
429. Christensen DP, Gysemans C, Lundh M, Dahllof MS, Noesgaard D, Schmidt SF, Mandrup S, Birkbak N, Workman CT, Piemonti L, Blaabjerg L, Monzani V, Fossati G, Mascagni P, Paraskevas S, Aikin RA, Billestrup N, Grunnet LG, Dinarello CA, Mathieu C, Mandrup-Poulsen T. Lysine deacetylase inhibition prevents diabetes by chromatin-independent immunoregulation and beta-cell protection. Proc Natl Acad Sci USA 2014;111:1055-1059
430. Lundh M, Scully SS, Mandrup-Poulsen T, Wagner BK. Small-molecule inhibition of inflammatory beta-cell death. Diabetes Obes Metab 2013;15:176-184
431. Hellmann J, Tang Y, Kosuri M, Bhatnagar A, Spite M. Resolvin D1 decreases adipose tissue macrophage accumulation and improves insulin sensitivity in obese-diabetic mice. FASEB J 2011;25:2399-2407
432. Brooks-Worrell B, Narla R, Palmer JP. Biomarkers and immune-modulating therapies for type 2 diabetes. Trends Immunol 2012;33:546-553
433. Sahraoui A, Jensen KK, Ueland T, Korsgren O, Foss A, Scholz H. Anakinra and tocilizumab enhance survival and function of human islets during culture: implications for clinical islet transplantation. Cell Transplant 2013;10.3727/096368913X667529

434. Shapiro AMJ. Islet transplantation in type 1 diabetes: ongoing challenges, refined procedures, and long-term outcome. The review of diabetic studies : RDS 2012;9:385-406
435. McCall M, Pawlick R, Kin T, Shapiro AM. Anakinra potentiates the protective effects of etanercept in transplantation of marginal mass human islets in immunodeficient mice. Am J Transplant 2012;12:322-329
436. Abdelli S, Ansite J, Roduit R, Borsello T, Matsumoto I, Sawada T, Allaman-Pillet N, Henry H, Beckmann JS, Hering BJ, Bonny C. Intracellular stress signaling pathways activated during human islet preparation and following acute cytokine exposure. Diabetes 2004;53:2815-2823
437. Marzorati S, Antonioli B, Nano R, Maffi P, Piemonti L, Giliola C, Secchi A, Lakey JR, Bertuzzi F. Culture medium modulates proinflammatory conditions of human pancreatic islets before transplantation. Am J Transplant 2006;6:2791-2795
438. Bertuzzi F, Marzorati S, Maffi P, Piemonti L, Melzi R, de Taddeo F, Valtolina V, D'Angelo A, Di Carlo V, Bonifacio E, Secchi A. Tissue factor and CCL2/monocyte chemoattractant protein-1 released by human islets affect islet engraftment in type 1 diabetic recipients. J Clin Endocrinol Metab 2004;89:5724-5728
439. Saudek F, Jirak D, Girman P, Herynek V, Dezortova M, Kriz J, Peregrin J, Berkova Z, Zacharovova K, Hajek M. Magnetic resonance imaging of pancreatic islets transplanted into the liver in humans. Transplantation 2010;90:1602-1606
440. Cardozo AK, Ortis F, Storling J, Feng YM, Rasschaert J, Tonnesen M, Van Eylen F, Mandrup-Poulsen T, Herchuelz A, Eizirik DL. Cytokines downregulate the sarcoendoplasmic reticulum pump Ca2+ ATPase 2b and deplete endoplasmic reticulum Ca2+, leading to induction of endoplasmic reticulum stress in pancreatic beta-cells. Diabetes 2005;54:452-461
441. Montolio M, Biarnés M, Téllez N, Escoriza J, Soler J, Montanya E. Interleukin-1beta and inducible form of nitric oxide synthase expression in early syngeneic islet transplantation. J Endocrinol 2007;192:169-177
442. Satoh M, Yasunami Y, Matsuoka N, Nakano M, Itoh T, Nitta T, Anzai K, Ono J, Taniguchi M, Ikeda S. Successful islet transplantation to two recipients from a single donor by targeting proinflammatory cytokines in mice. Transplantation 2007;83:1085-1092
443. Barshes NR, Wyllie S, Goss JA. Inflammation-mediated dysfunction and apoptosis in pancreatic islet transplantation: implications for intrahepatic grafts. J Leukoc Biol 2005;77:587-597
444. Movahedi B, Van de Casteele M, Caluwé N, Stangé G, Breckpot K, Thielemans K, Vreugdenhil G, Mathieu C, Pipeleers D. Human pancreatic duct cells can produce tumour necrosis factor-alpha that damages neighbouring beta cells and activates dendritic cells. Diabetologia 2004;47:998-1008
445. Fontaine MJ, Blanchard J, Rastellini C, Lazda V, Herold KC, Pollak R. Pancreatic islets activate portal vein endothelial cells in vitro. Ann Clin Lab Sci 2002;32:352-361
446. Barbé-Tuana FM, Klein D, Ichii H, Berman DM, Coffey L, Kenyon NS, Ricordi C, Pastori RL. CD40-CD40 ligand interaction activates proinflammatory pathways in pancreatic islets. Diabetes 2006;55:2437-2445
447. Abdulreda MH, Faleo G, Molano RD, Lopez-Cabezas M, Molina J, Tan Y, Echeverria OA, Zahr-Akrawi E, Rodriguez-Diaz R, Edlund PK, Leibiger I, Bayer AL, Perez V, Ricordi C,

Caicedo A, Pileggi A, Berggren PO. High-resolution, noninvasive longitudinal live imaging of immune responses. Proc Natl Acad Sci USA 2011;108:12863-12868
448. de Vos P, Smedema I, van Goor H, Moes H, van Zanten J, Netters S, de Leij LFM, de Haan A, de Haan BJ. Association between macrophage activation and function of micro-encapsulated rat islets. Diabetologia 2003;46:666-673
449. Kaufman DB, Platt JL, Rabe FL, Dunn DL, Bach FH, Sutherland DE. Differential roles of Mac-1+ cells, and CD4+ and CD8+ T lymphocytes in primary nonfunction and classic rejection of islet allografts. J Exp Med 1990;172:291-302
450. Benda B, Korsgren O. Interleukin-6 in islet xenograft rejection. Transpl Int 2001;14:63-71
451. Omer A, Keegan M, Czismadia E, De Vos P, Van Rooijen N, Bonner-Weir S, Weir GC. Macrophage depletion improves survival of porcine neonatal pancreatic cell clusters contained in alginate macrocapsules transplanted into rats. Xenotransplantation 2003;10:240-251
452. Rossi L, Migliavacca B, Pierigé F, Serafini S, Sanvito F, Olivieri S, Nano R, Antonioli B, Magnani M, Bertuzzi F. Prolonged islet allograft survival in diabetic mice upon macrophage depletion by clodronate-loaded erythrocytes. Transplantation 2008;85:648-650
453. Donath MY, Størling J, Maedler K, Mandrup-Poulsen T. Inflammatory mediators and islet beta-cell failure: a link between type 1 and type 2 diabetes. J Mol Med 2003;81:455-470
454. Waterland RA, Jirtle RL. Transposable elements: targets for early nutritional effects on epigenetic gene regulation. Mol Cell Biol 2003;23:5293-5300
455. Butler AE, Jang J, Gurlo T, Carty MD, Soeller WC, Butler PC. Diabetes due to a progressive defect in beta-cell mass in rats transgenic for human islet amyloid polypeptide (HIP Rat): a new model for type 2 diabetes. Diabetes 2004;53:1509-1516
456. Salvalaggio PRO, Deng S, Ariyan CE, Millet I, Zawalich WS, Basadonna GP, Rothstein DM. Islet filtration: a simple and rapid new purification procedure that avoids ficoll and improves islet mass and function. Transplantation 2002;74:877-879
457. Lynn DJ, Winsor GL, Chan C, Richard N, Laird MR, Barsky A, Gardy JL, Roche FM, Chan TH, Shah N, Lo R, Naseer M, Que J, Yau M, Acab M, Tulpan D, Whiteside MD, Chikatamarla A, Mah B, Munzner T, Hokamp K, Hancock RE, Brinkman FS. InnateDB: facilitating systems-level analyses of the mammalian innate immune response. Mol Syst Biol 2008;4:218
458. Spandidos A, Wang X, Wang H, Seed B. PrimerBank: a resource of human and mouse PCR primer pairs for gene expression detection and quantification. Nucleic Acids Res 2010;38:D792-799
459. Livak KJ, Schmittgen TD. Analysis of relative gene expression data using real-time quantitative PCR and the 2(-Delta Delta C(T)) Method. Methods 2001;25:402-408
460. Schneider CA RW, Eliceiri KW. NIH Image to ImageJ: 25 years of image analysis. Nature Methods 2012;9:671-675
461. Van Rooijen N, van Kesteren-Hendrikx E. "In vivo" depletion of macrophages by liposome-mediated "suicide". Meth Enzymol 2003;373:3-16
462. Hutton M, Soukhatcheva G, Johnson J. Role of the TLR signaling molecule TRIF in β-cell function and glucose homeostasis. Islets 2010;2:104-111
463. Kahn SE, Hull RL, Utzschneider KM. Mechanisms linking obesity to insulin resistance and type 2 diabetes. Nature 2006;444:840-846

464. Donath MY, Böni-Schnetzler M, Ellingsgaard H, Halban PA, Ehses JA. Cytokine production by islets in health and diabetes: cellular origin, regulation and function. Trends Endocrinol Metab 2010;21:261-267
465. Westermark P, Eizirik DL, Pipeleers DG, Hellerström C, Andersson A. Rapid deposition of amyloid in human islets transplanted into nude mice. Diabetologia 1995;38:543-549
466. Westermark GT, Westermark P, Berne C, Korsgren O, Transplantation NNfCI. Widespread amyloid deposition in transplanted human pancreatic islets. N Engl J Med 2008;359:977-979
467. Donath M, Weder C, Whitmore J, Bauer R. XOMA 052, an Anti-IL-1ß Antibody, in a Double-Blind, Placebo-Controlled, Dose Escalation Study of the Safety and Pharmacokinetics in Patients with Type 2 Diabetes. Diabetologia 2008;51:S7
468. Maezawa I, Zimin PI, Wulff H, Jin L-W. Amyloid-beta protein oligomer at low nanomolar concentrations activates microglia and induces microglial neurotoxicity. J Biol Chem 2011;286:3693-3706
469. Huang da W, Sherman BT, Lempicki RA. Systematic and integrative analysis of large gene lists using DAVID bioinformatics resources. Nat Protoc 2009;4:44-57
470. Huang da W, Sherman BT, Lempicki RA. Bioinformatics enrichment tools: paths toward the comprehensive functional analysis of large gene lists. Nucleic Acids Res 2009;37:1-13
471. Ogata H, Goto S, Sato K, Fujibuchi W, Bono H, Kanehisa M. KEGG: Kyoto Encyclopedia of Genes and Genomes. Nucleic Acids Res 1999;27:29-34
472. Kudva YC, Mueske C, Butler PC, Eberhardt NL. A novel assay in vitro of human islet amyloid polypeptide amyloidogenesis and effects of insulin secretory vesicle peptides on amyloid formation. Biochem J 1998;331 (Pt 3):809-813
473. Green JD, Goldsbury C, Kistler J, Cooper GJS, Aebi U. Human amylin oligomer growth and fibril elongation define two distinct phases in amyloid formation. J Biol Chem 2004;279:12206-12212
474. Ikejima T, Okusawa S, Ghezzi P, van der Meer JW, Dinarello CA. Interleukin-1 induces tumor necrosis factor (TNF) in human peripheral blood mononuclear cells in vitro and a circulating TNF-like activity in rabbits. J Infect Dis 1990;162:215-223
475. Juliana C, Fernandes-Alnemri T, Wu J, Datta P, Solorzano L, Yu J-W, Meng R, Quong AA, Latz E, Scott CP, Alnemri ES. Anti-inflammatory compounds parthenolide and Bay 11-7082 are direct inhibitors of the inflammasome. J Biol Chem 2010;285:9792-9802
476. Lamkanfi M, Mueller JL, Vitari AC, Misaghi S, Fedorova A, Deshayes K, Lee WP, Hoffman HM, Dixit VM. Glyburide inhibits the Cryopyrin/Nalp3 inflammasome. J Cell Biol 2009;187:61-70
477. Masters SL, Dunne A, Subramanian SL, Hull RL, Tannahill GM, Sharp FA, Becker C, Franchi L, Yoshihara E, Chen Z, Mullooly N, Mielke LA, Harris J, Coll RC, Mills KHG, Mok KH, Newsholme P, Nuñez G, Yodoi J, Kahn SE, Lavelle EC, O'Neill LAJ. Activation of the NLRP3 inflammasome by islet amyloid polypeptide provides a mechanism for enhanced IL-1β in type 2 diabetes. Nat Immunol 2010;11:897-904
478. Henson MS, Buman BL, Jordan K, Rahrmann EP, Hardy RM, Johnson KH, O'Brien TD. An in vitro model of early islet amyloid polypeptide (IAPP) fibrillogenesis using human IAPP-transgenic mouse islets. Amyloid 2006;13:250-259
479. de Koning EJ, van den Brand JJ, Mott VL, Chargé SB, Hansen BC, Bodkin NL, Morris JF, Clark A. Macrophages and pancreatic islet amyloidosis. Amyloid 1998;5:247-254

480. Carpenter S, Aiello D, Atianand MK, Ricci EP, Gandhi P, Hall LL, Byron M, Monks B, Henry-Bezy M, Lawrence JB, O'Neill LA, Moore MJ, Caffrey DR, Fitzgerald KA. A long noncoding RNA mediates both activation and repression of immune response genes. Science 2013;341:789-792
481. Bamberger ME, Harris ME, McDonald DR, Husemann J, Landreth GE. A cell surface receptor complex for fibrillar beta-amyloid mediates microglial activation. J Neurosci 2003;23:2665-2674
482. Kam TI, Song S, Gwon Y, Park H, Yan JJ, Im I, Choi JW, Choi TY, Kim J, Song DK, Takai T, Kim YC, Kim KS, Choi SY, Choi S, Klein WL, Yuan J, Jung YK. FcgammaRIIb mediates amyloid-beta neurotoxicity and memory impairment in Alzheimer's disease. J Clin Invest 2013;123:2791-2802
483. Cheng K, Wang X, Zhang S, Yin H. Discovery of small-molecule inhibitors of the TLR1/TLR2 complex. Angewandte Chemie 2012;51:12246-12249
484. Chang Y-C, Kao W-C, Wang W-Y, Wang W-Y, Yang R-B, Peck K. Identification and characterization of oligonucleotides that inhibit Toll-like receptor 2-associated immune responses. FASEB J 2009;23:3078-3088
485. Ajit D, Udan M, Paranjape G, Nichols M. Amyloid-(1-42) Fibrillar Precursors are Optimal for Inducing Tumor Necrosis Factor- Production in the THP-1 Human Monocytic Cell Line. Biochemistry 2009;48:9011-9021
486. Klegeris A, McGeer PL. Complement activation by islet amyloid polypeptide (IAPP) and alpha-synuclein 112. Biochem Biophys Res Commun 2007;357:1096-1099
487. Hull RL, Westermark GT, Westermark P, Kahn SE. Islet amyloid: a critical entity in the pathogenesis of type 2 diabetes. J Clin Endocrinol Metab 2004;89:3629-3643
488. Westwell-Roper C, Dai DL, Soukhatcheva G, Potter KJ, van Rooijen N, Ehses JA, Verchere CB. IL-1 Blockade Attenuates Islet Amyloid Polypeptide-Induced Proinflammatory Cytokine Release and Pancreatic Islet Graft Dysfunction. J Immunol 2011;187:2755-2765
489. Arnush M, Heitmeier MR, Scarim AL, Marino MH, Manning PT, Corbett JA. IL-1 produced and released endogenously within human islets inhibits beta cell function. J Clin Invest 1998;102:516-526
490. Yin N, Xu J, Ginhoux F, Randolph GJ, Merad M, Ding Y, Bromberg JS. Functional specialization of islet dendritic cell subsets. J Immunol 2012;188:4921-4930
491. Boillée S, Yamanaka K, Lobsiger CS, Copeland NG, Jenkins NA, Kassiotis G, Kollias G, Cleveland DW. Onset and progression in inherited ALS determined by motor neurons and microglia. Science 2006;312:1389-1392
492. Cameron B, Landreth GE. Inflammation, microglia, and Alzheimer's disease. Neurobiol Dis 2010;37:503-509
493. Lacy PE, Finke EH. Activation of intraislet lymphoid cells causes destruction of islet cells. Am J Pathol 1991;138:1183-1190
494. Cao S, Zhang X, Edwards JP, Mosser DM. NF-kappaB1 (p50) homodimers differentially regulate pro- and anti-inflammatory cytokines in macrophages. J Biol Chem 2006;281:26041-26050
495. Smith MF, Jr., Eidlen D, Arend WP, Gutierrez-Hartmann A. LPS-induced expression of the human IL-1 receptor antagonist gene is controlled by multiple interacting promoter elements. J Immunol 1994;153:3584-3593

496. Haluzik M, Colombo C, Gavrilova O, Chua S, Wolf N, Chen M, Stannard B, Dietz KR, Le Roith D, Reitman ML. Genetic background (C57BL/6J versus FVB/N) strongly influences the severity of diabetes and insulin resistance in ob/ob mice. Endocrinology 2004;145:3258-3264
497. Gordon S, Taylor PR. Monocyte and macrophage heterogeneity. Nat Rev Immunol 2005;5:953-964
498. Arnush M, Scarim AL, Heitmeier MR, Kelly CB, Corbett JA. Potential role of resident islet macrophage activation in the initiation of autoimmune diabetes. J Immunol 1998;160:2684-2691
499. Markmann JF, Jacobson JD, Kiumura H, Choti MA, Hickey WF, Fox IJ, Silvers WK, Barker CF, Naji A. Modulation of the major histocompatibility complex antigen and the immunogenicity of islet allografts. Transplantation 1989;48:478-486
500. Rabinovitch A, Alejandro R, Noel J, Brunschwig JP, Ryan US. Tissue culture reduces Ia antigen-bearing cells in rat islets and prolongs islet allograft survival. Diabetes 1982;31 Suppl 4:48-54
501. Heitmeier MR, Arnush M, Scarim AL, Corbett JA. Pancreatic beta-cell damage mediated by beta-cell production of interleukin-1. A novel mechanism for virus-induced diabetes. J Biol Chem 2001;276:11151-11158
502. Sheykhzade M, Nyborg N. Non-competitive antagonism of amylin on CGRP(1)-receptors in rat coronary small arteries. Br J Pharmacol 2000;130:386-390
503. Shi XX, Wang LL, Li XX, Sahbaie PP, Kingery WSW, Clark JDJ. Neuropeptides contribute to peripheral nociceptive sensitization by regulating interleukin-1β production in keratinocytes. Anesthes Analg 2011;113:175-183
504. Manczak M, Mao P, Nakamura K, Bebbington C, Park B, Reddy PH. Neutralization of granulocyte macrophage colony-stimulating factor decreases amyloid beta 1-42 and suppresses microglial activity in a transgenic mouse model of Alzheimer's disease. Hum Mol Genet 2009;18:3876-3893
505. Taylor-Fishwick DA, Weaver JR, Grzesik W, Chakrabarti S, Green-Mitchell S, Imai Y, Kuhn N, Nadler JL. Production and function of IL-12 in islets and beta cells. Diabetologia 2013;56:126-135
506. Wang P, Wu P, Siegel MI, Egan RW, Billah MM. Interleukin (IL)-10 inhibits nuclear factor kappa B (NF kappa B) activation in human monocytes. IL-10 and IL-4 suppress cytokine synthesis by different mechanisms. J Biol Chem 1995;270:9558-9563
507. Sunderkotter C, Nikolic T, Dillon MJ, Van Rooijen N, Stehling M, Drevets DA, Leenen PJ. Subpopulations of mouse blood monocytes differ in maturation stage and inflammatory response. J Immunol 2004;172:4410-4417
508. Arnaout MA. Structure and function of the leukocyte adhesion molecules CD11/CD18. Blood 1990;75:1037-1050
509. Oh DYD, Morinaga HH, Talukdar SS, Bae EJE, Olefsky JMJ. Increased macrophage migration into adipose tissue in obese mice. Diabetes 2012;61:346-354
510. Stout RD, Jiang C, Matta B, Tietzel I, Watkins SK, Suttles J. Macrophages sequentially change their functional phenotype in response to changes in microenvironmental influences. J Immunol 2005;175:342-349
511. Lee YS, Li P, Huh JY, Hwang IJ, Lu M, Kim JI, Ham M, Talukdar S, Chen A, Lu WJ, Bandyopadhyay GK, Schwendener R, Olefsky J, Kim JB. Inflammation is necessary for

long-term but not short-term high-fat diet-induced insulin resistance. Diabetes 2011;60:2474-2483
512. Zraika S, Hull RL, Udayasankar J, Utzschneider KM, Tong J, Gerchman F, Kahn SE. Glucose- and time-dependence of islet amyloid formation in vitro. Biochem Biophys Res Commun 2007;354:234-239
513. Maedler K, Schumann DM, Sauter N, Ellingsgaard H, Bosco D, Baertschiger R, Iwakura Y, Oberholzer J, Wollheim CB, Gauthier BR, Donath MY. Low concentration of interleukin-1beta induces FLICE-inhibitory protein-mediated beta-cell proliferation in human pancreatic islets. Diabetes 2006;55:2713-2722
514. Sloan-Lancaster J, Abu-Raddad E, Polzer J, Miller JW, Scherer JC, De Gaetano A, Berg JK, Landschulz WH. Double-blind, randomized study evaluating the glycemic and anti-inflammatory effects of subcutaneous LY2189102, a neutralizing IL-1beta antibody, in patients with type 2 diabetes. Diabetes Care 2013;36:2239-2246
515. Cavelti-Weder C, Babians-Brunner A, Keller C, Stahel MA, Kurz-Levin M, Zayed H, Solinger AM, Mandrup-Poulsen T, Dinarello CA, Donath MY. Effects of gevokizumab on glycemia and inflammatory markers in type 2 diabetes. Diabetes Care 2012;35:1654-1662
516. Rissanen A, Howard CP, Botha J, Thuren T. Effect of anti-IL-1beta antibody (canakinumab) on insulin secretion rates in impaired glucose tolerance or type 2 diabetes: results of a randomized, placebo-controlled trial. Diabetes Obes Metab 2012;14:1088-1096
517. van Asseldonk EJ, Stienstra R, Koenen TB, Joosten LA, Netea MG, Tack CJ. Treatment with Anakinra improves disposition index but not insulin sensitivity in nondiabetic subjects with the metabolic syndrome: a randomized, double-blind, placebo-controlled study. J Clin Endocrinol Metab 2011;96:2119-2126
518. Ardestani A, Sauter NS, Paroni F, Dharmadhikari G, Cho JH, Lupi R, Marchetti P, Oberholzer J, Conte JK, Maedler K. Neutralizing interleukin-1beta (IL-1beta) induces beta-cell survival by maintaining PDX1 protein nuclear localization. J Biol Chem 2011;286:17144-17155
519. Harmon JS, Bogdani M, Parazzoli SD, Mak SS, Oseid EA, Berghmans M, Leboeuf RC, Robertson RP. beta-Cell-specific overexpression of glutathione peroxidase preserves intranuclear MafA and reverses diabetes in db/db mice. Endocrinology 2009;150:4855-4862
520. Höppener JWM, Jacobs HM, Wierup N, Sotthewes G, Sprong M, de Vos P, Berger R, Sundler F, Ahrén B. Human islet amyloid polypeptide transgenic mice: in vivo and ex vivo models for the role of hIAPP in type 2 diabetes mellitus. Exp Diabetes Res 2008;2008:697035
521. Hull RL, Watts MR, Kodama K, Shen ZP, Utzschneider KM, Carr DB, Vidal J, Kahn SE. Genetic background determines the extent of islet amyloid formation in human islet amyloid polypeptide transgenic mice. Am J Physiol Endocrinol Metab 2005;289:E703-709
522. Huang C-J, Haataja L, Gurlo T, Butler AE, Wu X, Soeller WC, Butler PC. Induction of endoplasmic reticulum stress-induced beta-cell apoptosis and accumulation of polyubiquitinated proteins by human islet amyloid polypeptide. Am J Physiol Endocrinol Metab 2007;293:E1656-1662
523. MacArthur DL, de Koning EJ, Verbeek JS, Morris JF, Clark A. Amyloid fibril formation is progressive and correlates with beta-cell secretion in transgenic mouse isolated islets. Diabetologia 1999;42:1219-1227

524. Ling PR, Mueller C, Smith RJ, Bistrian BR. Hyperglycemia induced by glucose infusion causes hepatic oxidative stress and systemic inflammation, but not STAT3 or MAP kinase activation in liver in rats. Metabolism 2003;52:868-874
525. Huang W, Metlakunta A, Dedousis N, Zhang P, Sipula I, Dube JJ, Scott DK, O'Doherty RM. Depletion of liver Kupffer cells prevents the development of diet-induced hepatic steatosis and insulin resistance. Diabetes 2010;59:347-357
526. Sandberg JO, Andersson A, Eizirik DL, Sandler S. Interleukin-1 receptor antagonist prevents low dose streptozotocin induced diabetes in mice. Biochem Biophys Res Commun 1994;202:543-548
527. Ladefoged M, Buschard K, Hansen AM. Increased expression of toll-like receptor 4 and inflammatory cytokines, interleukin-6 in particular, in islets from a mouse model of obesity and type 2 diabetes. APMIS 2013;121:531-538
528. Ardestani A, Sauter NS, Paroni F, Dharmadhikari G, Cho J-H, Lupi R, Marchetti P, Oberholzer J, Conte JK, Maedler K. Neutralizing interleukin-1beta (IL-1beta) induces beta-cell survival by maintaining PDX1 protein nuclear localization. J Biol Chem 2011;286:17144-17155
529. McKinnon CM, Docherty K. Pancreatic duodenal homeobox-1, PDX-1, a major regulator of beta cell identity and function. Diabetologia 2001;44:1203-1214
530. Leibowitz G, Ferber S, Apelqvist A, Edlund H, Gross DJ, Cerasi E, Melloul D, Kaiser N. IPF1/PDX1 deficiency and beta-cell dysfunction in Psammomys obesus, an animal with type 2 diabetes. Diabetes 2001;50:1799-1806
531. Kushner JA, Ye J, Schubert M, Burks DJ, Dow MA, Flint CL, Dutta S, Wright CV, Montminy MR, White MF. Pdx1 restores beta cell function in Irs2 knockout mice. J Clin Invest 2002;109:1193-1201
532. Eizirik DL, Mandrup-Poulsen T. A choice of death--the signal-transduction of immune-mediated beta-cell apoptosis. Diabetologia 2001;44:2115-2133
533. Talchai C, Xuan S, Lin HV, Sussel L, Accili D. Pancreatic beta cell dedifferentiation as a mechanism of diabetic beta cell failure. Cell 2012;150:1223-1234
534. Matsuoka TA, Kaneto H, Stein R, Miyatsuka T, Kawamori D, Henderson E, Kojima I, Matsuhisa M, Hori M, Yamasaki Y. MafA regulates expression of genes important to islet beta-cell function. Mol Endocrinol 2007;21:2764-2774
535. Arend WP, Palmer G, Gabay C. IL-1, IL-18, and IL-33 families of cytokines. Immunol Rev 2008;223:20-38
536. Park YJ, Ao Z, Kieffer TJ, Chen H, Safikhan N, Thompson DM, Meloche M, Warnock GL, Marzban L. The glucagon-like peptide-1 receptor agonist exenatide restores impaired pro-islet amyloid polypeptide processing in cultured human islets: implications in type 2 diabetes and islet transplantation. Diabetologia 2013;56:508-519
537. Aston-Mourney K, Hull RL, Zraika S, Udayasankar J, Subramanian SL, Kahn SE. Exendin-4 increases islet amyloid deposition but offsets the resultant beta cell toxicity in human islet amyloid polypeptide transgenic mouse islets. Diabetologia 2011;54:1756-1765
538. Hou X, Ling Z, Quartier E, Foriers A, Schuit F, Pipeleers D, Van Schravendijk C. Prolonged exposure of pancreatic beta cells to raised glucose concentrations results in increased cellular content of islet amyloid polypeptide precursors. Diabetologia 1999;42:188-194

539. Cai K, Qi D, Wang O, Chen J, Liu X, Deng B, Qian L, Liu X, Le Y. TNF-α acutely upregulates amylin expression in murine pancreatic beta cells. Diabetologia 2011;54:617-626
540. Cai K, Qi D, Hou X, Wang O, Chen J, Deng B. MCP-1 Upregulates Amylin Expression in Murine Pancreatic β Cells through ERK/JNK-AP1 and NF-κB Related Signaling Pathways Independent of CCR2. PLoS ONE 2011;6:e19559
541. Ellingsgaard H, Hauselmann I, Schuler B, Habib AM, Baggio LL, Meier DT, Eppler E, Bouzakri K, Wueest S, Muller YD, Hansen AM, Reinecke M, Konrad D, Gassmann M, Reimann F, Halban PA, Gromada J, Drucker DJ, Gribble FM, Ehses JA, Donath MY. Interleukin-6 enhances insulin secretion by increasing glucagon-like peptide-1 secretion from L cells and alpha cells. Nat Med 2011;17:1481-1489
542. Panagiotopoulos C, Qin H, Tan R, Verchere CB. Identification of a beta-cell-specific HLA class I restricted epitope in type 1 diabetes. Diabetes 2003;52:2647-2651